

Montana Tech Library

Digital Commons @ Montana Tech

Graduate Theses & Non-Theses

Student Scholarship

Spring 2022

**CHARACTERIZING HYDROSTRATIGRAPHIC COMMUNICATION OF
THE SEMI-CONSOLIDATED SEDIMENT AQUIFERS OF THE
FLATHEAD VALLEY IN NORTHWESTERN MONTANA THROUGH
HYDROGEOPHYSICAL SURVEYS**

Elizabeth Katherine Breitmeyer

Follow this and additional works at: https://digitalcommons.mtech.edu/grad_rsch



Part of the [Geological Engineering Commons](#)

CHARACTERIZING HYDROSTRATIGRAPHIC COMMUNICATION OF
THE SEMI-CONSOLIDATED SEDIMENT AQUIFERS OF THE FLATHEAD
VALLEY IN NORTHWESTERN MONTANA THROUGH
HYDROGEOPHYSICAL SURVEYS

by

Elizabeth Katherine Breitmeyer

A thesis submitted in partial fulfillment of the
requirements for the degree of

Master of Science in Geoscience:
Geophysical Engineering Option

Montana Tech

2022



Abstract

To accurately forecast the cascading effects of increased stress to a hydrologic system, characterization of the continuity and permeability of the primary confining layer (PCL) separating the shallow and deep intermontane alluvial aquifers is required. Geophysical methods provide a faster cost-effective alternative to drilling to acquire additional information on the changes of hydrostratigraphy with depth. Geoelectric resistivity models recovered through inversion of TEM central loop sounding data to delineate changes in geoelectric properties with depth, providing information on the depth, thickness and resistivity of the hydrostratigraphy. Comparison of geoelectric resistivity models with well completion report lithologies yield information about the permeability of the hydrostratigraphy and can infer the potential for occurring hydrostratigraphic communication.

The geological history of the Flathead Valley created a complex stratigraphic sequence of glacial sediments comprising the primary confining layer (PCL). Glacial sediments include glaciolacustrine, glacioteconite tills, subglacial traction tills and melt-out tills. Characterization of the PCL is the primary target for geophysical investigation as a critical element in understanding the hydrostratigraphic communication. The geoelectrical resistivity of glacial sediments is highly variable. Whether the PCL of the Flathead Valley, Montana presents geoelectrical property distinctions that are targetable by electromagnetic surveys is unknown. To assess the targetability of the glacial deposits comprising the PCL, a series of central loop soundings were completed. Geoelectrical models recovered through inversion and compared to well completion report lithology indicate the PCL presents a resistivity target that can be imaged using electromagnetic methods. The PCL appears to be variable throughout the Flathead Valley with predictable geoelectric resistivity ranges.

Keywords: central loop sounding, geoelectric resistivity model, primary confining layer, glaciolacustrine, subglacial traction till, melt-out till

Dedication

I dedicate this work to my husband, Ron and our children Katie, Tess, Mandy and Eddie for their love and support. They generously and patiently gave me the time and support I needed to make my own dreams come true. I couldn't have done this without you.

I also dedicate this work to Dad, Grandpa Don and Grandpa Dusty who always believed in me and taught me to believe in myself. You planted the seeds of ability in me and nurtured them. None of you lived to see me finish but I made it.

Acknowledgements

I would like to thank the Montana Bureau of Mines and Geology (MBMG) Ground Water Investigation Program (GWIP) for funding the field surveys used for my research and providing a wealth of information on the hydrostratigraphy of the Flathead Valley.

I would also like to thank MBMG for awarding me the Unno Sahinen Memorial Scholarship and matching MBMG Scholarship to assist in funding my investigations of the data gathered.

I would like to thank the Montana Water Center for my Fellowship with them while working on my data inversions.

I would like to thank SM Energy for awarding me the SM Energy Endowed Scholarship to providing funds to complete my investigations.

I would like to thank Dr. Trevor Irons for his time and knowledge to teach and advise me as I progressed through my project.

I would like to thank Dr. James Berglund of the MBMG GWIP team for getting his hands dirty in the field collecting the surveys and his expertise on hydrostratigraphy of the Flathead Valley.

I would like to thank Dr. Ronald Breitmeyer of MBMG for his assistance in producing lithology-resistivity figures for this work.

I would like to thank my committee members, Dr. Trevor Irons, Dr. James Berglund, Dr. Glenn Shaw, and Dr. Xiaobing Zhou for their support and wisdom in helping me complete my project and degree.

I would like to thank all of the support staff on the Montana Tech campus for their assistance in making this work possible.

I would also like to thank Mark Ottey of Kalispell, Montana for allowing me to perform my hydrogeophysical surveys on his property.

Table of Contents

ABSTRACT	II
DEDICATION	III
ACKNOWLEDGEMENTS	IV
LIST OF TABLES	VIII
LIST OF FIGURES.....	X
LIST OF EQUATIONS	XVI
GLOSSARY OF TERMS.....	XVII
ABBREVIATIONS	XXI
1. INTRODUCTION	1
2. BACKGROUND.....	6
2.1. <i>Geology</i>	6
2.2. <i>Glaciation</i>	8
2.3. <i>Hydrogeologic Section</i>	8
2.3.1. Conceptual Flow Model.....	9
2.4. <i>Resistivity of Stratigraphy</i>	11
2.4.1. Geoelectric Resistivity of Sand and Gravel Aquifers.....	13
2.4.2. Geoelectric Resistivity of Glacial Till Deposits	14
2.4.2.1. Glaciotectonite Tills.....	15
2.4.2.2. Subglacial Traction Tills	15
2.4.2.3. Melt-Out Tills	16
2.4.3. Geoelectric Resistivity of Glaciolacustrine Deposits.....	18
3. METHODOLOGY	19
3.1. <i>Transient Electromagnetics</i>	19

3.1.1.	Survey Design of Central Loop Soundings	19
3.1.2.	Equipment	22
3.2.	<i>Data Noise</i>	28
4.	INVERSION MODELS	29
4.1.	<i>Beowulf Algorithm</i>	30
4.2.	<i>Python Processing</i>	30
4.3.	<i>Depth of Investigation</i>	33
5.	RESULTS.....	35
5.1.	<i>Site 1</i>	35
5.2.	<i>Site 2</i>	38
5.3.	<i>Site 3</i>	42
5.3.1.	Site 3-1	45
5.3.2.	Site 3-2	46
5.4.	<i>Site 4</i>	48
5.4.1.	Site 4-1	51
5.4.2.	Site 4-2	52
5.4.3.	Site 4-3	54
5.4.4.	Site 4-4	55
6.	DISCUSSION.....	57
6.1.	<i>Site 1</i>	58
6.2.	<i>Site 2</i>	63
6.3.	<i>Site 3</i>	71
6.3.1.	Site 3-1	72
6.3.2.	Site 3-2	79
6.4.	<i>Site 4</i>	82
6.4.1.	Site 4-1	87
6.4.2.	Site 4-2	92
6.4.3.	Site 4-3	95

6.4.4. Site 4-4	101
6.5. Valley-wide scale.....	103
7. CONCLUSION	111
REFERENCES.....	114
APPENDIX A: FUTURE WORK	118
APPENDIX B: DATA	120
APPENDIX C: PYTHON PROCESSING SCRIPTS.....	121
APPENDIX D: BIG FORK FARM WELL #5 REPORTS	155
APPENDIX E: OTHER WELL REPORTS	184

List of Tables

<i>Table 1. GDP data set FV-S5-TEM1 Sounding at 4 Hz. Time gate is centered at time Wn, the voltage out is MAG 1, and the apparent resistivity is Rho 1.</i>	<i>120</i>
<i>Table 2. plotZT.py script developed by Dr. Trevor Irons to invert the central loop sounding data and produce a geoelectric resistivity model using the Beowulf algorithm.</i>	<i>121</i>
<i>Table 3. Control.yaml script developed by Dr. Trevor Irons from the sounding data for Site 4-1 at 8 Hz; used as the control file for the python processing in plotZT.py.</i>	<i>141</i>
<i>Table 4. Beowulf.out output script for the 8 Hz sounding at Site 4-1 using the inputs in the Table 3 control.yaml script for a 7-layer model with a 55-meter circular loop (Wilson, Raiche, & Sugeng, 2007).</i>	<i>142</i>
<i>Table 5. Big Fork Farm well #5 completion report; GWIC ID 317644 (Ground Water Information Center; Montana Bureau of Mines and Geology; Montana Technological University, 1998-2022). Annotation of the corresponding Site 3-1 geoelectric inversion model recovered PCL result have been overlaid in green.</i>	<i>157</i>
<i>Table 6. Big Fork Farm well #5 Geophysical Summary Plot report, reproduced with permission of Montana Bureau of Mines and Geology Publication Office (Montana Tech - Montana Bureau of Mines and Geology, 2021). Annotation of the corresponding hydrostratigraphic interpretations have been overlaid in green.</i>	<i>159</i>
<i>Table 7. Big Fork Farm deep well #5 report for neutron and density testing. Reproduced with permission of Montana Bureau of Mines and Geology Publication Office (Montana Tech - Montana Bureau of Mines and Geology, 2021). Annotation of the PCL and deep aquifer top interpretations have been overlaid in green.</i>	<i>161</i>
<i>Table 8. Big Fork Farm deep well #5 report for three arm caliper, natural gamma with volume print. Reproduced with permission of Montana Bureau of Mines and Geology Publication Office (Montana Tech - Montana Bureau of Mines and Geology, 2021). Annotation of the PCL and deep aquifer top location interpretation have been overlaid in green.</i>	<i>170</i>
<i>Table 9. QWIC ID 85605 well completion report with lithology for comparison with 1D geoelectric resistivity model at Site 1 (Ground Water Information Center; Montana Bureau of Mines and Geology; Montana Technological University, 1998-2022).</i>	<i>187</i>

<i>Table 10. GWIC ID 310815 well completion report with lithology for comparison with 1D geoelectric resistivity model at Site 2 (Ground Water Information Center; Montana Bureau of Mines and Geology; Montana Technological University, 1998-2022).</i>	190
<i>Table 11. GWIC ID 318274 well completion report with lithology for comparison with 1D geoelectric resistivity model at Site 2 (Ground Water Information Center; Montana Bureau of Mines and Geology; Montana Technological University, 1998-2022).</i>	193
<i>Table 12. QWIC ID 28881 well completion report with lithology for comparison with 1D geoelectric resistivity model at Site 3-2 (Ground Water Information Center; Montana Bureau of Mines and Geology; Montana Technological University, 1998-2022).</i>	196
<i>Table 13. QWIC ID 74883 well completion report with lithology for comparison with 1D geoelectric resistivity model at Site 4 (Ground Water Information Center; Montana Bureau of Mines and Geology; Montana Technological University, 1998-2022).</i>	199
<i>Table 14. QWIC ID 74884 well completion report with lithology for comparison with 1D geoelectric resistivity model at Site 4 (Ground Water Information Center; Montana Bureau of Mines and Geology; Montana Technological University, 1998-2022).</i>	201
<i>Table 15. QWIC ID 74924 well completion report with lithology for comparison with 1D geoelectric resistivity model at Site 4 (Ground Water Information Center; Montana Bureau of Mines and Geology; Montana Technological University, 1998-2022).</i>	203

List of Figures

Figure 1. Flathead Valley research area in northwestern Montana is outlined in a red box within the state of Montana. The topographic base map highlights the rugged terrain of western Montana and nearby Glacier National Park (Montana State Library Geographic Information; National Geographic Society, i-cubed).....2

Figure 2. Geophysical survey sites in Flathead Valley, Montana indicated with red markers and annotation of the hydrogeologic cross section in Figure 4 indicated by orange line (LaFave, Smith, & Patton, 2004; Montana State Library GIS Services).....5

Figure 3. Geologic Map of Northwestern Montana (Montana Bureau of Mines and Geology).7

Figure 4. Hydrogeologic Cross Section of the Flathead Valley developed by LaFave, Smith and Patton in 2004 reproduced with permission from the Montana Bureau of Mines and Geology Publications Office (LaFave, Smith, & Patton, 2004).9

Figure 5. Conceptual Flow Model of the Flathead Valley developed by LaFave, Smith and Patton in 2004 reproduced with permission from the Montana Bureau of Mines and Geology Publications Office (LaFave, Smith, & Patton, 2004).....10

Figure 6. Range of geoelectrical resistivity values for post-glacial intermontane valleys, adapted from Palacky (1987) and Veleva (2005).12

Figure 7. Hydrostratigraphic Section of the Flathead Valley developed by LaFave, Smith and Patton in 2004 reproduced with permission from the Montana Bureau of Mines and Geology Publications Office (LaFave, Smith, & Patton, 2004).13

Figure 8. Transient Electromagnetic Loop Sounding survey design.20

Figure 9. Electromagnetic waves comprised of an electrical and a magnetic vector field.21

Figure 10. Field equipment set up of the transmitter and recording instrumentation under a shade structure.23

Figure 11. TEM transmitter and receiver graph of transmitter current over time and receiver output voltage over time; and TEM receiver output response curve over time from (Environmental Protection Agency, n.d.).....24

Figure 12. Transmitter waveforms collected at Site 1 using the ZPB-600 which raised the transmitter load voltage from 24-volts to around 100-volts. The current differential is nearly 30-amps with most of this in the form of the

<i>large surges associated with switching the transmitter on. The current stabilized to an effective 5 to 5.8-amp pulse. Frequencies greater than 4-hertz (8 Hz, 100 V graph) did not stabilize before the ramp off resulting in poor waveform using the DC-DC converter. The blue-gray lines represent the simplified waveforms used in inverse modeling and red are the recorded variations of the amplitude on the Siglent oscilloscope.</i>	<i>26</i>
<i>Figure 13. Digitized waveforms from ZT-30 shunt resistor when driven by 24-volt LiFePO₄ battery. The blue lines represent the simplified waveforms used in inverse modeling and red are the recorded variations of the amplitude on the Siglent oscilloscope.</i>	<i>28</i>
<i>Figure 14. 8-hertz soundings data stack from Site 3-2. Masked time gates include the first time gate to account for uncertainty in the starting time and late-time gates beneath the signal-to-noise threshold (dashed line in S:N graph at bottom). All time gates utilize the standard deviation of their average data value in the stack.</i>	<i>32</i>
<i>Figure 15. Site 1 is located at Kokanee Bend on the Flathead River in the northern end of the Flathead Valley (Montana State Library GIS Services). See Figure 2 for overview of entire survey area.</i>	<i>36</i>
<i>Figure 16. Stacked 1-hertz, 4-hertz and 8-hertz data for the soundings at Site 1.</i>	<i>37</i>
<i>Figure 17. Recovered 1D 6-layer geoelectric resistivity model of 8-hertz data at Site 1.</i>	<i>38</i>
<i>Figure 18. Site 2 is located along the eastern medial moraine of the Flathead Valley on the Ottey Property near the Creston Fish Hatchery (Montana State Library GIS Services). See Figure 2 for overview of entire survey area.</i>	<i>40</i>
<i>Figure 19. Recovered 1D 7-layer geoelectric resistivity model of 8-hertz data at Site 2.</i>	<i>42</i>
<i>Figure 20. Site 3 consisted of two nearby locations near the center of the Flathead Valley on the northern shore of Flathead Lake, Montana. Site 3-1 is located at the Big Fork Farm Water Treatment Facility and is the location of the new deep wells drilled by MBMG in 2021. Site 3-2 is located on the nearby Flathead Waterfowl Production Area, under management of U.S. Fish & Wildlife (Montana State Library GIS Services). See Figure 2 for overview of entire survey area.</i>	<i>44</i>
<i>Figure 21. Recovered 1D 6-layer geoelectric resistivity model of 8-hertz data at Site 3-1.</i>	<i>46</i>
<i>Figure 22. Recovered 1D 6-layer geoelectric resistivity model of 8-hertz data at Site 3-2.</i>	<i>48</i>
<i>Figure 23. Site 4 consisted of four central loop soundings located on the Crow Waterfowl Production Area, under management of U.S. Fish & Wildlife Services in the center of the Flathead Valley, south of Flathead Lake (Montana</i>	

State Library GIS Services). Pingos and glacial kettles riddle the surface in this region (Hyndman & Thomas, 2020).

See Figure 2 for overview of entire survey area.....50

Figure 24. Recovered 1D 7-layer geoelectric resistivity model of 8-hertz data at Site 4-1.52

Figure 25. Recovered 1D 6-layer geoelectric resistivity model of 8-hertz data at Site 4-2.53

Figure 26. Recovered 1D 7-layer geoelectric resistivity model of 8-hertz data at Site 4-3.55

Figure 27. Recovered 1D 7-layer geoelectric resistivity model of 8-hertz data at Site 4-4.57

Figure 28. 6-layer depth comparison of well 85605 well completion report lithology and the Site 1 1D 6-layer geoelectric model layer depths (Ground Water Information Center; Montana Bureau of Mines and Geology; Montana Technological University, 1998-2022).....60

Figure 29. 1D geoelectric resistivity model of Site 2 with lithology of well 310815 (Ground Water Information Center; Montana Bureau of Mines and Geology; Montana Technological University, 1998-2022).....65

Figure 30. 1D geoelectric resistivity model of Site 2 with lithology of well 318274 (Ground Water Information Center; Montana Bureau of Mines and Geology; Montana Technological University, 1998-2022).....66

Figure 31. 1D geoelectric resistivity model of Site 3-1 with lithology of the Geophysics Summary Plot lithology by Colog, Inc (Montana Tech - Montana Bureau of Mines and Geology, 2021).74

Figure 32. 1D geoelectric resistivity model of Site 3-1 with lithology of well 317644 (Ground Water Information Center; Montana Bureau of Mines and Geology; Montana Technological University, 1998-2022).....75

Figure 33. 6-layer depth comparison of well 28881 well completion report lithology and the Site 3-2 1D 6-layer geoelectric resistivity model geoelectric layer depths (Ground Water Information Center; Montana Bureau of Mines and Geology; Montana Technological University, 1998-2022).80

Figure 34. 7-layer depth comparison of the Site 4 1D 6 and 7-layer geoelectric resistivity model layer depths.83

Figure 35. 1D geoelectric resistivity model of Site 4-1 with lithology of well 74924 (Ground Water Information Center; Montana Bureau of Mines and Geology; Montana Technological University, 1998-2022).....88

Figure 36. 6-layer depth comparison of wells 74924, 74883 and 74884 well completion report lithologies (Figure 50 and Tables 13-15, Appendix E) and the Site 4-2 1D 6-layer geoelectric model layer depths (Ground Water Information Center; Montana Bureau of Mines and Geology; Montana Technological University, 1998-2022).....93

<i>Figure 37. 7-layer depth comparison of well 74883 well completion report lithologies (Figure 50 and Tables 13-15, Appendix E) and the Site 4-3 1D 7-layer recovered geoelectric resistivity model geoelectric layer depths (Ground Water Information Center; Montana Bureau of Mines and Geology; Montana Technological University, 1998-2022)).</i>	96
<i>Figure 38. 7-layer depth comparison of well 74884 well completion report lithologies (Figure 50 and Tables 13-15, Appendix E) and the Site 4-3 1D 7-layer recovered geoelectric resistivity model geoelectric layer depths (Ground Water Information Center; Montana Bureau of Mines and Geology; Montana Technological University, 1998-2022).</i>	97
<i>Figure 39. 3D model of the 1D recovered model geoelectric resistivities in Ohm-meters for layers 1-6 along the series of soundings across the Flathead Valley, Montana with annotation of the predominant glacial depositional type represented at each site in green.</i>	104
<i>Figure 40. 3D Model of the 1D recovered geoelectric resistivity model thicknesses in meters for layers 1- 6 along the series of soundings across the Flathead Valley, Montana with annotation of the predominant glacial depositional type represented at each site.</i>	105
<i>Figure 41. Over-arching geometry of the geoelectric resistivity of the PCL in Ohm-meters along the series of soundings across the Flathead Valley, Montana.</i>	108
<i>Figure 42. Over-arching geometry of the geoelectric resistivity layer thickness of the PCL in meters along the series of soundings across the Flathead Valley, Montana. Sites 1 and 4-2 recorded the PCL as the basement geoelectric layer and had no geoelectric resistivity layer thickness to report.</i>	109
<i>Figure 43. Over-arching geometry of the geoelectric resistivity layer depth to the top of the PCL in meters below the surface along the series of soundings across the Flathead Valley, Montana.</i>	110
<i>Figure 44. Diagram of helicopter airborne electromagnetic survey design.</i>	118
<i>Figure 45. Site 3-1 TEM and nearby well locations located on or near the Big Fork Farm Water Treatment Facility (Montana State Library GIS Services). Star indicates the new (2021) deep well 317644 with well completion report lithology and additional geophysical reports (Ground Water Information Center; Montana Bureau of Mines and Geology; Montana Technological University, 1998-2022).</i>	156

Figure 46. Map of central loop sounding sites and all well locations in the GWIC database for the Flathead Valley, Montana (Montana State Library GIS Services; Ground Water Information Center; Montana Bureau of Mines and Geology; Montana Technological University, 1998-2022) Annotation of TEM sounding sites in red and the hydrogeologic cross section from Figure 4. Only a small percentage of the wells in the GWIC system contain well completion reports with lithology, many are only mapped locations with no additional information available.....185

Figure 47. Site 1 TEM location and locations of all nearby wells in the GWIC database located on or near the Kokanee Bend of the Flathead River (Montana State Library GIS Services). Star indicates well (85605) with a well completion report with lithology (Ground Water Information Center; Montana Bureau of Mines and Geology; Montana Technological University, 1998-2022). All wells within the image were checked for the availability of a well completion report with lithology to use.186

Figure 48. Site 2 TEM and all well locations in the GWIC database located on or near the private property where the soundings were performed (Montana State Library GIS Services). Star indicates GWIP drilled well completion reports with lithology, wells 318274 and 310815 (Ground Water Information Center; Montana Bureau of Mines and Geology; Montana Technological University, 1998-2022).189

Figure 49. Site 3-2 TEM and all well locations in the GWIC database located on or near the Flathead Waterfowl Production Area under management of U.S. Fish & Wildlife Services (Montana State Library GIS Services). Star indicates well 28881 with well completion report with lithology (Ground Water Information Center; Montana Bureau of Mines and Geology; Montana Technological University, 1998-2022). All wells within the image were checked for the availability of a well completion report with lithology.....195

Figure 50. Site 4 TEM and all well locations in the GWIC database located on or near the Crow Waterfowl Production Area under management of U.S. Fish & Wildlife Services (Montana State Library GIS Services). Star indicates wells 74924, 74883 and 74884 with well completion reports with lithology (Ground Water Information Center; Montana Bureau of Mines and Geology; Montana Technological University, 1998-2022). All wells within the image were checked for the availability of a well completion report with lithology to use for correlation with the 1D geoelectric resistivity models.....198

Figure 51. Southwest to northeast cross section of lithology defining the near subsurface between Quigley on the north bank of the Flathead River near Kalispell, Montana and Ottey at Site 2 near the Creston Fish Hatchery (Smith, Flathead SW-NE Cross Section of Deep Aquifer Drilling Report, report in preparation 2022).205

List of Equations

1.....20

2.....21

3.....21

5.....25

6.....33

Glossary of Terms

Term	Definition
Eddy Currents	<i>Eddy Currents</i> (also known as Foucault's currents) are coils of electrical current induced within conductive bodies in the subsurface by a changing magnetic field in the surrounding subsurface described by Faraday's Law of Induction. These eddy currents flow perpendicular to the magnetic field component as it changes with time. The eddy currents induce a secondary magnetic field in the subsurface whose decay rate is recorded by the geophysical electromagnetic receiver.
Electromagnetism	<i>Electromagnetism</i> is the study of the electromagnetic force – the physical interaction of electrically charged particles between electric and magnetic fields. Electromagnetism is identified by the frequency or wavelength of the electromagnetic field in the electromagnetic spectrum.
Englacial	<i>Englacial</i> describes sediment that is carried in the inner parts of a glacier and to the deposition of those sediments.
Faraday's Law of Induction	<i>Faraday's Law of Induction</i> (also known as Faraday's Law) is used to describe how the electromotive force (the work done on a unit of charge when it has traveled one coil of an eddy current) around a closed path (or within a conductive body) is equal to the negative of the time rate of change of the magnetic flux (Φ) enclosed by the path (or outer surface of the conductive body).
Fluvial	<i>Fluvial</i> refers to deposits of sediment that are sorted and deposited by flowing streams or rivers. These deposits are stratified.
Glacial (or rock) Flour	<i>Glacial Flour</i> are a fine-grained, silt-sized rock particles generated by the glacial erosion of bedrock.
Gauss's Law for Magnetism	<i>Gauss's Law for Magnetism</i> states that the total magnetic flux (Φ) through a closed surface is equal to zero.
Glacial Lake Missoula	<i>Glacial Lake Missoula</i> is a glacial lake formed in northwestern Montana during the Pleistocene time. Formed by an ice dam of the Cordilleran Ice Sheet on the Clark Fork River in Montana. The ice dam broke in regular intervals flooding a portion of Washington State.
Glacial Outwash	<i>Glacial outwash</i> is stratified sand and gravel deposits "washed out" from a glacier by meltwater streams and deposited in front of the end moraine. Coarser material is deposited nearest the source.
Glacial Till	<i>Glacial till</i> is material deposited directly by glacial ice. Till is commonly massive, unsorted and unstratified sediment.

Glaciofluvial	<i>Glaciofluvial</i> deposits are glacially derived sediment that is sorted and deposited by streams flowing from the melting ice. These deposits are stratified and may occur in the form of outwash plains, valley trains, deltas, kames and eskers.
Glaciolacustrine	<i>Glaciolacustrine</i> deposits are related to lake depositional processes of material ranging from fine clay to gravel that is released from a glacier and deposited into a glacial lake by water or floating ice. They are bedded or laminated with varves or rhythmites and may contain large erratic rock fragments carried within the glacier.
Glaciotectonite	<i>Glaciotectonite</i> originally defined by (Banham, 1977); (Benn & Evans, 2010); and (Pedersen, 1988), refers to shearing and deformation of rocks and sediments which still retain some of the structural characteristics of the parent material. They can display either brittle and ductile deformation or a combination of the two processes. (Clark, 2018; Evans, Phillips, Hiemstra, & Auton, 2006)
Ground Moraines	<i>Ground Moraines</i> are deposits of glacial till from glaciers retreating at a constant to rapid rate. They can be characterized by the presence of a corrugated surface with irregular ridges transverse to the ice flow.
Hummocky Disintegrated Moraines	<i>Hummocky Disintegrated Moraines</i> are glacial till deposits formed during the stagnation of the glacial ice during retreat. They consist of variable topography with numerous knobs, kettles and pingos. They usually have a round, broad shape that does not stand out from the landscape and grade gently into ground moraines.
Johnson Noise	<i>Johnson noise</i> is electronic noise generated by thermal agitation of electrons inside an electrical conductor at equilibrium, regardless of voltage applied. Thermal noise increases with temperatures.
Kettles	<i>Kettles</i> are steep-sided, bowl-shaped depressions in glacial till deposits, often containing a lake or swamp. Irregularly shaped due to formation through melting of a large, detached block of stagnant ice that had been wholly or partially buried in the till.
Ohm's Law	<i>Ohm's Law</i> states that the electric current is proportional to voltage and inversely proportional to resistance.
Porosity	<i>Porosity</i> is the percentage of open space within an unconsolidated sediment or rock. Represented first by the spaces between the grains of the sediment or sedimentary rock; second by fractures within the rock. Unconsolidated sediments usually have a higher porosity than consolidated sediments because they are not cemented and usually not compressed. Fine-grained materials like silt and clay usually have a greater porosity than coarser materials like gravel. Well-sorted sediments usually have a higher porosity than poorly-sorted sediments. "Glacial till, which has a wide range of grain sizes and is typically formed under compression beneath glacial ice, has relatively low porosity." (Earle, 2015)

Lateral Moraines	<i>Lateral Moraines</i> are glacial till formed by material eroded from the valley walls.
Loess	<i>Loess</i> are silt-sized particles transported and deposited by wind. Deposits typically thin at edges with the mean-particle size decreasing with distance from the source. Commonly picked up from glacial meltwaters.
Magnetic Flux (ϕ)	<i>Magnetic Flux (ϕ)</i> through a surface is the mathematical integral of the normal component of the magnetic field over that surface. When determining the total magnetic flux through a surface, only the boundary of the surface needs to be defined without knowledge of the surface shape. The integral over any surface sharing the same boundary will be equal.
Matrix	<i>Matrix</i> is the natural material (such as soil or rock) in which something is embedded (Dictionary, 1828).
Maxwell's Equations	<i>Maxwell's Equations</i> describe mathematically how electric and magnetic fields are generated and altered by electrical charges, currents and changes to the electric and magnetic fields.
Medial Moraines	<i>Medial Moraines</i> are glacial till deposits formed by the joining of two lateral moraines at the confluence of two glaciers.
Melt-Out Till	<i>Melt-out till</i> is englacial and supraglacial drift sediment released by the melting of stagnant or slowly moving debris-rich glacial ice that has been directly deposited without subsequent transport or deformation (Evans, Phillips, Hiemstra, & Auton, 2006; Benn & Evans, 2010; Clark, 2018).
Peat	<i>Peat</i> is soil composed primarily of variably decomposed, unconsolidated organic matter accumulated in wetlands.
Pingo	<i>Pingo</i> refers to a conical mound of soil-covered ice raised in part by hydrostatic pressure within and below the permafrost of arctic regions. Results in circular depressions containing lakes, ponds or swamps.
Permafrost	<i>Permafrost</i> is ground, soil or rock that remains at or below 0°C for at least two years. It is defined on the basis of temperature and not necessarily containing ground ice.
Plucking	<i>Plucking</i> is the process of glacial erosion by which blocks of rock are pulled away from fractured bedrock.
Rhythmite	<i>Rhythmite</i> are an individual unit in a succession of beds developed by rhythmic sedimentation. There is no limit to the thickness or complexity of the bedding and has no time-related or seasonality.
Silt	<i>Silt</i> is an unconsolidated fine sand, clay or organic material carried by running water and deposited as a sediment. Particle size is usually on the order of 1/20 th of a millimeter or less in diameter. In soil it must contain less than 12% clay (Dictionary, 1828).

Subglacial Drift	<i>Subglacial Drift</i> is used to describe glacial till deposits of substrate material that was eroded beneath the sole of a glacier. This can include the re-working of prior glacial deposits. Rounding, faceting and scratching of the larger clasts from the shear-force abrasion are characteristic of these deposits.
Subglacial Traction Till	<i>Subglacial Traction Till</i> is subglacial drift deposited by a glacial sole that has slid over and/or deformed its bed and then released the sediment from the ice via pressure melting and/or plucking followed by disaggregation and homogenizing through shear-force abrasion (Evans, Phillips, Hiemstra, & Auton, 2006). Subglacial traction till is “very dense with a low water content because of the combination of the pressures of the ice and shear” (p.263) (Clark, 2018). “These tills have bimodal or multimodal particle size distributions with distinct rock flour and gravel ranges. Cobbles and boulders are aligned with the direction of the ice flow” (p.264) (Clark, 2018).
Supraglacial Drift	<i>Supraglacial Drift</i> is used to describe glacial till deposits that were carried in the upper reaches or on top of the glacier and later deposited during glacial retreat. In valley glaciers where the confining walls provide material, deposits are characterized by angular clasts with lenses of finer, waterlaid sediments and small amounts of entrapped loess.
Terminal Moraines	<i>Terminal Moraines</i> are the bulldozed glacial till deposits from the leading edge of the glacier. This moraine deposit marks the farthest extent the glacier progressed.
Time Domain Electromagnetics (TDEM)	<i>Time Domain Electromagnetics</i> (TDEM) are transient electromagnetic (TEM) geophysical survey techniques that use time as an independent variable to describe the electromagnetic waveform using Maxwell’s Equations.
Transient Electromagnetics (TEM)	<i>Transient Electromagnetics</i> (TEM) are an active-source geophysical method using an electromagnetic field induced by transient pulses of electric current and the measurement of the secondary magnetic fields decay to determine the electrical conductivity in the near subsurface.
Varves	<i>Varves</i> are a thin pair of graded glaciolacustrine layers seasonally deposited with a coarser thicker summer layer and a finer-grained thinner winter layer.

Unless otherwise noted: Electromagnetic Terminology (Reynolds, 2011; Griffiths, 2019; Environmental Protection Agency, n.d.); Glacial Terminology (Martini, Brookfield, & Sadura, 2001).

Abbreviations

Abbreviation	Full Name
DOI	Depth of Investigation
GWIC	Ground Water Information Center of the Montana Bureau of Mines and Geology
GWIP	Ground Water Investigation Program of the Montana Bureau of Mines and Geology
H-AEM	Helicopter Airborne Electromagnetics
MBMG	Montana Bureau of Mines and Geology
PCL	primary confining layer
TDEM	Time Domain Electromagnetics
TEM	Transient Electromagnetics

1. Introduction

The Flathead Valley in Montana, north of Missoula (Figure 1) is known for its prized Flathead cherries. This largely agricultural area has been growing at a rapid rate. The United States Census Bureau estimates a population growth of 14.2 % from 2010 to 2019 in Flathead County, which encompasses the northern end of the Flathead Valley and therefore the upper end of the watershed (United States Census Bureau). The 2017 census of agriculture indicates that the farmland area had increased by 7% between 2012 and 2017 and that 12% of this farmland was irrigated at that time (United States Department of Agriculture). Flathead Valley is also a gateway to Glacier National Park and known for the scenic beauty of its lake and forests, bringing in tourists from around the world. The county population increases by 40% during the months of June through August according to the Flathead County Montana website (Flathead County Montana).

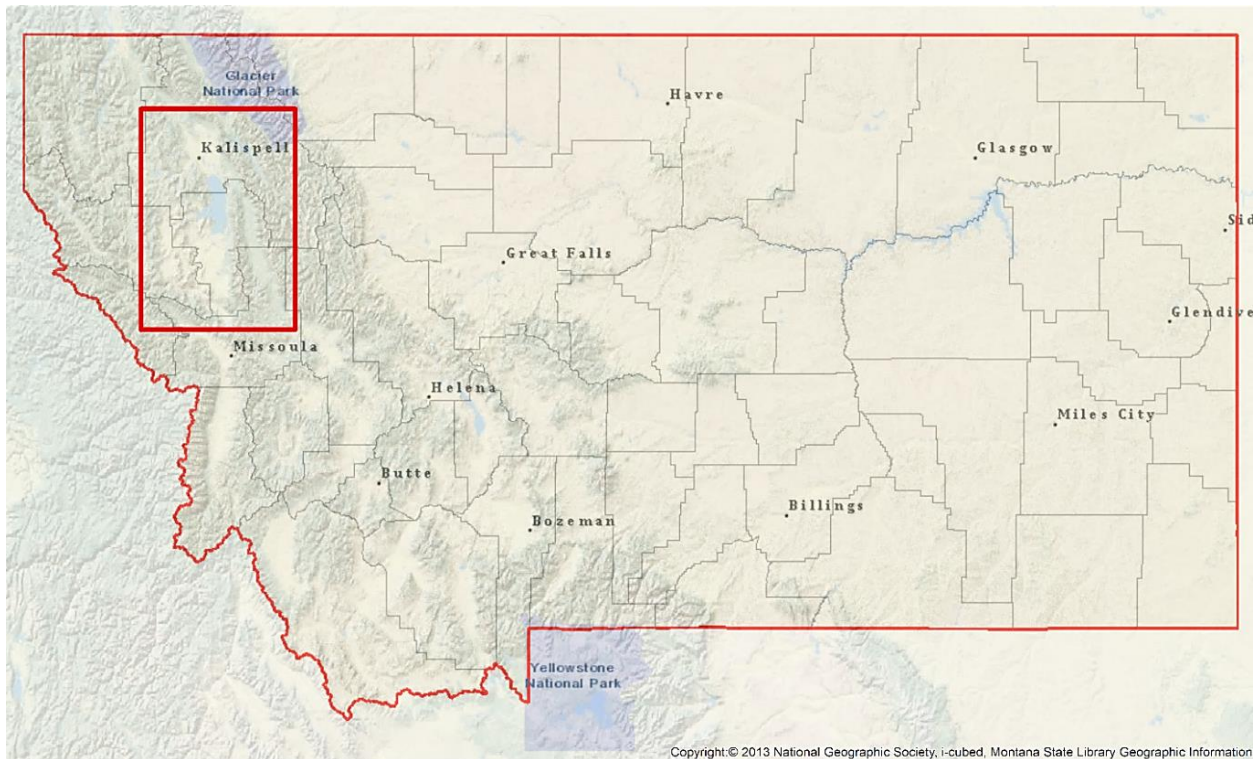


Figure 1. Flathead Valley research area in northwestern Montana is outlined in a red box within the state of Montana. The topographic base map highlights the rugged terrain of western Montana and nearby Glacier National Park (Montana State Library Geographic Information; National Geographic Society, i-cubed).

Concern over the ability of the valley to sustain growth without compromising the treasured surface waters prompted the Montana State Legislature to task the Montana Bureau of Mines and Geology's (MBMG) Ground Water Investigation Program (GWIP) with conducting an investigation to develop a calibrated numerical groundwater flow model capable of forecasting the impact of increased groundwater development scenarios on the area aquifers and surface waters on the east side of Flathead Valley (Bobst, Berglund, & Snyder, 2020). A critical component of understanding the interconnection between the groundwater and surface waters of Flathead Valley requires characterization of the continuity and permeability of the primary confining layer (PCL) separating the shallow and deep intermontane alluvial aquifers. The

leakiness and variability of this layer is the key characteristic in accurately forecasting the cascading effects on increased stress to the system.

Traditionally the hydrostratigraphy is inferred through interpolation of surface geology and geospatial water resource data including the use of well completion reports. This gives both a general picture of the subsurface stratigraphy and detailed point data of the subsurface hydrostratigraphy. Central repositories of regional groundwater resource data, such as the Ground Water Information Center (GWIC) at MBMG are maintained and updated to provide current information for use in water-resource management projects and studies. The GWIC repository contains data on well-completion reports from commercial drillers, measurements of well performance and water quality from site visits, water-level measurements for some wells dating back 60 years, and water-quality reports for thousands of samples (Ground Water Information Center; Montana Bureau of Mines and Geology; Montana Technological University, 1998-2022). The GWIC Repository provides a wealth of water resource data, however the reliability and quality of lithology logs are highly variable in commercially logged well completion reports.

The ambiguity and sparsity of well log completion reports with lithology creates the need to validate the hydrostratigraphy for development of a high-accuracy numerical flow model. To do this new data needs to be generated to provide additional information on the over-arching geometry of the hydrostratigraphy. Drilling a new well with core logging by scientists such as those on the GWIP team at MBMG is expensive, time-consuming and only provides a single high-accuracy data point. Hydrogeophysical surveys can provide additional data quickly and at a lower cost than drilling a single deep well.

Hydrogeophysical surveys using electromagnetic geophysical methods detect variations in the electrical properties of the substrata subjected to an electromagnetic field. The resistivity of the substrata is dependent on the fluid content as well as the resistive nature of the mineral content. The GWIP research team contracted the Geophysical Engineering Department of Montana Technological University to collect a series of Transient Electromagnetic (TEM) central loop soundings in the Flathead Valley in August of 2020 to aid in the validation and refinement of understanding the near subsurface hydrostratigraphy.

Very few geophysical surveys have been conducted in the Flathead Valley of Montana and no hydrogeophysical surveys have targeted the glacial sediments of the valley. Glacial sediments make a challenging target for geoelectric methods due to the large range of potential geoelectrical resistivities they can have. Inverse modelling of this geoelectric resistivity data provides a new image of the subsurface geometry and comparison with the hydrostratigraphic model and local lithology tell us where changes in the stratigraphic units are occurring. This provides validation of the over-arching geometry and continuity of the hydrostratigraphy and increases confidence in the results of the numerical groundwater flow model forecast.

The purpose of this study is to use the data from the survey sites (Figure 2) to test the efficacy of electromagnetic property geophysics in characterizing the glacial sediments composing the PCL of the Flathead Valley in northwestern Montana. Additionally, we aim to investigate the continuity and over-arching geometry of the PCL located between the semi-consolidated sediment aquifers of the Flathead Valley.

Flathead Valley, Montana

Geophysical Survey Sites

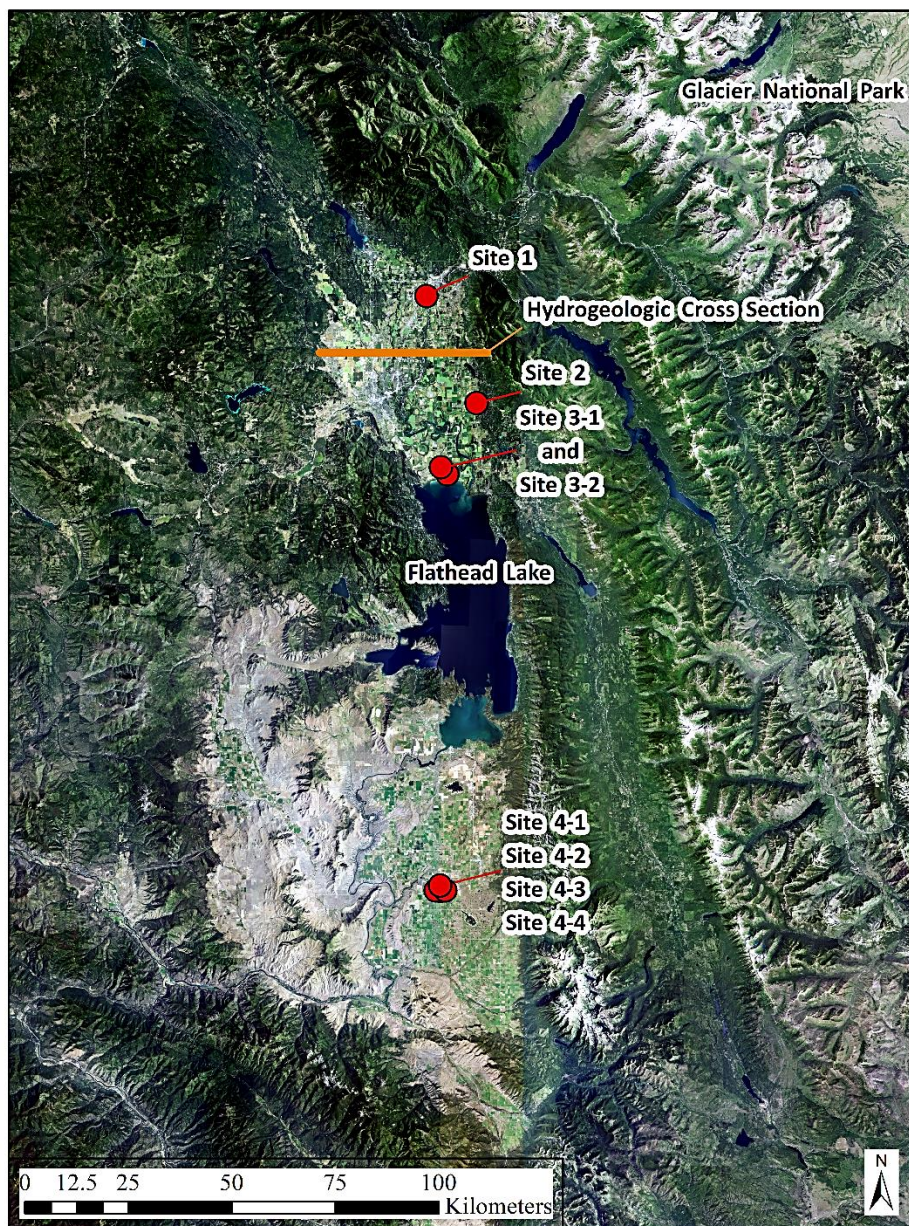


Figure 2. Geophysical survey sites in Flathead Valley, Montana indicated with red markers and annotation of the hydrogeologic cross section in Figure 4 indicated by orange line (LaFave, Smith, & Patton, 2004; Montana State Library GIS Services).

2. Background

2.1. Geology

The entirety of northwestern Montana, located west of the Rocky Mountain front and north of the Lewis and Clark fault zone is a region in which the continental crust uplifted, folded, fractured, broke and slid eastward in great slabs, stacking up and sliding over one another (Hyndman & Thomas, 2020). These Belt Formations, also known as the Belt Supergroup sedimentary rocks have the unusual characteristic of older Precambrian formations overlying younger Tertiary formations (LaFave, Smith, & Patton, 2004). The Flathead Valley is part of the Rocky Mountain Trench, some 1,600 kilometers-long combination of valleys extending from Alaska along the western side of British Columbia's Rockies through Yukon and British Columbia, Canada to St. Ignatius, Montana, marking the western edge of the Belt Formations (Hyndman & Thomas, 2020). Figure 3 is a geologic map of the study area detailing the complex geology resulting from the periods of tectonic compression and relaxations followed by erosion and deposition.




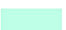

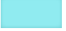








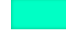











Northwestern Montana

Legend

Geologic Map

Geologic Units

Unit_Name

	Alluvium		Mount Pablo Formation through Ellis Group: Mount Pablo, Morrison, Swift, Rierdon, and Sawtooth Formations
	Blackleaf Formation		Piegan Group: Helena and Wallace Formations
	Devils Glen through Flathead Formation: Devils Glen, Switchback, Steamboat, Pentagon, Pagoda, Dearborn, Damnation or Elko, Gordon, and Flathead Formations		Ravalli Group: St. Regis, Revett, and Burke Formations; or Empire and Grinnell Formations; or Empire and Spokane Formations
	Garnet Range Formation: locally includes upper Libby Formation and Pilcher Formation in northwestern Montana		Red Lion through Flathead Formation: Red Lion, Pilgrim, Park, Meagher, Wolsey, and Flathead Formations; or Red Lion, Hasmark, Silver Hill, and Flathead Formations
	Glacial deposit		Sediment or sedimentary rock
	Glacial lake deposit		Three Forks through Maywood Formation: Three Forks, Jefferson, and Maywood Formations or Palliser and Alexo Formations, and Fairholme Group in northwestern Montana near Canadian border
	Granitic rock		Upper Missoula Group: McNamara, Bonner, and Mount Shields Formations; locally includes lower Libby Formation in northwestern Montana
	Gravel		Upper Prichard or Appekunny Formation
	Helena Formation		Volcanic rock: locally includes Challis Volcanics in southwestern Montana
	Kishenehn Formation		water
	Kootenai Formation		
	Lower Greyson Formation		
	Lower Missoula Group: Shepard and Snowslip Formations; or Shepard Formation and unresolved Snowslip Formation equivalent		
	Lower Prichard Formation		
	Madison Group: Mission Canyon and Lodgepole Formations; or Castle Reef and Allan Mountain Formations		
	Mafic intrusive rock		
	Marias River Formation		

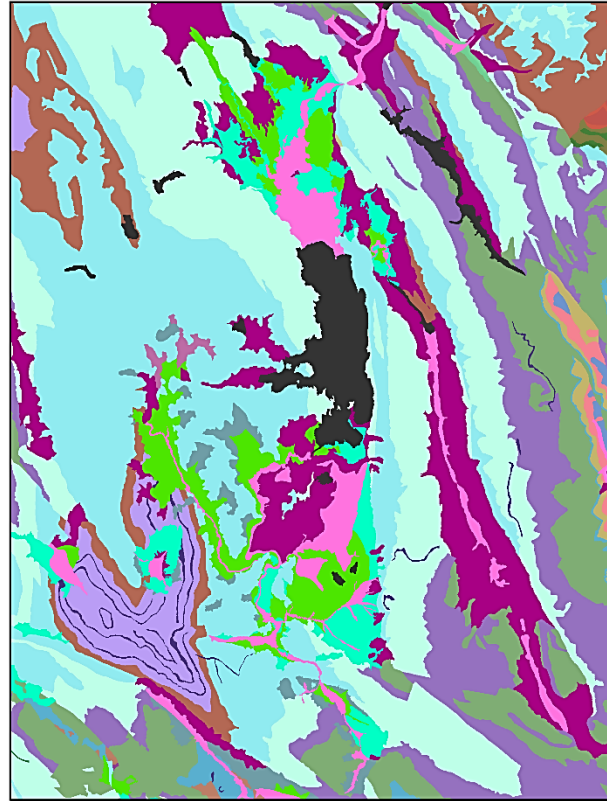


Figure 3. Geologic Map of Northwestern Montana (Montana Bureau of Mines and Geology).

2.2. Glaciation

Flathead Valley underwent multiple complex glaciations. The most recent glaciation occurred 15,000 years ago when the Flathead Lobe of the Cordilleran Ice Sheet gouged its way down the Rocky Mountain Trench during the Pinedale Glaciation eroding the Belt Formations (LaFave, Smith, & Patton, 2004; Hyndman & Thomas, 2020). Present-day Flathead Lake resides in the depression left from the weight of the Flathead Glacier as it melted. The lake is confined to the west and south by the Elmo, Big Arm and Polson terminal moraines. Glacial deposits in the Flathead Valley are a mix of Belt Supergroup glacio-erosional deposits in the form of moraines made of glacial till, glacial outwash sediments and glaciolacustrine deposits from the melting of the Flathead Glacier and flooding by Glacial Lake Missoula south of the Polson terminal moraine.

2.3. Hydrogeologic Section

The hydrogeologic cross-section of the valley in Figures 2 and 4 was developed by LaFave, Smith and Patton (2004) depicting the interpolated geometry of the valley subsurface. Within the bowl of bedrock are semi-consolidated Tertiary sediments composed of clay, silt and sand deposited during the relaxation period of the Belt Formation. This is overlain by the Deep Alluvium sand and gravel layer, deposited between the end of the Tertiary and prior to the period of complex glaciation. The PCL composed of glacial drift deposits and glaciolacustrine deposits overlies the Deep Alluvium. Finally, a layer of Shallow Alluvium deposited after the final melting of the Flathead Glacier with inter-fingering of glacial and intermediate-aged alluvium deposited at the margins of the glaciers during their advances and retreats comprises the uppermost strata.

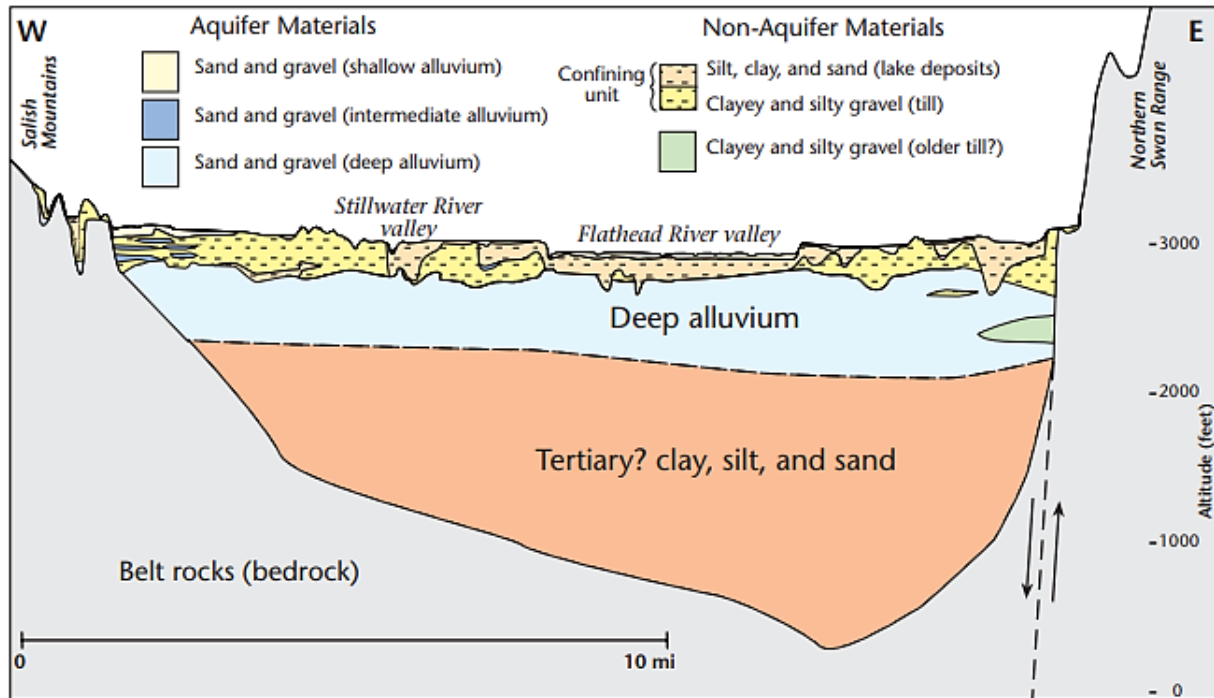


Figure 4. Hydrogeologic Cross Section of the Flathead Valley developed by LaFave, Smith and Patton in 2004 reproduced with permission from the Montana Bureau of Mines and Geology Publications Office (LaFave, Smith, & Patton, 2004).

2.3.1. Conceptual Flow Model

The Shallow and Deep Alluvium layers contain the primary aquifers of the Flathead Valley. The conceptualized subsurface flow model of the Flathead Valley developed by LaFave, Smith and Patton (2004) is in Figure 5. In the Flathead Valley flow system, all strata except the uppermost layer of alluvium are saturated. Recharge in the valley occurs as meltwater off the mountain ranges either infiltrates directly into the shallow system as runoff or into the network of rock fractures moving to deeper hydrostratigraphic layers. Groundwater flows down valley split by the PCL into shallow and deep flow systems. The continuity and over-arching geometry of the PCL is largely unknown. Well completion report lithology and depth to flowing water suggest the presence of either intermediate aquifers or holes in the PCL.

The importance of this confining layer is understanding how it controls the flow regime of the primary aquifer system. The water budget of the valley is dependent upon the volume of groundwater storage and the residence time of water within the various parts of the aquifer system. If there is significant hydrostratigraphic communication occurring between the Shallow and Deep Sand and Gravel Aquifers, over-pumping of the Deep Aquifer could lead to a draw-down effect in the Shallow Aquifer and ultimately to drawdown of the surface waters of the Flathead Lake, in effect taxing the regional ecological system.

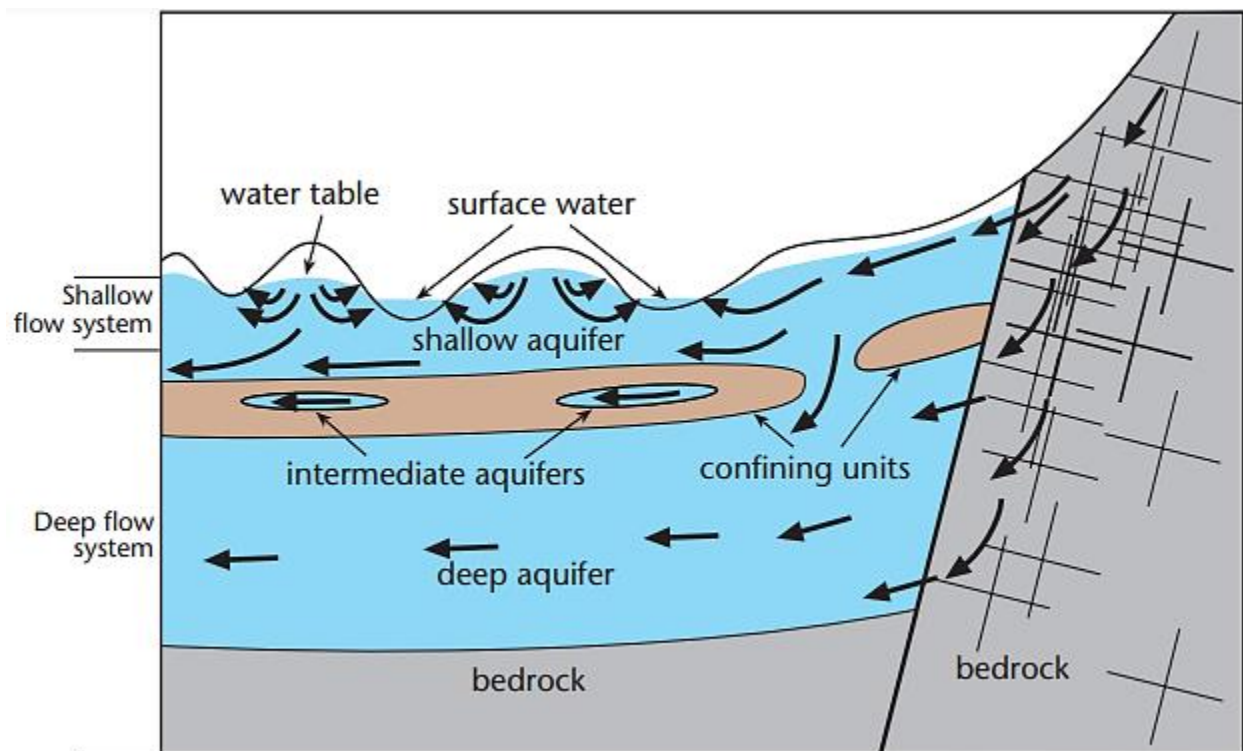


Figure 5. Conceptual Flow Model of the Flathead Valley developed by LaFave, Smith and Patton in 2004 reproduced with permission from the Montana Bureau of Mines and Geology Publications Office (LaFave, Smith, & Patton, 2004).

2.4. Resistivity of Stratigraphy

Electromagnetic geophysical investigations are used to detect variations in the electrical properties of the geologic units. Geoelectrical resistivity of saturated and semi-saturated units is often dependent on both the fluid content of the geologic unit and the resistive nature of the fluid and mineral content making up the stratigraphy. Fluid content is related to the pore volume porosity and the porosity caused by the interconnection of fractures in the unit (Earle, 2015). Fluid resistivity will determine the bulk electrical resistivity of most saturated strata and can be a variable of consideration where water quality causes the electrical resistivity to decrease with increasing ionic content.

Do electromagnetic methods have the ability to differentiate between the glacial deposits comprising the PCL of the Flathead Valley, Montana and the semi-consolidated sand and gravel aquifers? Palacky (1987) found that “in Canada and Scandinavia, glacial or glaciolacustrine sediments cover most of the previously glaciated areas [which may be similar to those found in the Flathead Valley]. Although moraine sediments (gravel, sand, tills) are resistive to poorly conductive (50 to 10 000 Ohm meters), clays deposited in lakes formed after the retreat of glaciers are conductive (5 to 100 Ohm meters)” (Palacky, 1987). Common resistivity ranges of strata found in postglacial intermontane valley fill adapted from Palacky (1987) and Veleva (2005) have been compiled in Figure 6 to provide guidelines for the geoelectric resistivity ranges that will be seen in the Flathead Valley data.

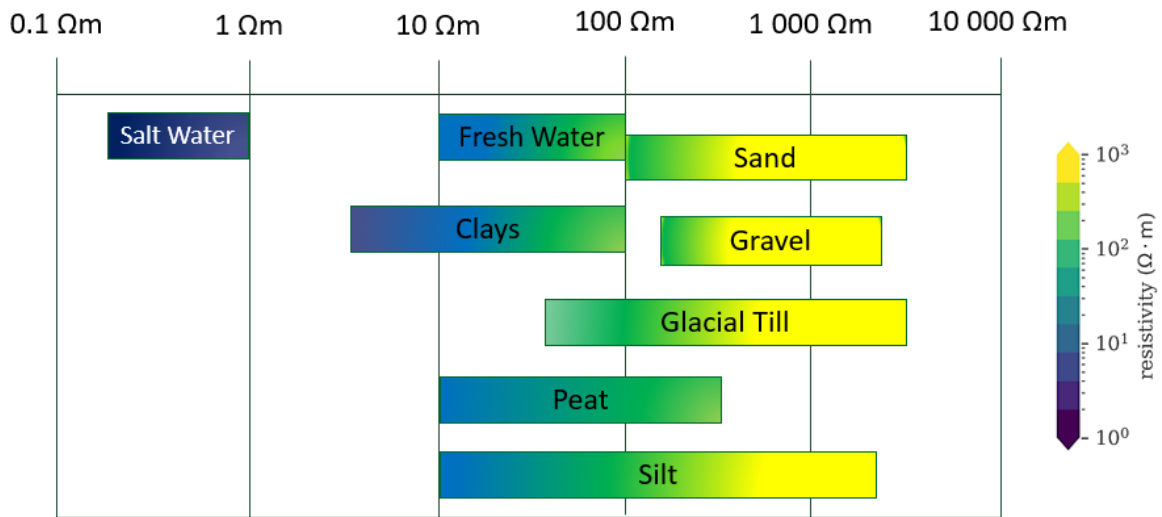


Figure 6. Range of geoelectrical resistivity values for post-glacial intermontane valleys, adapted from Palacky (1987) and Veleva (2005).

The geoelectrical resistivity changes with depth can be estimated under the guidelines of Figure 6 and the Flathead Valley stratigraphic section by LaFave, Smith and Patton (2004) in Figure 7. In unconsolidated glacial sediments, glacial development of both glacial and non-glacial unconsolidated material creates a primary porosity inferred from depositional processes (p.434) (Ravier & Buoncristiani, 2018). Therefore, understanding of glacial depositional processes throughout the valley will be necessary to differentiate the geoelectrical resistivity of the various glacial deposits making up the PCL from the sand and gravel aquifers.

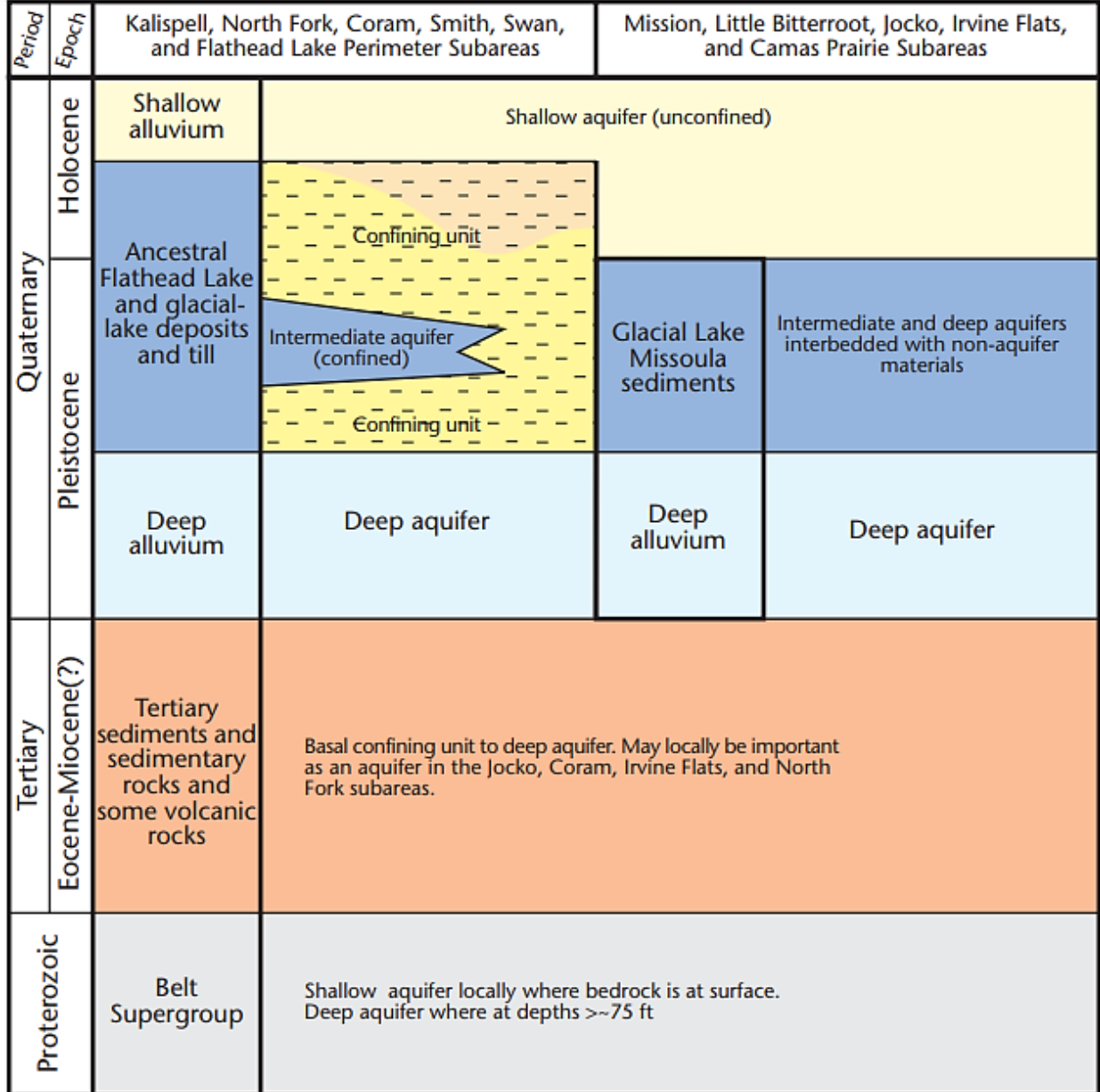


Figure 7. Hydrostratigraphic Section of the Flathead Valley developed by LaFave, Smith and Patton in 2004 reproduced with permission from the Montana Bureau of Mines and Geology Publications Office (LaFave, Smith, & Patton, 2004).

2.4.1. Geoelectric Resistivity of Sand and Gravel Aquifers

Semi-consolidated alluvial sand and gravel aquifers containing fresh groundwater (with low ionic content) will have a moderate geoelectrical resistivity with increasing geoelectrical

resistivity where they lose water content. These stratigraphic units will make up the layers immediately above and below the PCL.

2.4.2. Geoelectric Resistivity of Glacial Till Deposits

In locations where the PCL is predominately composed of saturated semi-consolidated glacial outwash and till, rock flour or silt, the geoelectrical resistivity will be heavily influenced by the material porosity and resistivity of its groundwater content. Glacial till is best classified based on modes of transportation and deposition due to the effects of each producing differences in the physical properties of tills with similar composition (Clark, 2018). Clark (2018) and Evans et al. (2006) defined glacial tills as (a) deformation-based (glaciotectonite), (b) a combination of deposition and deformation (subglacial traction till) or (c) deposition-based (melt-out till) (Evans, Phillips, Hiemstra, & Auton, 2006; Clark, 2018).

Glacial tills are complex, spatially variable, and dense composite soils (Clark, 2018). A till can be classified as: I) fine-grained fully homogenized soil; II) matrix-dominated soil behaving as a fine-grained soil with some coarse-grained particles; III) clast-dominated soil behaving as a coarse-grained soil with fine-grained particles; or IV) coarse-grained soil (Clark, 2018). “The density depends on the pore pressure regime that existed during deposition” (Clark, 2018). In a glacial outwash with high silt content, which has a high porosity and low permeability (Earle, 2015), the geoelectrical resistivity of the layer will be heavily influenced by the water resistivity. The type of composite soil and its density will need to be considered in defining the geoelectrical properties of the glacial tills encountered.

2.4.2.1. Glaciotectonite Till

Glaciotectonite are formed in areas where the glacier moved over solid or superficial geology, deforming the substrate (Clark, 2018). Glaciotectonite deposits are subject to shear and gravitational forces during deposition resulting in brittle shear planes, faults, ductile folds and laminations (Clark, 2018). These deposits are a type III clast-dominated composite soil with 0-15% fines (Clark, 2018). It is important to note that even a 15% content of fine-matrix particles can have a significant influence on the physical properties (Clark, 2018) yielding a low porosity and moderate permeability (Earle, 2015).

A type III glaciotectonite till of clast-dominated glacial outwash made of a small percentage of till, rock flour or silt matrix will have a moderate density, moderate-to-high permeability and low porosity. The geoelectrical resistivity of the layer will be heavily influenced by the water resistivity yielding a moderately geoelectrical resistive layer when saturated with fresh groundwater.

Glaciotectonite till may have geoelectrical resistivities difficult to differentiate from the sand and gravel aquifers lying above and below.

2.4.2.2. Subglacial Traction Till

Subglacial traction tills are formed as a result frictional movement of a glacier. These subglacial drift deposits are “usually very dense with a low water content because of the combination of the [gravitational] pressures of the ice and shear” (p.263) force of the glacial-ice passage (Clark, 2018). Subglacial traction tills can be described as over-consolidated because they are dense rather than consolidated by geotechnical processes (Clark, 2018). These deposits can be type I-IV composite soils.

A type I subglacial traction till of fine-grained fully homogenized soil matrix with 70-100% fines will have a moderate-to-high density, low permeability and low porosity yielding a moderately-high geoelectrical resistive layer (Earle, 2015; Clark, 2018).

A type II subglacial traction till of matrix-dominated soil behaving as a 45-70% fine-grained soil with some coarse-grained particles will have a moderate-to-high density, low-to-moderate permeability and moderately-low porosity. The geoelectrical resistivity of the layer will be somewhat influenced by the water resistivity yielding a moderately geoelectrical resistive layer when saturated with fresh groundwater (Earle, 2015; Clark, 2018).

A type III subglacial traction till of clast-dominated soil behaving as a coarse-grained soil with 15-45% fine-grained particles will have a moderate-to-high density, low permeability and moderately-low porosity yielding a moderate geoelectrical resistive layer (Earle, 2015; Clark, 2018).

A type IV subglacial traction till of coarse-grained soil (0-15% fines) will have a moderate density, moderate permeability and low porosity. The geoelectrical resistivity of the layer will be somewhat influenced by the water resistivity yielding a moderately geoelectrical resistive layer when saturated by fresh groundwater (Earle, 2015; Clark, 2018).

Subglacial traction tills may have geoelectrical resistivities difficult to differentiate from the sand and gravel aquifers lying above and below.

2.4.2.3. Melt-Out Tills

Melt-out tills are formed of englacial and supraglacial drift deposits resulting from stagnant or slow-moving ice (Benn & Evans, 2010; Clark, 2018). “The clast content reflects high-level transport in which particles retain their angularity,” is “generally poorly consolidated

because it has not been subjected to high pressures or shear,” and has a “relatively low density compared to other tills” (p.264) (Clark, 2018). These deposits can be type I-IV composite soils.

A type I melt-out till of fine-grained fully homogenized soil matrix with 70-100% fines will have a low-to-moderate density, moderately-low permeability and moderately-low porosity. The geoelectrical resistivity of the layer will be somewhat influenced by the water resistivity yielding a moderately geoelectrical resistive layer when saturated with fresh groundwater (Earle, 2015; Clark, 2018).

A type II melt-out till of matrix-dominated soil behaving as a 45-70% fine-grained soil with some coarse-grained particles will have a low-to-moderate density, low-to-moderate permeability and moderately-low porosity. The geoelectrical resistivity of the layer will be somewhat influenced by the water resistivity yielding a moderately geoelectrical resistive layer when saturated by fresh groundwater (Earle, 2015; Clark, 2018).

A type III melt-out till of clast-dominated soil behaving as a coarse-grained soil with 15-45% fine-grained particles will have a low-to-moderate density, low-to-moderate permeability and moderately-low porosity. The geoelectrical resistivity of the layer will be somewhat influenced by the water resistivity yielding a moderately geoelectrical resistive layer when saturated by fresh groundwater (Earle, 2015; Clark, 2018).

A type IV melt-out till of coarse-grained soil (0-15% fines) will have a moderately-low density, moderately-high permeability and low porosity. The geoelectrical resistivity of the layer will be heavily influenced by the water resistivity yielding a high-to-moderately geoelectrical resistive layer when saturated by fresh groundwater (Earle, 2015; Clark, 2018).

Melt-out tills may have geoelectrical resistivities difficult to differentiate from the sand and gravel aquifers lying above and below.

2.4.3. Geoelectric Resistivity of Glaciolacustrine Deposits

In locations where the PCL is predominately composed of glaciolacustrine deposits containing both organic silts and clay minerals, the geoelectrical resistivity will be heavily influenced by the material porosity and permeability. High clay content will yield a high porosity, low permeability and geoelectrical low-resistivity layer. High silt content will be heavily influenced by the water resistivity yielding a moderate-to-low geoelectrical resistivity layer when saturated by fresh groundwater.

Glaciolacustrine deposits containing primarily clay will have low geoelectrical resistivities easy to differentiate from the sand and gravel aquifers lying above and below. Glaciolacustrine deposits containing primarily silt may have geoelectrical resistivities difficult to differentiate from the sand and gravel aquifers lying above and below.

3. Methodology

3.1. Transient Electromagnetics

Electromagnetic property geophysics can be used to define the continuity and over-arching geometry of the PCL between semi-consolidated sediment aquifers. Transient Electromagnetics (TEM) is an active-source geophysical method using an electromagnetic field induced by transient pulses of electric current to determine changes in the geoelectrical resistivity in the near subsurface. Electrical resistivity (in Ohm-meters) and its reciprocal electrical conductivity (in Siemens-per-meter) are a measurement of the ease of which electrical current can flow through a substance.

3.1.1. Survey Design of Central Loop Soundings

A loop of wire is laid out on the surface of the earth with a receiver located at the center (Figure 8). A transmitter connected to the loop sends pulses of a square wave form of electric current through the wire. During the transmitter shut-off part of the electrical current pulse cycle, a perpendicular magnetic field is induced which travels out similar to smoke rings, both growing and diffusing with time. When this magnetic field interacts with a conductive material in the subsurface electrical eddy currents are induced within the conductor. These eddy currents generate a secondary magnetic field. This magnetic field moves out through the subsurface from the conductive body and is recorded by the receiver when the decaying magnetic field induces a voltage response within the receiver. The recording of the magnetic field can then be mathematically converted using Maxwell's Equations (Equation 1) to derive the electrical resistivity of the subsurface strata that interacted with the magnetic field (Griffiths, 2019).

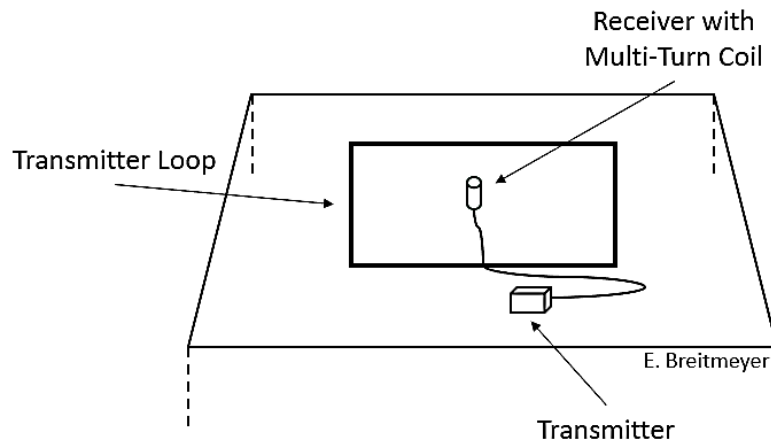


Figure 8. Transient Electromagnetic Loop Sounding survey design.

Maxwell's Equations are:

$$\nabla \cdot \mathbf{E} = \frac{\rho}{\epsilon_0} \quad \text{Gauss' Law}$$

$$\nabla \cdot \mathbf{B} = 0 \quad \text{Gauss' Law for Magnetism}$$

$$\nabla \times \mathbf{E} = -\frac{\partial \mathbf{B}}{\partial t} \quad \text{Faraday's Law of Induction}$$

$$\nabla \times \mathbf{B} = \mu_0 \left(\sigma \mathbf{E} + \epsilon_0 \frac{\partial \mathbf{E}}{\partial t} \right) \quad \text{Ampere's Law}$$

1

where \mathbf{E} is the electrical field intensity, \mathbf{B} is the magnetic flux density, μ_0 is the magnetic permeability of the subsurface, ϵ_0 is the electrical permittivity of the subsurface. σ is the electrical conductivity of the subsurface and the reciprocal ρ , is the electrical resistivity (Reynolds, 2011; Griffiths, 2019).

The electrical and magnetic fields are perpendicularly polarized with respect to each other (Figure 9) and propagate through air at the speed of light, C , and can be calculated in the subsurface using the equations

$$c = \frac{E}{B} \quad \text{and} \quad c = \frac{1}{\sqrt{\mu_0 \epsilon_0}}$$

2

(Reynolds, 2011; Griffiths, 2019).

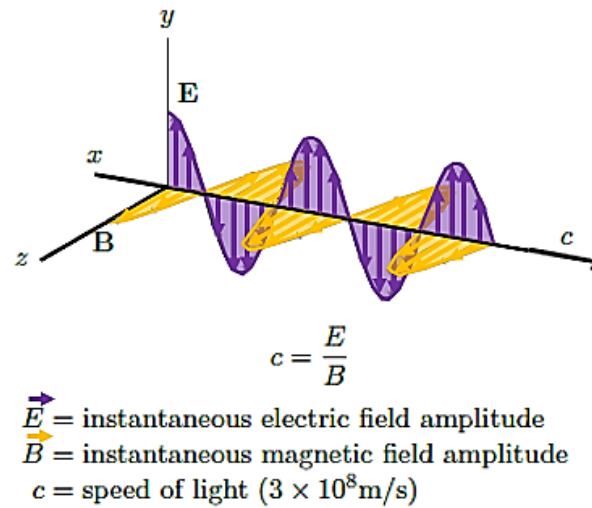


Figure 9. Electromagnetic waves comprised of an electrical and a magnetic vector field.

Only the vertical z component of the magnetic \mathbf{H} -field intensity is measured so the data are the

$$\frac{\partial H_z}{\partial t} = \dot{H}_z,$$

3

where \mathbf{H} is the magnetic flux density of the secondary magnetic field induced by the eddy currents within the conductor. Early time variations of the recorded magnetic \mathbf{H} -field intensity are associated with the geoelectrical resistivity at shallow depths. Later time magnetic \mathbf{H} -field intensity variations are subject to the geoelectrical resistivity with increasing depth where the increase in decay coupled with the decrease in resolution results in a loss of usable signal.

3.1.2. Equipment

The wire loop was laid out using a field tape and Brunton compass to locate each of the loop's corners manually followed by precision locating of each corner with an EMLID Differential GPS. The differential GPS was then used to precisely locate the center for placement of the receiver coil. The transmitter and recording equipment were sited outside of the wire loop under a shade structure to reduce the heat of the electronics (Figure 10). A Zonge ZeroTEM ZT-30 transmitter, Zonge GDP-32^{II} digitizer and Zonge ANT/2 TEM receiver antenna with an effective coverage of 10,000 square meters were used. The transmitter was powered by a high output 24-volt LiFePO₄ battery developed at Montana Tech with the optional use of a Zonge ZPB-600 DC-DC converter capable of stepping up transmitter input to 600-volt. Higher voltage enables larger transmission currents which create stronger magnetic fields and increase the depth of investigation.



Figure 10. Field equipment set up of the transmitter and recording instrumentation under a shade structure.

A variety of transmitter loop configurations were tested including square loops with 100-meter sides, circular loops with a 55-meter radius, and a square 93-meter sided loop. Circular loops deployed the most efficiently and were used when the ground was clear of obstacles. In all cases the receiver was located in the center of the transmitter loop to recover the 1D geoelectrical resistivity structure.

The TEM transmitter and GDP digitizer that were used in the survey do not record the transmitter waveform. This information is necessary for data inversion as small changes can have a large effect on the data and can mask the geoelectrical resistivity response (Figure 11). In an

attempt to work around this limitation, the waveforms were recorded using an external Siglent field oscilloscope connected to a shunt resistor across the transmitter circuit (Figure 9). This allowed for the collection of full digitized waveforms for each sounding.

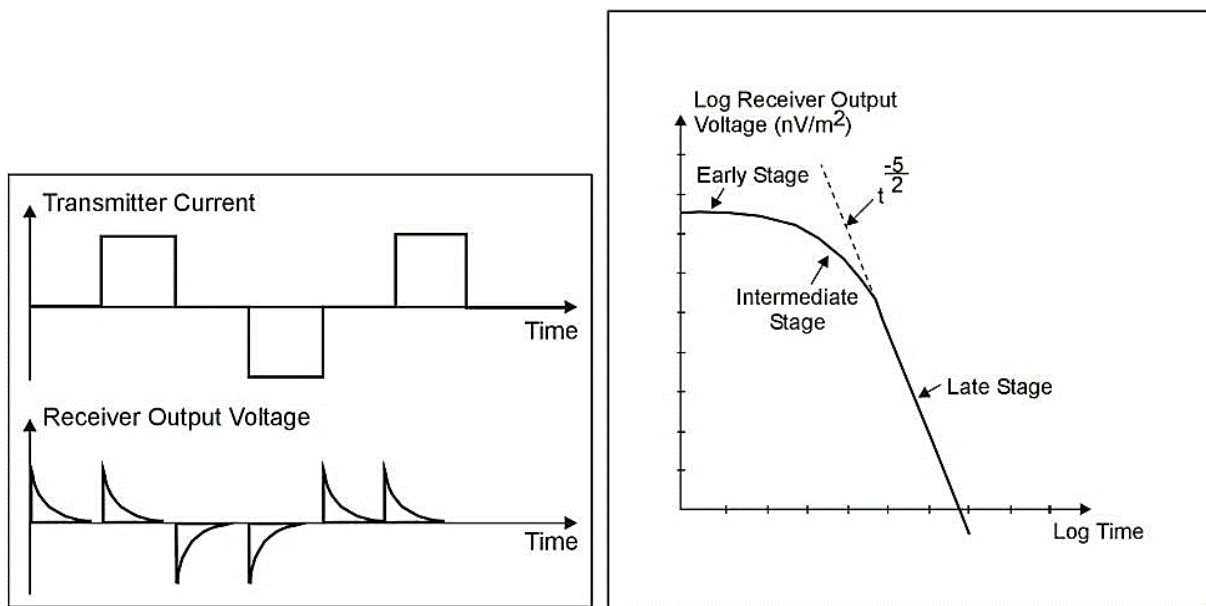


Figure 11. TEM transmitter and receiver graph of transmitter current over time and receiver output voltage over time; and TEM receiver output response curve over time from (Environmental Protection Agency, n.d.).

There is no absolute mechanism to tie the external oscilloscope waveform time to the digitized GDP recording time. The Zonge GDP-32^{II} digitizer manual states data times are referenced from the ‘start’ of the ramp-off, but neglect to provide a definitive method to tie the independent waveform times recorded by the Siglent oscilloscope to the GDP recordings (Zonge International, 2002). To account for the unknown ramp-off time, the GDP digitizer time gates are adjusted as an independent variable to reduce the RMS error in the final inversion.

The TEM transmitter is capable of transmitting up to 30-amp pulses. This rating is measured differentially between oppositely polarized transmitter pulses which equates to 15-amp maximum pulse amplitude. Above this amplitude limit the transmitter fails requiring restart of

data acquisition. Since depth of investigation is directly proportional to transmitter turn off step, large pulse amplitudes are desirable. Ohm's Law

$$I = \frac{V}{R}$$

4

dictates that the current (I) through a transmitter wire is proportional to the voltage (V) driving the current (I) divided by the total resistance (R) of the wire (Reynolds, 2011; Griffiths, 2019). To achieve as large a transmitter pulses as possible the ZPB-600 DC-DC converter was used to step up the voltage load from our 24-volt high output LiFePO₄ battery to a voltage that drove an approximately 30-amp differential current. Example waveforms using the ZPB-600 from Site 1 are shown in Figure 12. The differential pulse current was approximately 30-amps (15-amps positive and negative) using the ZPB-600 yielding approximately 100-volt output. Most of this current was associated with switching transients which took time to stabilize. In Figure 12, it is evident frequencies higher than 4-hertz did not stabilize before the onset of the switch off ramp resulting in poor transmitter waveforms for higher frequencies. The poor transmitter waveforms at higher frequencies necessitated the predominate collection of 1-hertz data at sites using the DC-DC converter, which is slow to acquire and does not provide a strong magnetic-field, resulting in shallower returned subsurface data. Additionally, the effective pulse amplitude was closer to 5.8-amps, well below the 15-amp theoretical limit.

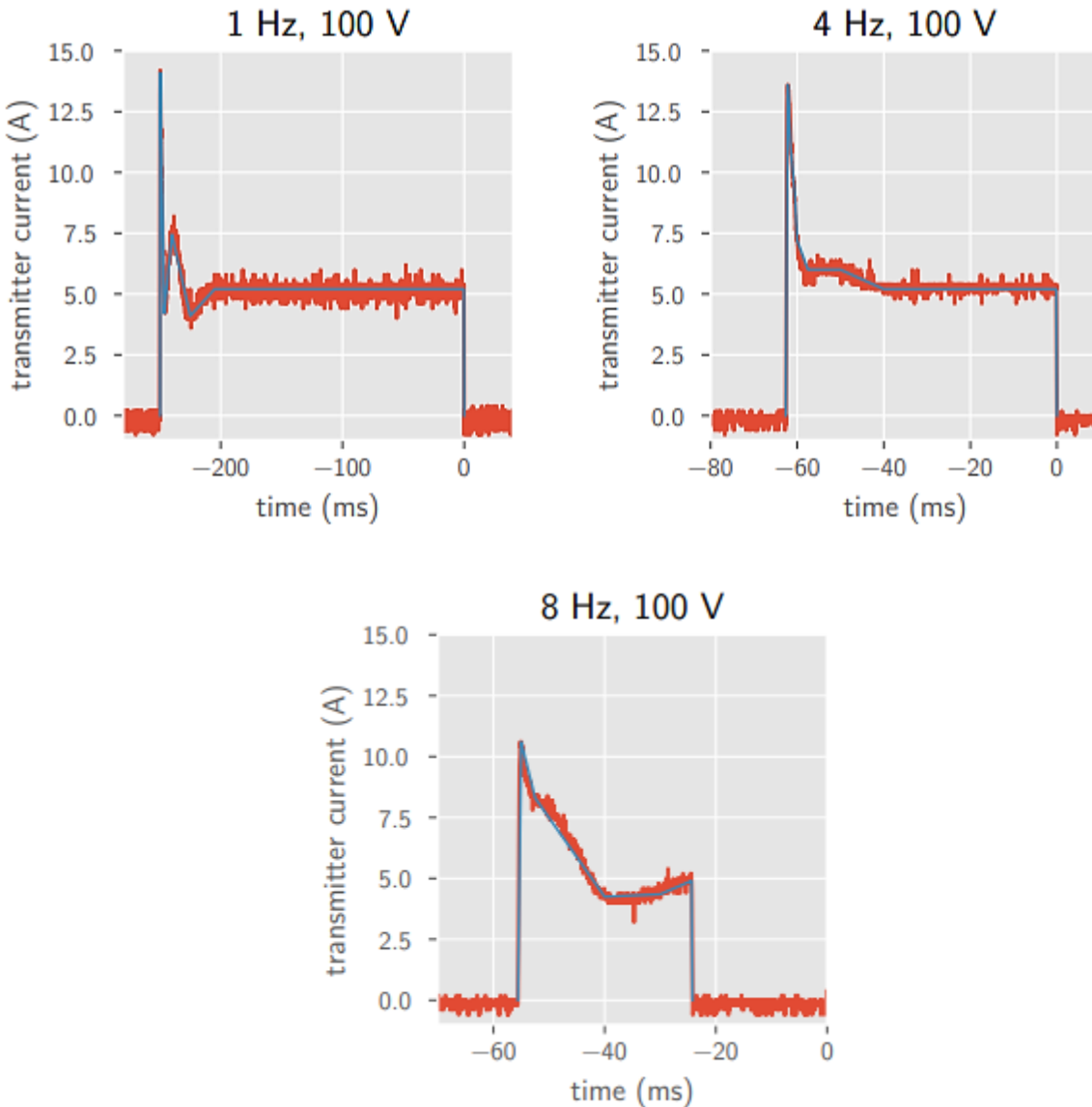


Figure 12. Transmitter waveforms collected at Site 1 using the ZPB-600 which raised the transmitter load voltage from 24-volts to around 100-volts. The current differential is nearly 30-amps with most of this in the form of the large surges associated with switching the transmitter on. The current stabilized to an effective 5 to 5.8-amp pulse. Frequencies greater than 4-hertz (8 Hz, 100 V graph) did not stabilize before the ramp off resulting in poor waveform using the DC-DC converter. The blue-gray lines represent the simplified waveforms used in inverse modeling and red are the recorded variations of the amplitude on the Siglent oscilloscope.

The high output LiFePO₄ battery was connected directly to the TEM transmitter, bypassing the DC-DC converter to overcome the poor waveforms of the higher frequencies observed at Site 1. This resulted in much cleaner waveforms, improving the quality of the data

(Figure 13). The TEM transmitter had much lower switching transients in this case and the pulse amplitude was approximately 4.2-amps, not far below the 5.8-amps realized with the DC-DC converter. Higher frequencies remained stable when the DC-DC converter was bypassed and allowed the collection of higher frequency data capable of visualizing the shallower changes in the subsurface. For these reasons the Flathead EM survey did not use the ZPB-600 after the second TEM survey collected.

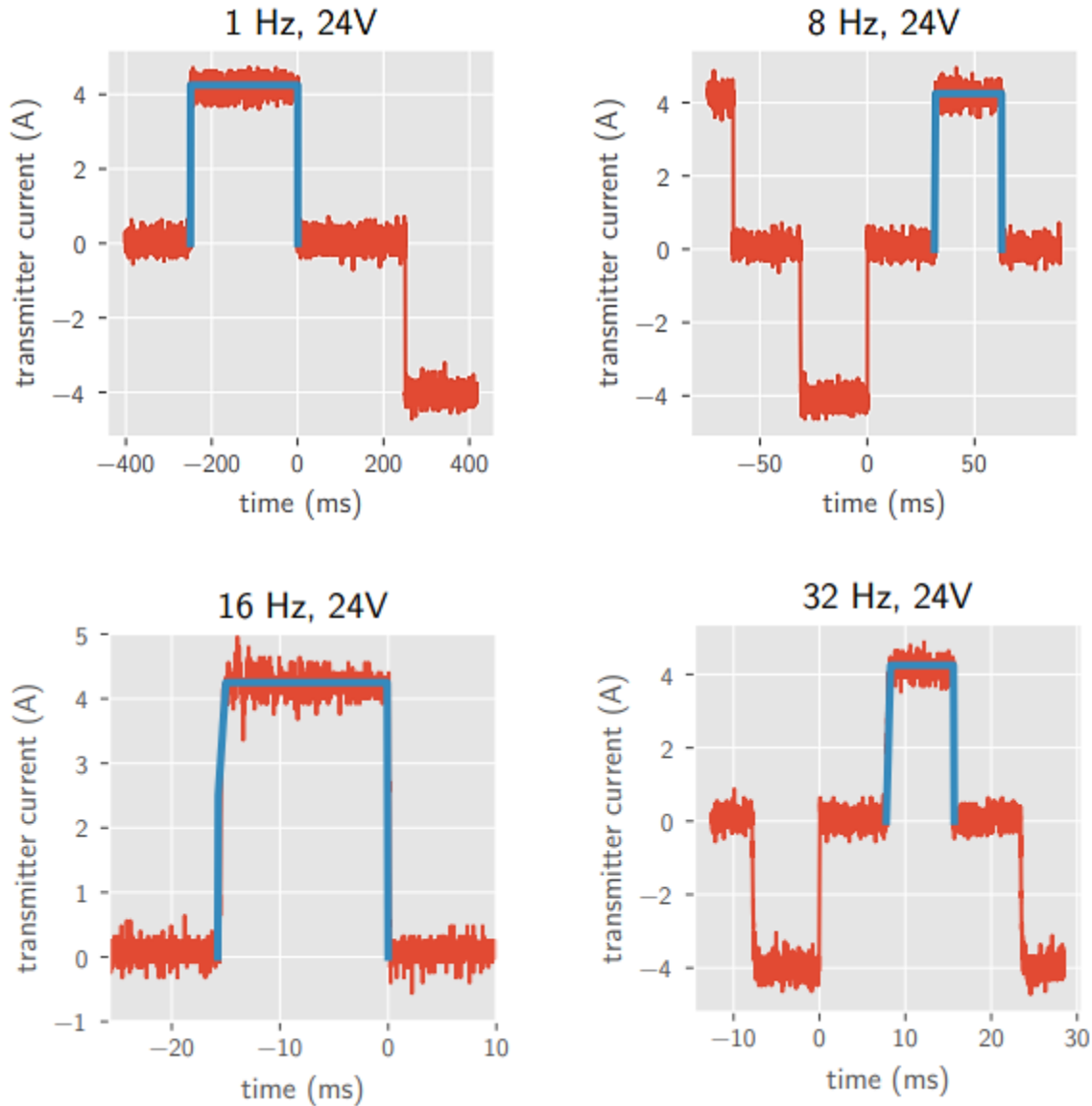


Figure 13. Digitized waveforms from ZT-30 shunt resistor when driven by 24-volt LiFePO₄ battery. The blue lines represent the simplified waveforms used in inverse modeling and red are the recorded variations of the amplitude on the Siglent oscilloscope.

3.2. Data Noise

The signal-to-noise ratio of the data was kept as low as possible during survey collection by avoiding and attempting to mitigate as many noise sources as possible. Noise sources in TEM data can result from Johnson noise due to hot instrumentation, long run times, and conductive infrastructures or infrastructures generating electromagnetic radio frequency radiation.

Temperatures ran into the mid-to-high 90s (degrees Celsius) during collection of field data in late July through early August 2020. Hot instrumentation and wiring resulting from long run times and external conditions increase the noise in the data. A shade structure was used for the transmitter and recording instrumentation while collecting data to reduce the external temperature.

Cultural noise is created by infrastructure that generates electromagnetic waves such as overhead power lines, powered irrigation systems and buried power conduits. When in range of the receiver the electromagnetic waves overlapping with our transmitted ones mask the signal of interest.

Other cultural noise sources in the data can be created by conductive objects such as fences, signs, culverts, buried pipelines, and cattleguards on or near the surface. These can mask the near-subsurface geoelectrical resistivity readings by returning a stronger magnetic field than our subsurface strata target. All survey locations were chosen as the optimal area of the properties surveyed to have the cleanest data.

At Site 1 while testing the parameters and configurations, 4-hertz soundings appeared to be highly sensitive to noise, so this frequency was not collected at the other sites. 8-hertz data were collected at all sites and provides fair a representation of the TEM data for all of the sites and was the frequency providing the best combination of returned depth and quality.

4. Inversion Models

Deterministic inversion modelling of the geoelectrical resistivity data creates a visual representation of the finite geometric solution of the combined variations in the recorded geoelectrical resistivity with depth. Comparison of the recovered geoelectric model with the

hydrostratigraphic model and local lithology reports are used to identify where the changes in geoelectric profile of the hydrostratigraphy are occurring.

4.1. Beowulf Algorithm

The layered earth inversion algorithm *Beowulf* developed in Australia by the Commonwealth Scientific and Industrial Research Organization was used to model the data (Wilson, Raiche, & Sugeng, 2007). *Beowulf* is characterized as a deterministic inversion, meaning a single solution is obtained for each dataset and then the programming searches for an ideal solution where the simulated data matches the observed data to a certain degree (Wilson, Raiche, & Sugeng, 2007). Cultural noise due to the infrastructures are difficult to keep away from and imperfections in instrumentation and acquisition make it impossible to have complete accuracy, therefore the program employs a least squares measure of data misfits to provide the best accuracy it can. The best reported RMS values were used to determine how many layers best represented each sounding site.

4.2. Python Processing

A processing workflow was developed for the Flathead TEM data by Dr. Trevor Irons. Python scripts (Tables 2 and 3, Appendix C) were developed to parse the GDP digitizer output data into directories of soundings based on site name, line number, and transmitter frequency. An example sounding file is shown in Table 1 of Appendix B. The sounding file contains the recorded $\partial\mathbf{H}_z/\partial t$ magnetic field data at each of the 31-time gates recorded. Each sounding file contains an internal stack of repeated cycles. In Table 1, Appendix B, the sounding was produced from 128 averaged cycles of 4-hertz data.

The sounding files (Table 1, Appendix B) do not contain any information about the noise level of the recorded data. Noise level is a critical input for the inversion and model appraisal. To address this limitation multiple sounding files of the same frequency were generated and averaged. The standard deviation of the average at each time gate of a frequency provides a reasonable measure of data uncertainty at each time gate. This approach allows for the removal of statistically significant outliers as well as the determination of a signal-to-noise threshold below which the record does not contain statistically significant information (Figure 14). The late-time data below this threshold are masked to improve the accuracy.

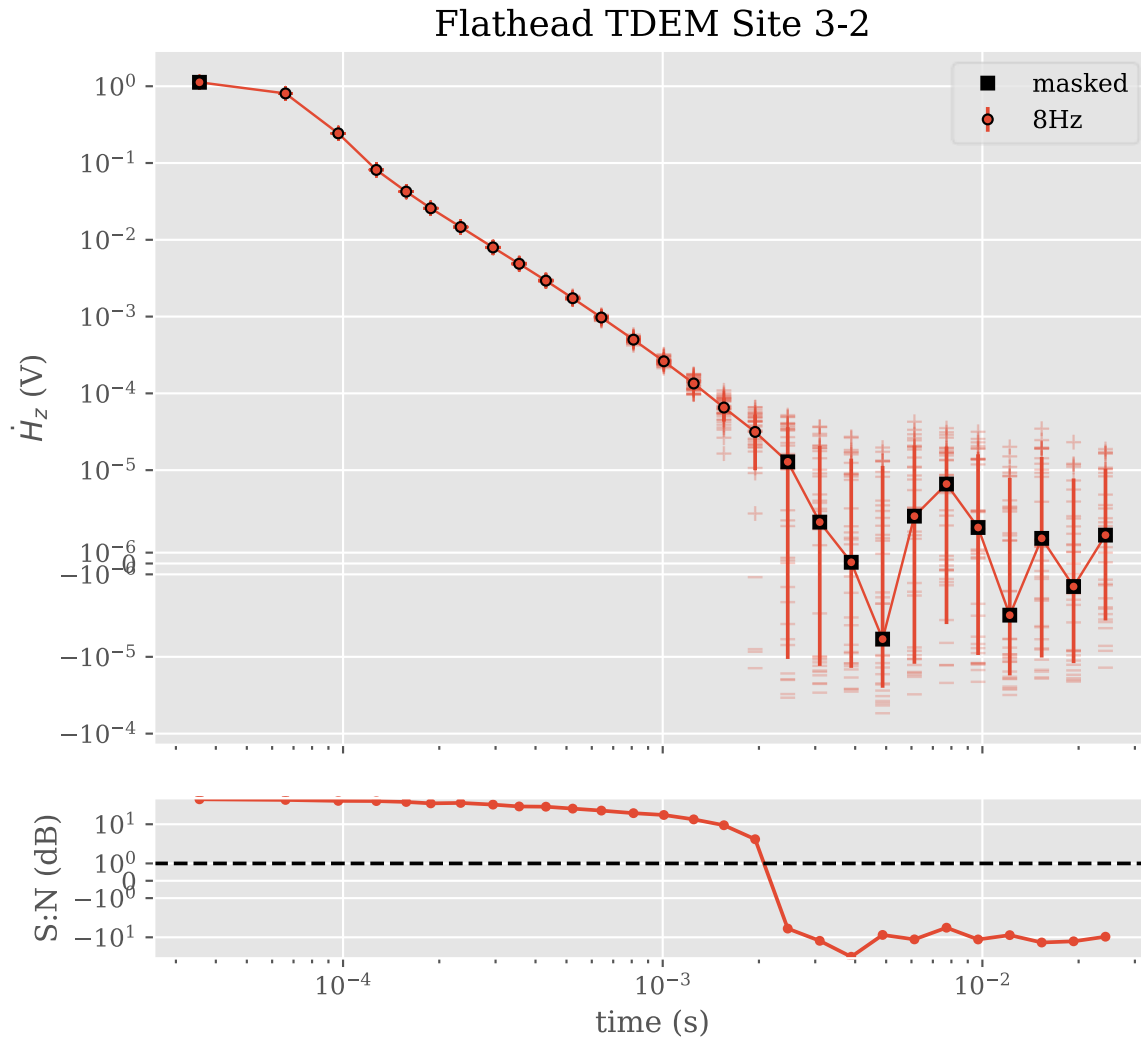


Figure 14. 8-hertz soundings data stack from Site 3-2. Masked time gates include the first time gate to account for uncertainty in the starting time and late-time gates beneath the signal-to-noise threshold (dashed line in S:N graph at bottom). All time gates utilize the standard deviation of their average data value in the stack.

The first time-gate data containing recording time uncertainty due to the lack of recorded waveform by the instrumentation was also masked through the input of the transmitter time delay as an independent variable to reduce the RMS value during inversion. This allowed the *Beowulf* inversion algorithm to more effectively differentiate between the layers by masking the less certain data (Wilson, Raiche, & Sugeng, 2007).

4.3. Depth of Investigation

The Depth of Investigation (DOI) using Spies (1989) equations to locate the threshold depth where we can have a high confidence in the accuracy of our inversion model.

The depth of investigation (DOI) is an important consideration for interpreting geophysical inversions and data. The depth we are able to model to is reliant on numerous factors such as at what depth the subsurface geoelectrical resistivity fails to impact the recorded data. The depth of resolution is another factor to be accounted for. Estimates of the DOI based on the sensitivity of the model are best used to describe the maximum depth of investigation.

While this approach affords a more straightforward answer, the depth of investigation is dependent upon the geoelectrical resistivity of the earth, meaning the DOI estimate is dependent on the recovered model in an after-knowledge sense. This is problematic as the DOI estimate cannot be incorporated in the solution of the inverse problem since it is a dependency of the inversion. DOI approximations have been made numerous times in the literature and are commonly employed. The depth of investigation used in this work is estimated as

$$DOI = 0.55 \left(\frac{IA\rho_a}{\beta} \right)^{0.2}$$

5

(Spies, 1989).

In this equation I is the transmitter current before ramp off, A is the area of the transmitter, ρ_a is the apparent resistivity of the earth (recovered through inversion), and β is an estimate of the signal-to-noise threshold (Figure 14). The maximum depth of investigation is of interest, therefore the standard deviation of the last non-masked datapoint is used as an estimate of β . For the sites using the DC-DC converter, multiple soundings were not taken of all frequencies, for these soundings β was assigned the value of 1×10^{-5} to represent a near zero

estimate of the signal-to-noise threshold in the calculations. Inversion results in this report denote the depth of investigation as a dashed line labeled *DOI (Spies, 1989)*.

The resolution consideration approaches the depth of investigation by studying how deeply a deviation in the earth's geoelectrical resistivity from a model assumed to be correct will be recovered in an inversion. This is also a function of the realized noise, survey geometry, instrumentation, and the geoelectrical resistivity model of the solution. This report does not include any resolution analysis of the results, but could make a good future work utilizing the dataset.

TEM inversion is a non-unique problem with an infinite number of potential solutions which will fit a particular dataset. The inversion algorithm employed in this report is a deterministic one which begins searching for the solution that best matches the collected data at a set starting point (Table 4, Appendix C). The best match is reported as the 1D recovered geoelectric resistivity model. However, such an approach does not explore the myriad other models which could fit the data. Bayesian inversions for example do not provide a single model which fit the data, but rather a large ensemble of models which fit the data. The computational cost of such an inversion is much higher, additionally determining which models to use from such an inversion is a complicated question as well. This approach could also make a good future work utilizing the data set and methodology such as that laid out in the paper by Enemark et al (2020) (Enemark, Peeters, Mallants, Flinchum, & Batelaan, 2020). This report does not include any exploration of the non-uniqueness of the solution and such analysis will be an important further consideration.

5. Results

5.1. Site 1

Site 1, Figures 2 and 15, is located at Kokanee Bend on the Flathead River in the northern end of the Flathead Valley near Columbia Falls, Montana. Cultural noise sources included overhead power to the south of the sounding location, an unknown well to the northeast, barbwire fences separating some of the field margins, potential unseen culverts and residences to the north, south and east. This sounding was performed using a 100-meter square central loop sounding with the ZPB-600 DC-DC converter. Soundings were collected in 1-hertz, 4-hertz and 8-hertz. The waveform issues related to the DC-DC converter were unknown during this survey. Only a single 8-hertz sounding was performed at this site while testing of the optimal combination of frequency, transmitter loop size and input power were being conducted. β for 8-hertz was assigned as 1×10^{-5} , as no standard deviation could be established for this data set. The graph in Figure 16 of stacked data in one, four and eight hertz show the 8-hertz data was the best average of the three data sets available at this site despite the poor waveform.

Flathead Valley, Montana

Site 1

TEM Survey Sites



Figure 15. Site 1 is located at Kokanee Bend on the Flathead River in the northern end of the Flathead Valley (Montana State Library GIS Services). See Figure 2 for overview of entire survey area.

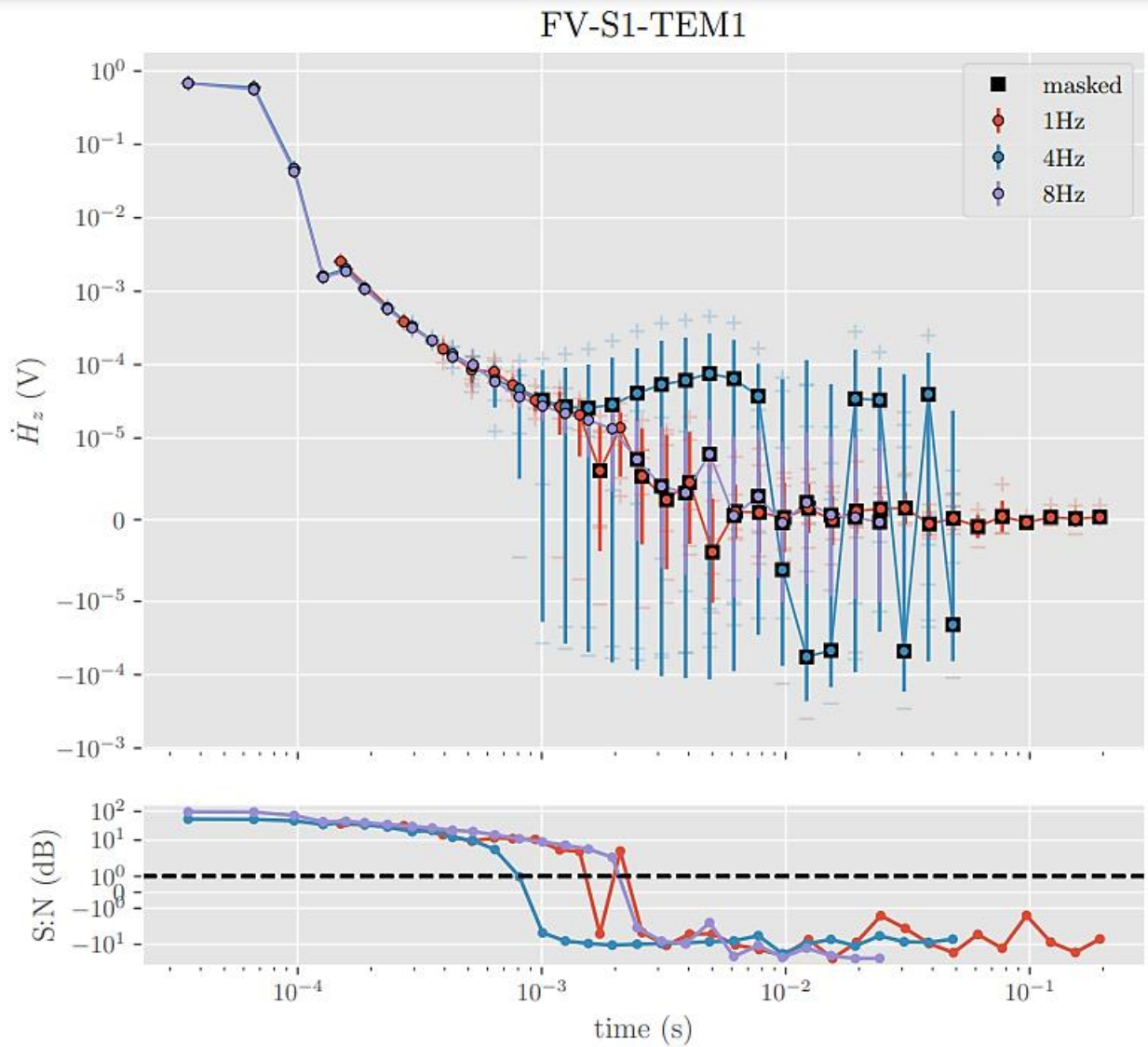


Figure 16. Stacked 1-hertz, 4-hertz and 8-hertz data for the soundings at Site 1.

The 1D 6-layer recovered geoelectric resistivity model from the 8-hertz data in Figure 17 shows shallow low resistivity geoelectric layers with progressively resistive geoelectric layers beneath and a geoelectric layer with a less certain drop in geoelectrical resistivity beneath the DOI. This puts the top of geoelectric layer-4 around 20-meters below the surface with a thickness around 200-meters and a geoelectrical resistivity of 5,172 Ohm-meters. The top of geoelectric layer-5 is around 220-meters below the surface, 140-meters thick and has a

geolectrical resistivity of 1,446 Ohm-meters. The bottom of geoelectric layer-5 lies just below the DOI making its thickness less certain.

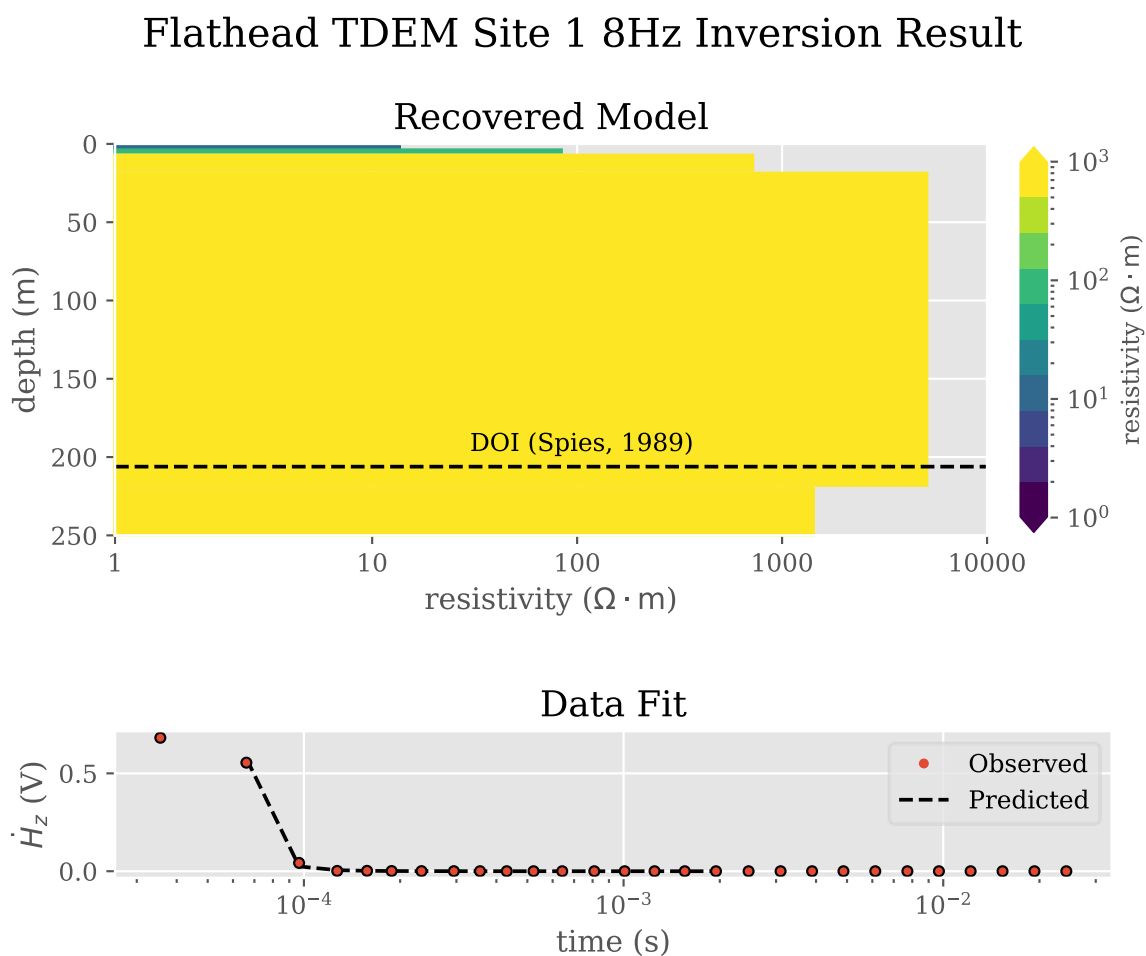


Figure 17. Recovered 1D 6-layer geoelectric resistivity model of 8-hertz data at Site 1.

5.2. Site 2

Site 2, Figures 2 and 18, is located along the eastern medial moraine on the Ottey property near the Creston Fish Hatchery in Kalispell, Montana. Site 2 had two new wells drilled by MBMG as part of their study of the East Flathead Valley in 2020 and 2021, the well locations and well completion reports are in Figure 48 and Tables 10 and 11 of Appendix E. This sounding

was performed using a 55-meter circular central loop sounding due to space limitations. The transmission was performed with only the 24-volt battery. Both the deployment speed and waveforms using the 24-volt battery were an improvement on previous soundings. The property owner reported the presence of a buried power conduit running along the road on the western edge of his property so cultural noise issues are expected. Additional cultural noise sources included an unknown well to the east of the sounding, possible unseen culverts and residences to the north and southeast of the sounding. Soundings were collected in 1-hertz and 8-hertz. The 1-hertz data contained significant noise levels.

Flathead Valley, Montana

Site 2

TEM Survey Site

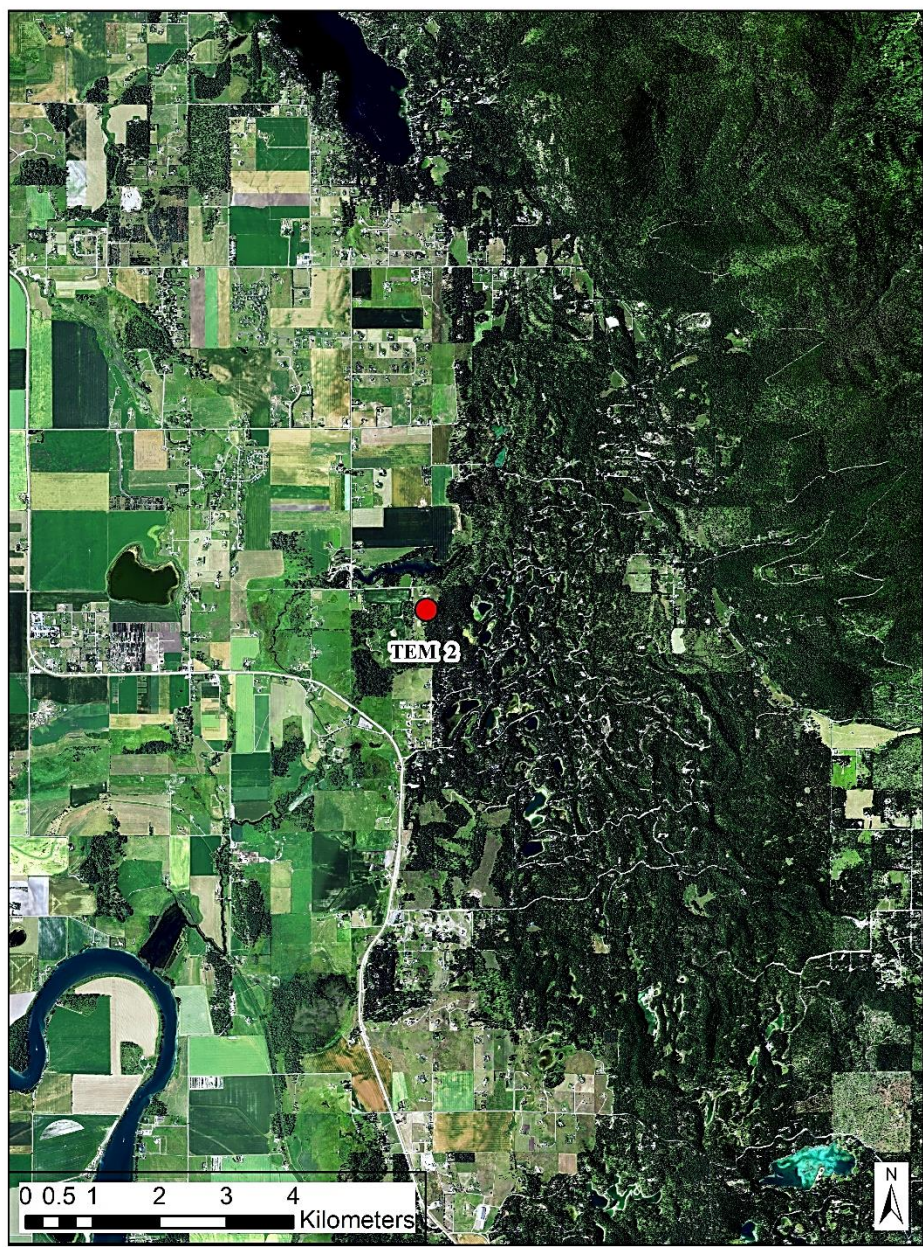


Figure 18. Site 2 is located along the eastern medial moraine of the Flathead Valley on the Ottey Property near the Creston Fish Hatchery (Montana State Library GIS Services). See Figure 2 for overview of entire survey area.

The 1D 7-layer recovered geoelectric resistivity model from the 8-hertz data in Figure 19 shows shallow low resistivity geoelectric layers with progressively resistive geoelectric layers beneath and a geoelectric layer with a drop in geoelectrical resistivity right above the DOI. This puts the top of geoelectric layer-3 at 10-meters below the surface with a thickness around 10-meters and a geoelectrical resistivity of 145 Ohm-meters. The top of geoelectric layer-4 around 20-meters below the surface with a thickness around 95-meters and a geoelectrical resistivity of 1,914 Ohm-meters. The top of geoelectric layer-5 is around 115-meters below the surface, about 65-meters thick and has a geoelectrical resistivity of 957 Ohm-meters. The top of geoelectric layer-6 lies just above the DOI at about 175-meters with a geoelectrical resistivity of 25 Ohm-meters. Due to the location of the DOI, the thickness of geoelectric layer-6 is less certain.

Flathead TDEM Site 2 8Hz Inversion Result

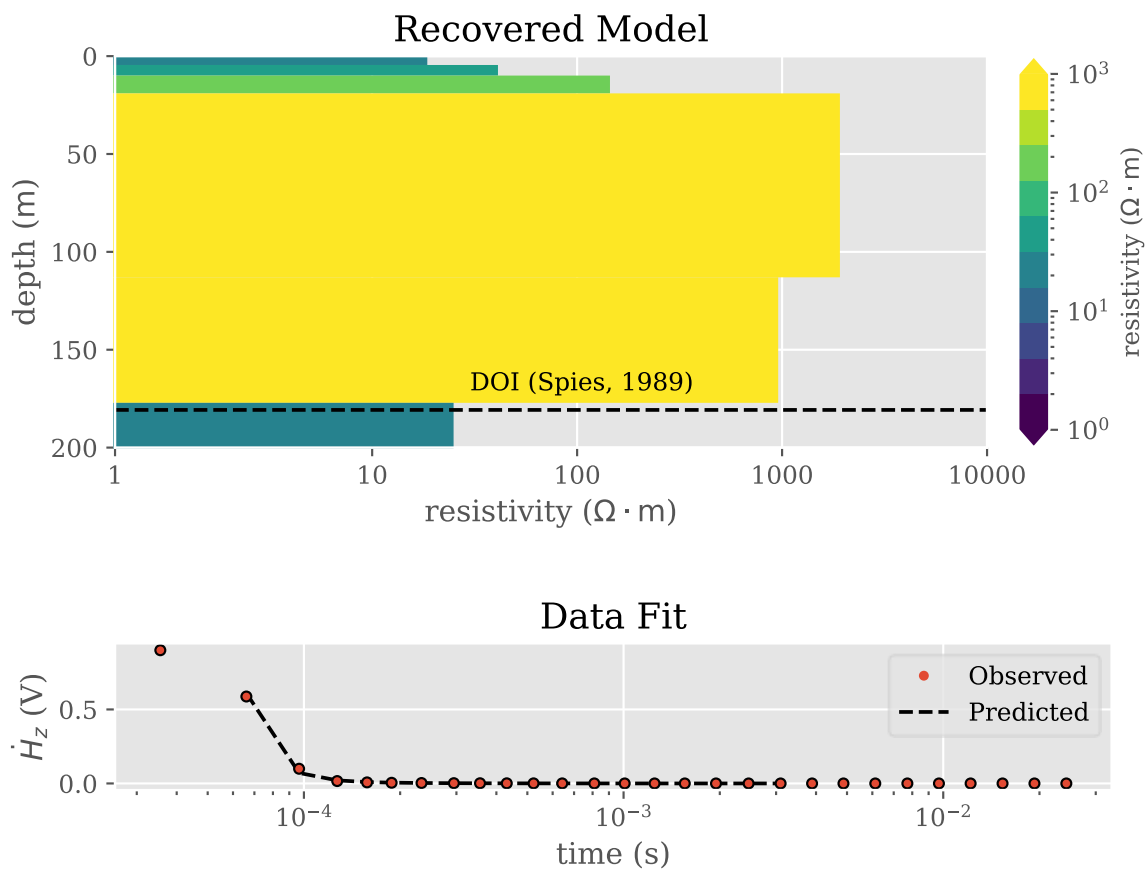


Figure 19. Recovered 1D 7-layer geoelectric resistivity model of 8-hertz data at Site 2.

5.3. Site 3

Two locations were surveyed at Site 3 due to the proximity and ability to obtain permission to collect an additional TEM sounding on the Flathead Waterfowl Production Area (managed by U.S. Fish & Wildlife Services) near the scheduled Big Fork Farm site at the Big Fork Farm Water Treatment Facility near Big Fork Farm, Montana (Figures 2 and 20). Site 3-1 is of special importance due to the MBMG project drilling a new deep well at this location in 2021 yielding a high accuracy lithologic drill core. The well logs obtained during drilling have been

included in this paper to correlate the success of the methodology and can be reviewed in Appendix D.

Flathead Valley, Montana
Site 3
TEM Survey Sites

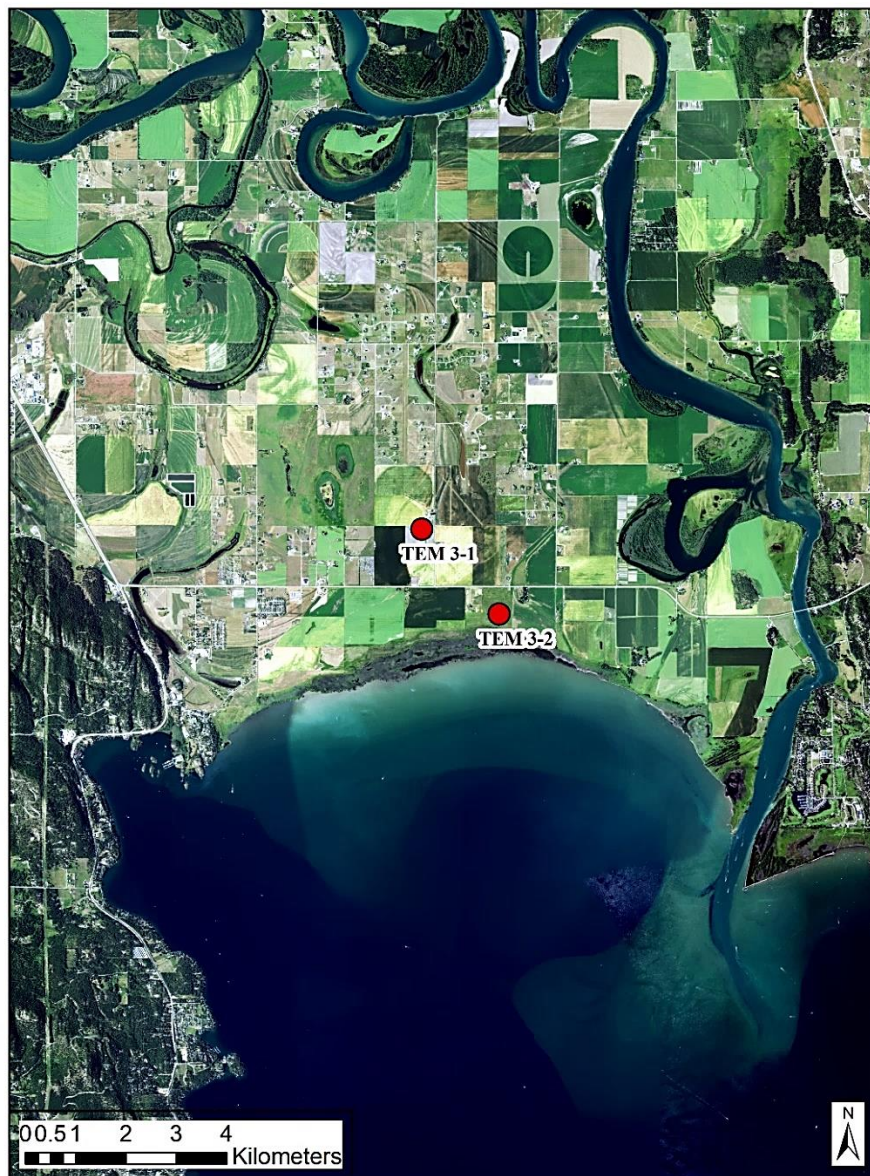


Figure 20. Site 3 consisted of two nearby locations near the center of the Flathead Valley on the northern shore of Flathead Lake, Montana. Site 3-1 is located at the Big Fork Farm Water Treatment Facility and is the location of the new deep wells drilled by MBMG in 2021. Site 3-2 is located on the nearby Flathead Waterfowl Production Area, under management of U.S. Fish & Wildlife (Montana State Library GIS Services). See Figure 2 for overview of entire survey area.

5.3.1. Site 3-1

Site 3-1 is located at the northern end of Flathead Lake at the Big Fork Farm Water Treatment Facility near Big Fork Farm, Montana. This sounding was performed using a 100-meter square central loop sounding with the ZPB-600 DC-DC converter. Many single soundings were performed with many cycles to test a variety of combinations. The waveform issues related to the DC-DC converter were unknown during this survey, as were the missing initial waveform timing data in the GDP digitizer recordings until preliminary processing had been completed. Cultural noise issues were expected as the property contains significant infrastructure from both the treatment facility to the northeast, overhead power to the north, east and south, potential unseen culverts, and potential buried power conduits related to the central-pivot irrigation network of the wheat fields adjoining the facility, including the un-planted field in which the sounding was conducted (see Figure 45, Appendix D). Soundings were collected in 1-hertz and 8-hertz. The 1-hertz data contained significant noise levels. Due to the collection of single soundings the stacking standard deviation is not known so β was assigned as 1×10^{-5} .

The 1D 6-layer recovered geoelectric resistivity model from the 8-hertz data in Figure 21 shows a range of low resistivity geoelectric layers. This puts the top of geoelectric layer-4 around 25-meters below the surface with a thickness around 40-meters and a geoelectrical resistivity of 280 Ohm-meters. The top of geoelectric layer-5 is around 65-meters below the surface, about 50-meters thick and has a geoelectrical resistivity of 44 Ohm-meters. The bottom of geoelectric layer-5 lies above the DOI. The top of geoelectric layer-6 is at 115-meters below the surface and has a geoelectrical resistivity of 226 Ohm-meters.

Flathead TDEM Site 3-1 8Hz Inversion Result

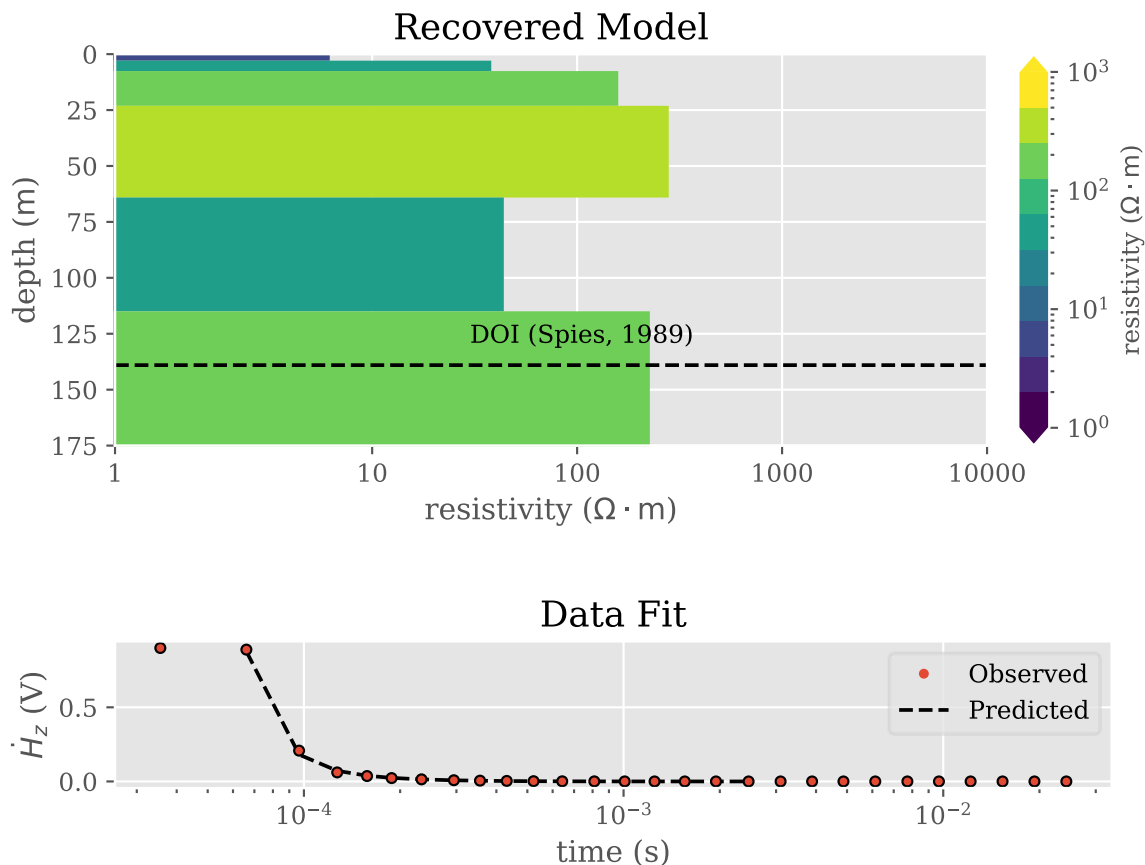


Figure 21. Recovered 1D 6-layer geoelectric resistivity model of 8-hertz data at Site 3-1.

5.3.2. Site 3-2

Site 3-2 is located on the northern shore of Flathead Lake at the Flathead Waterfowl Production Area, managed by U.S. Fish & Wildlife, near Big Fork Farm, Montana. This sounding was performed using a 100-meter square central loop sounding with the ZPB-600 DC-DC converter. Single soundings were performed with many cycles to further test a variety of combinations. The waveform issues related to the DC-DC converter had not been resolved at this time. Cultural noise issues were not expected as there was a good amount of space to the nearby residences to the north, east, and west (see Figure 49 in Appendix E). Additional cultural noise

sources include unknown wells to the east which may be related to irrigation in the fields and include buried power, barbwire fencing along the field boundaries, potential unseen culverts and overhead power on the north side of the road to the north of the sounding site. Soundings were collected in 1-hertz, 8-hertz and 16-hertz.

The 1D 6-layer recovered geoelectric resistivity model from the 8-hertz data in Figure 22 shows a range of low resistivity geoelectric layers overlying a very geoelectrical resistive geoelectric layer. This puts the top of geoelectric layer-4 around 30-meters below the surface with a thickness around 75-meters and a geoelectrical resistivity of 451 Ohm-meters. The top of geoelectric layer-5 is around 100-meters below the surface, about 30-meters thick and has a geoelectrical resistivity of 20 Ohm-meters. The DOI is well within the basement of the model beneath geoelectric layer-5.

Flathead TDEM Site 3-2 8Hz Inversion Result

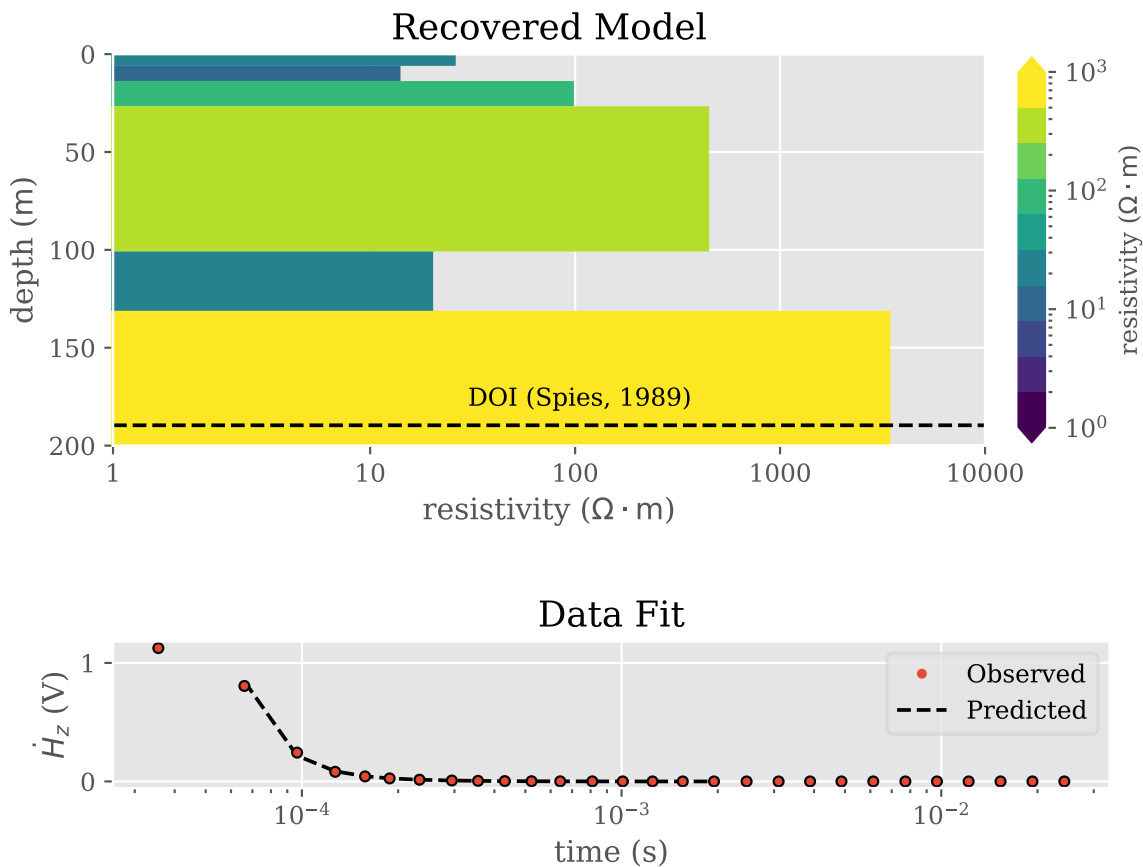


Figure 22. Recovered 1D 6-layer geoelectric resistivity model of 8-hertz data at Site 3-2.

5.4. Site 4

Due to vast area available to conduct surveys at the Crow Waterfowl Production Area, managed by U.S. Fish & Wildlife Services near Ronan, Montana, 4 locations were surveyed (Figures 2 and 23). A transect of three east-west oriented surveys (1-3) and one north of the central location. The Crow Waterfowl Production Area is located south of Flathead Lake, north of the Mission terminal moraine on the hummocky disintegrated moraines from the retreat of the Bull Lake Glacier (140,000 years ago) (Hyndman & Thomas, 2020). The area subsurface contains the uppermost alluvial layer over outwash from the Polson terminal moraine overtop the

Mission moraine. The region south of the Polson terminal moraine was also subject to repeated flooding from Glacial Missoula Lake giving the makeup of this areas substrata unique as compared to Sites 1-3 north of Flathead Lake (Hyndman & Thomas, 2020). Sounding locations 1-3 are on top of a hummocky disintegrated moraine made of melt-out till and sounding location 4 is on a ground moraine made of melt-out till.

Flathead Valley, Montana

Site 4

TEM Survey Sites



Figure 23. Site 4 consisted of four central loop soundings located on the Crow Waterfowl Production Area, under management of U.S. Fish & Wildlife Services in the center of the Flathead Valley, south of Flathead Lake (Montana State Library GIS Services). Pingos and glacial kettles riddle the surface in this region (Hyndman & Thomas, 2020). See Figure 2 for overview of entire survey area.

5.4.1. Site 4-1

Site 4-1 is located on the western end of the east-west transect of survey locations at Site 4. Site 4 soundings were performed using a 55-meter circular central loop sounding with the 24-volt battery. Multiple soundings were performed with many cycles to continue to provide a variety of combinations to obtain the best results. Cultural noise issues were not expected as there was a large amount of space to the nearby farms (see Figure 23). Cultural noise sources near sounding site 4-1 include an unknown well to the southeast, potential unseen culverts, distant cattleguards, and some barbwire fencing along the road and between adjacent properties. Soundings were collected in 1-hertz, 8-hertz, 16-hertz and 32-hertz.

The 1D 7-layer recovered geoelectric resistivity model from the 8-hertz data in Figure 24 shows shallow low resistivity geoelectric layers grading into progressively resistive geoelectric layers followed by a low resistivity geoelectric layer right below the DOI. This puts the top of geoelectric layer-4 around 10-meters below the surface with a thickness around 10-meters and a geoelectrical resistivity of 421 Ohm-meters. The top of geoelectric layer-5 is 20-meters below the surface, about 140-meters thick and has a geoelectrical resistivity of 1,589 Ohm-meters. The top of geoelectric layer-6 is around 160-meters below the surface, about 390-meters thick and has a geoelectrical resistivity of 226 Ohm-meters. The DOI is above the basement of the model at the bottom of geoelectric layer-6.

Flathead TDEM Site 4-1 8Hz Inversion Result

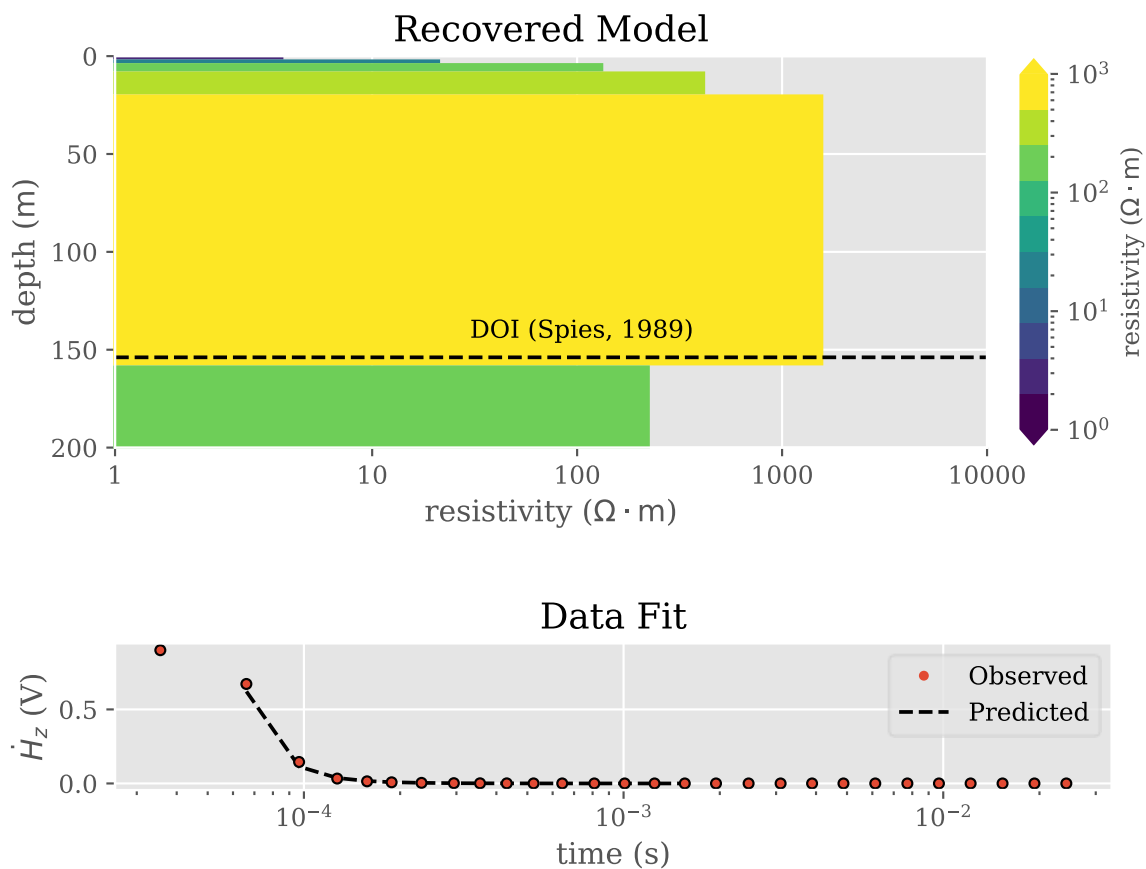


Figure 24. Recovered 1D 7-layer geoelectric resistivity model of 8-hertz data at Site 4-1.

5.4.2. Site 4-2

Site 4-2 is located at the center of the east-west transect of survey locations at Site 4. Site 4 soundings were performed using a 55-meter circular central loop sounding with the 24-volt battery. Multiple soundings were performed and cultural noise issues were not expected due to the vast size of the Crow Waterfowl Production Area (see Figure 23). Cultural noise sources near sounding site 4-2 include an unknown well to the southwest, potential unseen culverts, distant cattleguards, and some barbwire fencing along the road. Soundings were collected in 1-hertz, 8-hertz, and 16-hertz.

The 1D 6-layer recovered geoelectric resistivity model from the 8-hertz data in Figure 25 shows resistive geoelectric layers with a thin low resistivity geoelectric layer sandwiched between. The DOI does not breach end of geoelectric layer-5. This puts the top of geoelectric layer-4 around 20-meters below the surface with a thickness around 5-meters and a geoelectrical resistivity of 681 Ohm-meters. The top of geoelectric layer-5 is around 30-meters below the surface, 335-meters thick and has a geoelectrical resistivity of 5,159 Ohm-meters.

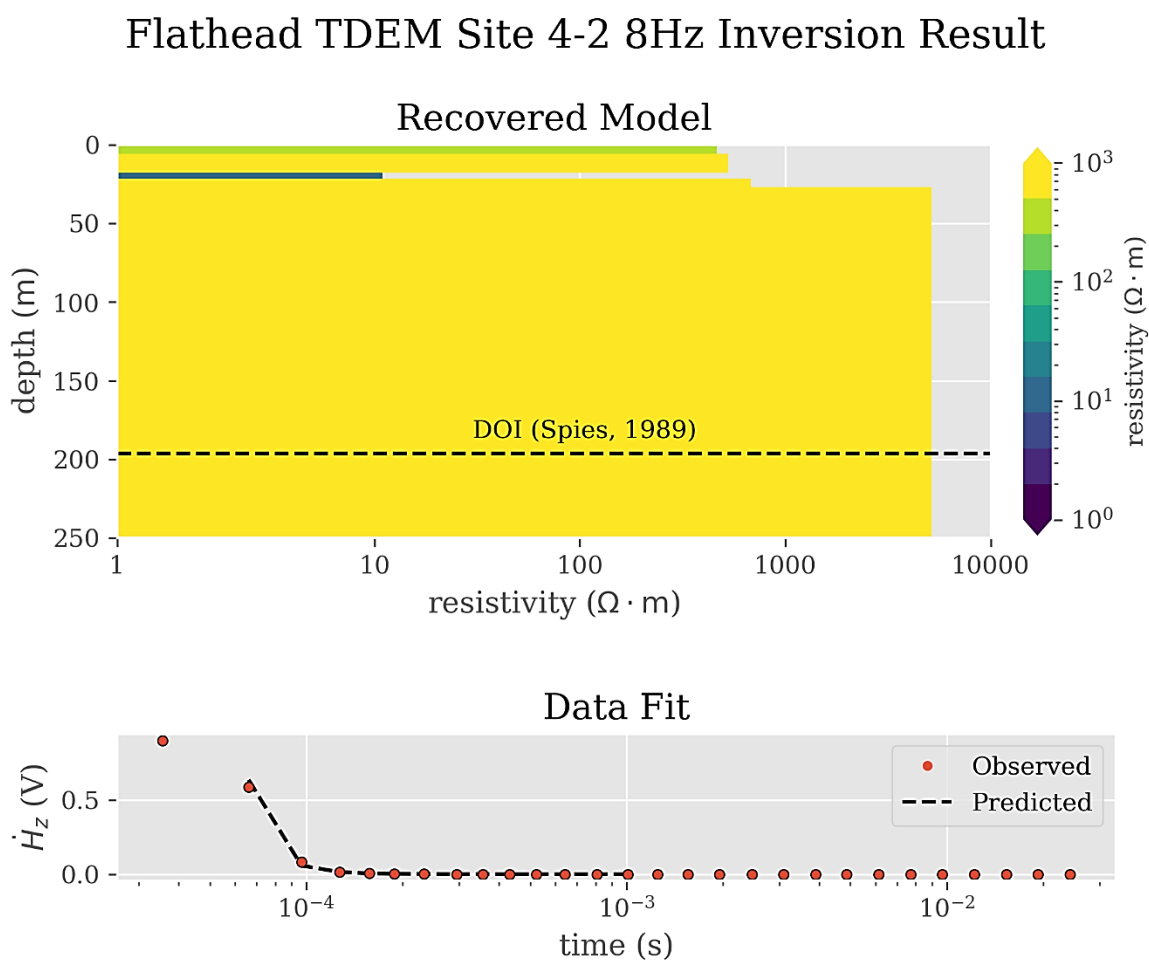


Figure 25. Recovered 1D 6-layer geoelectric resistivity model of 8-hertz data at Site 4-2.

5.4.3. Site 4-3

Site 4-3 is located on the eastern end of the east-west transect of survey locations at Site 4. Site 4 soundings were performed using a 55-meter circular central loop sounding with the 24-volt battery. Multiple soundings were performed and cultural noise issues were not expected due to the vast size of the Crow Waterfowl Production Area (see Figure 23). Cultural noise sources near sounding site 4-3 include some barbwire fencing along the road and between adjacent properties and wells to the east, potential unseen culverts and distant cattleguards. Soundings were collected in 1-hertz, 8-hertz, and 16-hertz.

The 1D 7-layer recovered geoelectric resistivity model from the 8-hertz data in Figure 26 shows a thin low resistivity geoelectric layer overlying a thick resistive geoelectric layer. The DOI does not breach end of geoelectric layer-5. This puts the top of geoelectric layer-4 around 5-meters below the surface with a thickness around 155-meters and a geoelectrical resistivity of 5,754 Ohm-meters. The top of geoelectric layer-5 is around 160-meters below the surface, about 310-meters thick and has a geoelectrical resistivity of 1,596 Ohm-meters.

Flathead TDEM Site 4-3 8Hz Inversion Result

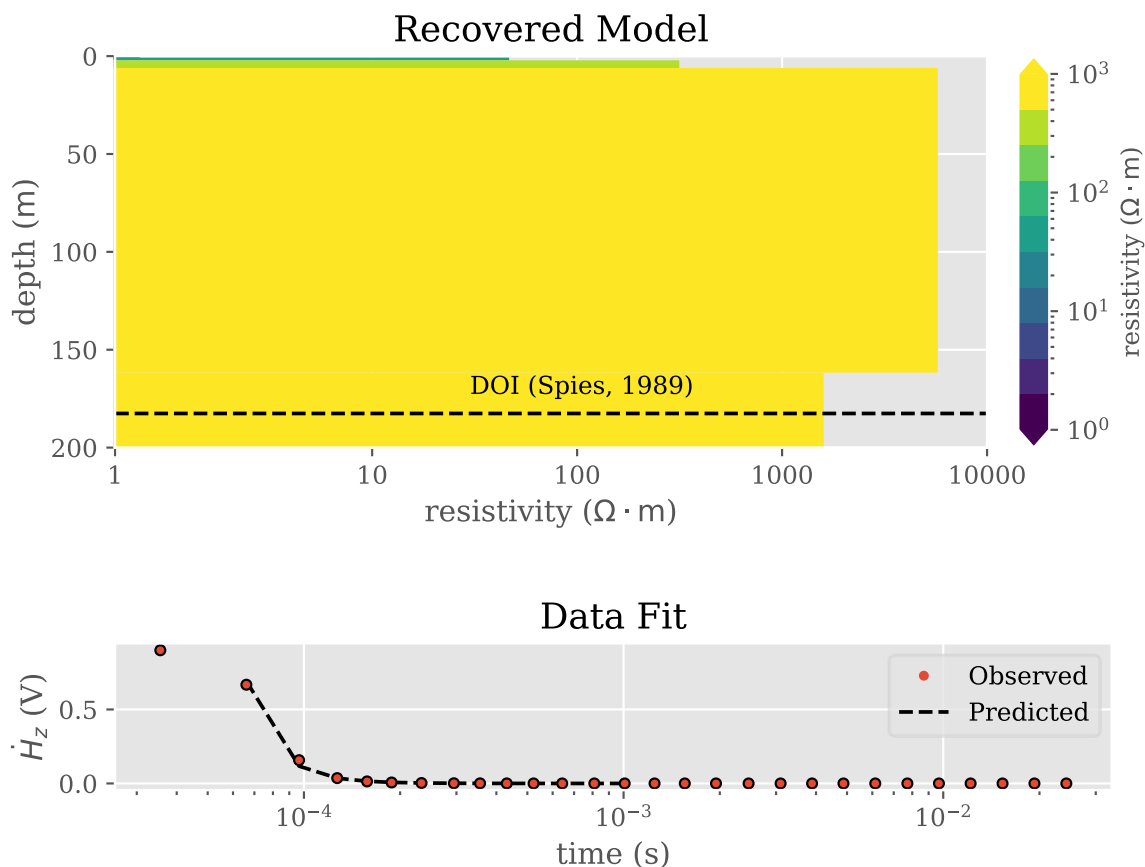


Figure 26. Recovered 1D 7-layer geoelectric resistivity model of 8-hertz data at Site 4-3.

5.4.4. Site 4-4

Site 4-4 is located north of the east-west transect of survey locations at Site 4. Site 4 soundings were performed using a 55-meter circular central loop sounding with the 24-volt battery. Multiple soundings were performed and cultural noise issues were not expected due to the vast size of the Crow Waterfowl Production Area (see Figure 23). Cultural noise sources near sounding site 4-4 include some barbwire fencing along the roads and between adjacent properties, potential unseen culverts, distant cattleguards and an unknown well to the west. Soundings were collected in 1-hertz, 8-hertz, and 16-hertz.

The 1D 7-layer recovered geoelectric resistivity model from the 8-hertz data in Figure 27 shows a thin low resistivity geoelectric layer overlying a thick resistive geoelectric layer with another low resistivity geoelectric layer beneath. The DOI does not breach end of geoelectric layer-6. This puts the top of geoelectric layer-4 around 20-meters below the surface with a thickness around 15-meters and a geoelectrical resistivity of 361 Ohm-meters. The top of geoelectric layer-5 is around 30-meters below the surface, 180-meters thick and has a geoelectrical resistivity of 3,238 Ohm-meters. The DOI is within geoelectric layer-6 with the depth to the top around 210-meters below the surface and a geoelectrical resistivity of about 153 Ohm-meters.

Flathead TDEM Site 4-4 8Hz Inversion Result

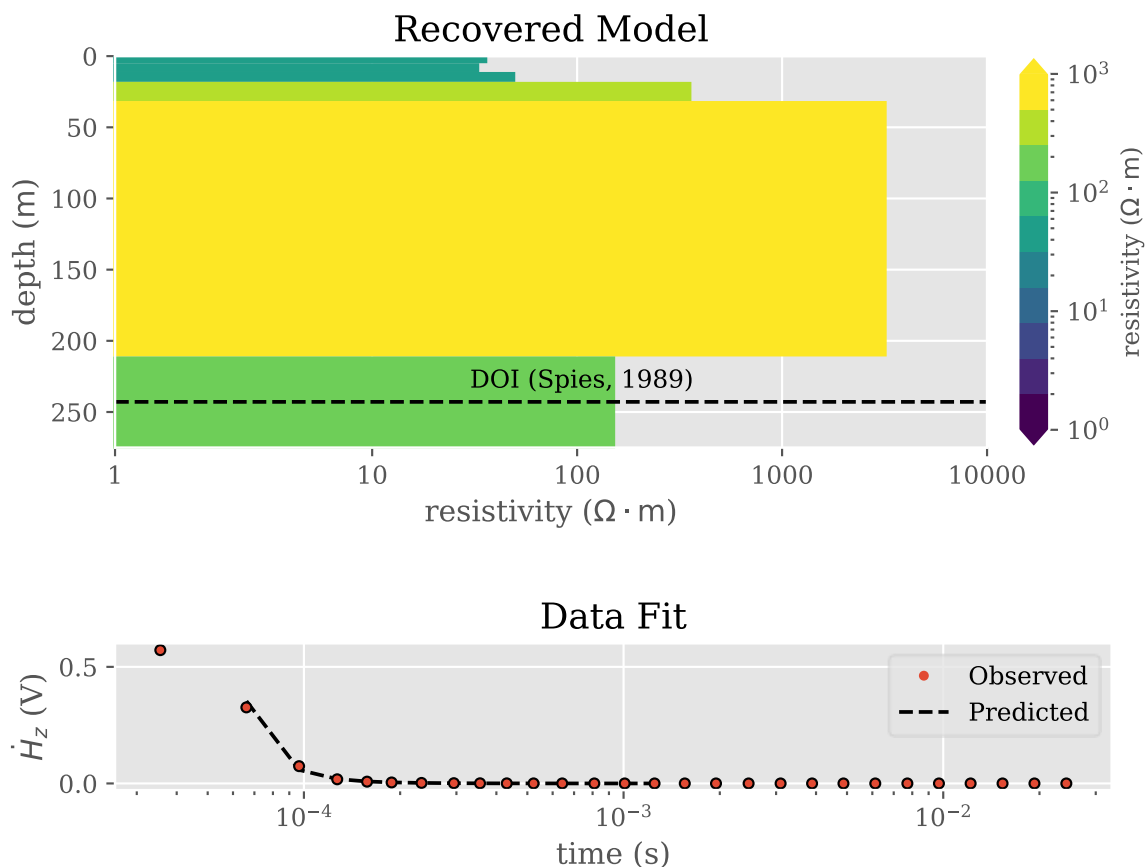


Figure 27. Recovered 1D 7-layer geoelectric resistivity model of 8-hertz data at Site 4-4.

6. Discussion

With a large range of possible geoelectrical resistivity values possible for the PCL (Figure 6) it is important to consider the location within the valley of each site and its unique glacial deposition and post-glacial composition. Next, consideration of how the probable depositional thickness of glacial sediments related to valley location and post-glacial depositional depth of overlying sediments. Lithology comparison with the nearest available well completion report with lithology provides guidance on the composite soil type trends of the upper alluvium. Finally, correlation of model statistics at near sounding locations and the

kilometers-long picture of the variability of the PCL over the series of locations rounded out the model analysis.

6.1. Site 1

Site 1 in the central-northern portion of the valley along the Flathead River near Columbia Falls, Montana could be inter-mixed glaciolacustrine and subglacial traction till deposits from periods of glacial retreat and advance causing the PCL profile to be a moderate geoelectrical resistivity to low geoelectrical resistivity. This is due to a primary component of subglacial traction till with the possibility of glaciolacustrine deposits composing the PCL in this location. Post-glacial deposition has been analyzed by LaFave, Smith and Patton to be generally more than 15-meters (p. 20) with the water level of the Shallow Aquifer in the Kalispell region, informally known as the Evergreen aquifer (Noble & Stanford, 1986) at an average depth of 8-meters (p.25) (LaFave, Smith, & Patton, 2004). Smith (2004) mapped the confining unit of the Kalispell Valley (the northern end of the Flathead Valley containing Sites 1-3) using geospatial well log data to determine the thickness; Smith found the thickness at Kokanee Bend of the Flathead River near Columbia Falls, Montana to be around 61-meters (Smith, Thickness of the Confining Unit in the Kalispell Valley, Flathead County, Montana, 2004). This value does not align with any of the modeled geoelectric resistivity layers. Geoelectric resistivity model layer-6 is well below the Depth of Investigation, making its depth and geoelectrical resistivity uncertain, yet is the most likely geoelectric model layer that could represent the PCL at this location with a geoelectrical resistivity suitable to the target layer. However, the poor waveform at this site reduces confidence in the quality of this data. Further, the proximity to the river and its erosional

forces which may have removed the glacial sediments of the PCL at this location are a likely reason for the disagreement with the mapping by Smith (2004).

Appendix E contains Figure 47 with the location of the well in relation to the TEM sounding and Table 9 of the nearest available well completion report with lithology. Figure 28 compares the results of the 1D 6-layer geoelectric resistivity model for Site 1 with the nearest available well completion report lithology.

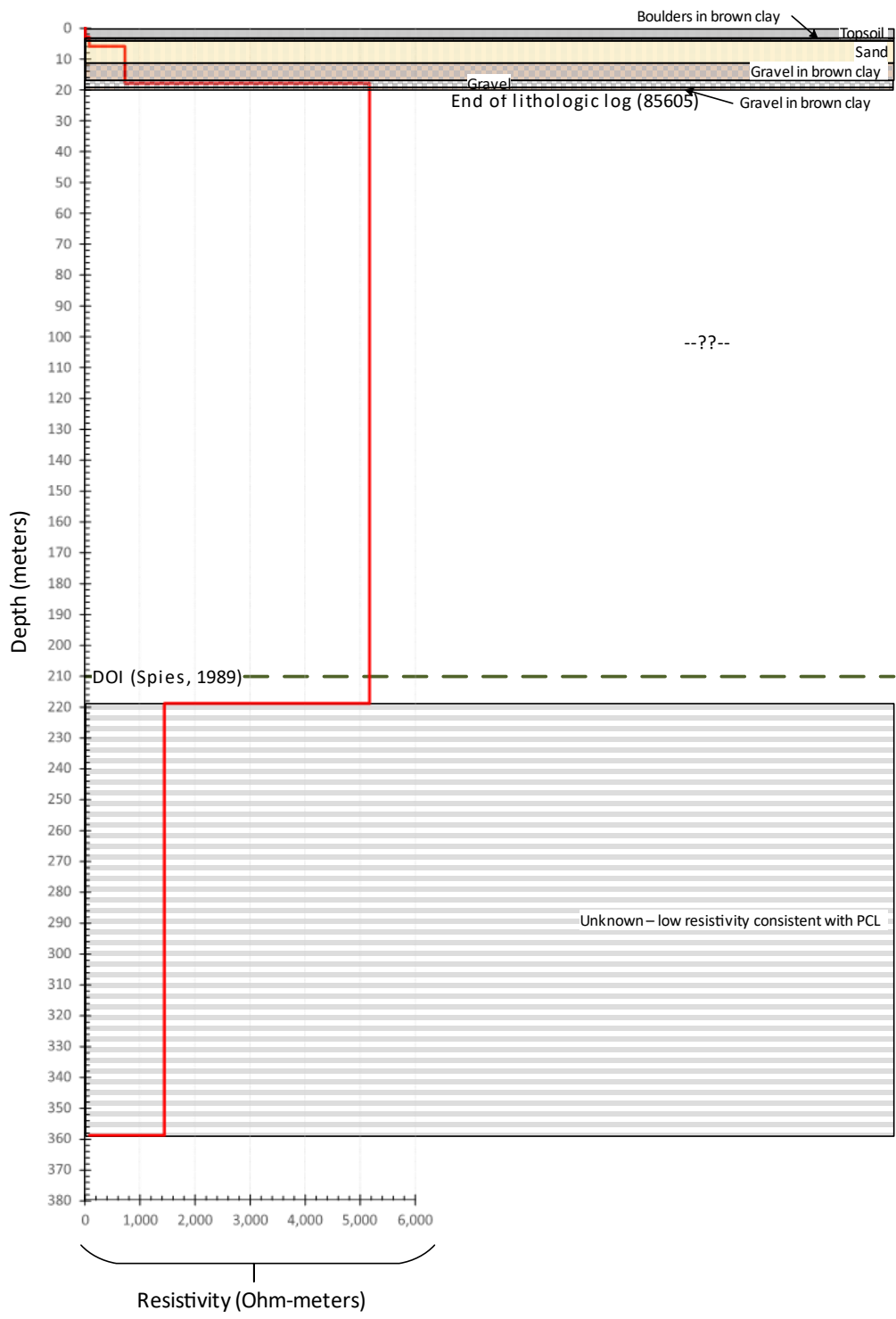


Figure 28. 6-layer depth comparison of well 85605 well completion report lithology and the Site 1 1D 6-layer geoelectric model layer depths (Ground Water Information Center; Montana Bureau of Mines and Geology; Montana Technological University, 1998-2022).

Geoelectric layer-1 of the recovered geoelectrical resistivity model in comparison with the Table 9 well completion report show agreement. Geoelectric layer-1 is a low geoelectrical resistivity (14 Ohm-meter) type I composite soil with a matrix of *topsoil* from 0-3 meters, representing the uppermost layer of alluvium (Ground Water Information Center; Montana Bureau of Mines and Geology; Montana Technological University, 1998-2022).

Geoelectric layer-2 of the recovered geoelectrical resistivity model in comparison with the Table 9 well completion report show agreement when combining the next two lithologic units. Geoelectric layer-2 is a low geoelectrical resistivity (85 Ohm-meters) type III to IV composite soil with a matrix of *boulders in brown clay* from 3-4 meters moving into the *sand* lithology from 4-11 meters (Ground Water Information Center; Montana Bureau of Mines and Geology; Montana Technological University, 1998-2022). The increase in geoelectrical resistivity, thickness and lithology indicates a fluvial braided river deposition in agreement with the location on the bend of the Flathead River.

Geoelectric layer-3 of the recovered geoelectrical resistivity model in comparison with the Table 9 well completion report show agreement when combining the next three lithologic units. Geoelectric layer-3 of the recovered geoelectrical resistivity model is a geoelectrical resistive (732 Ohm-meter) layer of type I grading into type III composite soil. The type I composite soil has a matrix of *sand* from 4-11 meters followed by *gravel in brown clay* from 11-17 meters and enters the *gravel and water* lithology from 17-19 meters (Ground Water Information Center; Montana Bureau of Mines and Geology; Montana Technological University, 1998-2022). The increase in geoelectrical resistivity, thickness and lithology indicates a continuation of the uppermost fluvial braided river deposition.

Geoelectric layer-4 of the recovered geoelectrical resistivity model is a very high resistivity (5,172 Ohm-meter) geoelectric layer from 18-219 meters. Geoelectric layer-4 has the DOI located just above the basal depth of 219-meters at about 210-meters depth. Lithology for upper portion of this geoelectric model layer is type IV composite soil with a matrix of *gravel and water* from 17-19 meters and type III composite soil with a matrix of *gravel in brown clay and water* from 19-20 meters (Ground Water Information Center; Montana Bureau of Mines and Geology; Montana Technological University, 1998-2022). There are no further lithologic units available for comparison with this sounding. The thickness and high geoelectrical resistivity of this geoelectric layer indicates it is likely a further continuation of the upper sand and gravel aquifer.

Geoelectric layer-5 of the recovered geoelectrical resistivity model is just below the DOI making the recovered model at this depth less certain. Geoelectric layer-5 is a very high resistivity (1,446 Ohm-meter) geoelectric layer from roughly 219-360 meters.

Geoelectric layer-6 is the basement of the recovered geoelectrical resistivity model, well below the DOI making the recovered model at this depth less certain. Geoelectric layer-6 is a moderately resistive (87 Ohm-meter) geoelectric layer at around 360-meters depth. Geoelectric layer-6 may be the PCL; however, it lies well below the DOI making it very uncertain and without a deep well with drill core lithology it is impossible to confirm the presence of glacial deposits. It is entirely possible here at the bend in the Flathead River that the PCL was severely eroded away and is representative of a hole in the glacial layer.

6.2. Site 2

Site 2 along the eastern front of the valley, nestled alongside the medial moraine separating the Flathead Valley Lobe from the Swan Valley Lobe, is at the base of the former ice-contact slope near Kalispell, Montana. The flat floor abutting the medial moraine of this survey location indicates there has been sufficient alluvial deposition to raise the valley floor to a flat levelness, while the steep slope abutting contains a heavy measure of supraglacial drift deposits in the medial moraine. Deposits below the alluvium will have come primarily from a mixture of subglacial traction till and supraglacial drift tills, any englacial inclusions carried within and pushed along under the glaciers, and glaciolacustrine deposits from periods of glacial meltwater flooding the valley during glacial retreat. It is also possible at this margin of the valley that an intermediate-aged alluvium may be inter-layered with the glacial deposits. Glaciotectonite is not expected in this location, though may be present in the medial moraine. The deposits making up the PCL will likely have a moderate geoelectric resistivity as subglacial traction till or supraglacial till deposits down to a low geoelectric resistivity as a glaciolacustrine deposit.

LaFave, Smith and Patton (2004) found post-glacial deposition to be generally more than 15-meters deep (p. 20) and Smith mapped the thickness of the PCL in this area between 30 and 61-meters (LaFave, Smith, & Patton, 2004; Smith, Thickness of the Confining Unit in the Kalispell Valley, Flathead County, Montana, 2004). Geoelectric resistivity model layer-4 starts 19-meters from the surface in the mapped range of LaFave, Smith and Patton but is a very high geoelectric resistivity of 1,914 Ohm-meters with a thickness of 94-meters. Not only is the geoelectric resistivity on the highest end of the subglacial traction tills range, but the thickness of geoelectric layer-4 is larger than Smith (2004) mapped, indicating the layer is most likely representative of a mixture of intermediate alluvial sediments and glacial layer deposits.

Geoelectric resistivity model layer-5 starts at 113-meters depth and is near the mapped thickness range of 30-61 meters for the PCL with a thickness of 67-meters. Geoelectric model layer-5 has a moderately high geoelectrical resistivity of 957 Ohm-meters which are in the high range of subglacial and supraglacial till geoelectric resistivities. Geoelectric model layer-5 could be representative of a mixture of subglacial and supraglacial tills with some intermediate alluvium, however the top of the layer is deeper than LaFave, Smith and Patton (2004) indicate.

Geoelectric resistivity model layer-6 has a notable low geoelectrical resistivity of 25 Ohm-meters that can be indicative of glaciolacustrine deposits. The thickness of geoelectric layer-6 is 37-meters, which is in the range of thickness mapped by Smith (2004). However, the depth to the top of geoelectric layer-6 is 177-meters which is significantly deeper than the 15-meters LaFave, Smith and Patton (2004) found. Further, the DOI starts around 180-meters creating uncertainty in the thickness of the recovered model values. The notable composition of geoelectric layer-6 may be worth further investigation to confirm the presence of glaciolacustrine deposits at this depth, possibly representing a lower extent of the PCL.

Two well completion reports with drill core lithologies from newly drilled wells installed by GWIP in 2020 and 2021 are located on site. Appendix E contains Figure 48 with the location of the wells in relation to the TEM sounding and Tables 10 and 11 contain copies of the well completion reports. Figures 29 and 30 compare the results of the 1D 7-layer geoelectric resistivity model for Site 2 with the well completion report lithologies. The diversity in the quality of lithologic descriptions can be appreciated in the Site 2 lithology-resistivity comparisons.

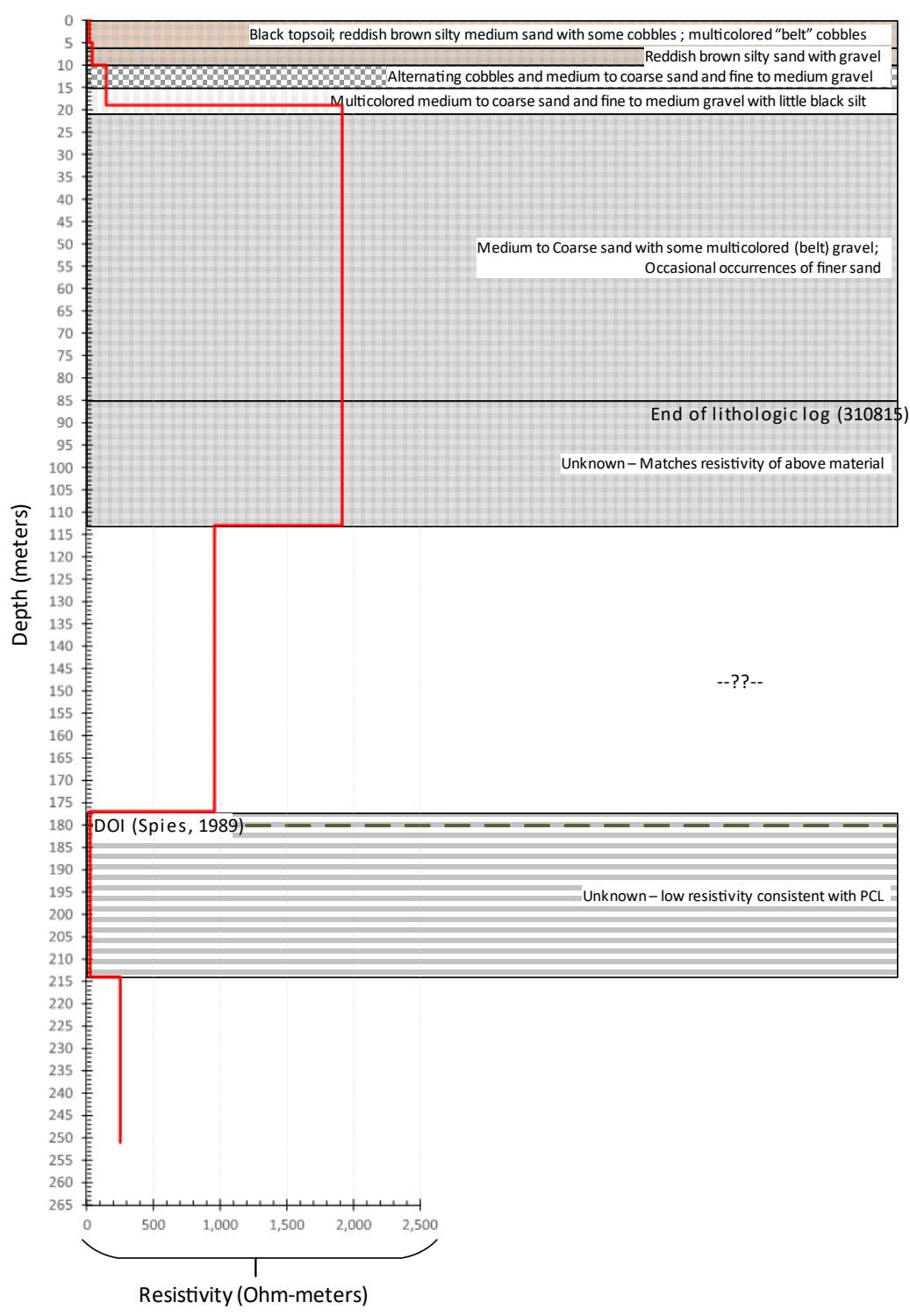


Figure 29. 1D geoelectric resistivity model of Site 2 with lithology of well 310815 (Ground Water Information Center; Montana Bureau of Mines and Geology; Montana Technological University, 1998-2022).

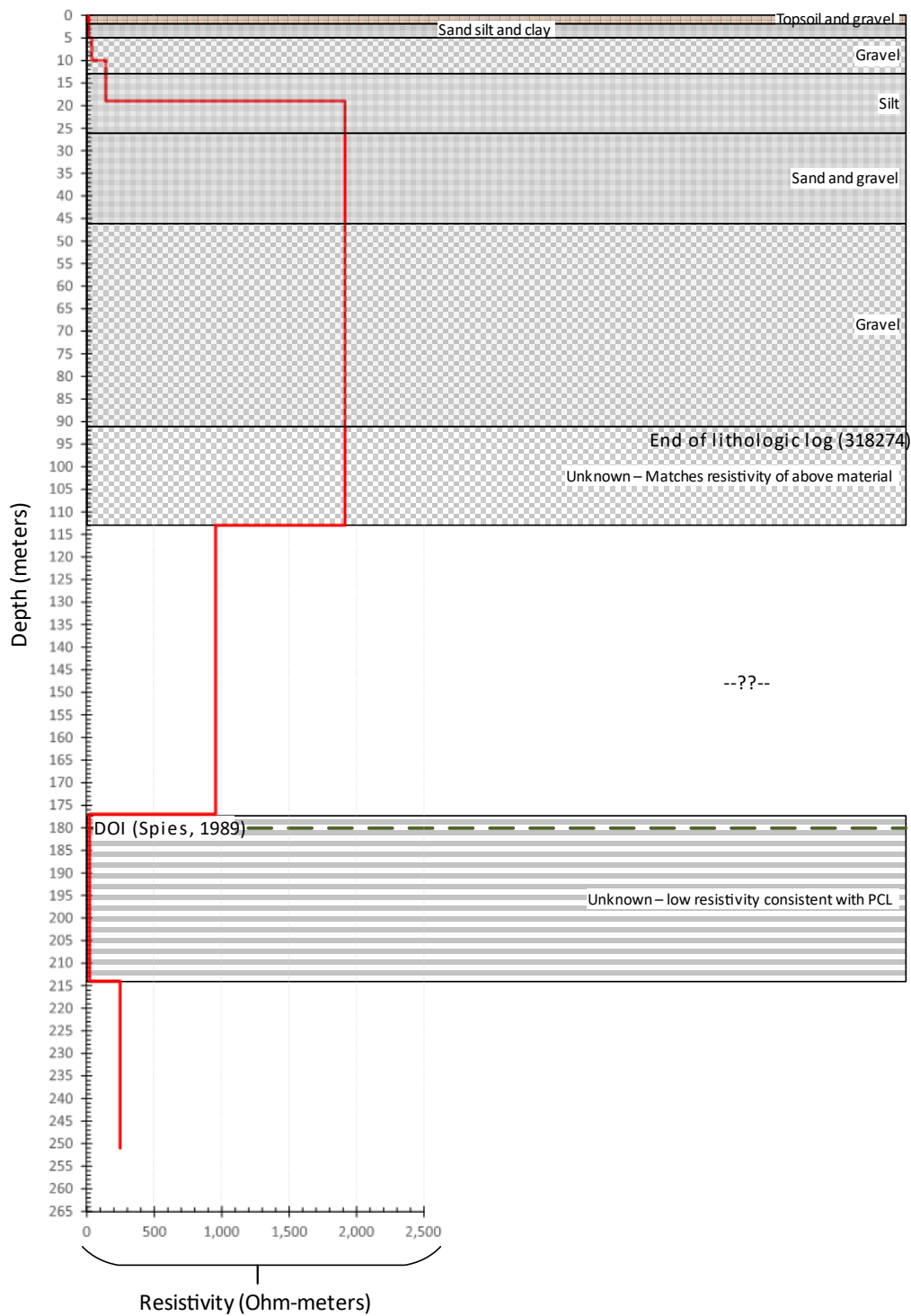


Figure 30. 1D geoelectric resistivity model of Site 2 with lithology of well 318274 (Ground Water Information Center; Montana Bureau of Mines and Geology; Montana Technological University, 1998-2022).

Geoelectric resistivity layer-1 of the recovered 1D geoelectric resistivity model in comparison with the well completion reports in Tables 10 and 11; reported lithology show some agreement. Well 310815 lithology from 0-0 meters, 0-2 meters and 2-5 meters combined closely matched the depths of the recovered geoelectrical resistivity model. 0-0 meters is reported as type I *black topsoil*; 0-2 meters is reported as type II *reddish brown silty medium sand with some cobbles and gravel*; and 2-5 meters is reported as type IV *multicolored (Belt) cobbles* (Table 10) (Ground Water Information Center; Montana Bureau of Mines and Geology; Montana Technological University, 1998-2022). Well 318274 lithology from 0-0 meters, 0-2 meters and 2-5 meters also combined closely match depths of the recovered geoelectrical resistivity model. 0-0 meters is reported as type I *top soil*; 0-2 meters is reported as type III *gravels*; and 2-5 meters is reported as type II *sand, silt and clay* (Table 11) (Ground Water Information Center; Montana Bureau of Mines and Geology; Montana Technological University, 1998-2022). While not separated by much physical distance, the differences in lithology of the same dimensions gives an appreciation for the spatial variability of the area. Geoelectric resistivity layer-1 is a low geoelectric resistivity (19 Ohm-meter) layer of type II-IV composite soil.

Geoelectric resistivity layer-2 of the recovered geoelectrical resistivity model in comparison with the well completion reports lithology show some agreement. Well 310815 lithology from 5-6 meters, 6-9 meters, and 9-10 meters combined to match the depth of the recovered geoelectrical resistivity model. 5-6 meters reported type III a *multicolored (Belt) gravel with little reddish brown sand* lithology; from 6-9 meters reported type II *reddish brown silty sand with little fine gravel*; and from 9-10 meters reported type II *reddish brown silty sand and fine to medium multicolored (Belt) gravel* (Table 10) (Ground Water Information Center; Montana Bureau of Mines and Geology; Montana Technological University, 1998-2022). Well

318274 lithology from 5-13 meters reported a type III *gravel* lithology (Table 11) (Ground Water Information Center; Montana Bureau of Mines and Geology; Montana Technological University, 1998-2022). Geoelectric resistivity layer-2 is a moderately low geoelectric resistivity (41 Ohm-meter) type II-III composite soil with a matrix of sand, silt and gravel; the lithology descriptions indicate the silt is a controlling factor in the geoelectrical resistivity of this unit.

Geoelectric resistivity layer-3 of the recovered geoelectrical resistivity model in comparison with the well completion reports lithology show some agreement in depth, but not in composition. Well 310815 lithology from 10-12 meters, 12-13 meters, 13-13 meters, 13-14 meters, 14-15 meters, 15-16 meters and 16-20 meters combined match the depth of the recovered geoelectrical resistivity model. 10-12 meters reported a type IV *multicolored (Belt) cobbles* lithology; from 12-13 meters reported type II *multicolored (Belt) medium to coarse sand and fine to medium gravel*; from 13-13 meters reported type IV *multicolored (Belt) cobbles*; from 13-14 meters reported type II-III *multicolored (Belt) medium to coarse sand and fine to medium gravel*; from 14-15 meters reported type IV *multicolored (Belt) cobbles*; from 15-16 meters reported type II-III *multicolored (Belt) medium to coarse sand and fine to medium gravel* and from 16-20 meters reported type II *multicolored (Belt) medium to coarse sand and fine to medium gravel with little black silt* (Table 10) (Ground Water Information Center; Montana Bureau of Mines and Geology; Montana Technological University, 1998-2022). Well 318274 lithology from 13-26 meters reported a type I *silt* lithology (Table 11) (Ground Water Information Center; Montana Bureau of Mines and Geology; Montana Technological University, 1998-2022). Geoelectric resistivity layer-3 is a moderately geoelectric resistive (145 Ohm-meter) type II-IV composite soil with a matrix of silt to layered sand, gravel and cobble. The alternate layering of well 310815 lithology is representative of cyclical deposition in the post-glacial period.

Geoelectric resistivity layer-4 of the recovered geoelectric resistivity model in comparison with the well completion reports lithology show mild agreement in depth, but not in composition. Well 310815 lithology from 20-meters until the end of the lithology record at 85-meters combined to match as much of the depth of the recovered geoelectric resistivity model as is available. 20-21 meters reported a type II-III *multicolored (Belt) medium to coarse sand and fine to medium gravel with little black silt and some cobbles* lithology; from 21-23 meters reported type II *reddish brown medium to coarse sand with little fine multicolored (Belt) gravel*; from 23-25 meters reported type II-III *medium to coarse sand with some fine multicolored (Belt) gravel and few cobbles*; from 25-26 meters reported type II *medium to coarse sand*; from 26-31 meters reported type II-III *fine to medium sand with some fine multicolored (Belt) gravel and some coarse sand*; from 31-35 meters reported type IV-III *multicolored (Belt) fine to medium gravel and medium to coarse sand*; from 35-38 meters reported type II *medium to coarse sand with some fine multicolored (Belt) gravel*; from 38-41 meters reported type II *medium to coarse sand with little fine multicolored (Belt) gravel*; from 41-54 meters reported type I *fine well sorted sand*; from 54-56 meters reported type II *medium to coarse sand with some fine gravel*; from 56-58 meters reported type I *fine to medium sand*; from 58-63 reported type I *fine sand*; from 63-67 meters reported type II *medium to coarse sand with some multicolored (Belt) fine gravel*; from 67-69 meters reported type III *multicolored (Belt) fine to medium gravel with some coarse sand*; and in continued layered sequences from 69-meters to the end of the lithology report at 85-meters reported sequences of type II *medium to coarse sand with* alternating sequences of type IV *some fine to medium multicolored (Belt) gravels* (Table 10) (Ground Water Information Center; Montana Bureau of Mines and Geology; Montana Technological University, 1998-2022). Well 318274 lithology from 26-46 meters and 46-91 meters reported a type II *sand and*

gravels and type IV *gravel* lithology respectively (Table 11) (Ground Water Information Center; Montana Bureau of Mines and Geology; Montana Technological University, 1998-2022).

Geoelectric layer-4 is a high geoelectric resistivity (1,914 Ohm-meter) layer of type I-IV composite soil with a matrix of layered sand, gravel and cobbles. The alternate layering of well 310815 lithology is representative of cyclical deposition in the depth range of LaFave, Smith and Patton's (2004) glacial deposition. The high geoelectrical resistivity indicates the cobbles and gravels are major controlling factor in the geoelectric resistivity. The cobbles and gravels are indicative of englacial and supraglacial till deposits. The presence of the intermediate alluvium we expect to see at the glacial margins is likely represented in the cyclical layering of the lithologies. Geoelectric resistivity layer-4 may be representative of the Pinedale glaciation before the final retreat of the glaciers.

Geoelectric resistivity layer-5 of the recovered geoelectrical resistivity model is a moderately geoelectric resistive (957 Ohm-meter) layer from 113-177 meters. There are no further lithologic units available for comparison with this sounding, however the decrease in geoelectrical resistivity and consideration of the previous lithologic units indicates a continuation of the type II composite soil with a matrix of primarily sand with some gravel and cobble components. The thickness is just above the PCL thickness range of Smith (2004) and given the overlying alluvial fan type lithologic sequence geoelectric resistivity layer-5 may have a larger component of intermediate alluvium and be representative of a longer glacial retreat period occurring prior to the Pinedale glaciation.

Geoelectric resistivity layer-6 has DOI around 180-meters deep, just inside the geoelectric layer. Geoelectric resistivity layer-6 is a very low geoelectric resistivity (25 Ohm-meter) layer from 177-meters to over 200-meters depth – the depth to the bottom being less

certain due to its location below the Depth of Investigation. The lithology of the two well completion reports combined with the sharp drop in geoelectrical resistivity may be an indication that geoelectric resistivity layer-6 is a deep glaciolacustrine deposit in the PCL from an early glacial retreat flood such as the Bull Lake glaciation a 140,000 years ago that created the Mission moraine at the southern end of the valley (Hyndman & Thomas, 2020).

Geoelectric resistivity layer-7 is the basement of the recovered geoelectrical resistivity model well below the DOI around 180-meters deep. Geoelectric resistivity layer-7 is a moderate resistivity (251 Ohm-meter) geoelectric layer. Being well below the Depth of Investigation creates uncertainty in the confidence of the model at this depth. However, we can be confident in a decrease in geoelectrical resistivity beneath Geoelectric resistivity layer-6.

Overall interpretations of Site 2 are alluvial fan type depositional layers recorded in the well completion report lithologies. A thin uppermost alluvial layer overlying an intermixing of intermediate alluvial sediments washed down from the higher reaches of the medial moraine with supraglacial and englacial deposits intermixed with subglacial traction tills from cycles of glacial advance and retreat overlying what may be glaciolacustrine deposits from an earlier glacial retreat flood such as the Bull Lake glaciation. Lack of deeper drill core lithology has created a need to rely on geologic interpretations of the geoelectric resistivity layers at depths below the lithology on record and indicate a need for further investigation of the notable low geoelectric resistivity layer-6 to confirm the presence of glaciolacustrine sediments at this depth.

6.3. Site 3

Site 3 at valley center just north of Flathead Lake near Big Fork Farm, Montana is composed of some type I subglacial traction till with cycles of thicker glaciolacustrine

deposition. This combination of glacial components yields a low geoelectrical resistivity PCL in agreement with Palacky's assessment of the lower geoelectrical resistivities of Canadian glaciolacustrine strata (Palacky, 1987). Both Sites 3-1 and 3-2 modelled the PCL as geoelectric layer-5 with geoelectric resistivities of 44 Ohm-meters and 20 Ohm-meters respectively. The depth to the top of the PCLs are around 65-meters and 100-meters respectively, showing a deepening of the local area PCL towards the lake. Site 3-1 model found the PCL to only be 51-meters thick and Site 3-2, southeast about 2.5-kilometers from the primary site and closer to the lake was about 100-meters thick, showing a thickening of the PCL glacial layer toward the lake in this local area. Smith (2004) geospatially mapped the PCL thickness between 152 and 183-meters thick at Site 3 which did not agree with the data model of Site 3-1, but was closer to the data model of Site 3-2 (Smith, Thickness of the Confining Unit in the Kalispell Valley, Flathead County, Montana, 2004).

6.3.1. Site 3-1

A new deep well was constructed in 2021 with an assortment of down borehole geophysics as well as drill core lithology reports at the location of Site 3-1 near Big Fork Farm, Montana. Appendix D contains Figure 45 with the location of the well in relation to the TEM sounding and annotated Tables 5-8 of new geophysical data taken in the near-surface range of our models. The BFF#5 well completion report (Ground Water Information Center; Montana Bureau of Mines and Geology; Montana Technological University, 1998-2022) in Table 5 recorded the PCL from 219-405 feet (67-123 meters) depth as a sticky tan clay – glaciolacustrine deposits. This is 57-meters thick and compellingly close to our 1D 6-layer recovered geoelectric resistivity model, geoelectric layer-5 thickness of 51-meters. The Geophysics Summary Plot

Report (Montana Tech - Montana Bureau of Mines and Geology, 2021) in Table 6 lithology found the PCL between 220-405 feet (67-123 meters) – again a thickness of 57-meters closely resembling the 1D 6-layer recovered geoelectric resistivity model of geoelectric layer-5. The Neutron and Density Report (Montana Tech - Montana Bureau of Mines and Geology, 2021) in Table 7 recorded a change in lithology and density at the bottom of the PCL (123-meters). The Three Arm Caliper Natural Gamma with Volume Report (Montana Tech - Montana Bureau of Mines and Geology, 2021) in Table 8 recorded an upward coarsening of grain size at the top of the PCL and a waning of grain size sequences at the bottom of the PCL indicating the change in deposition occurring at the upper and lower boundaries. All these methods recorded a layer sequence comparable to the 1D 6-layer recovered geoelectric resistivity model, geoelectric layer-5 results of the top at 64-meters below the surface and 51-meters thick. The geoelectric resistivity was in the predicted range for glaciolacustrine deposits at a geoelectric resistivity of 44 Ohm-meters.

Figure 31 is a 6-layer depth comparison of the 1D 6-layer modeled geoelectric resistivity model with Geophysics Summary Plot by Colog, Inc. Figure 32 is a 6-layer depth comparison of the 1D 6-layer modeled geoelectric resistivity model with the BFF#5 well completion report. Depth changes in the reported lithology near the recovered geoelectric resistivity inversion model depths are plotted together showing the success of the *Beowulf* algorithm in modeling the recovered geoelectric layers of the sounding data (Wilson, Raiche, & Sugeng, 2007). It is important to note that both sets of lithology were logged together at the same drill site, however the differences demonstrate the variability in lithology logging across multiple sites where judgement of the characteristics and changes in layer sequences are not always clear-cut.

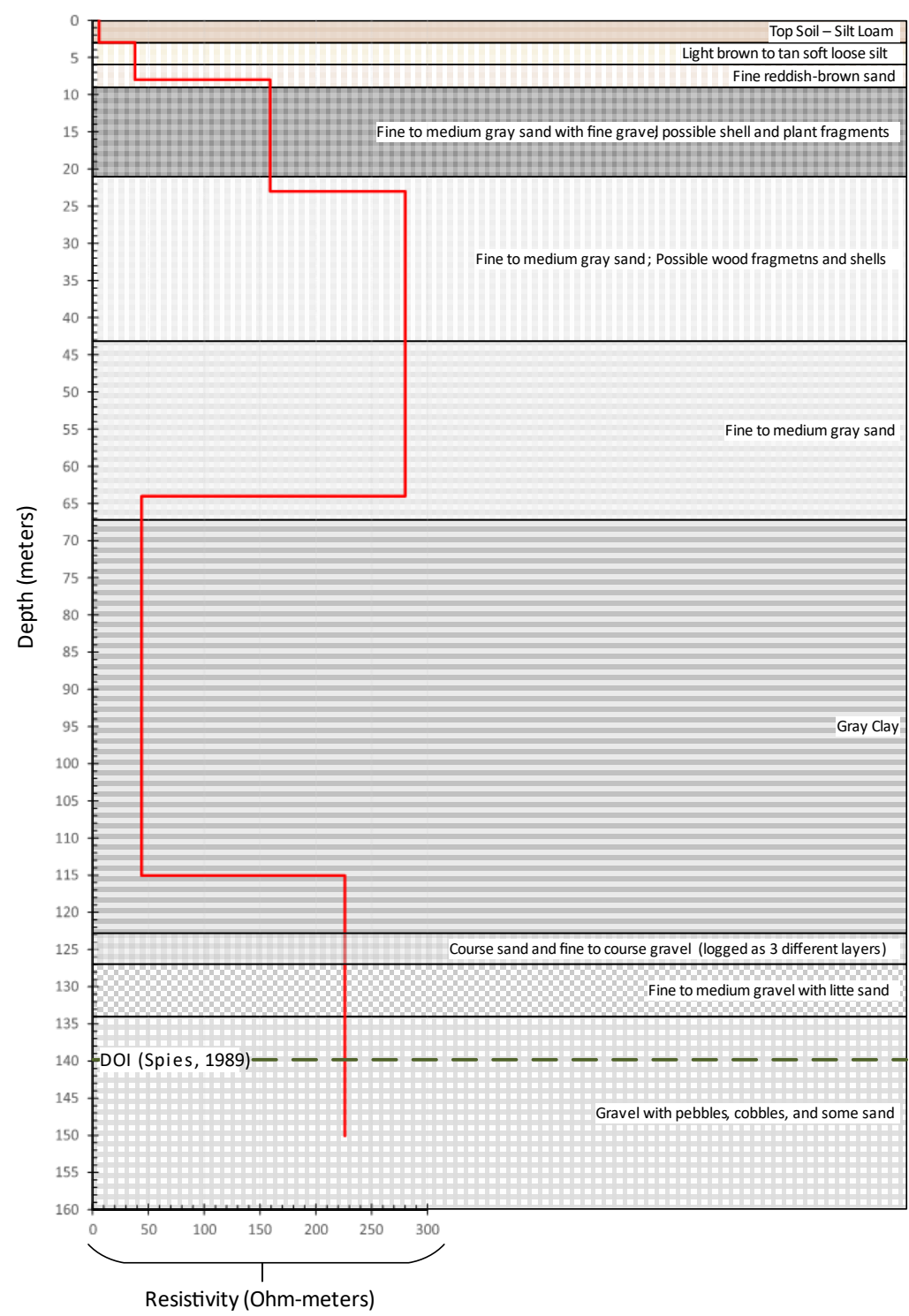


Figure 31. 1D geoelectric resistivity model of Site 3-1 with lithology of the Geophysics Summary Plot lithology by Colog, Inc (Montana Tech - Montana Bureau of Mines and Geology, 2021).

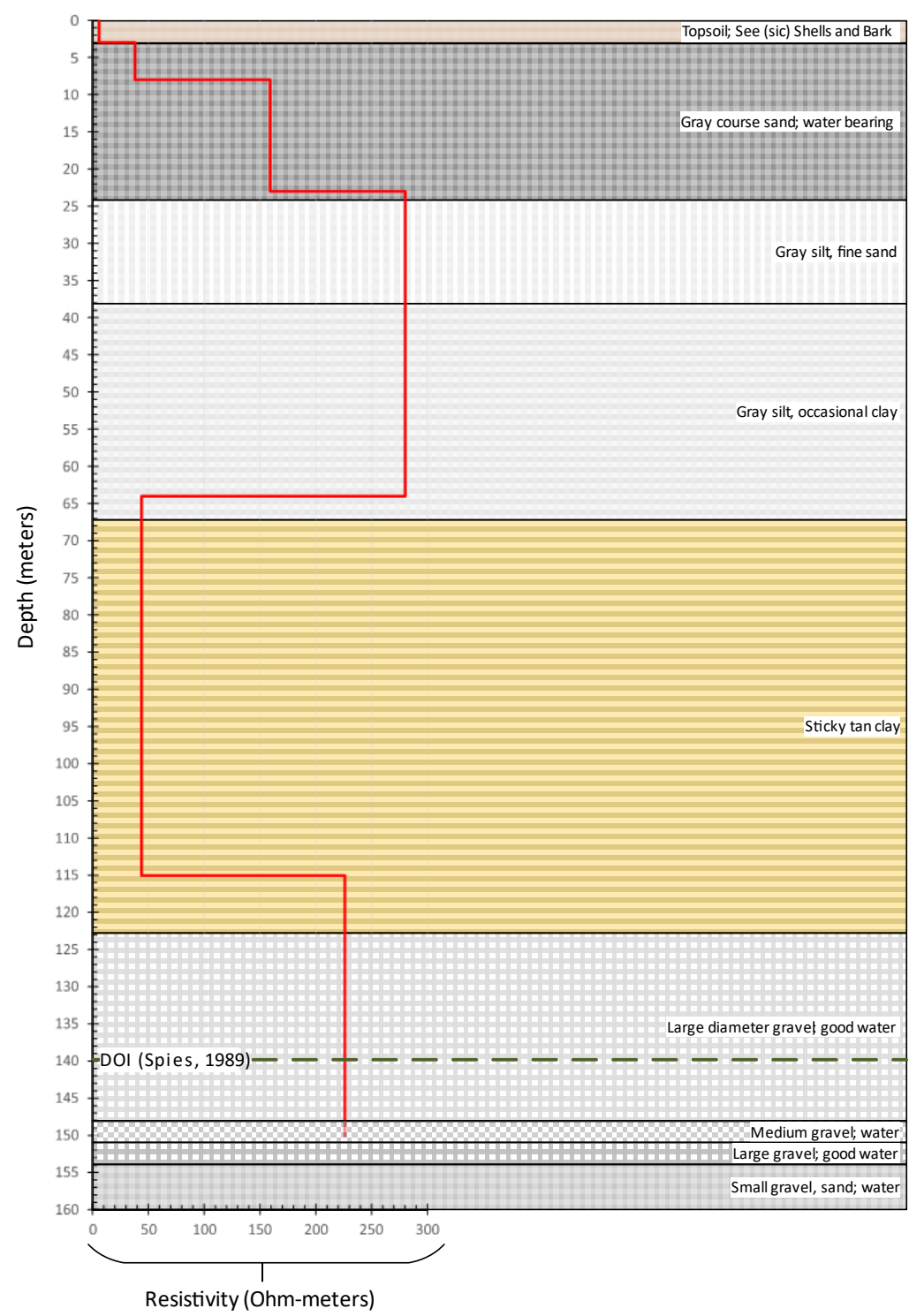


Figure 32. 1D geoelectric resistivity model of Site 3-1 with lithology of well 317644 (Ground Water Information Center; Montana Bureau of Mines and Geology; Montana Technological University, 1998-2022).

Geoelectric layer-1 of the 1D 6-layer recovered geoelectric resistivity model in comparison with the BFF#5 well completion report lithology and the Colog, Inc reported lithology are all in agreement. Geoelectric resistivity layer-1 is a low geoelectrical resistivity (6 Ohm-meter) type I composite soil with a matrix of *topsoil and silt loam with some sea shells and tree bark*. The shells provide evidence of inter-fingering of modern lacustrine deposition within the upper alluvium.

Geoelectric resistivity layer-2 of the recovered geoelectric resistivity model in comparison with the BFF#5 well completion report lithology and the Colog, Inc reported lithology show agreement. The BFF#5 well completion report logged a type II *water bearing coarse gray sand* lithology from 3-24 meters (Table 5) (Ground Water Information Center; Montana Bureau of Mines and Geology; Montana Technological University, 1998-2022). This is a much larger lithologic unit than both the recovered geoelectric resistivity model and the Colog, Inc reported lithology, demonstrating the variability in the lithology logging. The Colog, Inc lithology from 3-6 meters is reported as type I *light brown to tan soft loose silt* (Montana Tech - Montana Bureau of Mines and Geology, 2021), indicating geoelectric resistivity layer-2 is a low geoelectrical resistivity (38 Ohm-meter) type I composite soil with a silt matrix.

Geoelectric resistivity layer-3 of the 1D 6-layer recovered geoelectrical resistivity model in comparison with the BFF#5 well completion report lithology and the Colog, Inc reported lithology show strong agreement. The BFF#5 well completion report logged a type I *gray silt fine sand* lithology from 24-38 meters (Table 5) (Ground Water Information Center; Montana Bureau of Mines and Geology; Montana Technological University, 1998-2022). This is again a much larger lithologic unit than both the recovered geoelectrical resistivity model and the Colog, Inc reported lithology, demonstrating the variability in the lithology logging. The Colog, Inc

lithology from 6-9 meters and 9-21 meters combined closely matched the depths of the recovered geoelectrical resistivity model. 6-9 meters is reported as type I *fine reddish-brown sand* and 9-21 meters is reported as type II *fine to medium gray sand with some fine gravel, some shell fragments (mussels?) and some plant fragments* (Montana Tech - Montana Bureau of Mines and Geology, 2021). Both Colog, Inc layers are primarily sand indicating the *Beowulf* algorithm was unable to differentiate any change in geoelectrical resistivity between the two units (Wilson, Raiche, & Sugeng, 2007). Modeling of more (or fewer) geoelectric layers did not yield a closer result or improvement in the RMS value at this location. Geoelectric resistivity layer-3 is a moderate geoelectric resistivity (159 Ohm-meter) type II composite soil with a matrix of sand and gravel.

Geoelectric resistivity layer-4 of the 1D 6-layer recovered geoelectric resistivity model in comparison with the BFF#5 well completion report lithology and the Colog, Inc reported lithology show agreement. The BFF#5 well completion report logged a type I *gray silt occasional clay* lithology from 38-67 (Table 5) (Ground Water Information Center; Montana Bureau of Mines and Geology; Montana Technological University, 1998-2022). This is a close-matched lithologic unit to both the recovered geoelectric resistivity model and the Colog, Inc reported lithology. The Colog, Inc lithology from 21-43 meters and 43-67 meters combined closely matched the depths of the recovered geoelectric resistivity model and the BFF#5 lithology. 21-43 meters is reported as type I *fine to medium gray sand with some wood fragment and few shells* and 43-67 meters is reported as type I *fine to medium gray sand* (Montana Tech - Montana Bureau of Mines and Geology, 2021). Both Colog, Inc layers are primarily sand indicating the *Beowulf* algorithm was unable to differentiate any change in geoelectrical resistivity between the two units (Wilson, Raiche, & Sugeng, 2007). Modeling of more (or

fewer) geoelectric layers did not yield a closer result or improvement in the RMS value at this location. Geoelectric resistivity layer-4 is a moderate geoelectric resistivity (280 Ohm-meters) type I composite soil with a matrix of sand aquifer.

Geoelectric resistivity layer-5 of the 1D 6-layer recovered geoelectric resistivity model in comparison with the BFF#5 well completion report and the Colog, Inc reported lithology show agreement. The BFF#5 well completion report logged a glaciolacustrine *sticky tan clay* lithology from 67-123 meters (Table 5) (Ground Water Information Center; Montana Bureau of Mines and Geology; Montana Technological University, 1998-2022). The Colog, Inc lithology from 67-123 meters is reported a glaciolacustrine *gray clay; with few returns; composed of silt and finer material, mostly lost in the drilling mud; plastic clay in clumps on the screen* (Montana Tech - Montana Bureau of Mines and Geology, 2021). Geoelectric resistivity layer-5 is a moderately geoelectric resistive (33 Ohm-meter) glaciolacustrine clay – the PCL.

Geoelectric resistivity layer-6 is the basement of the 1D 6-layer recovered geoelectric resistivity model with the DOI around 140-meters deep. The lithology of the BFF#5 well completion report and the Colog, Inc report show agreement. The BFF#5 well completion report logged type IV *large diameter gravel in good water* from 123-148 meters, type IV *medium gravel and water* from 148-151 meters, type IV *large gravel and water* from 151-154 meters, and type III *small gravel sand and water* from 154-293 meters (Table 5) (Ground Water Information Center; Montana Bureau of Mines and Geology; Montana Technological University, 1998-2022). The Colog, Inc lithology from 123-125 meters is reported as type II *coarse sand and fine gravel; argillite*, from 125-126 meters is reported as type IV *coarse gravel*, from 126-127 meters is reported as type III *fine to medium gravel with some fine to coarse sand*, from 127-134 meters is reported as type IV *fine to medium gravel with little sand*, and 134-165 meters is

reported as type III-IV *gravel with pebbles, cobbles and some sand* (Montana Tech - Montana Bureau of Mines and Geology, 2021). Geoelectric resistivity layer-6 is a moderate geoelectric resistivity (226 Ohm-meter) type III-IV composite soil with a matrix of semi-consolidated gravel and sand aquifer.

Site 3-1 is fortunate to have a variety of strong correlation data to confirm the findings of the 1D recovered geoelectric resistivity model. The Geophysical Summary Plot by Colog Inc was able to clearly identify the glaciolacustrine clay of the PCL as well as confirm its boundaries utilizing the other down-borehole tests and drill core lithology included in this work (Montana Tech - Montana Bureau of Mines and Geology, 2021). The glaciolacustrine deposits were successfully identified by the *Beowulf* 1D recovered geoelectric resistivity model for Site 3-1 in geoelectric resistivity layer-5 (Wilson, Raiche, & Sugeng, 2007).

6.3.2. Site 3-2

Appendix E contains Figure 49 with the location of the well in relation to the TEM sounding and Table 12 of the nearest available well completion report with lithology near Big Fork Farm, Montana. Figure 33 compares the results of the 6-layer recovered geoelectric resistivity model for Site 3-2 with the nearest available well completion report lithology. It is important to note that the well driller used cable methodology to drill well 28881 indicating the lithology reported is of poor quality and they were likely collapsing the hole as they drilled causing the reported quicksand. Unfortunately, this well was the only one with reported lithology in the vicinity of the Site 3-2 soundings. Most interpretations will rely heavily on the results of nearby Site 3-1 where the correlation data is of a high quality.

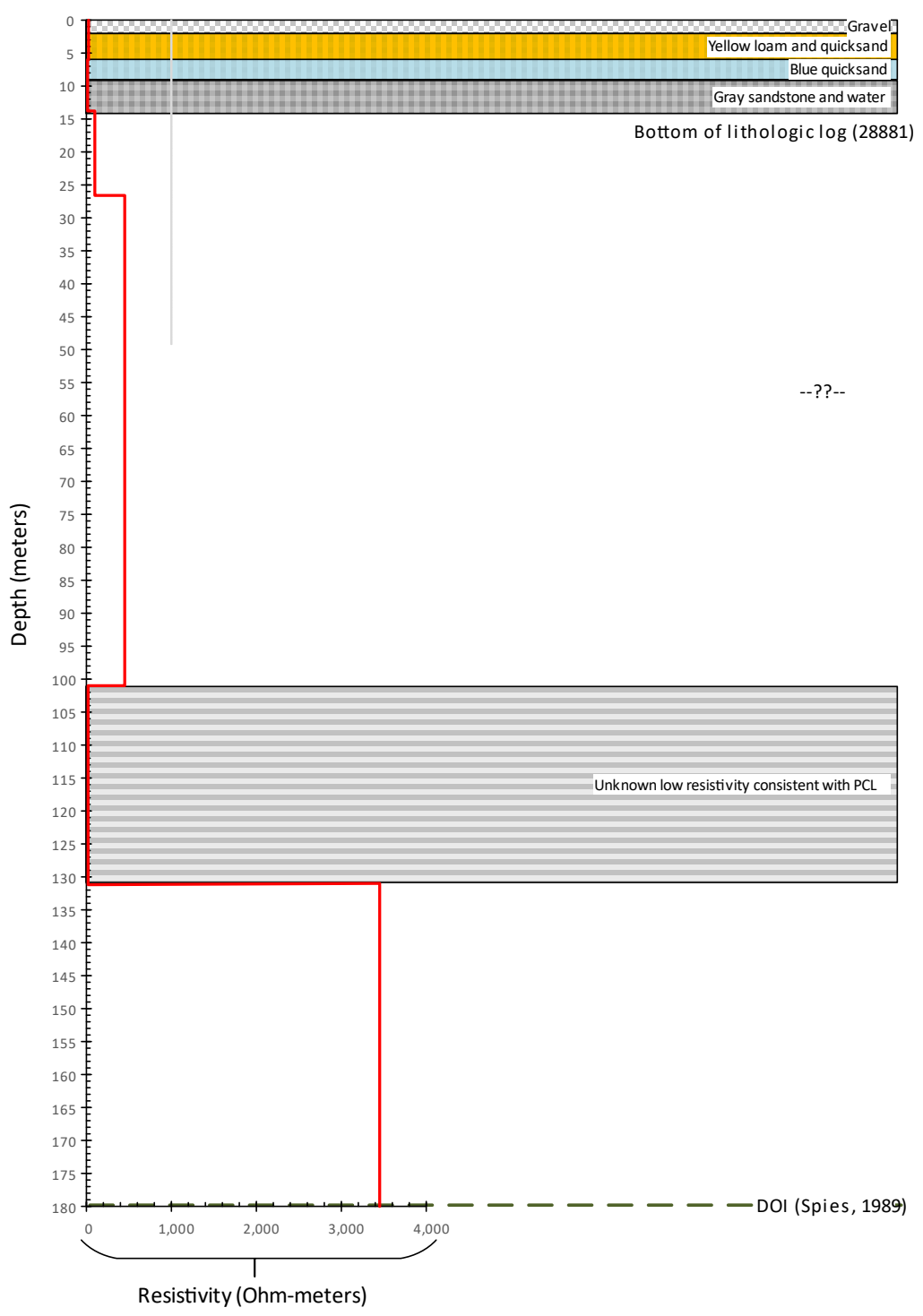


Figure 33. 6-layer depth comparison of well 28881 well completion report lithology and the Site 3-2 1D 6-layer geoelectric resistivity model geoelectric layer depths (Ground Water Information Center; Montana Bureau of Mines and Geology; Montana Technological University, 1998-2022).

Geoelectric resistivity layer-1 of the 1D 6-layer recovered geoelectric resistivity model in comparison with the Table 12 well completion report lithology show agreement when combining the first two lithologic units. Geoelectric resistivity layer-1 is a geoelectric resistive (26 Ohm-meter) type IV composite soil with a matrix of *gravel* from 0-2 meters and type I composite soil with a matrix of *yellow loam and quicksand* from 2-6 meters, representing the uppermost layer of alluvium (Ground Water Information Center; Montana Bureau of Mines and Geology; Montana Technological University, 1998-2022).

Geoelectric resistivity layer-2 of the 1D recovered geoelectric resistivity model in comparison with the Table 12 well completion report show agreement when combining the next two lithologic units. Geoelectric resistivity layer-2 is a geoelectric resistive (14 Ohm-meters) type I composite soil with a matrix of *blue quicksand* from 6-9 meters and *gray sandstone with water* from 9-14 meters, representing the uppermost layers of semi-consolidated sand aquifer where the water content highly influences the layer geoelectrical resistivity (Ground Water Information Center; Montana Bureau of Mines and Geology; Montana Technological University, 1998-2022).

Geoelectric resistivity layer-3 of the 1D recovered geoelectric resistivity model is a moderately geoelectric resistive (99 Ohm-meter) layer from 14-27 meters. There are no further lithologic units available for comparison with this sounding, however the increase in geoelectric resistivity and consideration of the previous lithologic unit indicates a continuation of the sand aquifer.

Geoelectric resistivity layer-4 of the 1D recovered geoelectric resistivity model is a moderately geoelectric resistive (451 Ohm-meter) layer from 27-101 meters. Geoelectric resistivity layer-4 is likely a further continuation of the sand aquifer.

Geoelectric resistivity layer-5 of the recovered geoelectrical resistivity model is a low geoelectric resistive (20 Ohm-meter) glaciolacustrine geoelectric layer from 101-131 meters. The sharp change in geoelectric resistivity is comparable to Site 3-1 and likely represents the PCL. The range of values between Sites 3-1 and 3-2 are reasonable considering the 2.5-kilometers between the sites and suggests a deepening of the top as it approaches the lake, which matches glaciolacustrine depositional patterns. The thickness of the PCL values suggests the thickness is thinning toward the lake. The geoelectric resistivity is becoming less geoelectrical resistive as the PCL approaches the lake and contains less subglacial drift and more glaciolacustrine elements.

Geoelectric resistivity layer-6 is the basement of the 1D recovered geoelectrical resistivity model with the DOI around 180-meters deep. Geoelectric resistivity layer-6 is a highly resistive (3,451 Ohm-meter) geoelectric layer and likely represents the deep alluvium aquifer encountered in Site 3-1.

6.4. Site 4

Site 4 in the central-southern end of Flathead Valley, near Ronan, Montana is on the retreating side of the Mission Moraine with predominant melt-out till deposits of glacial outwash, till and glaciofluvial channel deposits with some glaciolacustrine deposits from periods of Glacial Lake Missoula flooding (Hyndman & Thomas, 2020). The PCL deposits are likely thicker in this region and the melt-out till will have higher geoelectrical resistivity values than the glaciolacustrine deposits. The hummocky disintegrated moraine soundings 4-1, 4-2 and 4-3 are located on compared to the ground moraine sounding 4-4 is located on are reflected in the variety of depths of each layer of the recovered models at Site 4. Figure 34 compares the geoelectric resistivity layer depth results of the four soundings at Site 4. Note that the number of

geoelectric resistivity layers modeled was chosen based on the best RMS error value making Site 4-2 a 6-layer geoelectric resistivity model while the soundings for the remainder of the site are best modelled as 7-layer geoelectric resistivity models.

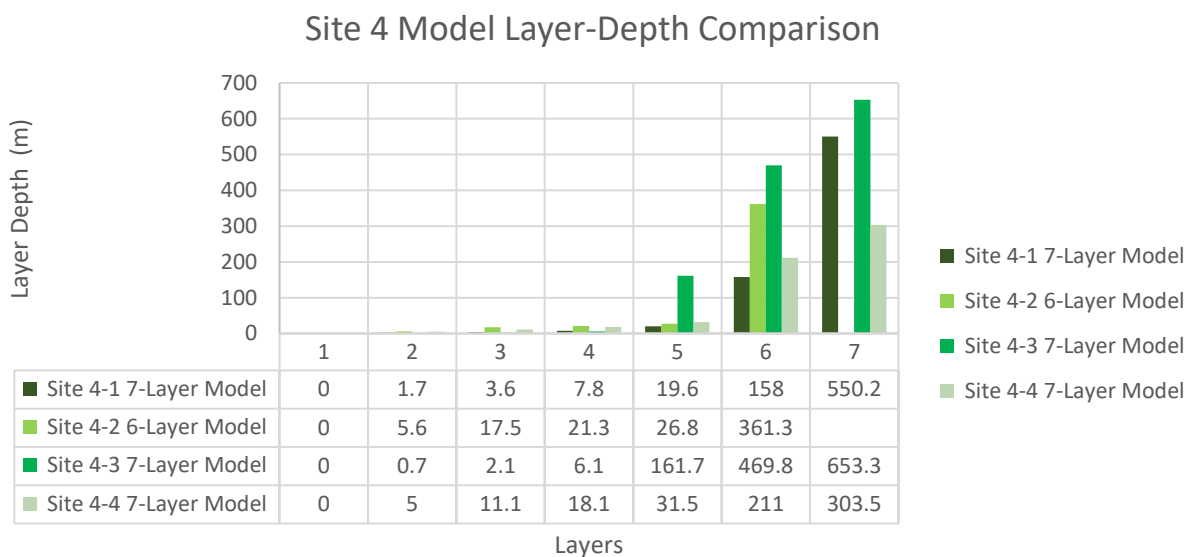


Figure 34. 7-layer depth comparison of the Site 4 1D 6 and 7-layer geoelectric resistivity model layer depths.

The variability in the geoelectric resistivity model layers clearly visualizes the variable nature of melt-out tills. The geoelectric resistivity models indicate a thin series of variable low-to-moderate geoelectric resistivity alluvial layers increasing in geoelectric resistivity with depth. At geoelectric resistivity layer-5, around 30-meters 3 of the 4 sites show an increase in geoelectric resistivity from 140 to 335 meters and Site 4-3 has its increasingly geoelectric resistive layers starting at 6-meters in geoelectric resistivity layer-4 and again at 162-meters in geoelectric resistivity layer-5. The high geoelectric resistivities of geoelectric resistivity layer-5 range from 1,500 to 5,800 Ohm-meters before decreasing in geoelectric resistivity again at geoelectric resistivity layer-6. Geoelectric resistivity layer-6 in all the models has geoelectrical resistivities ranging from 70 to 300 Ohm-meters with a large variability in thicknesses expected

of melt-out tills. The basement of Site 4-2 was geoelectric resistivity layer-6, while the remainder of the sites modeled best as 7-layer models. The basement of the geoelectric resistivity models at Sites 4-1 and 4-3 have a very low geoelectric resistivity for geoelectric layer-7 of 2 and 10 Ohm-meters which are likely representative of Glacial Lake Missoula glaciolacustrine deposits. The basement of Site 4-4 had another high geoelectric resistivity layer of around 5,300 Ohm-meters, indicating the presence of older high geoelectric resistivity deposits which were likely in place during the last cycle of Glacial Lake Missoula flooding.

Appendix E contains Figure 50 with the location of wells in relation to the TEM soundings and Tables 13-15 are the nearest available well completion reports with lithology. One well on the west side of Site 4 and two wells on the east side of Site 4 had well completion reports with lithology.

As anticipated, there is variability in the depths of the lithology sequences, even among the closely grouped east side wells. As previously discussed, the very nature of lithology logging in well completion reports is highly variable, relying on the experience and attention to fine details or gross changes to guide the author of such logs. Add to that the highly variable stratigraphic sequence due to the melt-out till and glaciolacustrine flood layers and a wide range of lithology sequencing is expected. Comparison of the well drill core lithology to the nearest sounding and site-by-site analysis to achieve an overall picture of melt-out till deposition may provide the clues needed to discern whether the Site 4 geoelectric resistivity models of melt-out tills are as successful as those north of Flathead Lake.

Well 74883 is closest to Site 4-3 (Appendix E Table 13). Well 74883 lithology from 0-0 meters are reported as type I *black dirt*; and 0-27 meters are reported as type I *hard gray rock* (Ground Water Information Center; Montana Bureau of Mines and Geology; Montana

Technological University, 1998-2022). Well 74883 lithology from 27-32 meters is reported as type I *medium hard brown and gray rock*; from 32-36 meters is reported as type I *hard gray rock*; from 36-38 meters is reported as type I *soft brown rock and a little water*; from 38-43 meters is reported as type I *broken brown and quartz rock with water*; 43-46 meters is reported as type I *medium hard brown rock and a little water*; and from 46-49 is reported as type I *hard gray rock* (Ground Water Information Center; Montana Bureau of Mines and Geology; Montana Technological University, 1998-2022).

Well 74884 is located near well 74883 and it is also closest to Site 4-3 (Appendix E Table 14). Well 74884 lithology 0-0 meters is reported as type I *black dirt*; 0-5 meters is reported as type I *broken gray rock*; and 5-43 meters is reported as type I *medium hard gray rock* (Ground Water Information Center; Montana Bureau of Mines and Geology; Montana Technological University, 1998-2022). Well 74884 lithology 43-44 meters is reported as type I *soft brown rock*; 44-50 meters is reported as type I *medium hard gray rock*; 50-55 meters is reported as type I *soft green and brown rock with a little water (2-3 gallons per minute)*; 55-68 meters is reported as type I *medium hard gray rock*; 68-79 meters is reported as type I *medium hard gray rock*; 79-90 meters is reported as type I *hard gray rock*; 90-91 meters is reported as type I *soft brown rock and water*; and 91-92 meters is reported as type I *hard gray rock* (Table 14) (Ground Water Information Center; Montana Bureau of Mines and Geology; Montana Technological University, 1998-2022).

Well 74924 is closest to Site 4-1 (Appendix E Table 15). It is important to note that the well driller used cable methodology to drill well 74924 indicating the lithology reported is of poor quality and they were likely collapsing the hole as they drilled causing the reported quicksand. Unfortunately, this well was one of only three wells with reported lithology in the

vicinity of the Site 4 soundings and the only well on the western side of the group of soundings. Lithology of well 74924 from 0-35 meters is type II *tan clay with gravel* (Ground Water Information Center; Montana Bureau of Mines and Geology; Montana Technological University, 1998-2022). Lithology of well 74924 from 35-38 meters is type I *wet clay*; from 38-44 meters is reported as type I *quicksand*; from 44-47 meters is reported as type I *clay with sand*; from 47-55 meters is reported as type I *light blue clay with sand*; from 55-81 meters is reported as type II *clay and gravel*; from 81-83 meters is reported as type III *gravel and clay*; from 83-102 meters is reported as type II *tan clay with gravel*; from 102-105 meters is reported as type I *wet sticky clay*; from 105-115 meters is reported as type II *clay and gravel*; from 115-116 meters is reported as type III *gravel and clay*; and from 116-119 meters is reported as type I *light grey fractured rock with water* (Ground Water Information Center; Montana Bureau of Mines and Geology; Montana Technological University, 1998-2022).

The eastern well lithologies have none of the clast components the western well lithology contains. The eastern well lithologies also show semi-consolidated to consolidated states which are not components of the western lithology. The eastern well sequences suggest a massive sequence of high geoelectric resistivity type I alluvium. The western well sequences suggest high geoelectric resistivity post-glacial outwash plane type I-III fluvial and alluvial fan type depositional layers. The gravel sequences in the western lithology suggest this location was part of a fluvial channel that is absent in the massive eastern lithologies. The lithologies serve to highlight the variability of the deposits in this region.

6.4.1. Site 4-1

Figure 35 compares the results of the 1D 7-layer geoelectric resistivity model for Site 4-1 with the well 74924 well completion report lithology. Well 74924 (Appendix E Table 15) is located closest to sounding Site 4-1 and will be the closest representation of the site conditions on the western end of Site 4 of the available well drill core lithologies. It is important to note that the well driller used cable methodology to drill well 74924 indicating the lithology reported is of poor quality and they were likely collapsing the hole as they drilled causing the reported quicksand. Unfortunately, this well was the only one with reported lithology in the vicinity of the Site 4-1 soundings. Furthermore, distance between well 74924 and Site 4-1 location (Figure 35) also decreases the accuracy of any comparison between the lithology and geoelectric resistivity. Well 74924 appears close to a fluvial channel to the west of the Site 4 sounding group, is further north than Site 4-1, and is more likely on the lower ground moraine than on the hummocky disintegrated moraine on which Site 4-1 is located. Interpretations of the 1D 7-layer geoelectric resistivity model for Site 4-1 with the well 74924 well completion report lithology need to be looked at in a more generalized way as a regional variation in the lithology to the west.

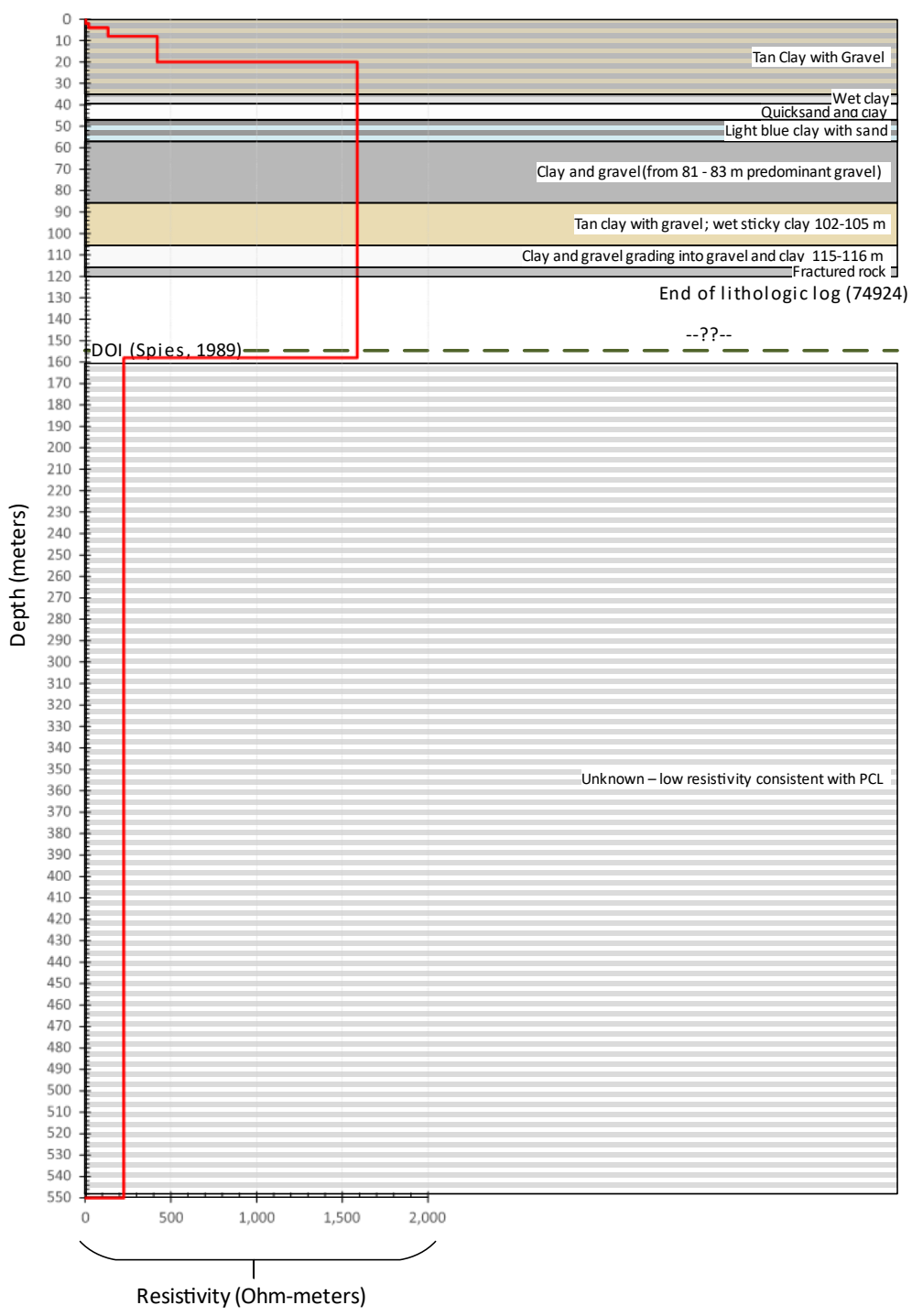


Figure 35. 1D geoelectric resistivity model of Site 4-1 with lithology of well 74924 (Ground Water Information Center; Montana Bureau of Mines and Geology; Montana Technological University, 1998-2022).

Well 74924 lithology from 0-35 meters encompasses geoelectric resistivity layers 1-4 of Site 4-1 (Appendix E Table 15). Lithology of well 74924 from 0-35 meters is type II *tan clay with gravel* (Ground Water Information Center; Montana Bureau of Mines and Geology; Montana Technological University, 1998-2022). Well 74924 lithology from 35-119 meters is within geoelectric resistivity layer 5 of Site 4-1. Lithology of well 74924 from 35-38 meters is type I *wet clay*; from 38-44 meters is reported as type I *quicksand*; from 44-47 meters is reported as type I *clay with sand*; from 47-55 meters is reported as type I *light blue clay with sand*; from 55-81 meters is reported as type II *clay and gravel*; from 81-83 meters is reported as type III *gravel and clay*; from 83-102 meters is reported as type II *tan clay with gravel*; from 102-105 meters is reported as type I *wet sticky clay*; from 105-115 meters is reported as type II *clay and gravel*; from 115-116 meters is reported as type III *gravel and clay*; and from 116-119 meters is reported as type I *light grey fractured rock with water* (Ground Water Information Center; Montana Bureau of Mines and Geology; Montana Technological University, 1998-2022).

Geoelectric resistivity layer-1 of the 1D 7-layer recovered geoelectric resistivity model in comparison with the well completion report in Figure 35; reported lithology show agreement. Geoelectric resistivity layer-1 is a low resistivity (4 Ohm-meter) geoelectric layer of type I soil composite matrix of clay-rich alluvium from 0-2 meters.

Geoelectric resistivity layer-2 of the 1D 7-layer recovered geoelectric resistivity model in comparison with the well completion report lithology show agreement. Geoelectric resistivity layer-2 is a low geoelectrical resistivity (21 Ohm-meter) type I soil composite matrix of clay-rich alluvium that is showing an increase in coarse-grained gravel components with depth.

Geoelectric resistivity layer-3 of the 1D 7-layer recovered geoelectric resistivity model in comparison with the well completion report lithology show some agreement in depth.

Geoelectric resistivity layer-3 is a moderately geoelectrical resistive (134 Ohm-meter) unit of soil composite matrix from type I to type II alluvium showing a marked increase in coarse-grained gravel components with depth.

Geoelectric resistivity layer-4 of the 1D 7-layer recovered geoelectric resistivity model in comparison with the well completion report lithology show some agreement in depth.

Geoelectric resistivity layer-4 is a moderately geoelectrical resistive (421 Ohm-meter) of soil composite matrix type II alluvium showing decreasing clay content and increasing coarse-grained gravel-based soil matrix where the gravel content is controlling the geoelectrical resistivity.

Geoelectric resistivity layer-5 of the 1D 7-layer recovered geoelectric resistivity model in comparison with the well completion report lithology show agreement. Geoelectric resistivity layer-5 of the recovered geoelectrical resistivity model is a high geoelectrical resistivity (1,589 Ohm-meter) layer from 20-158 meters. The DOI lies at the bottom of geoelectric resistivity layer-5 around 155-meters deep, decreasing the confidence of the results below this geoelectric resistivity layer. The lithologies of the nearby wells do not encompass the entire depth of geoelectric resistivity layer-5, however those within the geoelectric resistivity layer indicate a coarsening of the soil composite matrix from type II to type III alluvium with lessening clay content and increasing gravel components where the gravels are controlling the geoelectric resistivity. The lithological variations previously discussed between the well 74924 lithology and the Site 4-1 lithology likely include an increase in matrix sand with the increasing gravel to explain the increase in geoelectric resistivity values.

Geoelectric resistivity layer-6 lies just below the DOI at 158-meters deep. This causes a decreasing confidence in the results with depth below the top of this geoelectric resistivity layer.

Geoelectric resistivity layer-6 is a moderately geoelectric resistive (226 Ohm-meter) layer from 158-meters to some 550-meters depth. The 1D 7-layer recovered geoelectric resistivity model indicates a decrease in geoelectric resistivity and an increase in thickness to around 400-meters thick. Following the lithology sequence of the nearest well completion report (Well 74924, Appendix E Table 15) geoelectric resistivity layer-7 indicates a refining of the soil composite matrix from type III back to type II or type I alluvium with increasing clay content and decreasing gravel components. This sequence is supportive of post-glacial outwash plane and the fluvial type depositional layers recorded in the well completion report lithology of Well 74924 (Appendix E Table 15).

Geoelectric resistivity layer-7 is the basement of the 1D 7-layer recovered geoelectric resistivity model well below the DOI some 550-meters deep. Geoelectric resistivity layer-7 is a low resistivity (2 Ohm-meter) geoelectric layer. Being well below the Depth of Investigation creates uncertainty in the precision of the returned values of the model at this depth. However, we can be confident in a sharp decrease in geoelectric resistivity beneath geoelectric resistivity layer-6.

Without deep enough lithologic units for comparison with this sounding, let alone the physical distance separating the well site from the sounding site, determining the PCL cannot be easily confirmed. However, the sharp decrease in geoelectric resistivity after geoelectric resistivity layer-5 and consideration of the previous lithologic units indicate geoelectric resistivity layer-6 and geoelectric resistivity layer-7 are likely representatives of the PCL where the melt-out tills (geoelectric resistivity layer-6) overlie glaciolacustrine clay layers (geoelectric resistivity layer-7) from earlier cycles of glaciofluvial and glaciolacustrine deposits. Further, the clay-rich alluvium deposits over-top of the PCL washed across the glacial outwash plane from

first the glaciolacustrine deposits of the upper watershed, then later the modern lacustrine clays of present-day Flathead Lake.

6.4.2. Site 4-2

Figure 36 compares the results of the 1D recovered 6-layer geoelectrical resistivity model for Site 4-2 with the well completion report lithologies. Being roughly equidistant from both eastern and western wells, none of the well lithologies will provide a better representation of sounding Site 4-2 lithology over the other(s). All interpretations are drawn from the similarities of the grouped soundings and from the generalized well lithologies both near Site 4-2 and throughout the Flathead Valley.

Site 4-2 and Well Lithology Depth Comparison

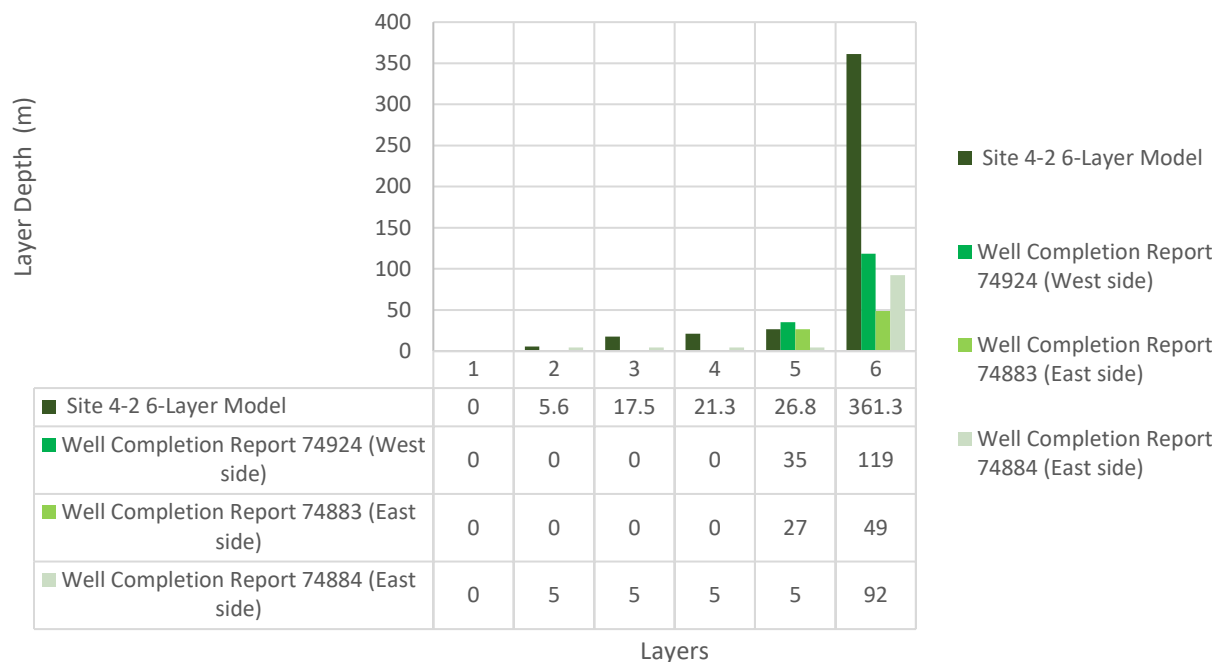


Figure 36. 6-layer depth comparison of wells 74924, 74883 and 74884 well completion report lithologies (Figure 50 and Tables 13-15, Appendix E) and the Site 4-2 1D 6-layer geoelectric model layer depths (Ground Water Information Center; Montana Bureau of Mines and Geology; Montana Technological University, 1998-2022). Highlights the range of lithological variations available for comparison with the site.

Geoelectric resistivity layer-1 of the 1D 6-layer recovered geoelectrical resistivity model in comparison with the well completion reports in Tables 13-15; reported lithology show agreement in depth. Geoelectric resistivity layer-1 is a very shallow moderately geoelectric resistive (465 Ohm-meter) layer of unknown soil composite matrix of alluvium from 0-6 meters.

Geoelectric resistivity layer-2 of the 1D 6-layer recovered geoelectric resistivity model in comparison with the well completion report lithology show agreement in depth. Geoelectric resistivity layer-2 is a very shallow moderately geoelectric resistive (527 Ohm-meter) layer of unknown soil composite matrix of alluvium from 6-18 meters.

Geoelectric resistivity layer-3 of the 1D 6-layer recovered geoelectric resistivity model in comparison with the well completion report lithology show little agreement in depth. Geoelectric resistivity layer-3 is a very shallow low geoelectric resistive (11 Ohm-meter) layer of unknown soil composite matrix of presumably clay-rich alluvium from 18-21 meters that is showing a sharp decrease in geoelectrical resistivity with depth. It is too shallow and too near the surface to be representative of the PCL.

Geoelectric resistivity layer-4 of the 1D 6-layer recovered geoelectric resistivity model in comparison with the well completion report lithology within the geoelectric layer show little agreement. Geoelectric resistivity layer-4 is a very shallow geoelectric layer of moderate geoelectric resistivity (681 Ohm-meter) of unknown soil composite matrix of alluvium from 21-27 meters showing a sharp increase in geoelectrical resistivity with depth.

Geoelectric resistivity layer-5 of the 1D 6-layer recovered geoelectric resistivity model in comparison with the well completion report lithology within the geoelectric layer show some agreement in depth. Geoelectric resistivity layer-5 of the recovered geoelectric resistivity model is a very high geoelectric resistivity (5,159 Ohm-meter) layer of unknown soil composite matrix of alluvium from 27-360 meters. The DOI lies near the middle of geoelectric resistivity layer-5 around 195-meters deep, decreasing the confidence of the results below this depth.

Geoelectric resistivity layer-6 is the basement of the 1D 6-layer recovered geoelectric resistivity model and has a moderate geoelectric resistivity (302 Ohm-meter) showing a decreasing trend in the geoelectrical resistivity that indicates this is most likely the PCL. This geoelectric resistivity layer will be primarily melt-out till with any glaciolacustrine layers beneath the depth recovered by the geoelectric resistivity model.

6.4.3. Site 4-3

Figures 37 and 38 compares the results of the 1D 7-layer geoelectric resistivity model for Site 4-3 with the well completion report lithologies of wells 74883 and 74884. Wells 74883 and 74884 are located closest to sounding Site 4-3 and will be the closest representation of the site conditions on the eastern end of Site 4. The similarities between the well lithologies are encouraging as to their accuracy and both wells appear to be located on the same hummocky disintegrated moraine as Site 4-3. Due to similarities in the locations of wells 74883 and 74884 to the location of Site 4-3 the lithological comparison can allow closer interpretations.

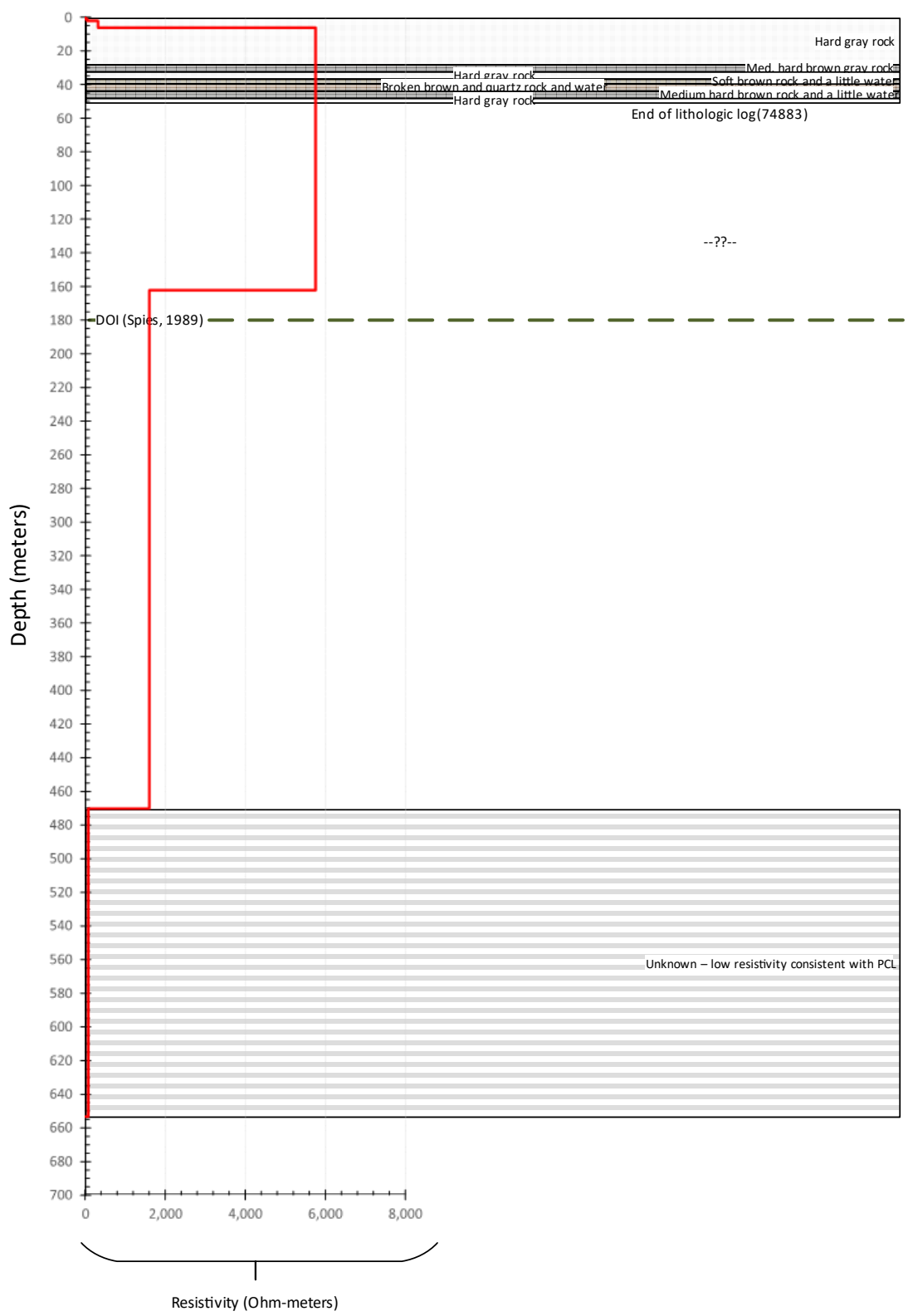


Figure 37. 7-layer depth comparison of well 74883 well completion report lithologies (Figure 50 and Tables 13-15, Appendix E) and the Site 4-3 1D 7-layer recovered geoelectric resistivity model geoelectric layer depths (Ground Water Information Center; Montana Bureau of Mines and Geology; Montana Technological University, 1998-2022)).

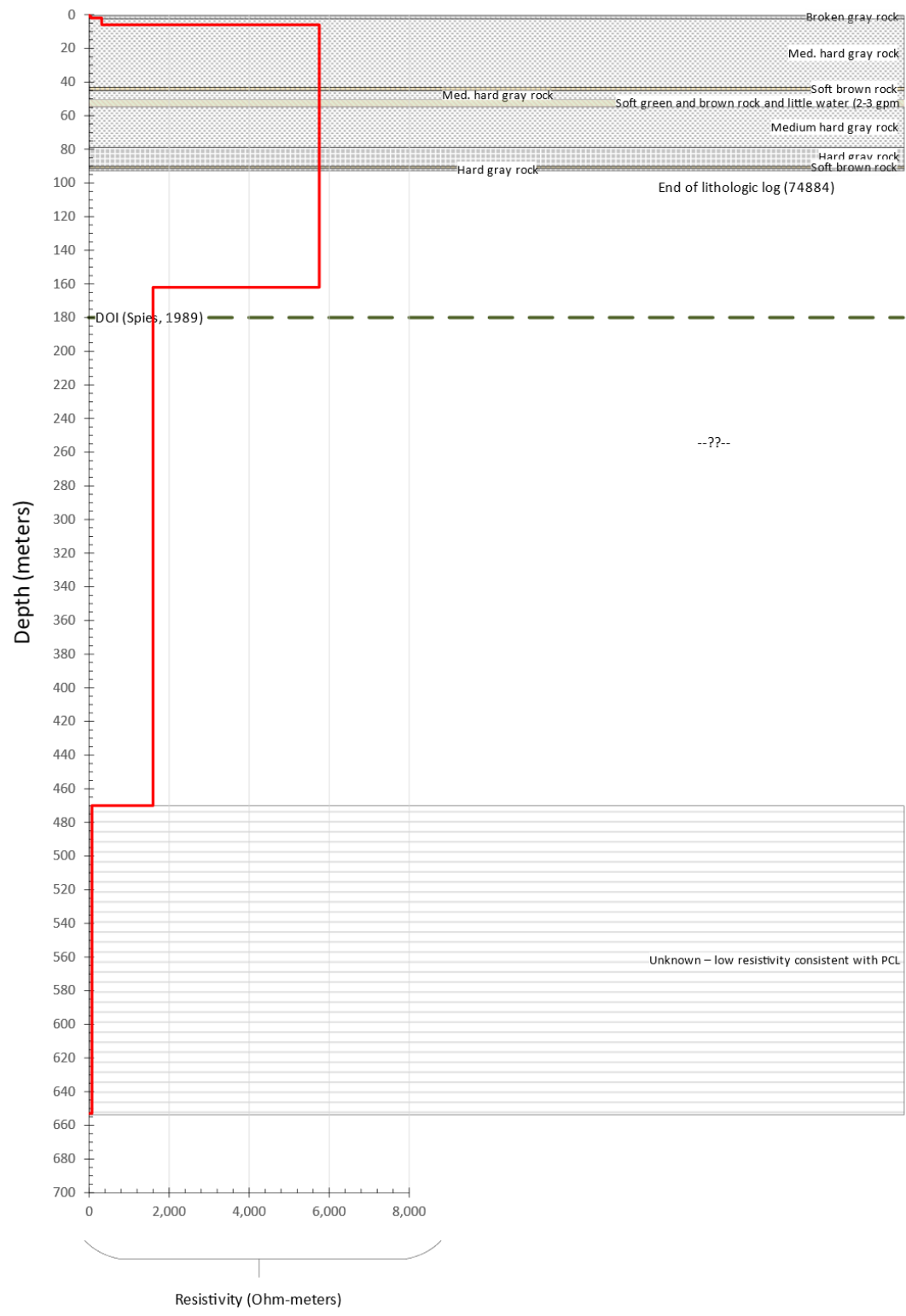


Figure 38. 7-layer depth comparison of well 74884 well completion report lithologies (Figure 50 and Tables 13-15, Appendix E) and the Site 4-3 1D 7-layer recovered geoelectric resistivity model geoelectric layer depths (Ground Water Information Center; Montana Bureau of Mines and Geology; Montana Technological University, 1998-2022).

Well 74883 lithology from 0-49 meters encompass geoelectric resistivity layers 1-4 of Site 4-3 (Appendix E Table 13). Well 74883 lithology from 0-0 meters are reported as type I *black dirt*; and 0-27 meters are reported as type I *hard gray rock* (Ground Water Information Center; Montana Bureau of Mines and Geology; Montana Technological University, 1998-2022). Well 74883 lithology from 27-32 meters is reported as type I *medium hard brown and gray rock*; from 32-36 meters is reported as type I *hard gray rock*; from 36-38 meters is reported as type I *soft brown rock and a little water*; from 38-43 meters is reported as type I *broken brown and quartz rock with water*; 43-46 meters is reported as type I *medium hard brown rock and a little water*; and from 46-49 is reported as type I *hard gray rock* (Table 13) (Ground Water Information Center; Montana Bureau of Mines and Geology; Montana Technological University, 1998-2022).

Well 74884 lithology from 0-5 meters encompass geoelectric resistivity layers 1-3 of the of Site 4-3 and 5-92 encompasses geoelectric resistivity layer-4 (Appendix E Table 14). Well 74884 lithology from 0-0 meters is reported as type I *black dirt*; 0-5 meters is reported as type I *broken gray rock*; and 5-43 meters is reported as type I *medium hard gray rock* (Ground Water Information Center; Montana Bureau of Mines and Geology; Montana Technological University, 1998-2022). Well 74884 lithology from 43-44 meters is reported as type I *soft brown rock*; 44-50 meters is reported as type I *medium hard gray rock*; 50-55 meters is reported as type I *soft green and brown rock with a little water (2-3 gallons per minute)*; 55-68 meters is reported as type I *medium hard gray rock*; 68-79 meters is reported as type I *medium hard gray rock*; 79-90 meters is reported as type I *hard gray rock*; 90-91 meters is reported as type I *soft brown rock and water*; and 91-92 meters is reported as type I *hard gray rock* (Table 14) (Ground Water

Information Center; Montana Bureau of Mines and Geology; Montana Technological University, 1998-2022).

Geoelectric resistivity layer-1 of the 1D 7-layer recovered geoelectric resistivity model in comparison with the well completion reports in Tables 13-15; reported lithology show agreement. Geoelectric resistivity layer-1 is a very shallow low geoelectrical resistivity (1 Ohm-meter) geoelectric resistivity layer of type I soil composite matrix of clay-rich alluvium from 0-1.7 meters.

Geoelectric resistivity layer-2 of the 1D 7-layer recovered geoelectric resistivity model in comparison with the well completion report lithology show agreement. Geoelectric resistivity layer-2 is a very shallow low geoelectric resistivity (47 Ohm-meter) semi-consolidated type I soil composite matrix of clay-rich alluvium with a likely increase in coarser grains to explain the increase in geoelectric resistivity.

Geoelectric resistivity layer-3 of the 1D 7-layer recovered geoelectric resistivity model in comparison with the well completion report lithology show some agreement in depth. Geoelectric resistivity layer-3 is a shallow moderately geoelectric resistive (315 Ohm-meter) semi-consolidated unit of soil composite matrix from type I alluvium that is showing an increase in consolidation with depth.

Geoelectric resistivity layer-4 of the 1D 7-layer recovered geoelectric resistivity model in comparison with the well completion report lithology within the geoelectric resistivity layer show some agreement. Geoelectric resistivity layer-4 is a thick geoelectric resistivity layer of very high geoelectric resistivity (5,754 Ohm-meter) soil composite matrix of type I alluvium showing variations in the matrix content and state of consolidation.

Geoelectric resistivity layer-5 of the 1D 7-layer recovered geoelectric resistivity model lies deeper than the well completion report lithology. Geoelectric resistivity layer-5 of the recovered geoelectric resistivity model is a high geoelectric resistivity (1,596 Ohm-meter) layer from 162-470 meters. The DOI lies near the top of geoelectric layer-5 around 180-meters deep, decreasing the confidence of the results below this depth. The lithology sequence of the geoelectric resistivity layers above in comparison with the trending decrease in geoelectrical resistivity indicate a possible increase in clay content of the type I soil composite matrix.

Geoelectric resistivity layers 6 and 7 lie deep below the DOI around 180-meters deep. This causes a decreasing confidence in the results with depth.

Geoelectric resistivity layer-6 is a low geoelectric resistive (70 Ohm-meter) layer from around 470-meters to some 650-meters depth. The recovered geoelectric resistivity model indicates a decrease in geoelectrical resistivity and a decrease in thickness to around 180-meters thick.

Geoelectric resistivity layer-7 is the basement of the 1D 7-layer recovered geoelectric resistivity model and has a low geoelectric resistivity (10 Ohm-meter).

Being well below the Depth of Investigation creates uncertainty in the precision of the returned values of the model at this depth. However, we can be confident in a sharp decrease in geoelectric resistivity beneath geoelectric resistivity layer-5. There are no further lithologic units available for comparison with this sounding, however the marked decrease in geoelectrical resistivity and consideration of the previous lithologic units indicate geoelectric resistivity layer-6 and geoelectric resistivity layer-7 are likely representative of the PCL where the melt-out tills (geoelectric resistivity layer-6) are overlying glaciolacustrine clay layers (geoelectric resistivity layer-7) from earlier cycles of glaciofluvial and glaciolacustrine deposits. Further, the clay-rich

alluvium deposits over-top of the PCL washed across the glacial outwash plane from the glaciolacustrine deposits of the upper watershed, then later from the modern lacustrine clays of present-day Flathead Lake.

6.4.4. Site 4-4

Being roughly equidistant from both eastern and western wells, none of the well lithologies will provide a better representation of sounding Site 4-4 lithology over the other(s). All interpretations are drawn from the similarities of the grouped soundings and from the generalized well lithologies both near Site 4-2 and throughout the Flathead Valley.

Geoelectric resistivity layer-1 of the 1D 7-layer recovered geoelectric resistivity model in comparison with the well completion reports in Tables 13-15; reported lithology show agreement in depth. Geoelectric resistivity layer-1 is a very shallow low geoelectric resistivity (36 Ohm-meter) layer of unknown soil composite matrix of presumably clay-rich alluvium from 0-5 meters.

Geoelectric resistivity layer-2 of the 1D 7-layer recovered geoelectric resistivity model in comparison with the well completion report lithology show agreement in depth. Geoelectric resistivity layer-2 is a very shallow low geoelectric resistivity (33 Ohm-meter) layer of unknown soil composite matrix of presumably clay-rich alluvium from 5-11 meters.

Geoelectric resistivity layer-3 of the 1D 7-layer recovered geoelectric resistivity model in comparison with the well completion report lithology show some agreement in depth. Geoelectric resistivity layer-3 is a very shallow low geoelectric resistivity (50 Ohm-meter) layer of unknown soil composite matrix of presumably clay-rich alluvium from 11-18 meters.

Geoelectric resistivity layer-4 of the 1D 7-layer recovered geoelectric resistivity model in comparison with the well completion report lithology within the geoelectric layer show some agreement. Geoelectric resistivity layer-4 is a shallow geoelectric layer of moderately geoelectric resistivity (361 Ohm-meter) of unknown soil composite matrix of alluvium from 18-32 meters showing an increase in geoelectric resistivity with depth.

Geoelectric resistivity layer-5 of the 1D 7-layer recovered geoelectric resistivity model in comparison with the well completion report lithology within the geoelectric layer show agreement in depth. Geoelectric resistivity layer-5 of the recovered geoelectric resistivity model is a very high geoelectric resistivity (3,238 Ohm-meter) geoelectric resistivity layer of unknown soil composite matrix of alluvium from 32-211 meters.

Geoelectric resistivity layer-6 of the 1D 7-layer recovered geoelectric resistivity model in comparison with the well completion report lithology within the geoelectric resistivity layer show little agreement in depth. Geoelectric resistivity layer-6 of the recovered geoelectric resistivity model is a moderate geoelectric resistivity (153 Ohm-meter) layer showing an increasing trend in the geoelectric resistivity. The DOI lies near the middle of geoelectric resistivity layer-6 around 240-meters deep, decreasing the confidence of the results below this depth. This geoelectric resistivity layer is the most likely candidate for the PCL sandwiched between two very high geoelectric resistivity layers.

Geoelectric resistivity layer-7 is the basement of the 1D 7-layer recovered geoelectric resistivity model and has a very high geoelectric resistivity (5,292 Ohm-meter) showing a varying trend in the geoelectric resistivity with depth and highlighting the variability of the melt-out till deposits.

6.5. Valley-wide scale

What do the results look like on a valley-wide scale? In Figure 39 the 1D recovered model geoelectric resistivities for all the soundings are combined into a 3D model highlighting an overview of what the over-arching geometry of the geoelectric resistivity layers are doing along the series of soundings across the valley. While the locations are not in a true transect and the data is sparse at best, annotations of the predominant glacial depositional type represented at each site lend clarity to the variability of the valley wide geoelectric resistivity distributions and highlight the challenge of geoelectric identification. Geoelectric resistivity peaks at the valley margins to the east, north and south where supraglacial tills, subglacial traction till and melt-out tills are predominant and dips where the glaciolacustrine deposits dominate as was predicted based on the range of geoelectric resistivities of the hydrostratigraphy. Despite the sparsity of data and irregularity of the locations, the 3D model of geoelectric resistive layers across the valley does provide an overview of the variability of the geoelectric subsurface layers in post-glacial intermontane valley systems.

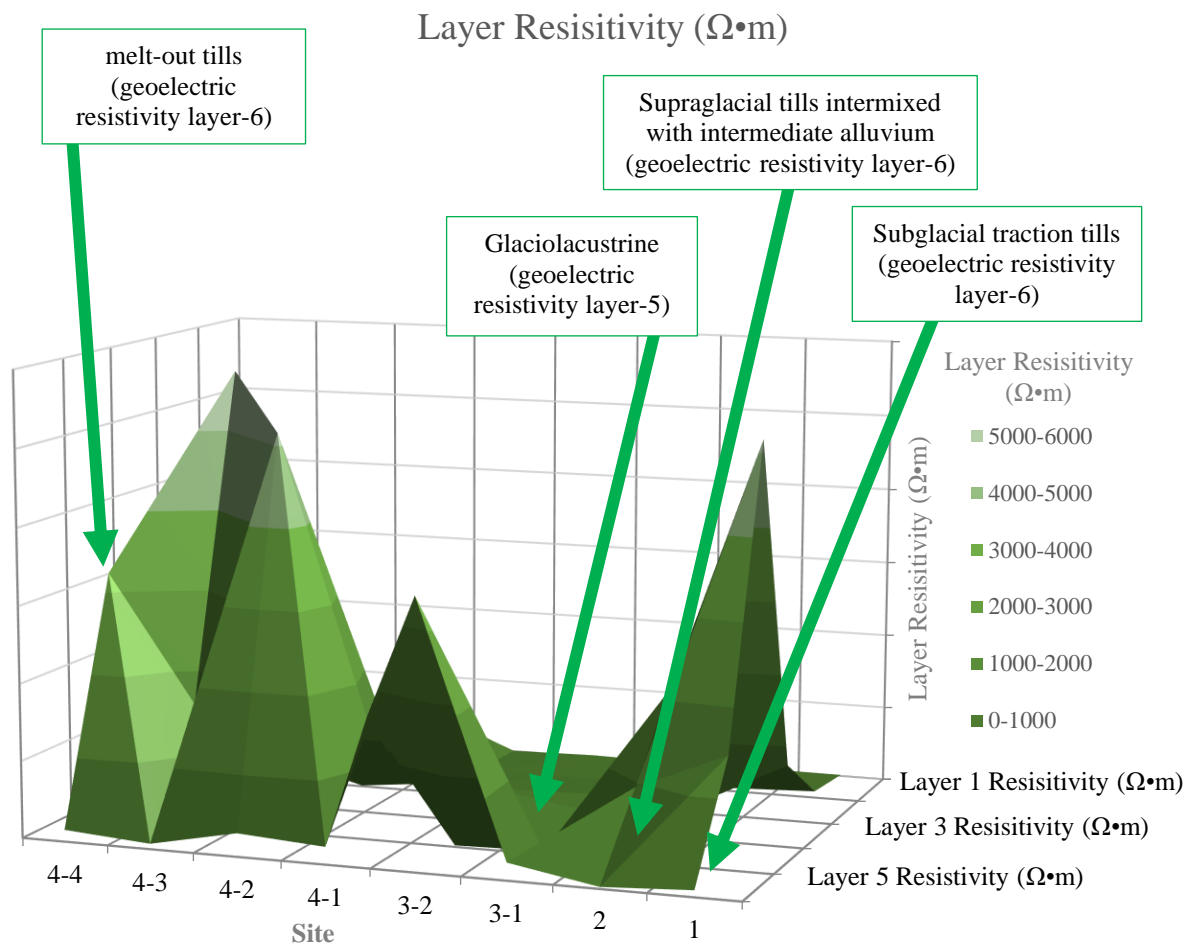


Figure 39. 3D model of the 1D recovered model geoelectric resistivities in Ohm-meters for layers 1-6 along the series of soundings across the Flathead Valley, Montana with annotation of the predominant glacial depositional type represented at each site in green.

In Figure 40 the 1D recovered model geoelectric resistivity layer thicknesses for all the soundings are combined into a 3D model highlighting an overview of what the over-arching geometry of the geoelectric resistivity layer thicknesses are doing along the series of soundings across the valley. While the locations are not in a true transect and the data is sparse at best, annotations of the predominant glacial depositional type represented at each site lend clarity to the variability of the valley wide geoelectric resistivity layer thickness distributions and highlight the challenge of geoelectric identification. Thickness peaks along the central axis of the valley to

the north and south (Sites 1 and 4) where subglacial traction till and melt-out tills are predominant and dips at the valley center where the glaciolacustrine deposits dominate (Site 3) with supraglacial tills falling into the mid-range of thicknesses at the valley margins. This agrees with intermontane glacial depositional patterns of thicker sequences at the terminal end of glaciers and thinner marginal sequences (Martini, Brookfield, & Sadura, 2001).

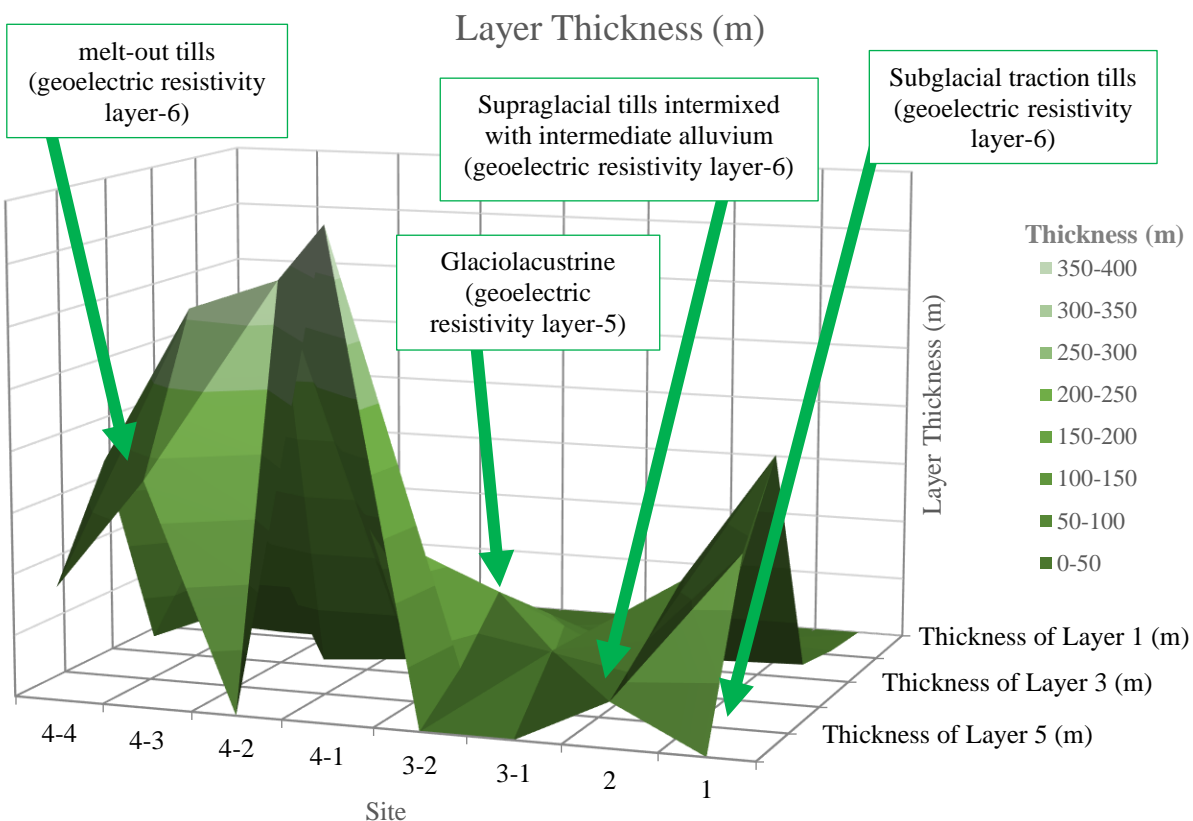


Figure 40. 3D Model of the 1D recovered geoelectric resistivity model thicknesses in meters for layers 1- 6 along the series of soundings across the Flathead Valley, Montana with annotation of the predominant glacial depositional type represented at each site.

Further agreement in the PCL thicknesses at the northern end of the Flathead Valley is found in Smith's new 2022 southwest to northeast cross section of the lithology based on newly drilled well cores (drilled in 2021) from a site named Quigley on the north bank of the Flathead

River and from the Ottey property wells 310815 and 318274 on Site 2 inter-filled with the well completion report lithologies available along the transect (Smith, Flathead SW-NE Cross Section of Deep Aquifer Drilling Report, report in preparation 2022). Smith's map can be found in Figure 51 in Appendix E. At Site 2, Smith (2022) found melt-out tills (sometimes called *ablation tills*) predominate the near-surface region with coarse lake deposits beneath, making the overall composition of the PCL at Site 2 very thin. This agrees with the Site 2 1D recovered model geoelectric resistivity, Figure 19, where geoelectric resistivity layer-1 defined the uppermost topsoil alluvium and geoelectric resistivity layer-2 captured the upper sand and gravel alluvium. Geoelectric resistivity layers 3-5 using Smith's 2022 cross sectional interpretation of the upper stratigraphy, are sequences of melt-out till material deposited during the final glacial retreat. This is a plausible alternative interpretation of the lithology and geoelectric resistivity at this location to the assessment in this paper that geoelectric resistivity layers 3-5 contained cyclical alluvial fan deposition of washed down subglacial and supraglacial deposits from the medial moraine intermixed with intermediate-age alluvium. Finally, Smith's (2022) interpretation does not account for the deep notably low geoelectric resistivity of the 1D recovered geoelectric resistivity model geoelectric resistivity layer-6 glaciolacustrine deposits overlying a higher geoelectrical resistivity deep alluvium layer that is likely the deep alluvium. This indicates recommendation of further study of the eastside marginal glacial deposition to account for the notable deep low geoelectric resistivity layer.

As the Smith (2022) cross section moves southwest across the north end of the valley, his interpretation of the mid-valley PCL glaciolacustrine deposits show thinner coarse-grained deposits near the northeastern edge of the valley grading into fine grained deposits of variable

thicknesses before thinning again at the approach of the southwestern edge of the valley where the cross section ends in more undefined till deposits.

In Figure 41 the 1D recovered model geoelectric resistivities of all the PCL sounding geoelectric resistivity layers are combined into a plot highlighting an overview of what the overarching geometry of the PCL's geoelectric resistivity is doing along the series of soundings across the valley. Note that these do not include Smith's (2022) interpreted tills in geoelectric resistivity layers 3-5 of Site 2, whose inclusion would raise the Site 2 level from the glaciolacustrine deposits 25 Ohm-meters to 145 Ohm-meters for geoelectric resistivity layer-3, a peak of 1,914 Ohm-meters for geoelectric resistivity layer-4, and 957 Ohm-meters for geoelectric resistivity layer-5 of supraglacial till which would make this the highest geoelectric resistivity portion of the PCL in the Flathead Valley of Montana. From the interpretations in this paper, geoelectric resistivity peaks at the south end of the valley where the melt-out tills of Site 4 are predominant and variable and geoelectric resistivity dips where the clay-rich glaciolacustrine deposits dominate at Sites 1 and 2. The subglacial traction tills of Site 1 at 87 Ohm-meters and melt-out tills of Site 4-3 at 70 Ohm-meters are in the middle ground of the glacial deposit geoelectric resistivity range for the Flathead Valley of Montana.

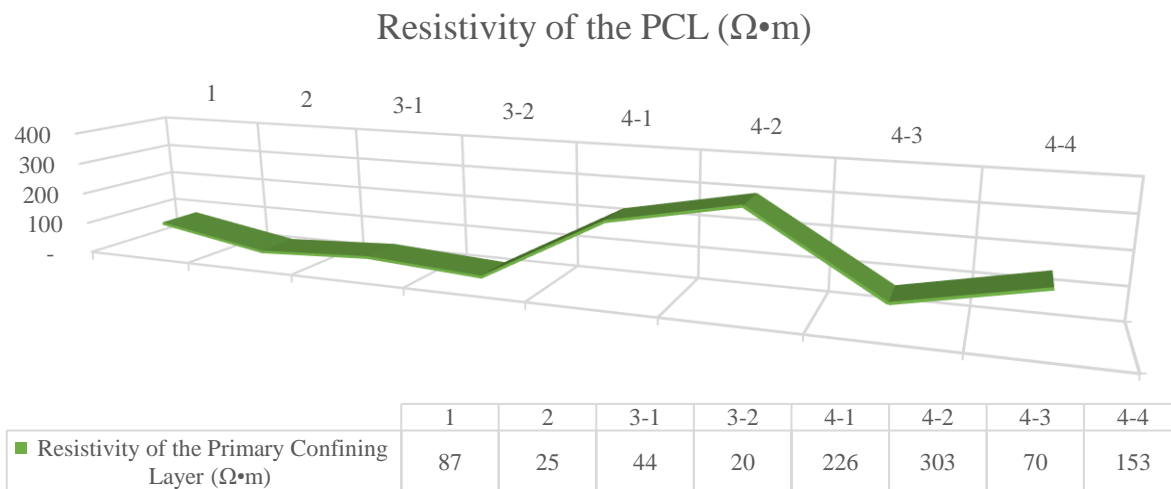


Figure 41. Over-arching geometry of the geoelectric resistivity of the PCL in Ohm-meters along the series of soundings across the Flathead Valley, Montana.

In Figure 42 the 1D recovered model geoelectric resistivity thicknesses of all the PCL soundings are combined into a plot highlighting an overview of what the over-arching geometry of the PCL's geoelectric resistivity layer thickness is doing along the series of soundings across the valley. Models where the PCL was represented as the basement of the model have no modeled thickness. Note that these thicknesses do not include Smith's (2022) interpreted tills in geoelectric resistivity layers 3-5 of Site 2, whose inclusion would raise the Site 2 level from the glaciolacustrine deposits 37-meters to, 9-meters for geoelectric resistivity layer-3, a peak of 94-meters for geoelectric resistivity layer-4 and 64-meters for geoelectric resistivity layer-5 of supraglacial till which would together make this 204-meters – and put Site 2 closer in range to the melt-out tills of Site 4 of the PCL in the Flathead Valley of Montana. From the interpretations in this paper, thickness peaks at the south end of the valley where the variable melt-out till predominates and dips where the glaciolacustrine deposits dominate. The average geoelectric resistivity layer thickness of the series of soundings is 131-meters thick. The variability of geoelectric resistivity layer thickness is especially evident in the southern end of

our series where the hummocky nature of the glacial deposits is reflected in the extreme variations at the Site 4 soundings.

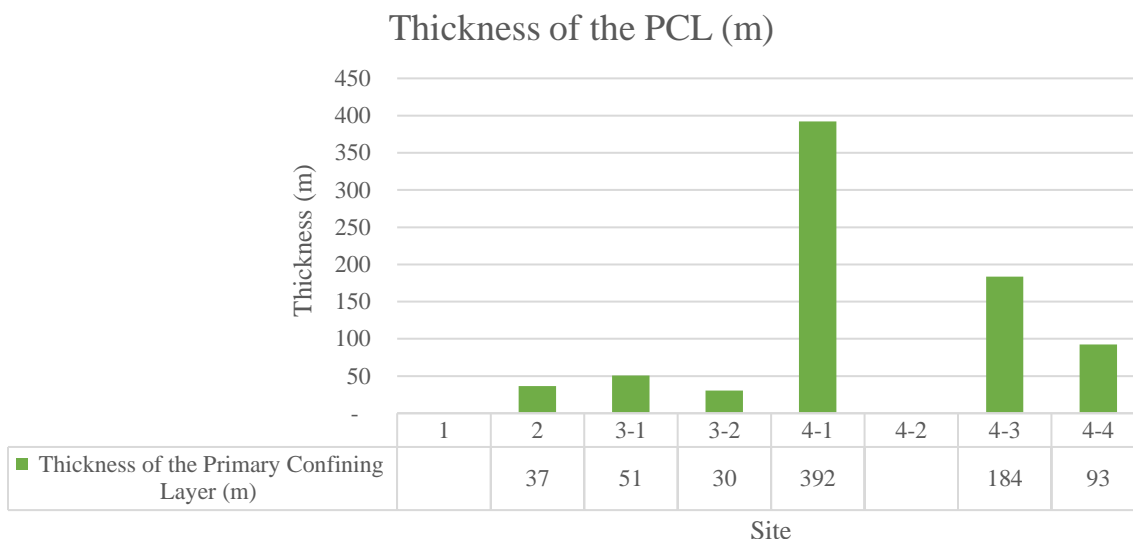


Figure 42. Over-arching geometry of the geoelectric resistivity layer thickness of the PCL in meters along the series of soundings across the Flathead Valley, Montana. Sites 1 and 4-2 recorded the PCL as the basement geoelectric layer and had no geoelectric resistivity layer thickness to report.

In Figure 43 the 1D recovered model geoelectric resistivity depth to top of all the PCL soundings are combined into a plot highlighting an overview of what the over-arching geometry of the PCL's depth to top is doing along the series of soundings across the valley. Note that these depths to the top of the PCL layer do not include Smith's (2022) interpreted tills in geoelectric resistivity layers 3-5 of Site 2, whose inclusion would raise the Site 2 PCL shallowest depth from the glaciolacustrine deposit at 177-meters to 10-meters for geoelectric resistivity layer-3, 19-meters for geoelectric resistivity layer-4 and 113-meters for geoelectric resistivity layer-5 of supraglacial till and place Site 2 at the shallowest depth to the top of the PCL in the Flathead Valley of Montana. From the interpretations in this paper, the average depth to top of the PCL is 238-meters deep. The depth to top of the PCL fluctuates with its shallowest component

corresponding to the glaciolacustrine deposits at 64-meters. The PCL is buried deeper where melt-out tills and subglacial tills predominate along the central-axis of the valley, except where fluvial and lacustrine processes have dominated in the post-glacial depositional period. The increase in depth is related to the post-glacial intermontane alluvial depositional processes. The shallower lacustrine alluvium overlying the glaciolacustrine are much finer sediments and as such take up less physical space than the coarser alluvial fan deposits overlying the remainder of the valley basin.

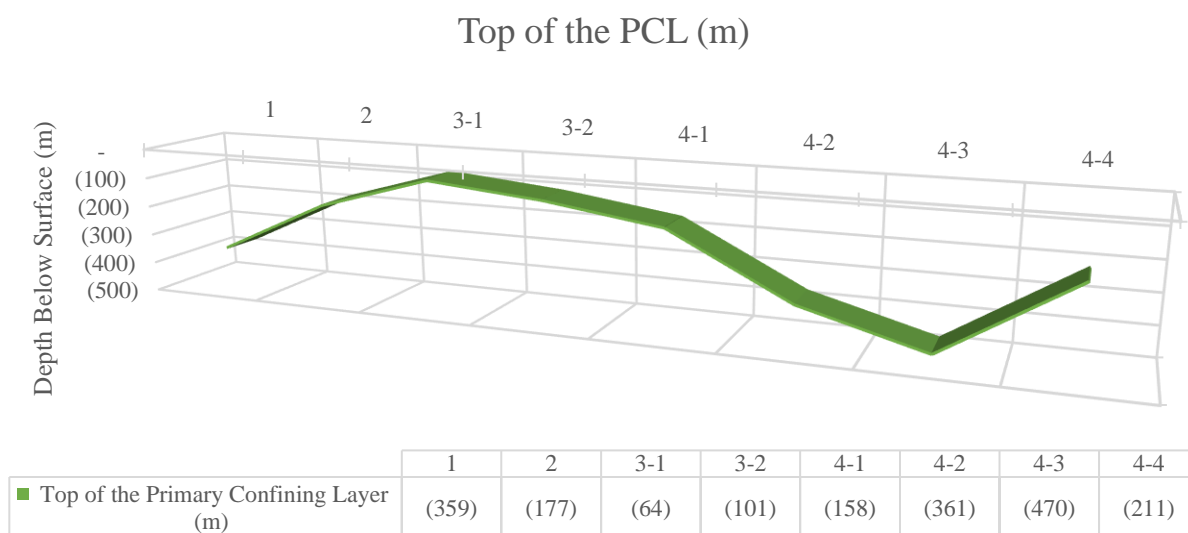


Figure 43. Over-arching geometry of the geoelectric resistivity layer depth to the top of the PCL in meters below the surface along the series of soundings across the Flathead Valley, Montana.

7. Conclusion

To accurately forecast the cascading effects of increased stress to a hydrologic system, characterization of the continuity and permeability of the primary confining layer (PCL) separating the shallow and deep intermontane alluvial aquifers is required. Geophysical methods provide a faster cost-effective alternative to drilling to acquire additional information on the changes of hydrostratigraphy with depth. Geoelectric resistivity models recovered through inversion of TEM central loop sounding data delineate changes in geoelectric resistivity properties with depth, providing information on the depth, thickness and geoelectrical resistivity of the hydrostratigraphy. Comparison of geoelectric resistivity models with well completion report lithologies and knowledge of the geologic history yield information about the estimated permeability of the hydrostratigraphy. When employed on a valley-wide scale, the geoelectric resistivity models can also divulge information on the spatial continuity of lithologies with distinct geoelectric properties.

In the Flathead Valley of northwestern Montana, a complex stratigraphic sequence of glacial sediments comprises the PCL. Intermontane valley glacial sediments include glaciolacustrine, glaciotectonite, supraglacial tills, subglacial traction tills and melt-out tills. The range of geoelectric resistivity of glacial sediments is highly variable and dependent on the composite soil composition as well as water content and resistivity. The key findings on the PCL composition of the Flathead Valley are the following:

- Glaciolacustrine sediments in the Flathead Valley are a very low geoelectric resistivity. The glaciolacustrine sediments are a clay-rich matrix yielding geoelectric resistivities between 20 and 50 Ohm-meters. The thickness of the deposit is a confirmed 56-meters at the BFF#5 well and around 50-meters at

nearby Site 3-1 at the Big Fork Farm Water Treatment Facility. The thickness varies down to around 30-meters at Site 3-2 and around 40-meters at Site 2. The depth from the surface varies from a confirmed 64-meters at Site 3-1 down to around 175-meters at Site 2 and 100-meters at Site 3-2. The PCL is present at Site 3-1 and 3-2 in confining glaciolacustrine sediments. Indication of a deeper low geoelectric resistivity layer at Site 2 indicates the potential presence of an unmapped deep confining unit along the eastern edge of the Flathead Valley warranting further investigation. Glaciolacustrine sediments represent a fully confining PCL.

- Subglacial traction tills may have been present in inter-mixed layers with glaciolacustrine deposits at Site 1 at one time, however the geoelectric resistivity data do not find evidence of the PCL in the known depth range of the area north of Flathead Lake. The possibility the PCL was severely eroded away by the Flathead River at Site 1 and is representative of a hole in the glacial layer is the most likely scenario. Subglacial traction tills could not be confirmed at Site 1.
- Supraglacial tills and subglacial traction tills intermixed with intermediate alluvium are present at Site 2 in the Flathead Valley as moderately to highly geoelectric resistive layers ranging from 1,914 Ohm-meters in layer-4 to 957 Ohm-meters at geoelectric resistivity layer-5. Correlating lithology indicates a thin uppermost alluvial layer overlying an intermixing of intermediate alluvial sediments washed down from the higher reaches of the medial moraine with supraglacial and englacial deposits intermixed with subglacial traction tills from

cycles of glacial advance and retreat. Supraglacial tills and subglacial traction tills intermixed with intermediate alluvium represent a leaky confining PCL.

- Melt-out tills in the Flathead Valley are moderately geoelectrical resistive layers with geoelectric resistivities ranging from 70 Ohm-meters at 4-3 to 303 Ohm-meters at 4-2 with 153 Ohm-meters at 4-4 and 226 Ohm-meters at 4-1. The thickness of the melt-out tills ranged from a low of 93-meters at sounding 4-4 to 392-meters at site 4-1 with 4-3 recovering a thickness of 184-meters and 4-2 had no thickness reported due to being the basement of the recovered model. Depth to top ranged from 158-meters for 4-1 to 470-meters at 4-3 with intermediate depths of 211-meters at 4-4 and 361-meters at 4-2. The differences between the depths to the top of the PCL at Site 4 are indicative of the hummocky nature of melt-out tills. The eastern and western lithologies are as variable as the soundings, with the eastern lithologies semi-consolidated to consolidated massive type I composite soils and western lithology consistent with fluvial deposition containing type I and type II composite soils with gravel sequences. Melt-out tills represent a leaky-confining PCL.

References

- Banham, P. (1977). Glacitectorites in till stratigraphy. *Boreas*, 6(2), 101-105.
doi:10.1111/j.1502-3885.1977.tb00339.x
- Benn, D., & Evans, D. (2010). *Glaciers and Glaciation*. London, UK: Routledge.
- Bobst, A., Berglund, J., & Snyder, D. (2020, July). The East Flathead Groundwater Investigation. Montana: Montana Bureau of Mines and Geology.
- Clark, B. (2018). The engineering properties of glacial tills. *Geotechnical Research*, 5(4), 262-277. doi:10.1680/jgere.18.00020
- Dictionary*. (1828). Retrieved from Merriam-Webster Dictionary: <http://www.merriam-webster.com/dictionary>
- Earle, S. (2015). Chapter 14.1: Groundwater and Aquifers. In *Physical Geology*. Pressbooks.
- Enemark, T., Peeters, L., Mallants, D., Flinchum, B., & Batelaan, O. (2020). A Systematic Approach to Hydrogeologic Conceptual Model Testing, Combining Remote Sensing and Geophysical Data. *Water Resources Research*, 56(8). doi:10.1029/2020WR027578
- Environmental Protection Agency. (n.d.). *EPA Web Archives*. Retrieved from <https://archive.epa.gov>
- Evans, D., Phillips, E., Hiemstra, J., & Auton, C. (2006). Subglacial till: Formation, sedimentary characteristics and classification. *Earth-Science Reviews*, 115-176.
doi:10.1016/j.earscirev.2006.04.001
- Flathead County Montana. (n.d.). *About Flathead County*. Retrieved from Flathead County Montana: https://www.flathead.mt.gov/about_flathead_county/index.php
- Griffiths, D. J. (2019). *Introduction to Electrodynamics*. Cambridge University Press.

- Ground Water Information Center; Montana Bureau of Mines and Geology; Montana Technological University. (1998-2022). Retrieved from Montana's Ground Water Information Center: <http://www.mbmggwic.mtech.edu>
- Hyndman, D., & Thomas, R. (2020). *Roadside Geology of Montana* (2 ed.). Missoula, Montana: Mountain Press Publishing.
- LaFave, J., Smith, L., & Patton, T. (2004). *Ground-Water Resources of the Flathead Lake Area: Flathead, Lake, Missoula, and Sanders Counties, Montana*. Montana Bureau of Mines and Geology.
- Martini, I., Brookfield, M., & Sadura, S. (2001). *Principles of Glacial Geomorphology and Geology*. Prentice Hall.
- Montana Bureau of Mines and Geology. (n.d.). GM 62-D GIS packed map `usgs_Geology_500k.mpk`. (E. Breitmeyer, Ed.)
- Montana State Library Geographic Information. (n.d.). Montana Base Layer Map.
- Montana State Library GIS Services. (n.d.). Base Map from MDSI-Framework database. *NAIP 2019 digital orthographic image*.
- Montana Tech - Montana Bureau of Mines and Geology. (2021). *3 Arm Caliper Volume & Natural Gamma Log Report for BFF#5 FVDeep Project*. Flathead: Colog, Inc.
- Montana Tech - Montana Bureau of Mines and Geology. (2021). *Geophysical Summary Plot of FV Deep BFF#5*. Colog, Inc.
- Montana Tech - Montana Bureau of Mines and Geology. (2021). *Neutron and Density Log Report for BFF#5 FVDeep Project*. Flathead: Colog Inc.
- National Geographic Society, i-cubed. (n.d.). `USA_Topo_Maps`.

- Noble, R., & Stanford, J. (1986). *Ground-water resources and water quality of unconfined aquifers in the Kalispell valley, Montana: Montana Bureau of Mines and Geology Open-File Report 177*. Montana Bureau of Mines and Geology.
- Palacky, G. (1987). Resistivity Characteristics of Geologic Targets. In M. Nabighian (Ed.), *Electromagnetic Methods in Applied Geophysics - Theory* (Vol. 1, pp. 53-56). Tulsa, Oklahoma: Society of Exploration Geophysicists.
- Pedersen, S. (1988). *Glacitectonite: Brecciated Sediments and Cataclastic Sedimentary Rocks Formed Subglacially* (Vol. 43). Copenhagen, Denmark: Geological Survey of Denmark.
- Petite, B. (2022, January 5). Vertical Rewind: Dr. Hans Lundberg, the prospecting pioneer. *Vertical*.
- Ravier, E., & Buoncristiani, J. (2018). Chapter 12: Glaciohydrogeology. *Past Glacial Environments*, 431-466. doi:10-1016/B978-0-08-100524-8.00013-0
- Reynolds, J. (2011). *An Introduction to Applied and Environmental Geophysics* (2 ed.). John Wiley & Sons, Ltd.
- SkyTem. (2022, April 3). *Groundwater and Environmental*. Retrieved from SkyTEM: <https://skytem.com/water-mapping/>
- Smith, L. (2004). Thickness of the Confining Unit in the Kalispell Valley, Flathead County, Montana. In L. Smith, J. LaFave, C. Carstarphen, D. Mason, & M. Richter, *Ground-water resources of the Flathead Lake Area: Flathead, Lake, and parts of Missoula and Sanders counties. Part B-Maps: Montana Bureau of Mines and Geology Ground-water Assessment Atlas 2-B*. Montana Bureau of Mines and Geology - A Department of Montana Tech of The University of Montana.

Smith, L. (report in preparation 2022). *Flathead SW-NE Cross Section of Deep Aquifer Drilling Report*. Montana Bureau of Mines & Geology.

Spies, B. (1989). Depth of investigation in electromagnetic sounding methods. *GEOPHYSICS*, 54(7), 872-888.

United States Census Bureau. (n.d.). *Cumulative Estimates of Resident Population Change for Counties and County Rankings: April 1, 2010 to July 1, 2019*. Retrieved from County Population Totals: 2010-2019: <https://www.census.gov/data/datasets/time-series/demo/popest/2010s-counties-total.html> Montana: co-est2019-cumchg-30.xlsx

United States Department of Agriculture. (n.d.). *2017 Census of Agriculture*. Retrieved from National Agricultural Statistics Service: https://www.nass.usda.gov/Publications/AgCensus/2017/Online_Resources/County/Profiles/Montana/cp30029.pdf

Veleva, L. (2005). Soils and Corrosion. In *Corrosion Tests and Standards Manual* (2 ed.).

Wilson, G. A., Raiche, A., & Sugeng, F. G. (2007). Practical 3D EM Inversion - The P223F Software Suite. *ASEG Extended Abstracts*, 1(1), 1-5. doi:10.1071/ASEG2007ab165

Zonge International. (2002). Section 12. Transient Electromagnetic Program. In *GDP-32II Instruction Manual* (pp. 1-52).

Appendix A: Future Work

Helicopter Airborne Electromagnetics (H-AEM)

First developed in the 1946 by Hans Lundberg (Petite, 2022). H-AEM technology has the ability to collect millions of data points in a fraction of the time ground surveys can be laid out. An H-AEM survey is capable of providing a valley-wide map of the PCL that can fully delineate the continuity and over-arching geometry.

The survey design consists of a rigid electromagnetic transmitter loop and receiver suspended below the helicopter, Figure 44. Flight lines are run parallel and provide a cross-sectional view of the returned data along the flight path. All of the flight paths can then be stitched together using the industry standard Seequent Oasis Montaj software suite to provide 2D or 3D models of the subsurface data.

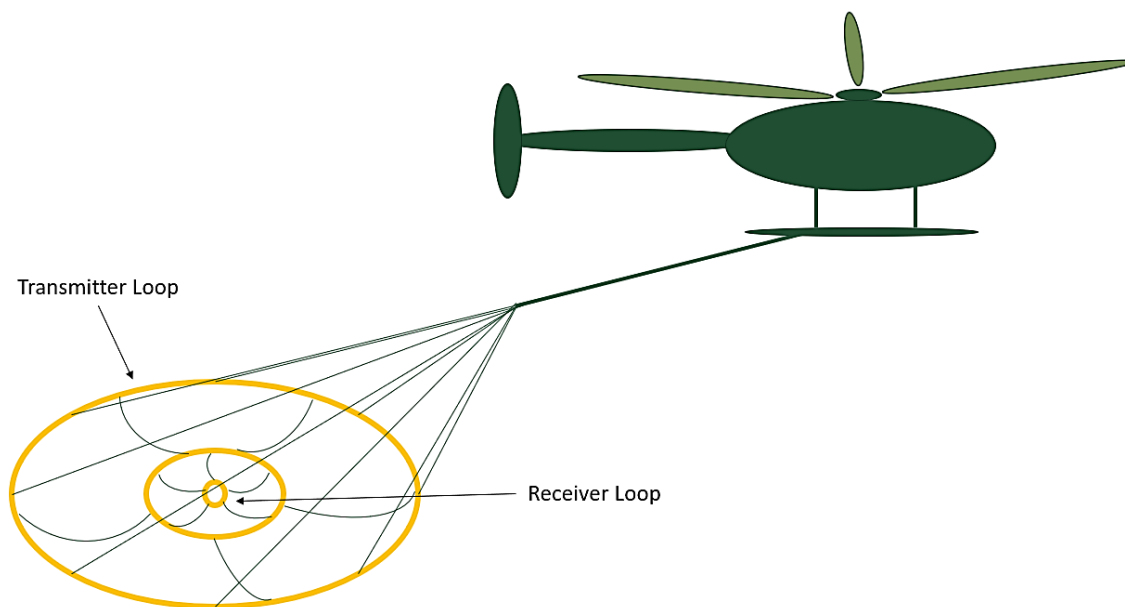


Figure 44. Diagram of helicopter airborne electromagnetic survey design.

SkyTEM is a world-wide full-service provider of H-AEM geophysical services. They are able to characterize aquifers from the very near surface to over 500-meters depth (SkyTem,

2022). Their collection rate is comparable to collection of a borehole data point every 3-meters and they can cover up to 1,000-kilometers per day in ideal conditions (SkyTem, 2022).

Appendix B: Data

Table 1. GDP data set FV-S5-TEM1 Sounding at 4 Hz. Time gate is centered at time W_n , the voltage out is $MAG I$, and the apparent resistivity is $Rho I$.

0117								
TEM	0859	2020-08-07	15:32:14	12.9v	INL	58.2%	22.8 DegC	
Tx		1 Rx	2 N OUT					
	4 Hz	128 Cyc Tx	Curr 5	91.55u	26u	30.52u		
1 Hz	0	377.96u	810.0u	33.60	0000	164.2u	-3.98	0
	W_n	Mag 1	Rho 1					
35.55u		-0.9000	34.505					
66.07u		-0.5566	16.923					
96.59u		-71.162m	35.409					
127.1u		-4.5743m	139.64					
157.6u		-626.03u	367.33					
188.1u		-29.290u	2106.4					
233.3u		212.48u	392.64					
294.5u		295.42u	213.82					
355.6u		320.58u	147.87					
431.1u		304.84u	110.95					
522.9u		364.67u	71.376					
642.8u		375.12u	49.644					
810.0u		377.96u	33.603					
1.008m		353.56u	24.409					
1.250m		316.72u	18.342					
1.554m		247.86u	15.033					
1.946m		111.20u	17.623					
2.461m		-78.868u	14.982					
3.099m		-222.61u	5.1087					
3.888m		-493.72u	2.0592					
4.874m		-634.06u	1.1957					
6.129m		-674.74u	0.7829					
7.723m		-516.37u	0.6367					
9.695m		-237.47u	0.7315					
12.18m		433.26u	0.3350					
15.33m		583.31u	0.1872					
19.29m		-125.63u	0.3553					
24.27m		-488.16u	97.997m					
30.57m		489.61u	66.609m					
38.45m		-376.85u	54.101m					
48.42m		263.37u	46.787m					

Appendix C: Python Processing Scripts

Table 2. `plotZT.py` script developed by Dr. Trevor Irons to invert the central loop sounding data and produce a geoelectric resistivity model using the *Beowulf* algorithm.

```

import numpy as np
import matplotlib.pyplot as plt
from matplotlib import cm
import matplotlib as mpl

plt.rcParams.update({
    "font.family": "serif", # use serif/main font for text elements
    "text.usetex": True, # use inline math for ticks
    "pgf.rcfonts": False # don't setup fonts from rc parameters
})

import sys
import glob
import scipy.stats
from io import StringIO
plt.style.use('ggplot')

import ruamel.yaml as yaml
import subprocess

#TXDLY = 15e-6
#ANTDLY = 15e-6

# From the GDP manual, section 12.9.
# these apply to 32, 16, 8 and 4 Hz for centre
# values, others can be calculated.
WINTBL = """
1 1 0.0u 0.0u 0.0u
2 1 30.5u 30.5u 30.5u
3 1 61.0u 61.0u 61.0u
4 1 91.6u 91.6u 91.6u
5 1 122.1u 122.1u 122.1u
6 1 152.6u 152.6u 152.6u
7 2 197.8u 183.1u 213.6u
8 2 259.0u 244.1u 274.7u
9 2 320.1u 305.2u 335.7u
10 3 395.6u 366.2u 427.3u
11 3 487.3u 457.8u 518.8u
12 5 607.3u 549.3u 671.4u
13 6 774.5u 701.9u 854.5u
14 7 972.3u 885.0u 1.068m
15 9 1.215m 1.099m 1.343m
16 11 1.518m 1.373m 1.678m

```

```

17 15 1.911m 1.709m 2.136m
18 19 2.426m 2.167m 2.716m
19 23 3.064m 2.747m 3.418m
20 29 3.852m 3.449m 4.303m
21 36 4.838m 4.334m 5.402m
22 47 6.094m 5.432m 6.836m
23 58 7.687m 6.867m 8.606m
24 72 9.659m 8.637m 10.803m
25 92 12.14m 10.834m 13.611m
26 116 15.30m 13.642m 17.151m
27 145 19.25m 17.182m 21.576m
28 184 24.24m 21.607m 27.192m
29 231 30.53m 27.222m 34.241m
30 289 38.42m 34.272m 43.061m
31 369 48.38m 43.091m 54.322m
"""

def convert(number):
    """
    Converts GDP data which may contain scaling factors into floats

    Args:
        number (string) : String representation of a number, eg. 1.234u which is
            converted to 1.234e-6

    Returns:
        float: The converted number in floating point precision.

    """
    if number[-1].isalpha():
        sc = number[-1]
        if sc == 'M':
            return float(number[0:-1])*1e6
        elif sc == 'K':
            return float(number[0:-1])*1e3
        elif sc == 'm':
            return float(number[0:-1])*1e-3
        elif sc == 'u':
            return float(number[0:-1])*1e-6
        elif sc == 'n':
            return float(number[0:-1])*1e-9
    else:
        # default case of no scaling factor
        return float(number)

def extractWindowTuples(WIN):

```



```

"""Convenience function that converts a window matrix to tuples of
windows for a particular record.
"""
wt = []
for iw in range(len(WIN)):
    wt.append( np.array( [WIN[iw][1], WIN[iw][2]] ))
return np.array(wt)

class TEMSounding( ):
    """
    SuperClass for TEM soundings
    """

    def __init__( self ):
        self.nStack = 0
        self.nTimeGates = 0

class ZeroTEMSounding( TEMSounding ):
    """
    A ZeroTEM sounding as recorded by Zonge instrumentation.
    """

    def __init__(self):
        super(ZeroTEMSounding, self).__init__()
        self.stacks = []
        self.CTRL = []

    def loadStack(self, stackDir):
        """
        Loads a directory of stacks, each stack in the directory is assumed to have the same
        parameters including sampling frequency and current. If a series of stacks has already
        been
        loaded, they will be replaced by this record.

        Args:
            stackDir : Directory path containing the stacks
        """
        print(stackDir)

        try:
            self.CTRL = yaml.load(open(stackDir+'/control.yaml'), Loader=yaml.Loader)
        except:
            print("No Control file found!", stackDir+'/control.yaml')
            exit(1)

```

```

TXABS = self.CTRL['TxAbs']
TXAMP = self.CTRL['TxAmp']

self.WN, self.MAG, self.RHO = [],[],[]
for SND in glob.glob(stackDir+"/*.SND"):
    self.stacks.append(SND)
    wn, mag, rho, WIN = self.loadSND(SND)
    self.WN.append(wn)
    self.MAG.append(mag)
    self.RHO.append(rho)
    self.nStack += 1

self.WIN = WIN # all windows **should** be aligned, TODO be more careful
self.WN = np.array(self.WN).T
self.MAG = np.array(self.MAG).T
self.RHO = np.array(self.RHO).T
print ("Loaded", self.nStack, "soundings in", stackDir)

def plotStack(self, freq, site):
    """
    Plots the stacked and averaged data
    """
    global firstPlot
    global ax1
    global ax2

    fig = plt.figure(0, figsize=(7.0,6.0))
    if firstPlot:
        ax1 = fig.add_axes([.15,.300,.8,.65])
        ax2 = fig.add_axes([.15,.100,.8,.15], sharex=ax1)
        #ax2 = fig.add_axes([.15,.15,.75,.75], sharex=ax1)

    # calculate average
    self.AVG = np.average(self.MAG, axis=1)

    # go ahead and fix sign errors
    if self.AVG[0] < 0:
        self.AVG *= -1.
        self.MAG *= -1.

    neg = self.MAG <=0
    pos = self.MAG > 0

    ax1.plot(self.WN[neg], self.MAG[neg], '_', alpha=.25, color=colours[isnd]) # grey
    ax1.plot(self.WN[pos], self.MAG[pos], '+', alpha=.25, color=colours[isnd])

```

```

#ax1.plot(self.WN, self.MAG, 'o', alpha=.15, markersize=3, color=colours[isnd]) # grey

if np.shape(self.MAG)[1] > 1:
    self.STD = np.std( self.MAG, axis=1 )
else:
    self.STD = 1e-5*np.ones( len(self.AVG) )
    #self.STD = np.std(self.AVG[-8::]) * np.ones(len(self.AVG))
    #print("assigning dummy variance", self.STD)
#self.STD[self.STD<1e-5] += 5e-4

neg = self.AVG <=0
pos = self.AVG > 0

self.mask = np.abs(self.AVG) < 1. * self.STD
if self.STD[0] < 1e-7:
    # self.mask[0] = True
    self.STD[0] += self.STD[1]

#self.mask[0:1] = True
#self.mask[3:] = True

#ax1.plot(self.WN, self.mask, 'o', alpha=.25, markersize=8, color='black')

# average apparent resistivity
AVGR = np.average(self.RHO, axis=1)

# simple average
#plt.scatter(self.WN[neg,0], -1*AVG[neg], marker='_', color = colours[isnd], alpha=1,
s=80)
#plt.scatter(self.WN[pos,0],  AVG[pos], marker='+', color = colours[isnd], alpha=1,
s=80)
#plt.plot(self.WN[:,0], np.abs(AVG), '-', color=colours[isnd], alpha=1, label=freq)

ax1.plot(self.WN[:,0], self.AVG, '-', color=colours[isnd], alpha=1, linewidth=1)
ax1.errorbar(self.WN[:,0], self.AVG, yerr=self.STD, fmt='o', markersize=4,
markeredgecolor='black', markeredgewidth=.5, color=colours[isnd], alpha=1, label=freq)

if firstPlot:
    ax1.plot(self.WN[self.mask,0], self.AVG[self.mask], 's', color='black', alpha=1,
markersize=5, label='masked')
else:
    ax1.plot(self.WN[self.mask,0], self.AVG[self.mask], 's', color='black', alpha=1,
markersize=5)

```

```

# SNR
ax2.plot(self.WN[:,0], 20*np.log10(np.abs(self.AVG/(self.STD))), '-.',
color=colours[isnd], alpha=1, label=freq)
ax2.axhline(y=1, linestyle='--', color='black')

# reject above 2 STD
if False:
    #STD = np.std( self.MAG, axis=1 )
    OUT = self.MAG-np.tile(self.AVG, (self.nStack,1)).T > 2.*np.tile(self.STD,
(self.nStack,1)).T
    print("Removed", np.sum(OUT), "outliers")
    self.AVG = np.ma.masked_array(self.MAG, OUT==True).mean(axis=1)
    #plt.plot(self.WN[:,0], AVG2, '-', color=colours[isnd+1], alpha=1, label=freq)

if False:
# MAD outlier detection
MAD = scipy.stats.median_abs_deviation( self.MAG, axis=1, scale="normal" )
MED = np.tile(np.median(self.MAG, axis=1), (self.nStack,1)).T
OUT = ( np.abs(self.MAG-MED) / np.tile(MAD, (self.nStack,1)).T ) > 2
print("Removed", np.sum(OUT), "outliers")
self.AVG = np.ma.masked_array(self.MAG, OUT==True).mean(axis=1)
#plt.plot(self.WN[:,0], AVG2, '-', color=colours[isnd+1], alpha=1, label=freq)

ax1.set_yscale('symlog', linthresh=self.STD[-1:])
ax2.set_yscale('symlog') #, linthresh=1e-6)
#ax2.set_yscale('log')
#ax1.xaxis.set_ticklabels([])

ax1.set_xscale('log')
#ax1.set_xscale('symlog', linthresh=1e-5)
#ax2.set_xscale('log')
ax2.set_xlabel("time (s)")
ax1.set_ylabel("$\dot{H}_z$ (V)")
ax2.set_ylabel("S:N (dB)")
ax1.set_title(site)

# don't show tick labels on top plot
ax1.xaxis.set_tick_params(which='both', labelbottom=False)

ax1.legend( )

global pgfTitle
try:
    pgfTitle += "_" + str(freq)
except:

```

```

    pgfTitle = str(freq)

plt.savefig(pgfTitle+"_stack.pgf")
plt.savefig(pgfTitle+"_stack.pdf")

# apparent resistivity plot
if False:
    plt.figure(1, figsize=[3,4])
    plt.plot( self.WN[:,0], AVGR )
    plt.title("resistivity")
    plt.gca().set_ylabel("Apparent resistivity ( $\Omega \cdot \mathbf{m}$ )")
    #plt.gca().set_yscale('log')
    plt.gca().set_xscale('log')
    plt.gca().set_xlabel("time (s)")
    plt.savefig(pgfTitle+"_ar.pgf")

firstPlot = False

# write out Beowulf inversion files
#writeCFL("Beowulf.cfl")
#writeINV("Beowulf.inv", MAG)

def loadSND(self,filename):
    """
    Loads a sounding saved by a GDP

    Args:
        filename(string) : the filename to load

    """

    inp = open(filename, 'r')
    lines = inp.readlines()
    inp.close()

    header = []
    for hl in range(6):
        header.append(lines[hl])

    WIN = self.calculateWindows(header)

    wn, mag, rho = [],[], []
    for fl in range(6, len(lines)):
        parse = (lines[fl].split())
        if len(parse) > 0:

```

```

        wn.append(convert(parse[0]))
        mag.append(convert(parse[1]))
        rho.append(convert(parse[2]))

    if len(wn) != self.nTimeGates:
        if self.nTimeGates == 0:
            self.nTimeGates = len(wn)
        else:
            # TODO consider an exception here
            print("Attempt to stack non-aligned SND files")
            exit()

    return(np.array(wn),np.array(mag),np.array(rho),WIN)

def Window(self, hz, offset):
    """
    Determintes the windows based on Zonge table data which are a function
    of Tx, Rx, and sampling delay.
    """
    sc = 1.
    if hz < 4:
        sc = 4./hz
    return np.genfromtxt(StringIO(WINTBL), dtype=[('WN','i8'),('NP','i8'),('win_centre','f8'),
        ('win_beg','f8'),('win_end','f8)], comments="#", converters=\
        {2: lambda s: convert(s.decode('utf-8'))*sc + offset ,\
        3: lambda s: convert(s.decode('utf-8'))*sc + offset ,\
        4: lambda s: convert(s.decode('utf-8'))*sc + offset })

def calculateWindows(self, header):
    """
    Parses the header data of a GDP record in order to extract window information,
    Uses Window function to do this as well.
    """
    recordNumber = header[0] # just the GDP record index
    # Parse second line
    stype, gpdN, date, time, batt, rtype, humidity, temp, tunits = header[1].split()
    # Parse third line
    Tx, nRx, Rx, line, NSEW, out = header[2].split()
    # parse 4th line
    Freq, Hz, Ncycles, Cyc, Tx, Curr, Amps, sampDly, aAliasDly, offset = header[3].split()
    sampDly = convert(sampDly)
    aAliasDly = convert(aAliasDly)
    offset = convert(offset)

    self.Freq = Freq

```

```

self.sampDly = sampDly

# save
self.sampFreq = float(Freq)
self.Amps = Amps

# the time gates are adjusted for low frequency datasets
sc = 1.
if float(Freq) < 4:
    sc = 4./float(Freq)

# Calculate 1st time gate according to manual, seems consistent with table
First = sampDly - (self.CTRL["TXDLY"]+self.CTRL["ANTDLY"]+aAliasDly)

# 2e-7 is an ad hoc correction that seems to work across datasets
SAMPLING = np.arange(1,2000)*(offset - sc*2e-7)

# grab data from table, TODO can probably just grab the single column we need
samp = self.Window(float(Freq), offset) #-(TXDLY+ANTDLY))

wc,wb,we,ii = [First],[First],[First],[1]
sStart = 0 # always starts at a 1 sample at First
for iw in range(1,len(samp)):
    sEnd = sStart + samp[iw][1]

    wc.append( First + np.mean( SAMPLING[sStart:sEnd] ) )
    wb.append( First + SAMPLING[sStart] )
    we.append( First + SAMPLING[sEnd-1] )
    ii.append( samp[iw][1] )
    sStart = sEnd

return np.array( (wc,wb,we,ii) ).T

def export(self, sdir):

    self.writeCFL("Beowulf.cfl", sdir)
    self.writeINV("Beowulf.inv", np.average(self.MAG, axis=1))

def writeCFL(self, fname, sdir):

    try:
        CTRL = yaml.load(open(sdir+'control.yaml'), Loader=yaml.Loader)
    except:
        print("No Control file found! Cannot export CFL for inversion")
        exit(1)

```

```

if CTRL["Invert"] == "False":
    return

TXABS = CTRL['TxAbs']
TXAMP = CTRL['TxAmp']

# dummy waveform base length on
#TXAMP = [0., 4.5, 4.5, 0.5, 0.]
#TXABS = [0, 1.5, 1e3*0.5/self.sampFreq-0.125, 1e3*0.5/self.sampFreq] # Good for 1
Hz
#TXABS = [0, 1.5, \
# 1e3*0.5/self.sampFreq-0.025, \
# 1e3*0.5/self.sampFreq-0.015, \
# 1e3*0.5/self.sampFreq]

# if self.Freq == "1":
# #####
# # 1 Hz from WFM file
# TXABS = np.array([ 0. , 0.42 , 249.958, 250.09 ]) #
# TXAMP = [0.,4.25,4.25,0] # wfm file #
# #####
# elif self.Freq == "8":
# #####
# # 8 Hz from WFM file
# TXABS = np.array([ 0. , 0.5 , 31.22, 31.35]) # 8 Hz from #
# TXAMP = [0.,4.25,4.25,0] # wfm file #
# #TXABS = np.array([ 0. , 0.5 , 31.22, 31.249]) # 8 Hz from #
# #TXAMP = [0.,4.25,4.25,0] # wfm file #
# #####
# elif self.Freq == "16":
# #####
# # 16 Hz from WFM file
# TXABS = [0.,0.05,0.75,15.65,15.75] # 16 Hz, from WFM file #
# TXAMP = [0.,2.5,4.25,4.25,0] #
# #####
# elif self.Freq == "32":
# #####
# # 16 Hz from WFM file
# TXABS = [0.,0.495,7.809,7.92] # 32 Hz, from WFM file #
# TXAMP = [0.,4.25,4.25,0] #
# #####

# Good for 1 Hz

```



```

#TXABS = [0, 1.5, 1e3*0.5/self.sampFreq-0.025, 1e3*0.5/self.sampFreq] # Good for 16
Hz
#TXABS = [-1e3*0.5/self.sampFreq, -1e3*0.5/self.sampFreq+1.5, 0, 1.5] # TODO look
at WFM files

cw = open(fname, "w")
# RECORD 1
cw.write("Flathead inversion\n")
#####
# RECORD 2 #
#####
cw.write("1 0 0          !TDFD, ISYS, ISTOP\n")
#####
# RECORD 3 #
#####
# Step 0 = db/dt
# NSX = number of points to describe waveform
# NCHNL = number of time gates
# KRXW = time gates described as start to end (1) or centre and width (2)
# REFTYM = Zero time for data
# OFFTIME = time between cycles in ms
cw.write("0 %2.i " %len(TXAMP))
#cw.write( str(self.nTimeGates) + " 2 " ) # n time gates, KRXW
print("Number of non-masked time gates", np.sum(self.mask==0))
cw.write( str(np.sum(self.mask==0)) + " 2 " ) # n time gates, KRXW
# REFTYM : GDP starts the clock at the start of the ramp off...I THINK TODO verify
# OFFTIME is not saved explicitly in GDP files, this is a rough approximation...
#cw.write(" 0.0 %2.4f " %(.5/self.sampFreq))
#cw.write(" %2.4f %2.4f " %(TXABS[-2], 1e3*(.5/self.sampFreq)) )

#####
#
#cw.write(" %2.4f %2.4f " %(TXABS[-1]-.039, TXABS[-1])) # 16 Hz      #
#cw.write(" %2.4f %2.4f " %(TXABS[-1]-.03855, TXABS[-1]))          #
#cw.write(" %2.4f %2.4f " %(TXABS[-1]-.03863, TXABS[-1])) # From header #
cw.write(" %2.4f %2.4f " %(TXABS[-1] - CTRL['DlyOffset'], TXABS[-1]))
#cw.write(" %2.4f %2.4f " %( np.average(TXABS[-2:]) - CTRL['DlyOffset'], TXABS[-
1]))

#   if self.Freq == "1":
#       #cw.write(" %2.4f %2.4f " %(TXABS[-1]-.10, TXABS[-1]))
#       cw.write(" %2.4f %2.4f " %(TXABS[-1], TXABS[-1]))
#   elif self.Freq == "8":
#       cw.write(" %2.4f %2.4f " %(TXABS[-1]-.039, TXABS[-1])) # 10.04 RMS, S4-1
#       #cw.write(" %2.4f %2.4f " %(TXABS[-2]+.125, TXABS[-1])) # 10.04 RMS, S4-1

```

```

#      #cw.write(" %2.4f %2.4f " %(TXABS[-2], TXABS[-1])) # 10.04 RMS, S4-1
#      #cw.write(" %2.4f %2.4f " %(TXABS[-1], TXABS[-1])) # 10.04 RMS, S4-1
#      elif self.Freq == "16":
#      #cw.write(" %2.4f %2.4f " %(TXABS[-1]-.03863, TXABS[-1])) # 19.07 RMS, S3B
#      cw.write(" %2.4f %2.4f " %(TXABS[-1]-.038, TXABS[-1])) # 19.07 RMS, S3B
#      #cw.write(" %2.4f %2.4f " %(TXABS[-1], TXABS[-1]))
#      elif self.Freq == "32":
#      cw.write(" %2.4f %2.4f " %(TXABS[-1]-.040, TXABS[-1])) # 11.85 RMS, S4-1

#####
#

#cw.write(" %2.4f %2.4f " %(TXABS[-2], 1e3*(.5/self.sampFreq)) )
cw.write( " !STEP, NSX, NCHNL, KRXW, REFTYM, OFFTIME")

for ii in range(len(TXAMP)):
    cw.write("\n%8.3f %7.3f" %(TXABS[ii], TXAMP[ii]))
    cw.write("      !Tx Wvfm: abscissa (ms), current (A)\n")

# write out data gates...
width = self.WIN[:,2] - self.WIN[:,1]
width1 = (self.WIN[1,0]-self.WIN[0,0]) / 2
width[width<width1/2] = width1 # I'm not sure if zero length widths are allowed

# KRXW==1 start and off time
#for tg in range(self.nTimeGates):
#    cw.write( "%9.4f %7.4f\n"
%((round(1e3*self.WN[tg,0],5)),(round(1e3*width[tg],5))))

# KRXW==2 requires these to follow each other
for tg in range(self.nTimeGates):
    if self.mask[tg] == False:
        cw.write( "%9.4f\n" %((round(1e3*self.WN[tg,0],5))))
for tg in range(self.nTimeGates):
    if self.mask[tg] == False:
        cw.write( "%9.4f\n" %((round(1e3*width[tg],5))))

cw.write("1      !SURVEY_TYPE: General\n")

# Transmitter
Txtype = CTRL["Txtype"]
TxSz = CTRL["TxSize"]

#Txtype = "Circle"

```

```

if Txtype == "Circle":
    print("Using 55m CIRCULAR transmitter")
    rad = TxSz
    TXX = rad*np.sin(np.linspace(0,2*np.pi,32, endpoint=False))
    TXY = rad*np.cos(np.linspace(0,2*np.pi,32, endpoint=False))
else:
    print("Using 100m SQUARE transmitter")
    TXX = np.array( [-TxSz/2, TxSz/2, TxSz/2, -TxSz/2] )
    TXY = np.array( [-TxSz/2, -TxSz/2, TxSz/2, TxSz/2] )
#plt.figure()
#plt.plot(TXX, TXY)
#plt.show()

cw.write("1 1 1 1 50 1          !N LINES, MRXL, NTX, SOURCE_TYPE, MAXVRTX,
NTURNS\n")
cw.write("%2.i 0          !Nvertex, elevation z" %(len(TXX)))
for i in range(len(TXY)):
    cw.write( "\n%8.3f %8.3f" %(TXY[i],TXX[i]) )
cw.write( "          !Tx[i] East, Tx North (m)\n")

# specify rx
#LINE(J), IDTX(J), RX_TYPE(J), NRX(J), UNITS(J)
cw.write( "1000 1 1 1 1          !Line txid, rxtype, nrx, units (V)\n")
# units 11 = nT/s

#CMP(J), SV_AZM(J),KNORM(J), IPLT(J), IDH(J), RXMNT(J)
cw.write("3 0 0 1 0 10000          !cmp, sv_azm, knorm, iplt, idh, rxmoment\n")
cw.write("0 0 0          !receiver position\n")

# Record 10
SMOOTH = CTRL['Smooth']
nilay = CTRL['Nlay']

if len(CTRL['SRes']) == 1:
    res = CTRL['SRes']*np.ones(nilay)
else:
    res = CTRL["SRes"]

if SMOOTH:
    #####
    # SMOOTH INVERSION
    #####
    cw.write("%i %i          ! NLAYER, NLITH\n" %(nilay, nilay))
    thick = np.geospace(3, 60, nilay)
    #res = 20*np.ones(nilay) #np.array([26, 12., 87, 187, 307, 364, 237, 28, 2565])

```

```

    for ii in range(nilay):
        cw.write("%2.2f 1 1 0 0 0          ! RES, RMU, REPS, CHRG, CTAU,
CFREQ(1) - Lyr1\n" %(res[ii]))
        for ii in range(nilay):
            cw.write("%i %i          ! LITH, THICK - Layer 1\n" %(ii+1, thick[ii]))
    else:
        #####
        # MINIMUM LAYER INVERSION
        #####
        cw.write("%i %i          ! NLAYER, NLITH\n" %(nilay, nilay))
        thick = np.geomspace(5, 100, nilay)
        #res = 20*np.ones(nilay) #np.array([26, 12., 87, 187, 307, 364, 237, 28, 2565])
        #res[0] = .01
        for ii in range(nilay):
            cw.write("%2.2f 1 1 0 0 0          ! RES, RMU, REPS, CHRG, CTAU,
CFREQ(1) - Lyr1\n" %(res[ii]))
            for ii in range(nilay):
                cw.write("%i %i          ! LITH, THICK - Layer 1\n" %(ii+1, thick[ii]))

        #cw.write("200.6 1 1 0 0 0          ! RES, RMU, REPS, CHRG, CTAU, CFREQ(1) -
Lyr1\n")
        #cw.write("200.6 1 1 0 0 0          ! RES, RMU, REPS, CHRG, CTAU, CFREQ(1) -
Lyr1\n")
        #cw.write("200.6 1 1 0 0 0          ! RES, RMU, REPS, CHRG, CTAU, CFREQ(1) -
Lyr1\n")
        #cw.write("200.6 1 1 0 0 0          ! RES, RMU, REPS, CHRG, CTAU, CFREQ(1) -
Lyr1\n")
        #cw.write("200.6 1 1 0 0 0          ! RES, RMU, REPS, CHRG, CTAU, CFREQ(1) -
Lyr1\n")
        #cw.write("200.6 1 1 0 0 0          ! RES, RMU, REPS, CHRG, CTAU, CFREQ(1) -
Lyr1\n")
        #cw.write("200.6 1 1 0 0 0          ! RES, RMU, REPS, CHRG, CTAU, CFREQ(1) -
Lyr1\n")
        #cw.write("200.6 1 1 0 0 0          ! RES, RMU, REPS, CHRG, CTAU, CFREQ(1) -
Lyr1\n")
        #cw.write("200.6 1 1 0 0 0          ! RES, RMU, REPS, CHRG, CTAU, CFREQ(1) -
Lyr1\n")
        #cw.write("1 5          ! LITH, THICK - Layer 1\n")
        #cw.write("2 10          ! LITH, THICK - Layer 2\n")
        #cw.write("3 20          ! LITH, THICK - Layer 2\n")
        #cw.write("4 40          ! LITH, THICK - Layer 2\n")
        #cw.write("5 65          ! LITH, THICK - Layer 2\n")
        #cw.write("6 25          ! LITH, THICK - Layer 2\n")
        #cw.write("7 25          ! LITH, THICK - Layer 2\n")

```

```

#cw.write("8 25          ! LITH, THICK - Layer 2\n")
#cw.write("9 25          ! LITH, THICK - Layer 2\n")
#cw.write("10           ! LITH - basement\n")

if SMOOTH:
    cw.write("%i 90 10 2          ! NFIX, MAXITS, CNVRG, INVPRT\n" %(nilay-1))
else:
    cw.write("0 90 1 2          ! NFIX, MAXITS, CNVRG, INVPRT\n")

# write out std err W CNVRG = 2
#std = np.average(self.MAG, axis=1)
#for ii in range(len(self.STD[self.mask!=1]) ):
#    cw.write( str(self.STD[self.mask!=1][ii] ) + "\n")
#cw.write(str(.9) + "\n")

# derivative search
cw.write(" 3          ! NDSTP\n")
cw.write(" 5 3 1    ! KPCT (1:NDSTP)\n")

if SMOOTH:
    # fixed layer thickness
    for ilay in range(1, nilay):
        cw.write("1 " + str(ilay) + " 2\n")

cw.close()

def writeINV(self, fname, data):
    bw = open(fname, "w")

    bw.write("0          ! FD_ORDER\n") # time domain

    # LINE_CHK FID for consistency with cfl file
    # NSTAT is the number of receivers / stations
    # KMP is the component, 3 == z component
    bw.write("1000 1 3 ! LINE_CHK, NSTAT, KMP(J)\n")

    bw.write("0    ! DATA_FLOOR(J)\n") # 16

    # write out the data now
    bw.write(" 1") # leading white space is in AMIRA example files?, Receiver channel
index

    sc = 1.
    if data[0] < 0:
        sc = -1.

```

```

for ii in range(len(data)):
    #bw.write(" " + str( round(data[ii] * 1e4, 5) ))
    if self.mask[ii] == False:
        bw.write(" " + str(sc*1e-4*data[ii]) ) # rx moment
bw.write("\n")
bw.close()

def invert(self, sdir):
    """ Calls AMIRA Beowulf inversion.
    """
    subprocess.call("./Beowulf")
    subprocess.call(["mv", "Beowulf.mv1", sdir+".mv1"])

def readMV1(self, filename):
    with open(filename) as mv1:
        print("opening MV1", filename)
        for line in mv1:
            lsplit = line.split()
            if len(lsplit) > 1 and lsplit[1] == "TIMES(ms)=":
                tg = np.array(lsplit[2:], dtype=float)
            if len(lsplit) > 1 and lsplit[1][0:7] == "LAYERS=":
                #nlay = np.array(lsplit[1][8:], dtype=int)
                nlay = np.array(lsplit[1].split("=")[1], dtype=int)
            if len(lsplit) > 1 and lsplit[1] == "FINAL_MODEL":
                sig = np.array( lsplit[2:nlay+2], dtype=float )
                thick = np.array( lsplit[nlay+2:], dtype=float )
            if len(lsplit) > 1 and lsplit[0] == "SURVEY_DATA":
                obs = np.array(lsplit[4:], dtype=float)
            if len(lsplit) > 1 and lsplit[0] == "MODEL_DATA":
                pre = np.array(lsplit[4:], dtype=float)

            # make bottom layer thick...
            thick = np.concatenate( [thick, [500]] )
            depth = np.concatenate( [[0], np.cumsum(thick)] )
            depthc = (depth[0:-1] + depth[1:]) / 2

        return sig, thick, depth, depthc, obs, pre, tg

def modelAppraisal(self, sdir):

    sig, thick, depth, depthc, obs, pre, tg = self.readMV1(sdir+".mv1")
    tg *= 1e-3

    #subprocess.call(["python", "plotMV1.py", sdir+".mv1"])
    #print("std", self.STD[self.mask!=1])

```

```

#print("obs - pre", np.abs(obs-pre))

print( "L2 norm=", np.linalg.norm( 1e4*(obs-pre) / (self.STD[self.mask!=1]) ))

# Spies DOI estimate
CTRL = yaml.load(open(sdir+'/control.yaml'), Loader=yaml.Loader)
beta = self.STD[self.mask!=1][-1]
if CTRL["Txtype"] == "Square":
    area = CTRL["TxSize"]**2
else:
    area = np.pi*(CTRL["TxSize"]**2)
I = CTRL["TxAmp"][-2]
rhoa = np.sum(np.dot(sig,thick)) / np.sum(thick) # ohm m^2

DOI = 0.55 * ((I * area * rhoa ) / beta)**.2

print("rho_a", rhoa)
print("beta", beta)
print("DOI", DOI)

figa = plt.figure(3, figsize=(7,4.5))
figa.clf()

figa.suptitle(sys.argv[-1] + " " + sdir + " inversion result", fontsize=16)

aax1 = figa.add_axes([.125,.45,.700,.40])
aax2 = figa.add_axes([.850,.45,.025,.40])
wmap = cm.get_cmap("viridis", 10)

aax1.set_title("Recovered model")

aax3 = figa.add_axes([.125,.1,.80,.15])
#aax4 = figa.add_axes([.125,.15,.75,.325], sharex=aax3)
#aax3.set_yscale('log')
#aax3.set_xscale('log')

aax3.set_title("Data fit")

#nnorm = mpl.colors.LogNorm(vmin=np.min(sig), vmax=np.max(sig))
nnorm = mpl.colors.LogNorm(vmin=1, vmax=1e3)
sigc = wmap( nnorm( sig ) ) # mpl.colors.LogNorm(vmin=np.min(sig),
vmax=np.max(sig)) #same as above
aax1.barh(depthc, width=sig, height=thick, color=sigc, alpha=1.)#color=wmap.colors)

```

```

aax3.plot(self.WN, self.MAG, 'o', alpha=.15, markersize=3, color=colours[isnd]) #,
label="Observed") # grey
aax3.errorbar(self.WN[:,0], self.AVG, yerr=self.STD, fmt='o', markersize=4, \
    markeredgecolor='black', markeredgewidth=.5, color=colours[isnd], alpha=1)

aax3.plot(tg, 1e4*obs, '.', color=colours[isnd], label="Observed")
aax3.plot(tg, 1e4*pre, '--', color='black', label="Predicted")

aax1.text(30, DOI - 10, "DOI (Spies, 1989)", fontsize=10)
aax1.axhline(DOI, color='black', linestyle='--')

#aax4.plot(tg, (obs-pre)/(1e-4*self.STD[self.mask!=1]), '-.',label="misfit")

aax3.set_xlabel("time (s)")
aax3.set_ylabel("$\dot{H}_z$ (V)")

#aax1.set_ylim( [DOI + 50,0] )
aax1.set_ylim( [CTRL["PDepth"], 0] )
#aax1.set_ylim( aax1.get_ylim()[::-1] )
aax1.set_xlim( [1,1e4] )
aax1.set_xscale('symlog') # LaTeX complains unless this
#aax1.set_yscale('symlog')

aax1.xaxis.set_major_formatter(mpl.ticker.ScalarFormatter()) # only works for res > 1

#plt.colorbar(sigc)
aax1.set_xlabel("resistivity ($\Omega \cdot \mathrm{m}$)", fontsize=12)
aax1.set_ylabel("depth ($\mathrm{m}$)", fontsize=12)

cb1 = mpl.colorbar.ColorbarBase(aax2, cmap=wmap,
                                norm=norm,
                                orientation='vertical',
                                extend='both')
cb1.set_label("resistivity ($\Omega \cdot \mathrm{m}$)", fontsize=12)
aax3.legend()
figa.savefig( sdir+"_inv.pgf" )

if __name__ == "__main__":

    colours = plt.rcParams['axes.prop_cycle'].by_key()['color']

    #for SND in sys.argv[1:]:
    isnd = 0

```



```

MAG = []

firstPlot = True

for sdir in sys.argv[1:-1]:

    print("reading", sdir)

    # New class interface
    ZT = ZeroTEMSounding()
    ZT.loadStack(sdir) # + "/*.*.SND")
    ZT.plotStack(sdir, sys.argv[-1])

    CTRL = yaml.load(open(sdir+'/control.yaml'), Loader=yaml.Loader)
    if CTRL["invert"] != "False":
        ZT.export(sdir)

    # Call inversion
    ZT.invert(sdir)
    ZT.modelAppraisal(sdir)
    isnd += 1

plt.show()

#     for SND in glob.glob(sdir+"/*.*.SND"):
#
#         wn, mag, rho, WIN = loadSND(SND)
#         wint= extractWindowTuples(WIN)
#         neg = mag<=0
#         pos = mag>0
#         MAG.append(mag)
#         plt.scatter(wn[neg], -1*mag[neg], marker='.', color = colours[isnd], alpha=.25)
#         plt.scatter(wn[pos],  mag[pos], marker='+', color = colours[isnd], alpha=.25)
#         plt.plot( wiwintnt[0:len(wn)].T, np.ones((len(wn), 2)).T, color='grey' )
#         plt.plot( np.average(wint[0:len(wn)], axis=1).T, np.ones((len(wn))).T, '.',
color='black', )
#         #plt.plot( wint[0:len(wn)].T, np.ones((len(wn), 2)).T )
#
#     # calculate average
#     MAG = np.average(MAG, axis=0)
#
#     # write out Beowulf inversion files
#     #writeCFL("Beowulf.cfl")
#     #writeINV("Beowulf.inv", MAG)
#
#     plt.scatter(wn[neg], -1*MAG[neg], marker='_', color = colours[isnd], alpha=1, s=80)

```

```
# plt.scatter(wn[pos], MAG[pos], marker='+', color = colours[isnd], alpha=1, s=80)
# plt.plot(wn, np.abs(MAG), color = colours[isnd], alpha=1, label=sdir)
#
# isnd += 1
#
# plt.gca().set_yscale('log')
# plt.gca().set_xscale('log')
# plt.legend()
#
# plt.show()
```

Table 3. Control.yaml script developed by Dr. Trevor Irons from the sounding data for Site 4-1 at 8 Hz; used as the control file for the python processing in plotZT.py.

```
TxAbs: [ 0., 0.7, 15.65, 15.81]
TxAmp: [0.,3.75,3.75,0]
TxDly: .046
Txtype: "Circle"
TxSize: 55
Nlay: 7
SRes: [20.]
#SRes: [20.,10,100,100,300,800,1000,1000,5.]
Smooth: false
PDepth: 300
Invert: "True"
```

Table 4. Beowulf.out output script for the 8 Hz sounding at Site 4-1 using the inputs in the Table 3 control.yaml script for a 7-layer model with a 55-meter circular loop (Wilson, Raiche, & Sugeng, 2007).

Beowulf task started at 18:39 on 03 MAR 2022
 Beowulf - Version 1.0.3 7 November 2007
 Developed by: Art Raiche
 for: AMIRA project P223F

INPUT DATA

Flathead inversion

```

1 0 0          !TDFD, ISYS, ISTOP
0 4 15 2 15.7640 15.8100 !STEP, NSX, NCHNL, KRXW, REFTYM, OFFTIME
0.000 0.000
0.700 3.750
15.650 3.750
15.810 0.000      !Tx Wvfm: abscissa (ms), current (A)
0.0661
0.0966
0.1271
0.1576
0.1881
0.2333
0.2945
0.3556
0.4311
0.5229
0.6428
0.8100
1.0080
1.2500
1.5540
0.0152
0.0152
0.0152
0.0152
0.0152
0.0303
0.0303
0.0303
0.0606
0.0606
0.1213
0.1516

```

```

0.1819
0.2426
0.3032
1          !SURVEY_TYPE: General
1 1 1 1 50 1      !NLINES, MRXL, NTX, SOURCE_TYPE, MAXVRTX, NTURNS
32 0          !Nvertex, elevation z
55.000  0.000
53.943  10.730
50.813  21.048
45.731  30.556
38.891  38.891
30.556  45.731
21.048  50.813
10.730  53.943
0.000  55.000
-10.730 53.943
-21.048 50.813
-30.556 45.731
-38.891 38.891
-45.731 30.556
-50.813 21.048
-53.943 10.730
-55.000 0.000
-53.943 -10.730
-50.813 -21.048
-45.731 -30.556
-38.891 -38.891
-30.556 -45.731
-21.048 -50.813
-10.730 -53.943
-0.000 -55.000
10.730 -53.943
21.048 -50.813
30.556 -45.731
38.891 -38.891
45.731 -30.556
50.813 -21.048
53.943 -10.730      !Tx[i] East, Tx North (m)
1000 1 1 1 1      !Line txid, rxtype, nrx, units (V)
3 0 0 1 0 10000    !cmp, sv_azm, knorm, iplt, idh, rxmoment
0 0 0              !receiver position
7 7              !NLAYER, NLITH
20.00 1 1 0 0 0    ! RES, RMU, REPS, CHRG, CTAU, CFREQ(1) - Lyr1
20.00 1 1 0 0 0    ! RES, RMU, REPS, CHRG, CTAU, CFREQ(1) - Lyr1
20.00 1 1 0 0 0    ! RES, RMU, REPS, CHRG, CTAU, CFREQ(1) - Lyr1
20.00 1 1 0 0 0    ! RES, RMU, REPS, CHRG, CTAU, CFREQ(1) - Lyr1

```

```

20.00 1 1 0 0 0      ! RES, RMU, REPS, CHRG, CTAU, CFREQ(1) - Lyr1
20.00 1 1 0 0 0      ! RES, RMU, REPS, CHRG, CTAU, CFREQ(1) - Lyr1
20.00 1 1 0 0 0      ! RES, RMU, REPS, CHRG, CTAU, CFREQ(1) - Lyr1
1 5      ! LITH, THICK - Layer 1
2 8      ! LITH, THICK - Layer 1
3 13     ! LITH, THICK - Layer 1
4 22     ! LITH, THICK - Layer 1
5 36     ! LITH, THICK - Layer 1
6 60     ! LITH, THICK - Layer 1
7 100    ! LITH, THICK - Layer 1
0 90 1 2  ! NFIX, MAXITS, CNVRG, INVPRT
  3      ! NDSTP
  5 3 1  ! KPCT (1:NDSTP)

```

TDFD = 1; ISYS = 0; ISTOP = 0

```

+-----+
+ Time-Domain Ground System Information +
+-----+

```

STEP = 0; NSX = 4; NCHNL = 15; KRXW = 2; REFTYM = 15.76 ; OFFTYM = 15.81

TXON (ms) Transmitter current (amps)

	TXON (ms)	Transmitter current (amps)
1	0.000	0.000
2	0.700	3.750
3	15.650	3.750
4	15.810	0.000

Receiver channel origin INPUT is shifted by 15.764 ms from signal origin.

Receiver Window Specifications (ms - referenced to signal origin)

Window	Open	Close	Referenced		
			Width	Centre	Centre
1	15.823	15.838	0.015	15.830	0.066
2	15.853	15.868	0.015	15.861	0.097
3	15.884	15.899	0.015	15.891	0.127
4	15.914	15.929	0.015	15.922	0.158

5	15.944	15.960	0.015	15.952	0.188
6	15.982	16.012	0.030	15.997	0.233
7	16.043	16.074	0.030	16.059	0.294
8	16.104	16.135	0.030	16.120	0.356
9	16.165	16.225	0.061	16.195	0.431
10	16.257	16.317	0.061	16.287	0.523
11	16.346	16.467	0.121	16.407	0.643
12	16.498	16.650	0.152	16.574	0.810
13	16.681	16.863	0.182	16.772	1.008
14	16.893	17.135	0.243	17.014	1.250
15	17.166	17.470	0.303	17.318	1.554

SURVEY_TYPE = 1

NLINES = 1; MRXL = 1; NTX = 1; SOURCE_TYPE = 1; MXVRTX =50; NTRN = 1

Vertex Locations for Loop Sources

Transmitter 1 has 32 vertices:

	Easting	Northing	Elevation
	-----	-----	-----
1	55.00	0.00	0.00
2	53.94	10.73	0.00
3	50.81	21.05	0.00
4	45.73	30.56	0.00
5	38.89	38.89	0.00
6	30.56	45.73	0.00
7	21.05	50.81	0.00
8	10.73	53.94	0.00
9	0.00	55.00	0.00
10	-10.73	53.94	0.00
11	-21.05	50.81	0.00
12	-30.56	45.73	0.00
13	-38.89	38.89	0.00
14	-45.73	30.56	0.00
15	-50.81	21.05	0.00
16	-53.94	10.73	0.00
17	-55.00	0.00	0.00
18	-53.94	-10.73	0.00
19	-50.81	-21.05	0.00
20	-45.73	-30.56	0.00
21	-38.89	-38.89	0.00

22	-30.56	-45.73	0.00
23	-21.05	-50.81	0.00
24	-10.73	-53.94	0.00
25	0.00	-55.00	0.00
26	10.73	-53.94	0.00
27	21.05	-50.81	0.00
28	30.56	-45.73	0.00
29	38.89	-38.89	0.00
30	45.73	-30.56	0.00
31	50.81	-21.05	0.00
32	53.94	-10.73	0.00

Line 1000; Tx Index 1; Rx type = 1; NRX = 1; Units = 1

CMP = 3; KNORM = 0; IPLT = 1; IDH = 0; SV_AZM = 0.0; RXMNT = 0.1000E+05

Magnetic Dipole Receivers

	Easting	Northing	Elevation
	-----	-----	-----
1	0.0	0.0	0.0

NLAYER = 7; NLITH = 7

LITHOLOGY PROPERTIES

	Relative Resistivity	Relative MU	Relative Dielectric	Cole-Cole CHRG	Parameters CTAU	CFREQ
1	20.00	1.0	1.000	0.000	0.00	0.00
2	20.00	1.0	1.000	0.000	0.00	0.00
3	20.00	1.0	1.000	0.000	0.00	0.00
4	20.00	1.0	1.000	0.000	0.00	0.00
5	20.00	1.0	1.000	0.000	0.00	0.00
6	20.00	1.0	1.000	0.000	0.00	0.00
7	20.00	1.0	1.000	0.000	0.00	0.00

LAYERED EARTH INPUT DATA

```

1 1 5.0 J, LITHL(J), THK(J)
2 2 8.0 J, LITHL(J), THK(J)
3 3 13.0 J, LITHL(J), THK(J)
4 4 22.0 J, LITHL(J), THK(J)
5 5 36.0 J, LITHL(J), THK(J)
6 6 60.0 J, LITHL(J), THK(J)
7 7      Basement Lithology

```

Before computation begins, Beowulf may transform array and model coordinates from GPS coordinates where elevation increases positive upwards to a body-centred system where depth increases positive downwards. In this system, the dip of magnetic dipole transmitters and receivers = 0 for vertical dipoles and 90 for horizontal dipoles.

The computational horizontal origin remains unchanged.

Transformed transmitter and receiver locations for Line 1000
Survey azimuth = 0 degrees clockwise from North.

Transformed Vertex Locations for Loop Sources

Transmitter 1 has 32 vertices.

	Easting	Northing	
1	53.94	-10.73	0.00
2	50.81	-21.05	0.00
3	45.73	-30.56	0.00
4	38.89	-38.89	0.00
5	30.56	-45.73	0.00
6	21.05	-50.81	0.00
7	10.73	-53.94	0.00
8	0.00	-55.00	0.00
9	-10.73	-53.94	0.00
10	-21.05	-50.81	0.00
11	-30.56	-45.73	0.00
12	-38.89	-38.89	0.00
13	-45.73	-30.56	0.00
14	-50.81	-21.05	0.00
15	-53.94	-10.73	0.00
16	-55.00	0.00	0.00
17	-53.94	10.73	0.00
18	-50.81	21.05	0.00

19	-45.73	30.56	0.00
20	-38.89	38.89	0.00
21	-30.56	45.73	0.00
22	-21.05	50.81	0.00
23	-10.73	53.94	0.00
24	0.00	55.00	0.00
25	10.73	53.94	0.00
26	21.05	50.81	0.00
27	30.56	45.73	0.00
28	38.89	38.89	0.00
29	45.73	30.56	0.00
30	50.81	21.05	0.00
31	53.94	10.73	0.00
32	55.00	0.00	0.00

Transformed Locations for Magnetic Dipole Receivers in Line 1000

	Easting	Northing	Depth	Moment
	-----	-----	-----	-----
1	0.00	0.00	0.00	0.1000E+05

Plot points for receivers on Line 1000

	East	North	Elev
	----	-----	----
1	0.0	0.0	0.0

+-----+

+ Initial Layered Earth Model Parameters +

+-----+

	Depth							
Layer	Thickness	to Top	Resistivity	MU-R	EPS-R	CHRG	CFREQ	CTAU
	-----	-----	-----	-----	-----	-----	-----	-----
1	5.0	0.0	20.00	1.00	1.00	0.00	1.00	0.0
2	8.0	5.0	20.00	1.00	1.00	0.00	1.00	0.0
3	13.0	13.0	20.00	1.00	1.00	0.00	1.00	0.0
4	22.0	26.0	20.00	1.00	1.00	0.00	1.00	0.0
5	36.0	48.0	20.00	1.00	1.00	0.00	1.00	0.0
6	60.0	84.0	20.00	1.00	1.00	0.00	1.00	0.0
7		144.0	20.00	1.00	1.00	0.00	1.00	0.0

 END OF INPUT DATA DESCRIPTION

 Inversion Controls for Layer Parameters using Beowulf

NFIX = 0 MAXITS = 90 CNVRG = 1 INVPRT = 2

The inversion will finish if the RMS error is less than 0.1 percent
 or for some other as yet undisclosed reason.

A maximum of 90 iterations will be allowed.

The inversion sequence will use 2 numerical derivative steps

Values in percent: 5 3

All parameters will be allowed to vary during inversion

FD_ORDER = 0

Inversion controls and data for Line 1000

KMP = 3 CMP = 3

Time-Domain Data Floor = 0.000

SURVEY DATA

Line 1000 Magnetic dipole Rx Survey azimuth = 0 degrees Units = volts Plot point:
 Rx

Z : Vertical Component Survey Data for Line 1000

RECEIVER POSITIONS			CHNL 1	CHNL 2	CHNL 3	CHNL 4
CHNL 5	CHNL 6	CHNL 7	CHNL 8	CHNL 9	CHNL 10	CHNL 11
CHNL 12	CHNL 13	CHNL 14	CHNL 15			
Easting	Northing	Elev	0.1583E-01	0.1586E-01	0.1589E-01	0.1592E-01
0.1595E-01	0.1600E-01	0.1606E-01	0.1612E-01	0.1620E-01	0.1629E-01	0.1641E-01
0.1657E-01	0.1677E-01	0.1701E-01	0.1732E-01			

```

1      0.0      0.0      0.0  0.6719E-04  0.1450E-04  0.3299E-05  0.1431E-05  0.7755E-06
0.3945E-06  0.1903E-06  0.1043E-06  0.5953E-07  0.3261E-07  0.1653E-07  0.7648E-08
0.3975E-08  0.1593E-08  0.1054E-08

```

```

=====
=====

```

BEGIN INVERSION - TITLE = Flathead inversion

```

-----
Begin Inversion for Station 1 of Line 1000. NDATA = 15
Maximum iterations = 90 Derivative step = 5 percent.

```

0 iterations completed: RMS error = 126.90 percent. RSVT = 0.100

Model Description After 1 Iterations: RMS error = 103.17 RSVT = 0.050

Layer Resistivity Depth Thickness Conductance

```

-----
1  35.10   5.0   5.0   0.142
2  47.24  13.0   8.0   0.169
3  62.54  26.0  13.0   0.208
4  62.06  48.0  22.0   0.354
5  51.05  84.0  36.0   0.705
6  49.24 144.0  60.0   1.219
B   21.67

```

Model Description After 2 Iterations: RMS error = 89.02 RSVT = 0.025

Layer Resistivity Depth Thickness Conductance

```

-----
1  23.49   6.3   6.3   0.270
2  31.67  16.2   9.9   0.312
3  52.60  32.4  16.2   0.307
4  116.1   64.1  31.7   0.273
5  433.1  108.4  44.3   0.102
6  141.7  185.2  76.7   0.542
B   77.56

```

Model Description After 3 Iterations: RMS error = 31.72 RSVT = 0.013

Layer Resistivity Depth Thickness Conductance

	Resistivity	Depth	Thickness	Conductance
1	19.53	5.1	5.1	0.262
2	32.19	11.8	6.7	0.209
3	85.28	21.9	10.1	0.118
4	238.6	50.0	28.1	0.118
5	536.0	128.7	78.6	0.147
6	260.7	241.3	112.7	0.432
B	301.0			

Model Description After 4 Iterations: RMS error = 15.03 RSVT = 0.010

Layer Resistivity Depth Thickness Conductance

	Resistivity	Depth	Thickness	Conductance
1	16.51	5.1	5.1	0.309
2	26.86	11.2	6.1	0.225
3	94.45	18.9	7.7	0.082
4	396.5	39.8	20.9	0.053
5	938.7	138.7	98.9	0.105
6	230.6	256.3	117.6	0.510
B	1136.			

Model Description After 5 Iterations: RMS error = 10.13 RSVT = 0.010

Layer Resistivity Depth Thickness Conductance

	Resistivity	Depth	Thickness	Conductance
1	15.56	4.9	4.9	0.312
2	25.98	10.3	5.5	0.211
3	99.72	17.3	7.0	0.070
4	437.0	36.6	19.3	0.044
5	1028.	124.1	87.5	0.085
6	233.3	225.0	100.9	0.432
B	1818.			

Model Description After 6 Iterations: RMS error = 10.08 RSVT = 0.010

Layer Resistivity Depth Thickness Conductance

	Resistivity	Depth	Thickness	Conductance
1	17.85	5.2	5.2	0.292
2	24.12	11.0	5.8	0.240
3	95.99	18.1	7.1	0.073
4	443.7	37.5	19.5	0.044
5	1097.	140.6	103.1	0.094

6	229.4	248.7	108.2	0.471
B	2161.			

Model Description After 7 Iterations: RMS error = 10.02 RSVT = 0.010

Layer Resistivity Depth Thickness Conductance

	-----	-----	-----	-----
1	18.52	5.2	5.2	0.282
2	22.71	11.0	5.7	0.252
3	96.36	17.7	6.8	0.071
4	463.2	36.4	18.7	0.040
5	1160.	137.6	101.2	0.087
6	214.2	242.2	104.6	0.488
B	2617.			

Model Description After 8 Iterations: RMS error = 10.00 RSVT = 0.010

Layer Resistivity Depth Thickness Conductance

	-----	-----	-----	-----
1	19.25	5.3	5.3	0.274
2	21.84	11.0	5.7	0.263
3	96.54	17.7	6.7	0.069
4	472.5	36.2	18.5	0.039
5	1219.	140.1	103.9	0.085
6	209.5	244.4	104.3	0.498
B	2850.			

Model Description After 9 Iterations: RMS error = 9.97 RSVT = 0.010

Layer Resistivity Depth Thickness Conductance

	-----	-----	-----	-----
1	20.12	5.3	5.3	0.265
2	20.72	11.1	5.8	0.278
3	97.86	17.6	6.5	0.066
4	488.6	35.7	18.1	0.037
5	1293.	140.6	104.9	0.081
6	203.1	243.8	103.2	0.508
B	3106.			

Model Description After 10 Iterations: RMS error = 9.96 RSVT = 0.010

Layer Resistivity Depth Thickness Conductance

```

-----
1  19.82   5.2   5.2   0.262
2  20.02  10.8   5.6   0.281
3  99.01  17.1   6.3   0.064
4  498.2  34.9  17.8   0.036
5  1339.  138.5 103.6   0.077
6  198.6  240.7 102.1   0.514
B  3256.

```

Error reduction after last 2 iterations < 0.5 percent.
 No further error reduction can occur using a 5 percent derivative step.
 Test derivative step = 3 percent.

Error reduction after last 2 iterations < 0.5 percent.

12 Iterations completed: RMS error = 9.92 percent. RSVT = 0.010
 Inversion terminated

```

=====
Final Model After 12 Iterations: RMS error = 9.92

```

Layer Resistivity Depth Thickness Conductance ResImport ThkImport

```

-----
1  21.53   5.2   5.2   0.243   0.85   0.58
2  18.32  10.8   5.6   0.303   0.58   0.65
3  97.07  16.8   6.0   0.062   0.17   0.18
4  504.3  33.9  17.1   0.034   0.14   0.13
5  1386.  138.7 104.9   0.076   0.22   0.91
6  192.2  237.5  98.8   0.514   0.77   0.69
B  3313.                0.22

```

Data and Misfit Final - (East, North, Elevation) = 0.0 0.0 0.0

Z : Vertical Component data for Station 1 of Line 1000

```

-----
          CHNL 1   CHNL 2   CHNL 3   CHNL 4   CHNL 5   CHNL 6
CHNL 7   CHNL 8   CHNL 9   CHNL 10  CHNL 11  CHNL 12  CHNL 13
CHNL 14  CHNL 15

```

Survey data: 0.6719E-04 0.1450E-04 0.3299E-05 0.1431E-05 0.7755E-06 0.3945E-06 0.1903E-06 0.1043E-06 0.5953E-07 0.3261E-07 0.1653E-07 0.7648E-08 0.3975E-08 0.1593E-08 0.1054E-08

Model data: 0.7323E-04 0.1135E-04 0.3567E-05 0.1566E-05 0.8268E-06 0.4032E-06 0.1865E-06 0.1035E-06 0.5674E-07 0.3096E-07 0.1636E-07 0.7851E-08 0.3873E-08 0.1950E-08 0.9293E-09

Misfit (%):	-8.6	24.2	-7.8	-8.9	-6.4	-2.2	2.0	0.7
	4.8	5.2	1.0	-2.6	2.6	-20.1	12.6	

Beowulf task completed at 18:39 on 03 MAR 2022

Computation time = 4.31 seconds.

Appendix D: Big Fork Farm Well #5 Reports

Flathead Valley, Montana
Site 3-1
TEM and Well Completion Report

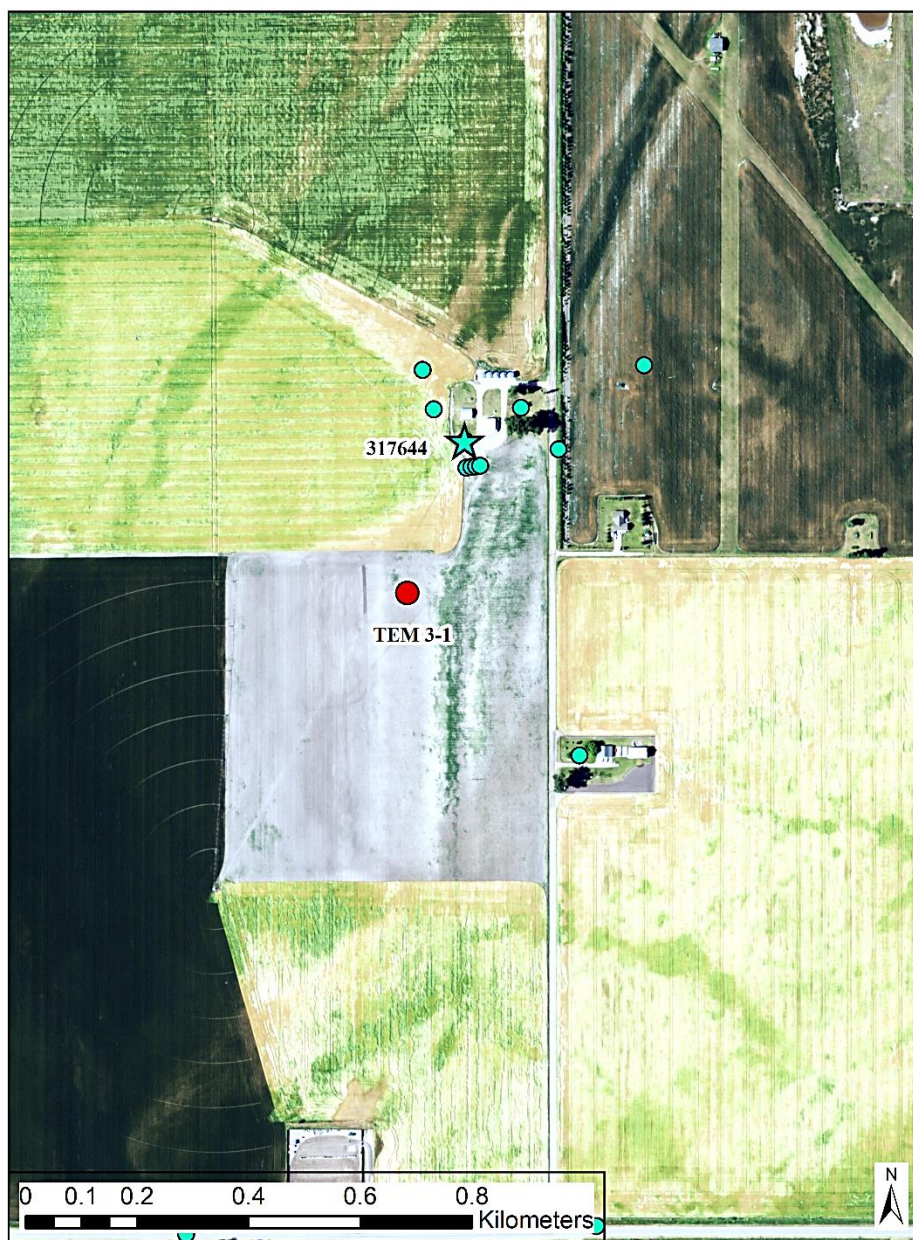


Figure 45. Site 3-1 TEM and nearby well locations located on or near the Big Fork Farm Water Treatment Facility (Montana State Library GIS Services). Star indicates the new (2021) deep well 317644 with well completion report lithology and additional geophysical reports (Ground Water Information Center; Montana Bureau of Mines and Geology; Montana Technological University, 1998-2022).

Table 5. Big Fork Farm well #5 completion report; GWIC ID 317644 (Ground Water Information Center; Montana Bureau of Mines and Geology; Montana Technological University, 1998-2022). Annotation of the corresponding Site 3-1 geoelectric inversion model recovered PCL result have been overlaid in green.

Site Name: BIG FORK WATER AND SEWER DISTRICT * BFF#5
GWIC Id: 317644

Section 1: Well Owner(s)

1) BIG FORK WATER AND SEWER DISTRICT (MAIL)
108 HARBOR HEIGHTS BLV
BIG FORK MONTANA 59911 [10/15/2021]

Section 2: Location

Township	Range	Section	Quarter Sections	
27N	20W	18	SE¼ NE¼	
County			Geocode	
FLATHEAD				
Latitude	Longitude	Geomethod	Datum	
48.103806	-114.182175	NAV-GPS	NAD83	
Ground Surface Altitude	Ground Surface Method	Datum	Date	
2908	DEM	NAVD88	10/20/2021	
Measuring Point Altitude	MP Method	Datum	Date Applies	
2911	DEM	NAVD88	10/20/2021	
Addition	Block		Lot	

Section 3: Proposed Use of Water

MONITORING (1)

Section 4: Type of Work

Drilling Method: ROTARY
Status: NEW WELL

Section 5: Well Completion Date

Date well completed: Friday, October 15, 2021

Section 6: Well Construction Details

Borehole dimensions

From	To	Diameter
0	380	16
380	1600	9.5

Casing

From	To	Diameter	Wall Thickness	Pressure Rating	Joint	Type
2	380	12	0.25		WELDED	A53B STEEL
2	540	10	0.25		WELDED	A53B STEEL
2	1540	6	0.188		THREADED	A53A STEEL

Completion (Perf/Screen)

From	To	Diameter	# of Openings	Size of Openings	Description
1540	1560	5		.020	SCREEN-CONTINUOUS-STAINLESS

Annular Space (Seal/Grout/Packer)

From	To	Description	Cont. Fed?
0	340	CEMENT	Y
1520	1600	SILICA SAND	Y

Section 7: Well Test Data

Total Depth: 1600
 Static Water Level: 15
 Water Temperature:

Air Test *

5 gpm with drill stem set at 500 feet for 1 hours.
 Time of recovery 1 hours.
 Recovery water level 15 feet.
 Pumping water level feet.

** During the well test the discharge rate shall be as uniform as possible. This rate may or may not be the sustainable yield of the well. Sustainable yield does not include the reservoir of the well casing.*

Section 8: Remarks

Section 9: Well Log

Geologic Source
 Unassigned

From	To	Description
0	11	TOPSOIL SEE SHELLS AND BARK
11	78	GRAY COURSE SAND WATER BEARING
78	125	GRAY SILT FINE SAND
125	219	GRAY SILT OCCASIONAL CLAY
219	405	STICKY TAN CLAY
405	485	LARGE DIAMETER GRAVEL GOOD WATER
485	495	MEDIUM GRAVEL WATER
495	505	LARGE GRAVEL GOOD WATER
505	960	SMALL GRAVEL SAND WATER
960	975	MOST SAND WITH SMALL AMOUNTS OF GRAVEL
975	983	SMOTHER DRILLING CLAY TYPE FORMATION
983	1003	SMALL GRAVEL LOTS OF SAND
1003	1025	SMALL LIGHT GRAVEL GRAVEL SMALL AMOUNTS OF SAND
1025	1085	MED SIZED GRAVEL W/SAND
1085	1095	SMALL GRAVEL A LOT OF SAND

Site 3-1 1D geoelectric resistivity inversion model recovered geoelectric resistivity layer 5 (PCL)

Driller Certification

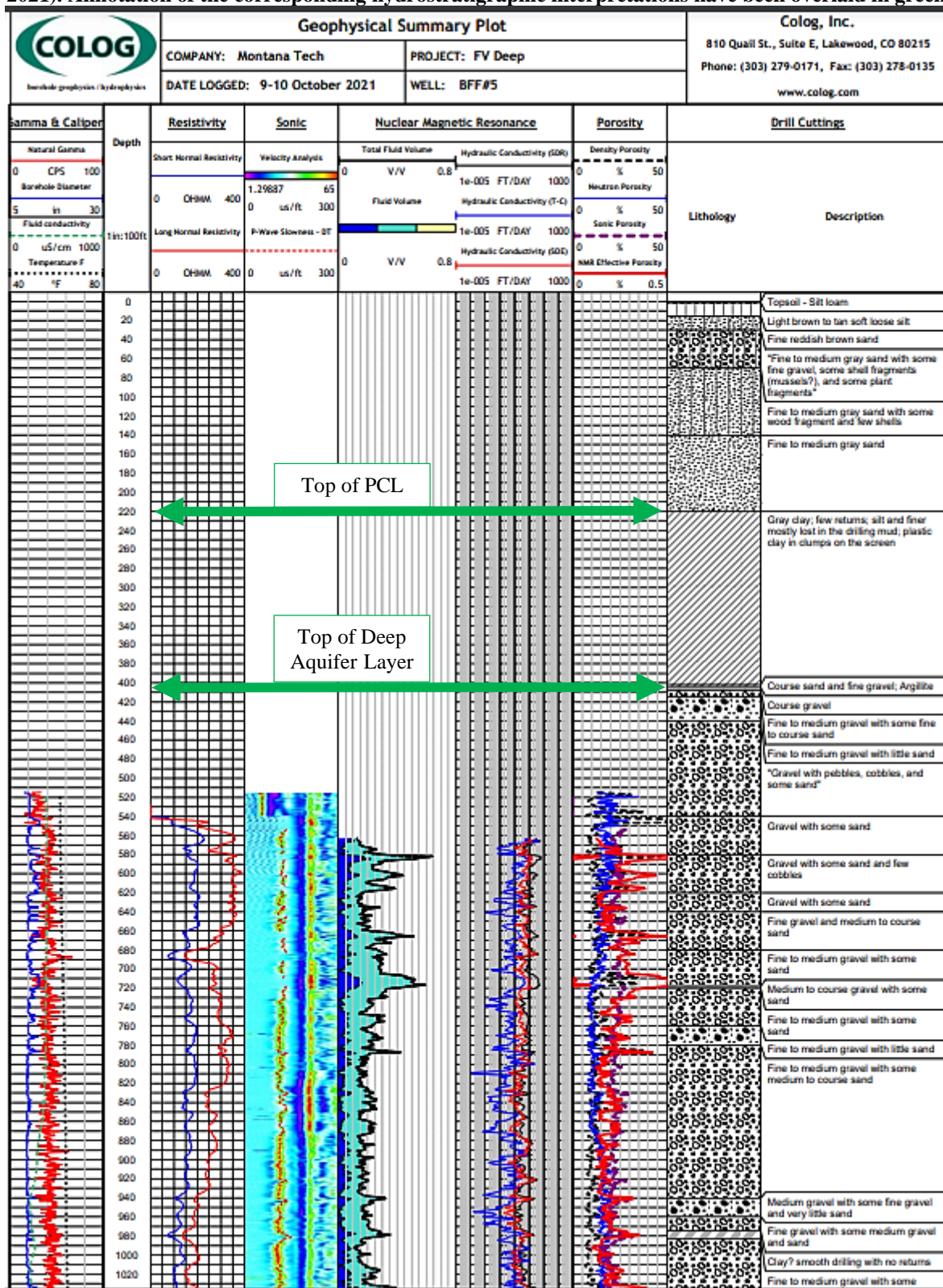
All work performed and reported in this well log is in compliance with the Montana well construction standards. This report is true to the best of my knowledge.

Name: CHAD DANIELSON
Company: RM DRILLING & WELL SERVICE INC.
License No: WWC-114
Date Completed: 10/15/2021

Site Name: BIG FORK WATER AND SEWER DISTRICT
 GWIC Id: 317644
 Additional Lithology Records

From	To	Description
1269	1380	SAND GRAY FINE W/WOOD CHIPS
1380	1473	FINE GRAY SAND
1473	1600	FINE GARY SAND W/WOOD CHIPS

Table 6. Big Fork Farm well #5 Geophysical Summary Plot report, reproduced with permission of Montana Bureau of Mines and Geology Publication Office (Montana Tech - Montana Bureau of Mines and Geology, 2021). Annotation of the corresponding hydrostratigraphic interpretations have been overlaid in green.



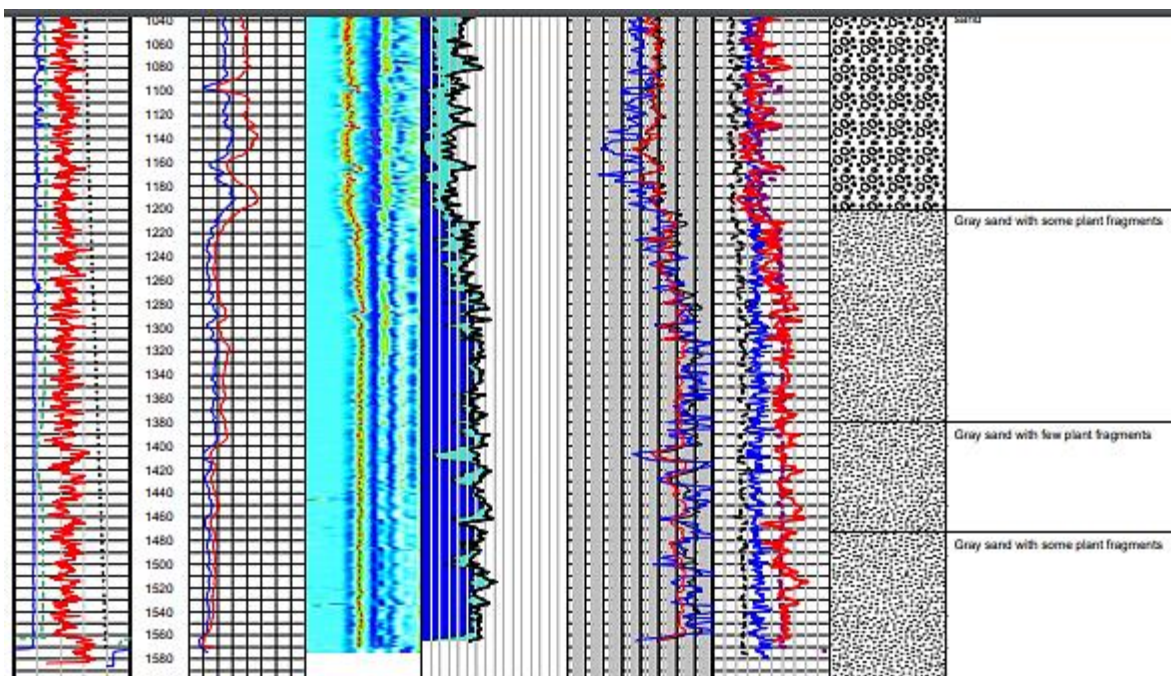



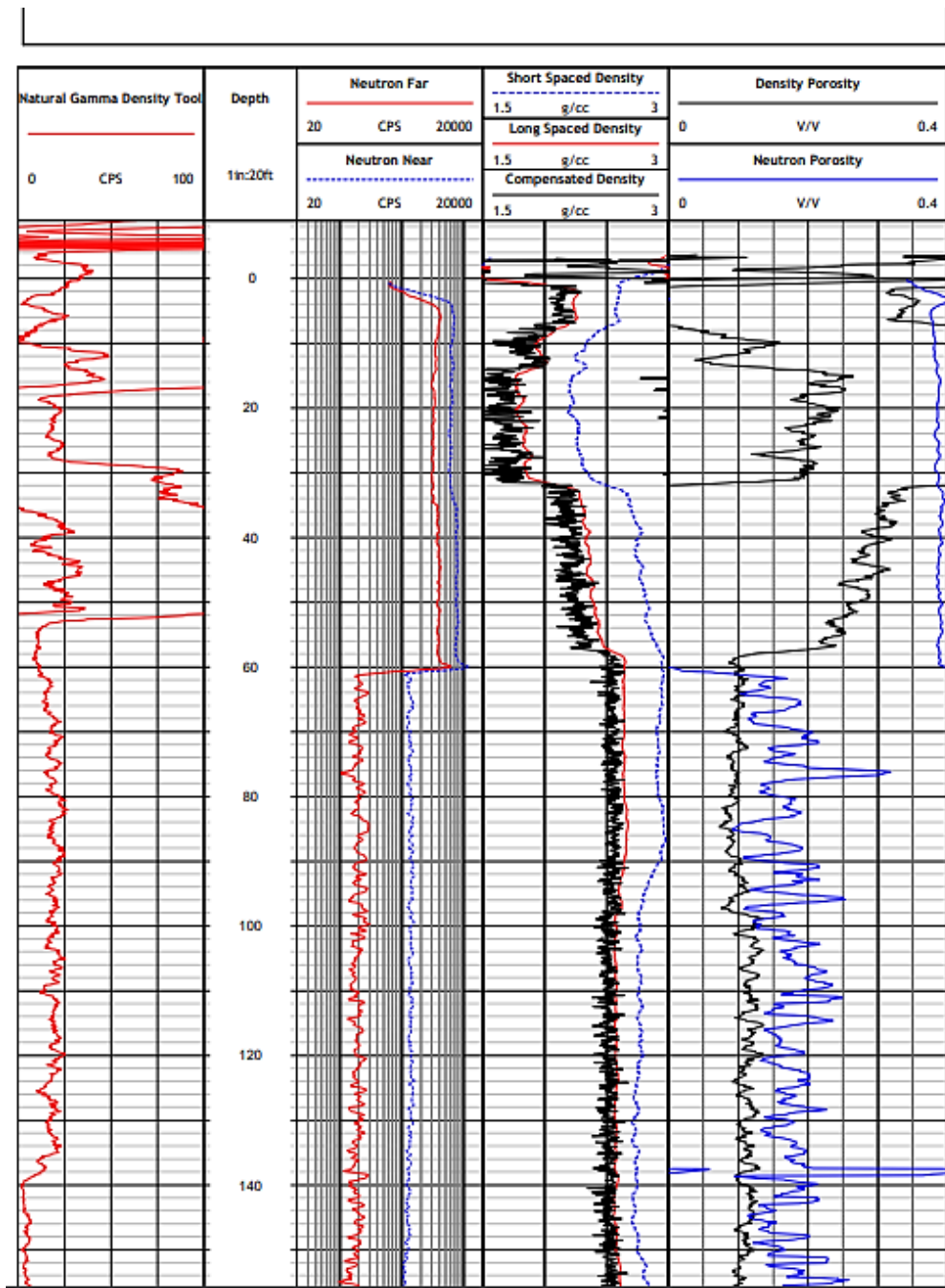
Table 7. Big Fork Farm deep well #5 report for neutron and density testing. Reproduced with permission of Montana Bureau of Mines and Geology Publication Office (Montana Tech - Montana Bureau of Mines and Geology, 2021). Annotation of the PCL and deep aquifer top interpretations have been overlaid in green.

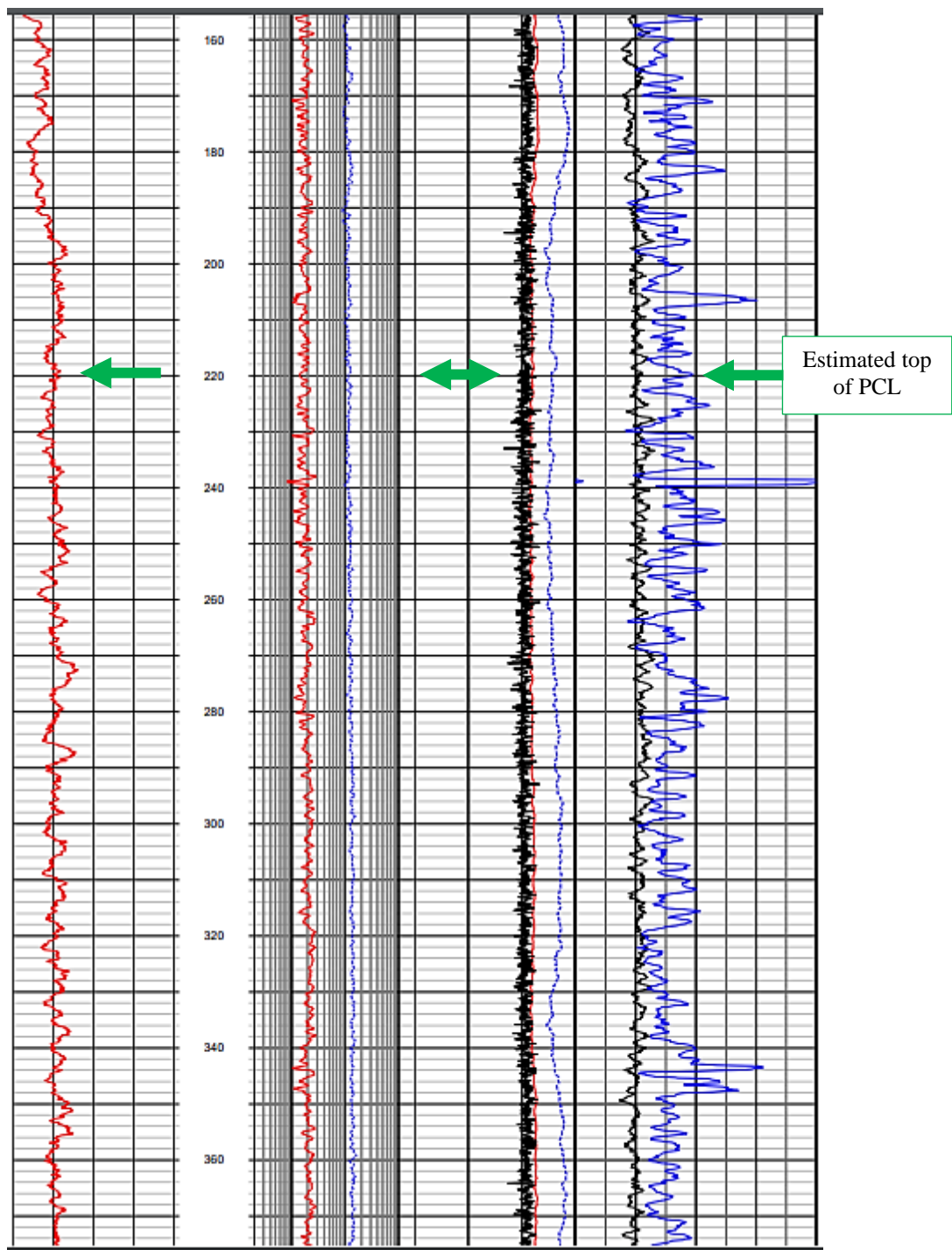
		\$10 Quail Street Suite E Lakewood, Colorado 80215 Office: 303.279.0171 Fax: 303.278.0135 www.colog.com		Neutron & Density	
		COMPANY WELL PROJECT COUNTY LOCATION Lat: 48.103531 Long: -114.18193	Montana Tech BFF#5 FVDeep Flathead SEC 18 TWP 27N RGE 20W ELEVATION 2907.64 ABOVE PERMANENT DATUM		
Company Montana Tech Well BFF#5 Project FVDeep County Flathead State Montana		PERMANENT DATUM NA LOG MEAS. FROM Ground Surface LOG MEAS. TO NA ABOVE PERMANENT DATUM		OTHER SERVICES Normal Resistivity Full Waveform Sonic Magnetic Resonance Fluid Temperature & Conductivity Neutron Density Three Arm Caliper Natural Gamma	
DRILLING MEAS. FROM Ground Surface					
DATE ACQUIRED	10 Oct 2021	10 Oct 2021			
RUN NUMBER	Seven	Seven			
LOG TYPE	Neutron	Density			
DEPTH-DRILLER	1600.0'	1600.0'			
DEPTH-CORREC	1575.0'	1575.0'			
RTM LOG INTERVAL	1575.0'	1575.0'			
TOP LOG INTERVAL	111.0'	111.0'			
REF ORDED BY	N. Walsh, M. Cullie	N. Walsh, M. Cullie			
WITNESSED BY	A. Bobel	A. Bobel			
PROBE TYPE, SN	Comprobe Slim, NSN	FDGS 5002			
LOGGING SPEED	40 f/min	40 f/min			
AS.D.E. / Sample Interval	3.3' / 1"	2.0' / 1"			
Final Level / Head Type	60' / WBM	60' / WBM			
BOREHOLE RECORD					
RUN No.	BIT	FROM	TO	SIZE	WGT
One	9.25"	540.0'	1600.0'	10"	Ss&G
				12"	Ss&G
					0.0'
					0.0'
					540.0'
					180.0'

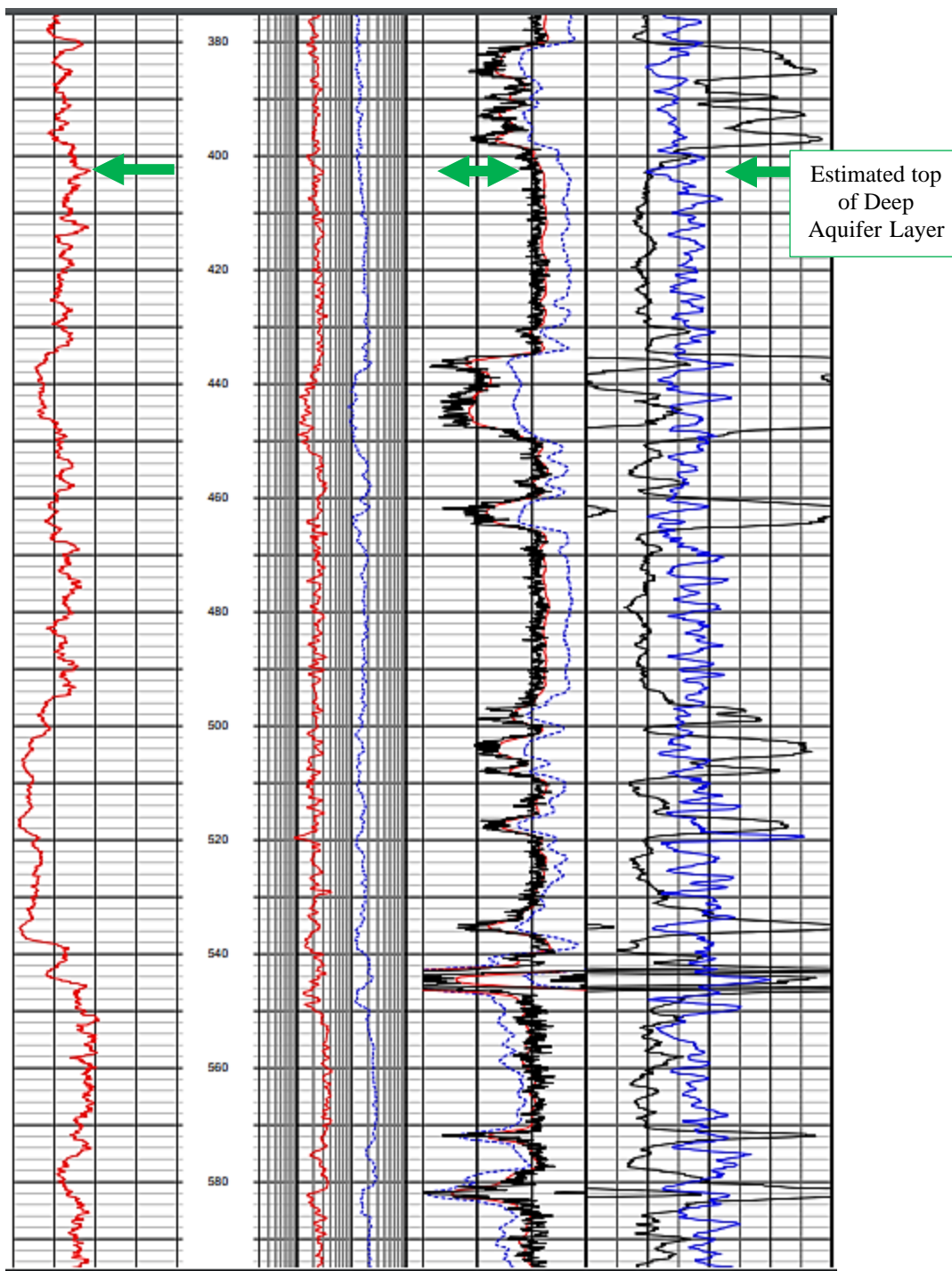
COMMENTS NA - Not Available, N/A - Not Applicable

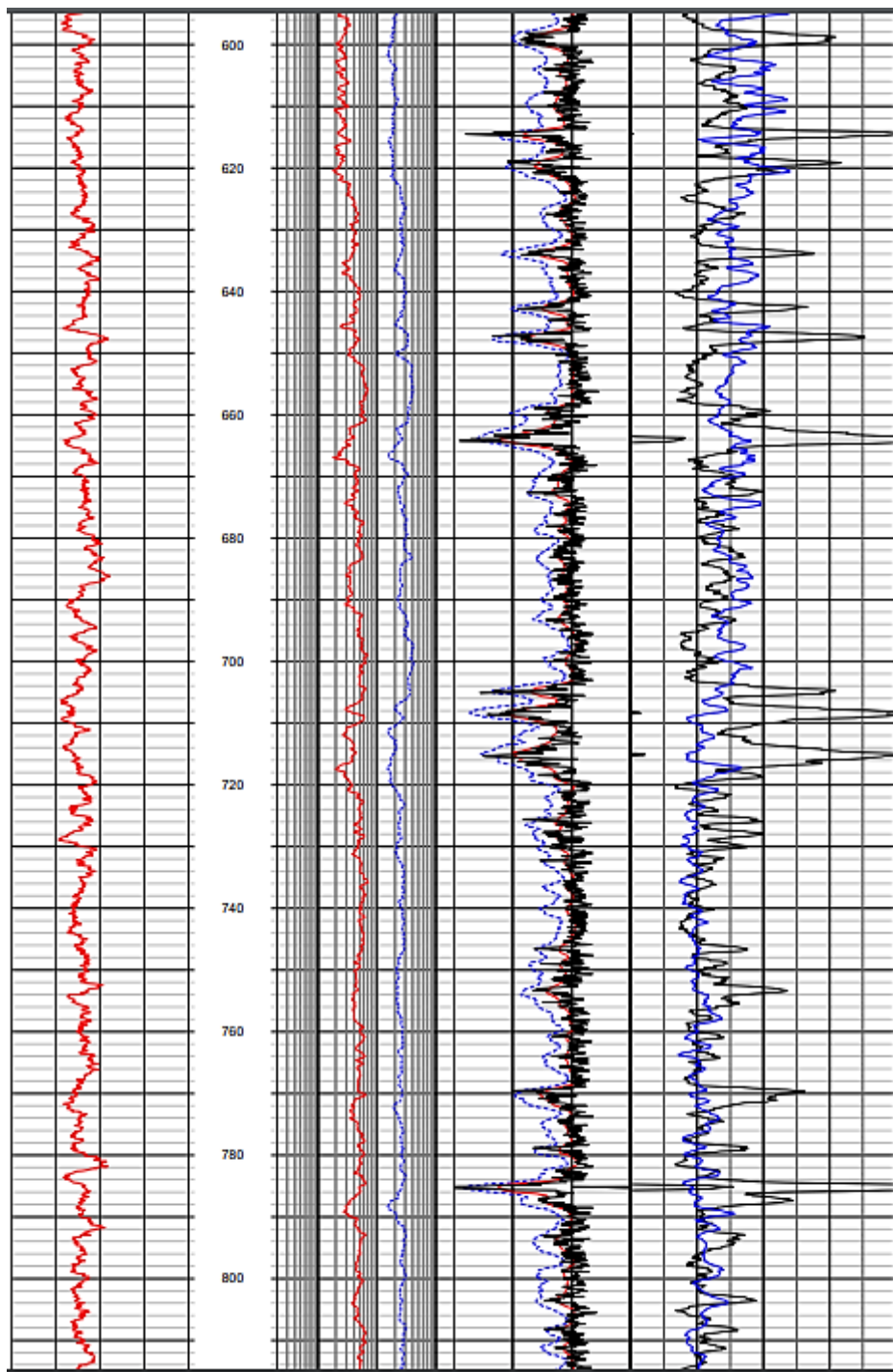
Source File: MontanaTech_FVDeep_BFF#5_Den-1UL.log, MontanaTech_FVDeep_BFF#5_Neu-Near-1UL.tdf, MontanaTech_FVDeep_BFF#5_Neu-Far-1UL.tdf,

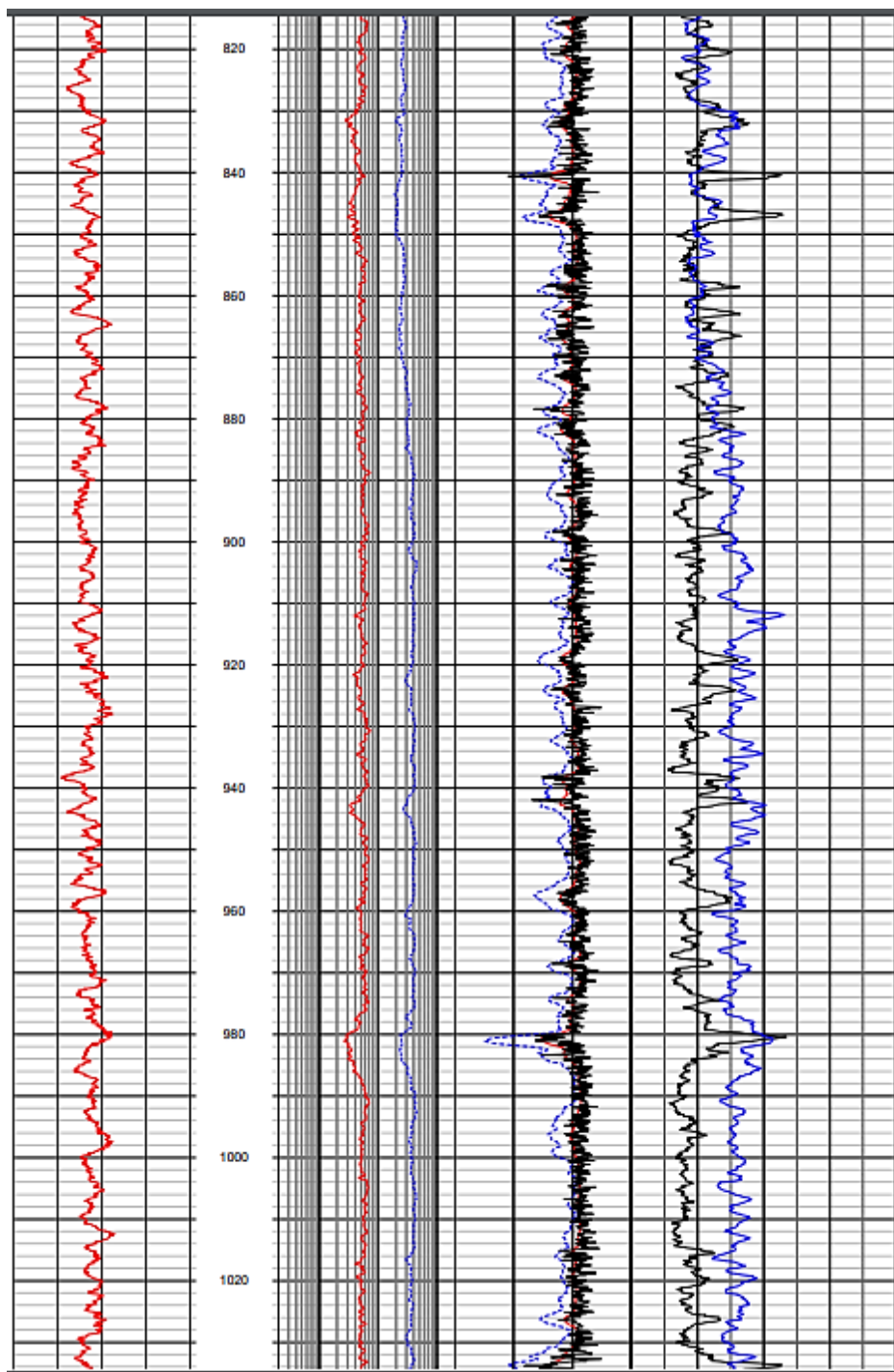
Formation matrix value of 2.71 used in porosity calculations.

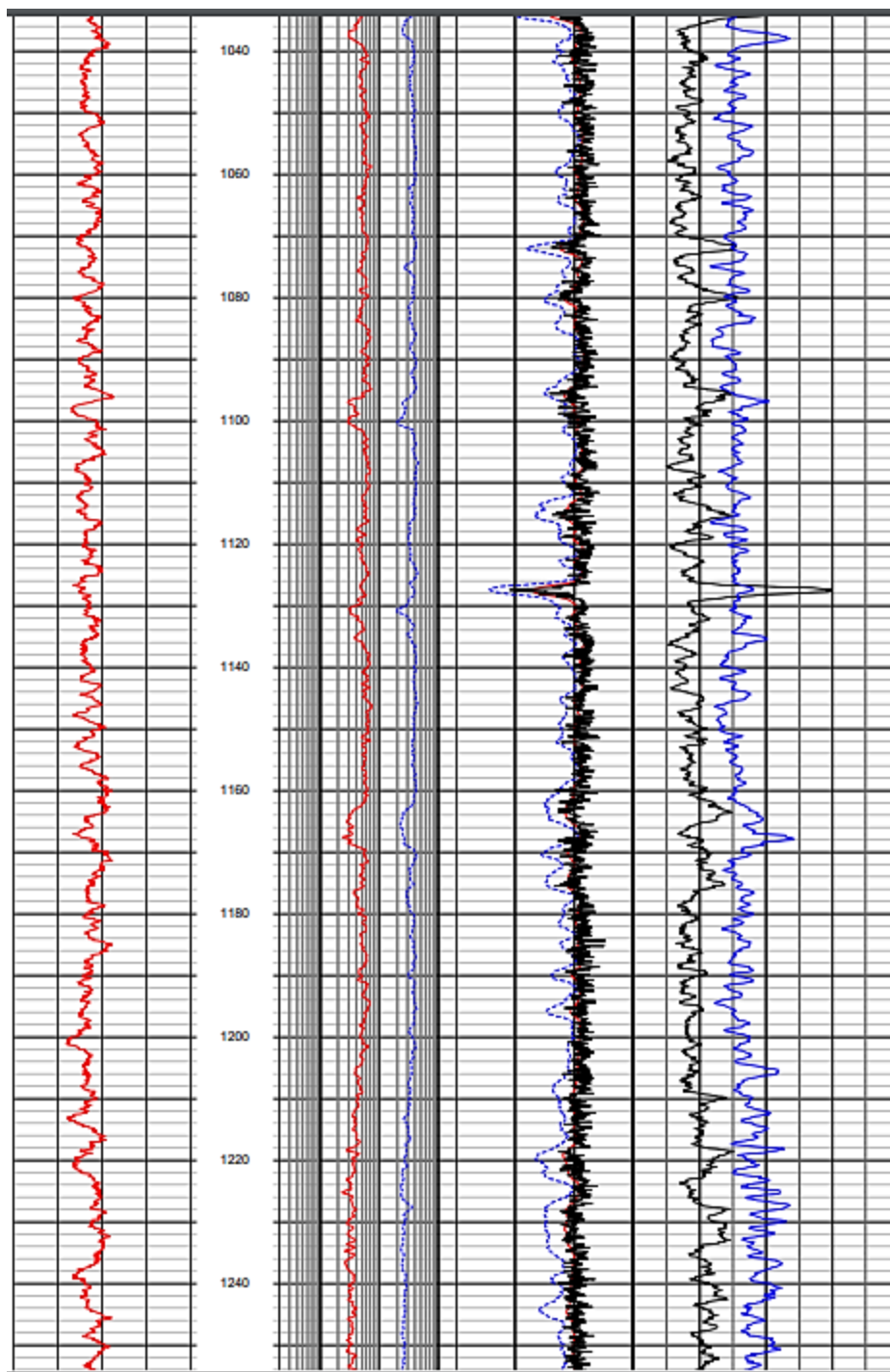


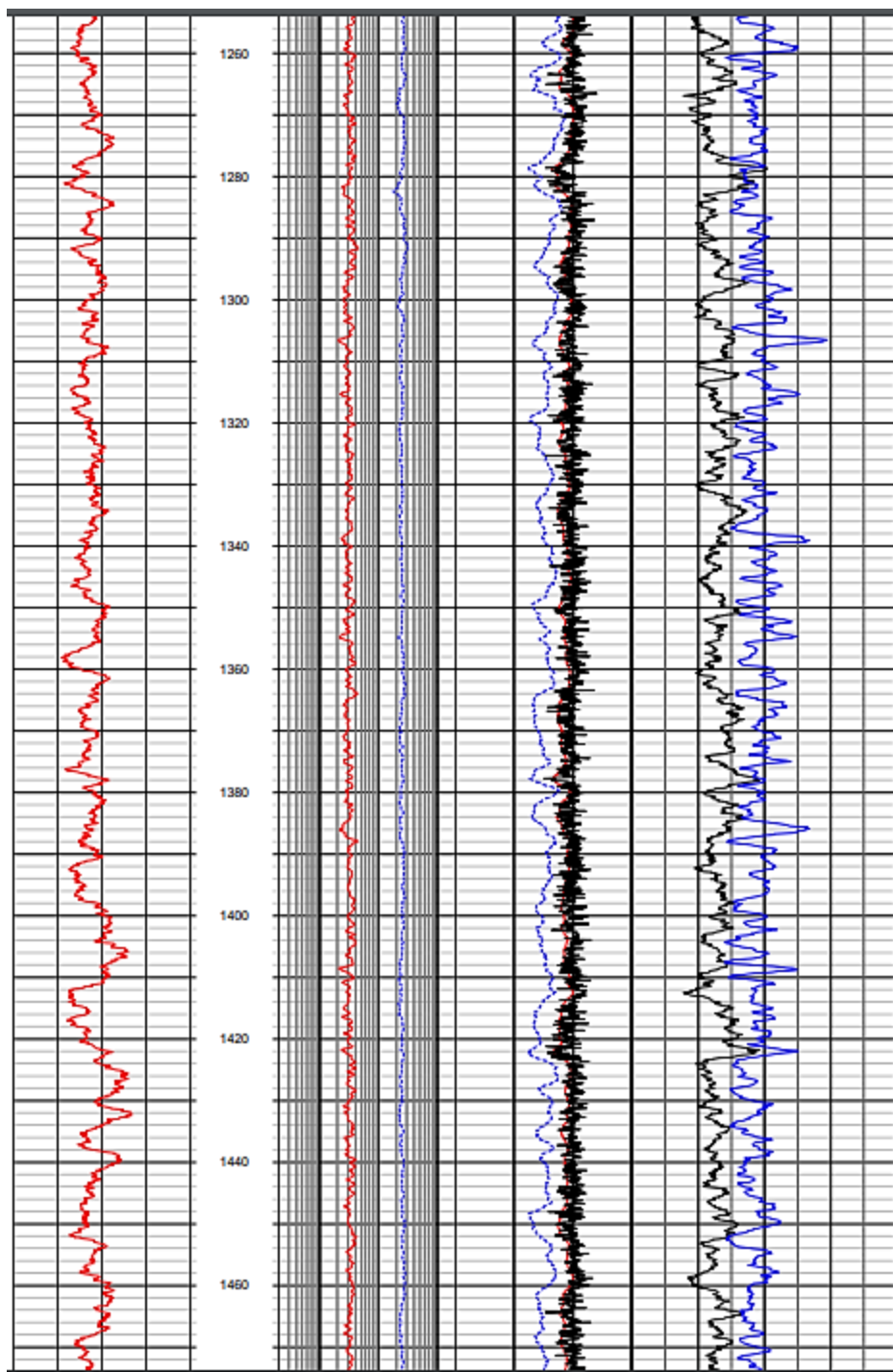












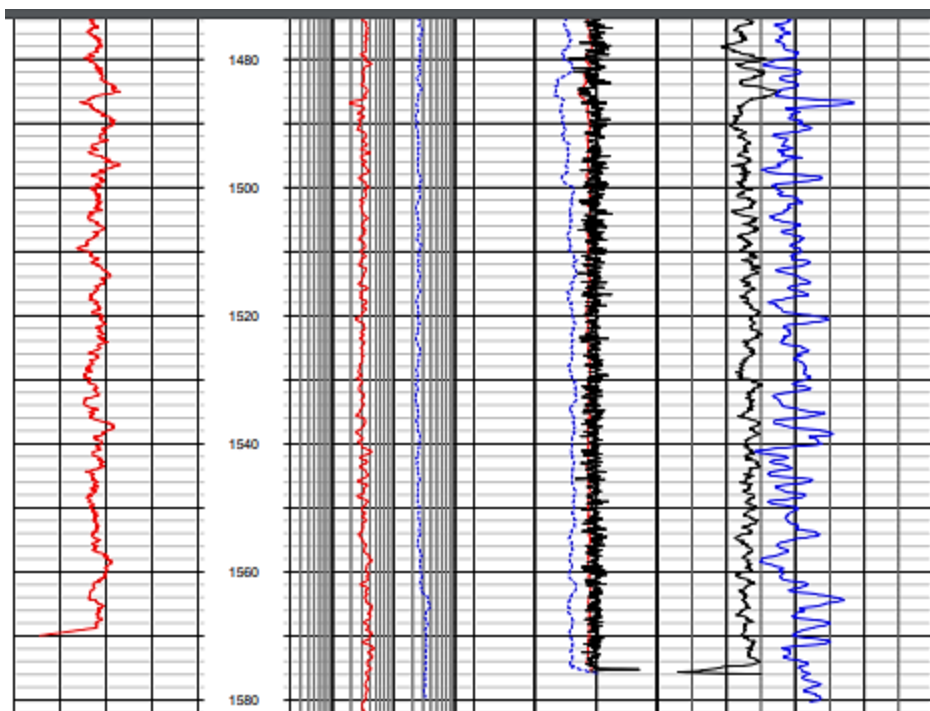
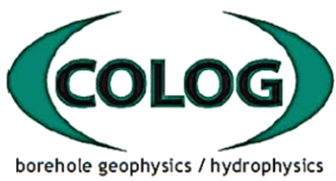


Table 8. Big Fork Farm deep well #5 report for three arm caliper, natural gamma with volume print. Reproduced with permission of Montana Bureau of Mines and Geology Publication Office (Montana Tech - Montana Bureau of Mines and Geology, 2021). Annotation of the PCL and deep aquifer top location interpretation have been overlaid in green.

		810 Quail Street Suite E Lakewood, Colorado 80215 Office: 303.279.0171 Fax: 303.278.0135 www.colog.com		Three Arm Caliper Natural Gamma w/Volume Print			
		COMPANY Montana Tech WELL BFF#5 PROJECT FVDeep COUNTY Flathead STATE MT					
Company Well Project County State	Montana Tech BFF#5 FVDeep Flathead Montana	LOCATION Lat: 48.10353 Long: -114.18193 QTR SE1/4SE1/4 SEC 18 TWP 27N RGE 20W			OTHER SERVICES Normal Resistivity Full Waveform Sonic Magnetic Resonance Fluid Temperature & Conductivity Neutron Density		
		PERMANENT DATUM NA ELEVATION 2907.64		LOG MEAS. FROM Ground Surface NA ABOVE PERMANENT DATUM		DRILLING MEAS. FROM Ground Surface	
DATE ACQUIRED	8 Oct 2021						
RUN NUMBER	One						
LOG TYPE	Caliper						
DEPTH-DRILLER	1600.0'						
DEPTH-LOGGER	1575.0'						
BTM LOG INTERVAL	1575.0						
TOP LOG INTERVAL	11.0'						
RECORDED BY	N. Welsh, M. Culig						
WITNESSED BY	A. Bobst						
PROBE TYPE, S/N	3ACS 117333						
LOGGING SPEED	40 ft/min						
A.S.D.E. / Sample Interval	3.86' / .1'						
Fluid Level / Fluid Type	10' / WBM						
BOREHOLE RECORD				CASING RECORD			
RUN No.	BIT	FROM	TO	SIZE	WGT.	FROM	TO
One	9.25"	540.0'	1600.0'	10"	Steel	0.0'	540.0'
				12"	Steel	0.0'	380.0'

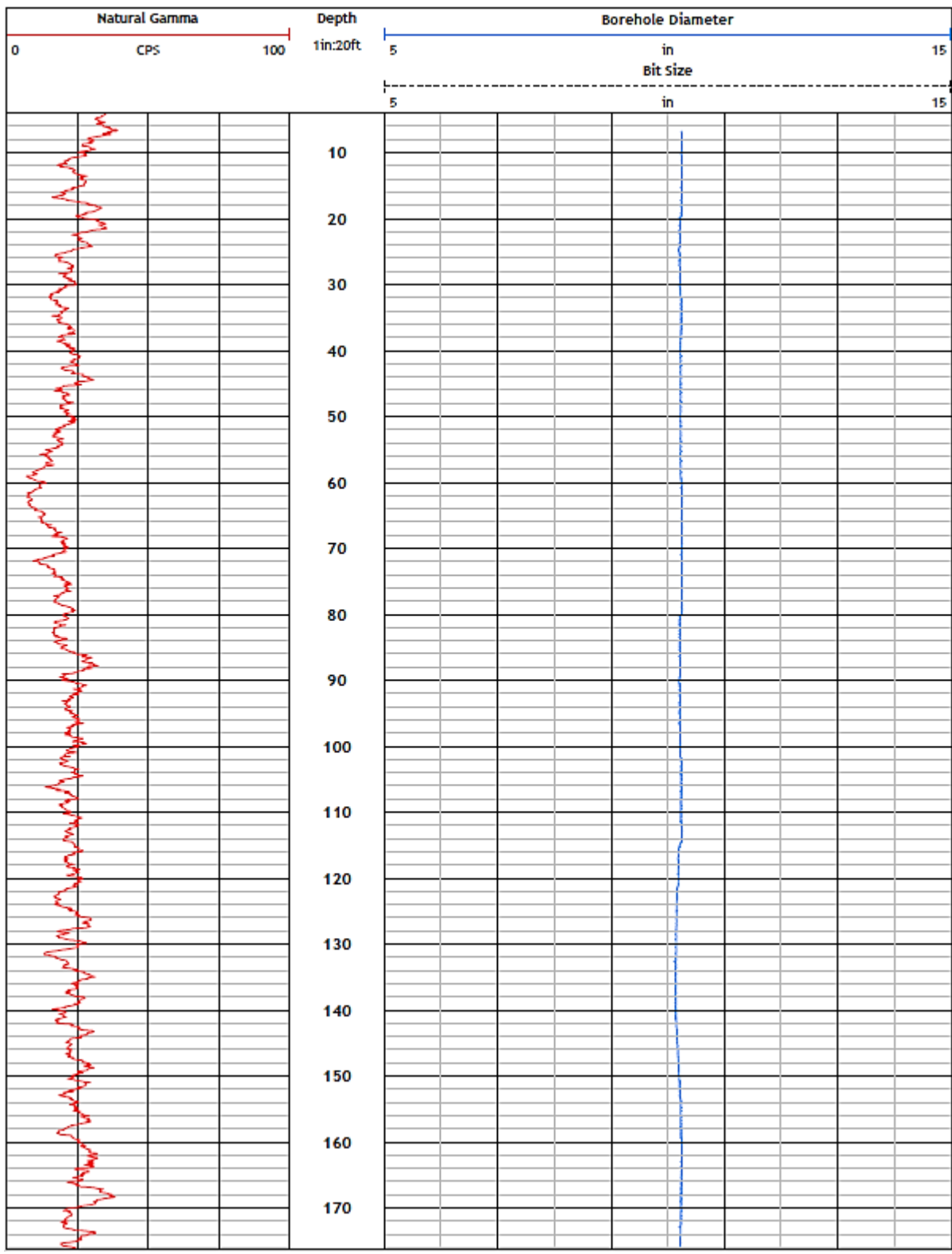
COMMENTS

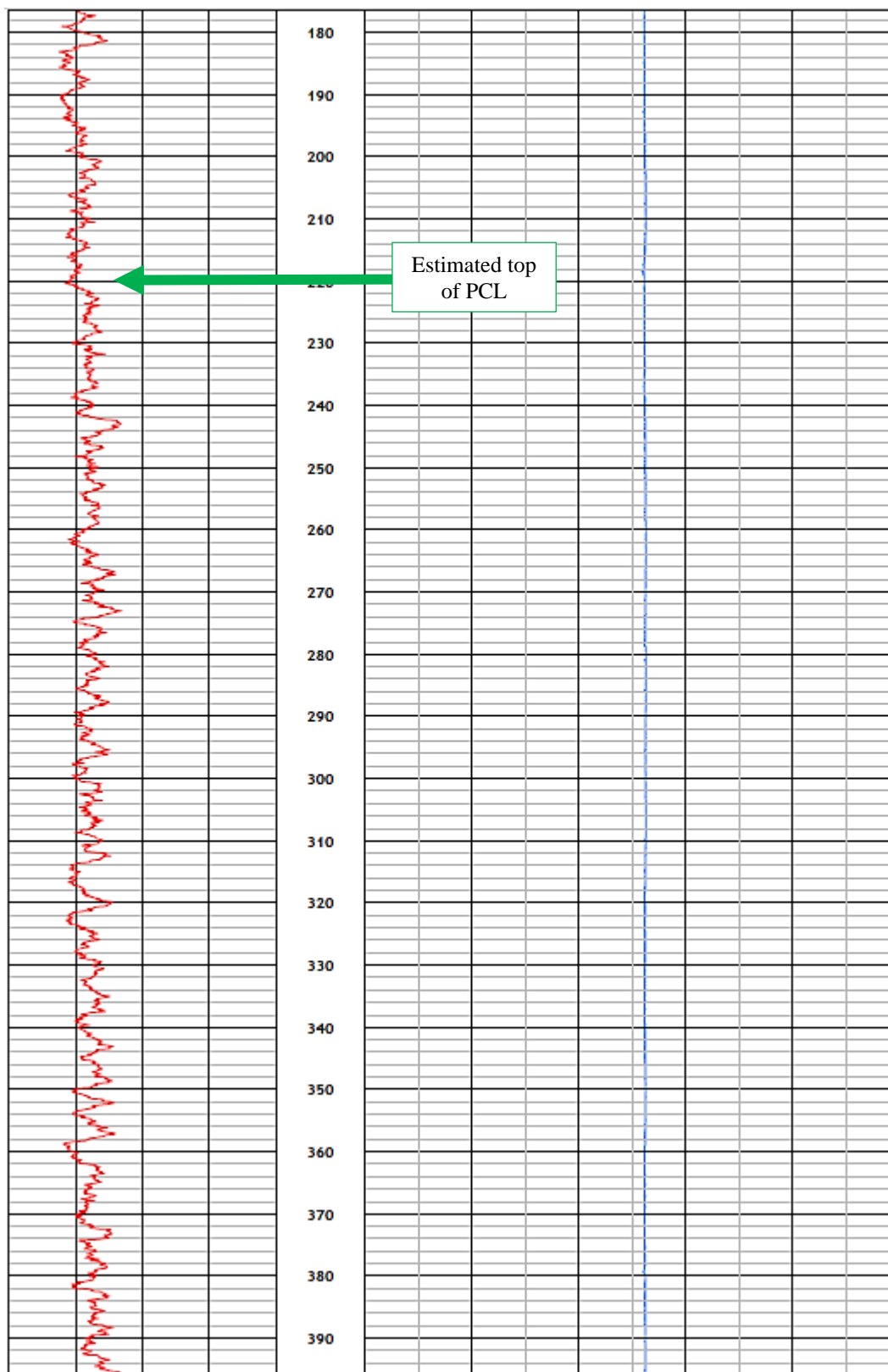
NA - Not Available, N/A - Not Applicable

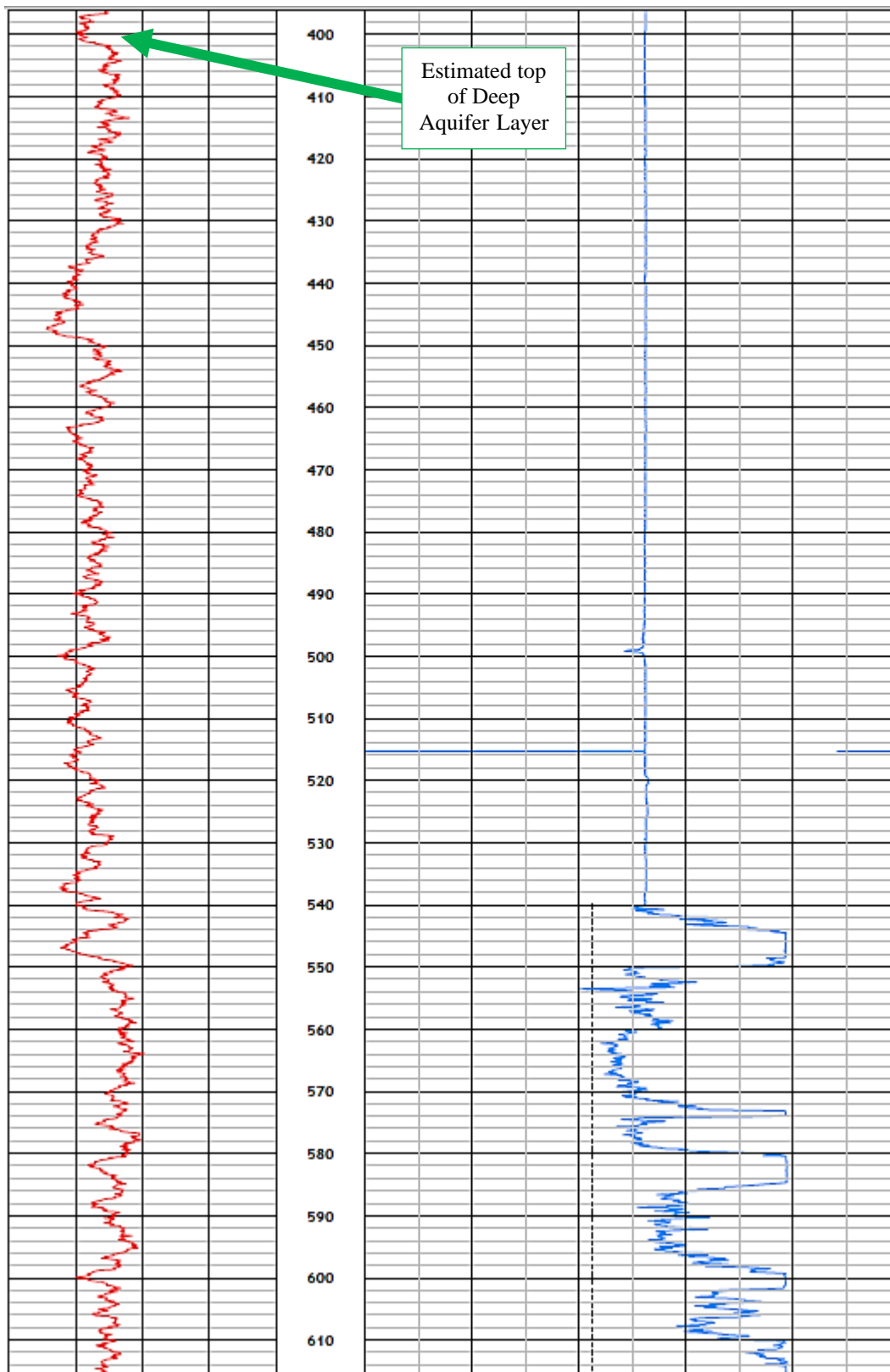
Source File: MontanaTech_FVDeep_BFF#5_Cal-1ULLOG

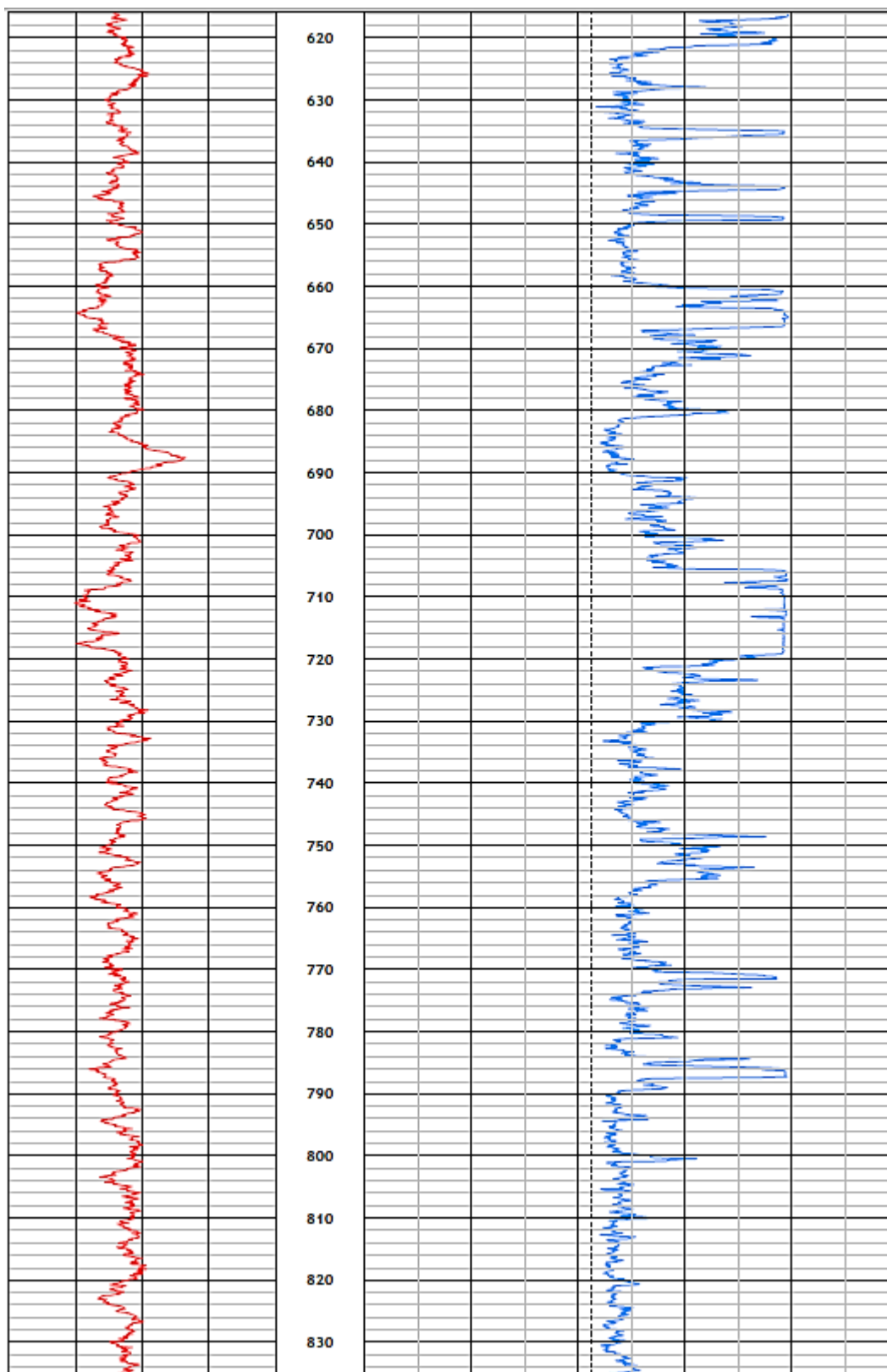
Future Casing of 6" used in volume calculation.

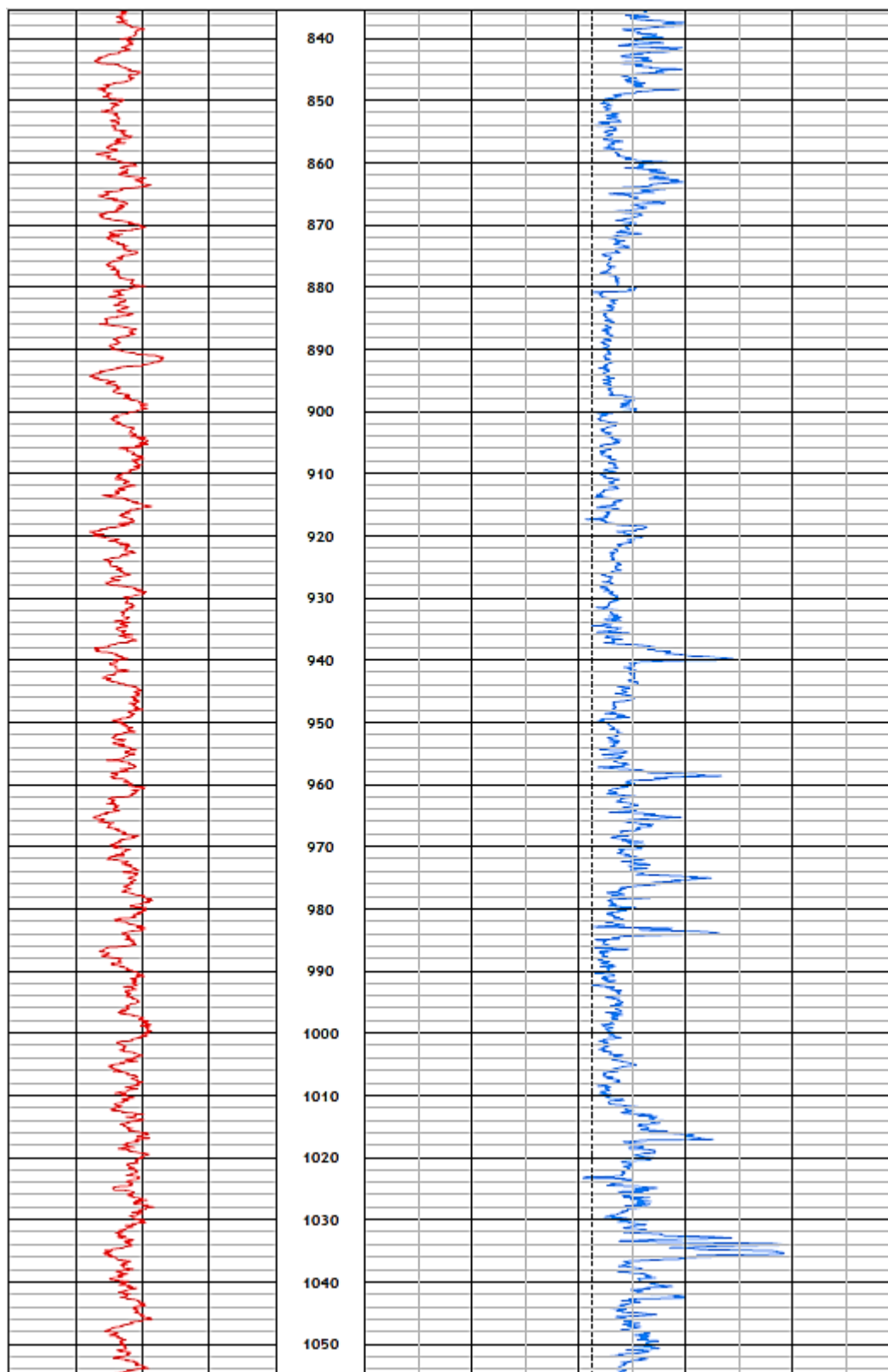
Natural Gamma logged to surface.

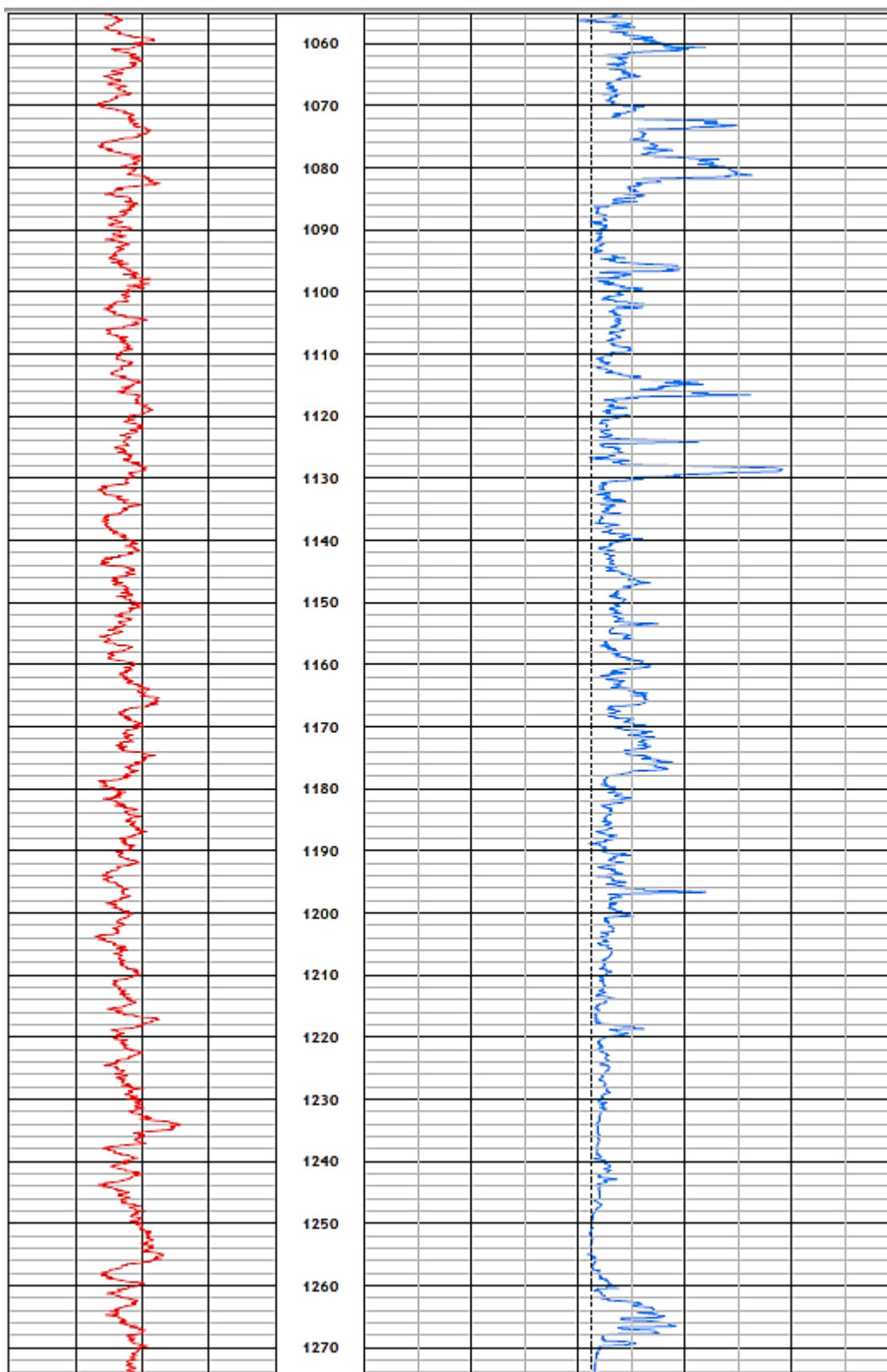


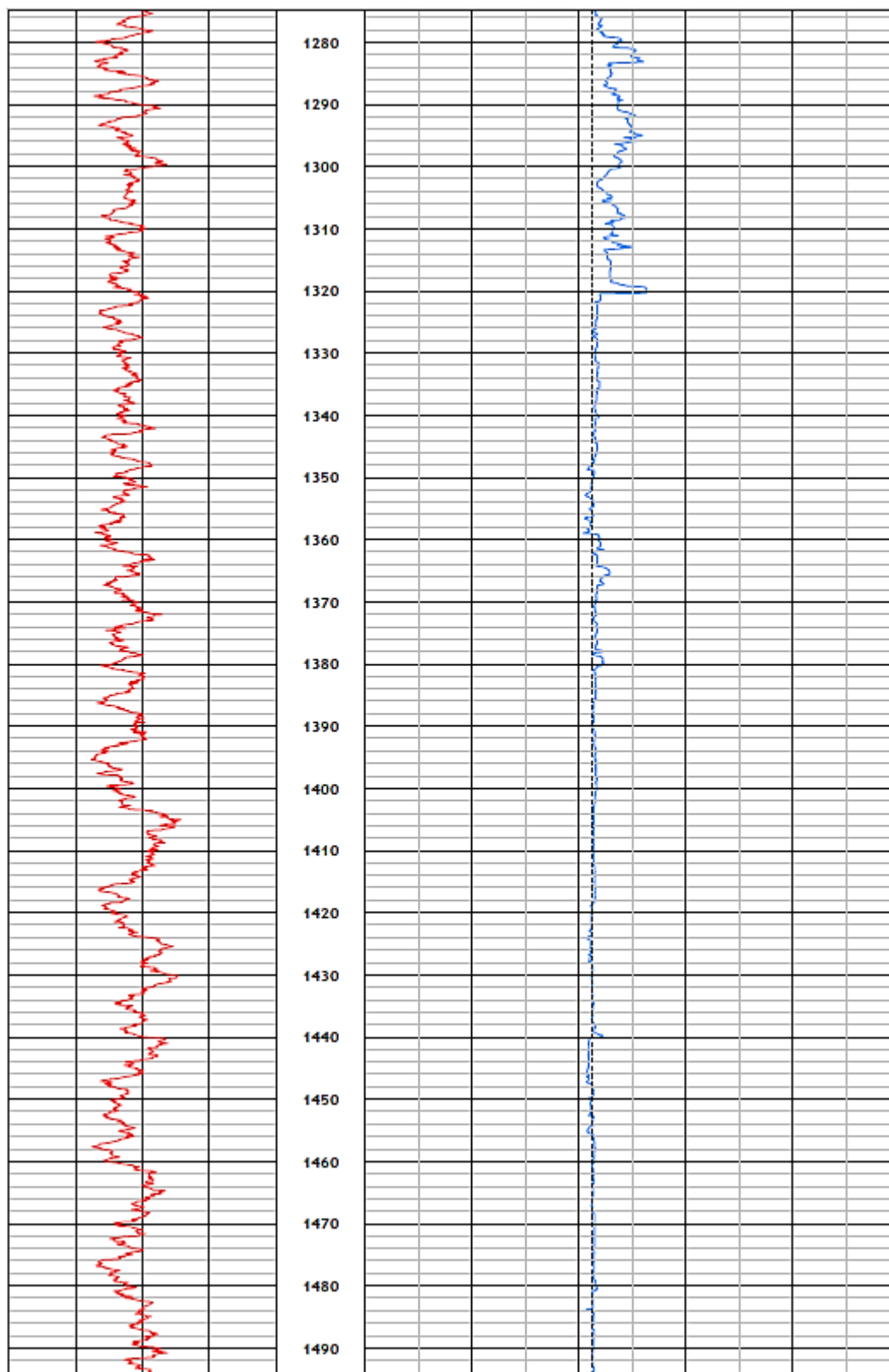


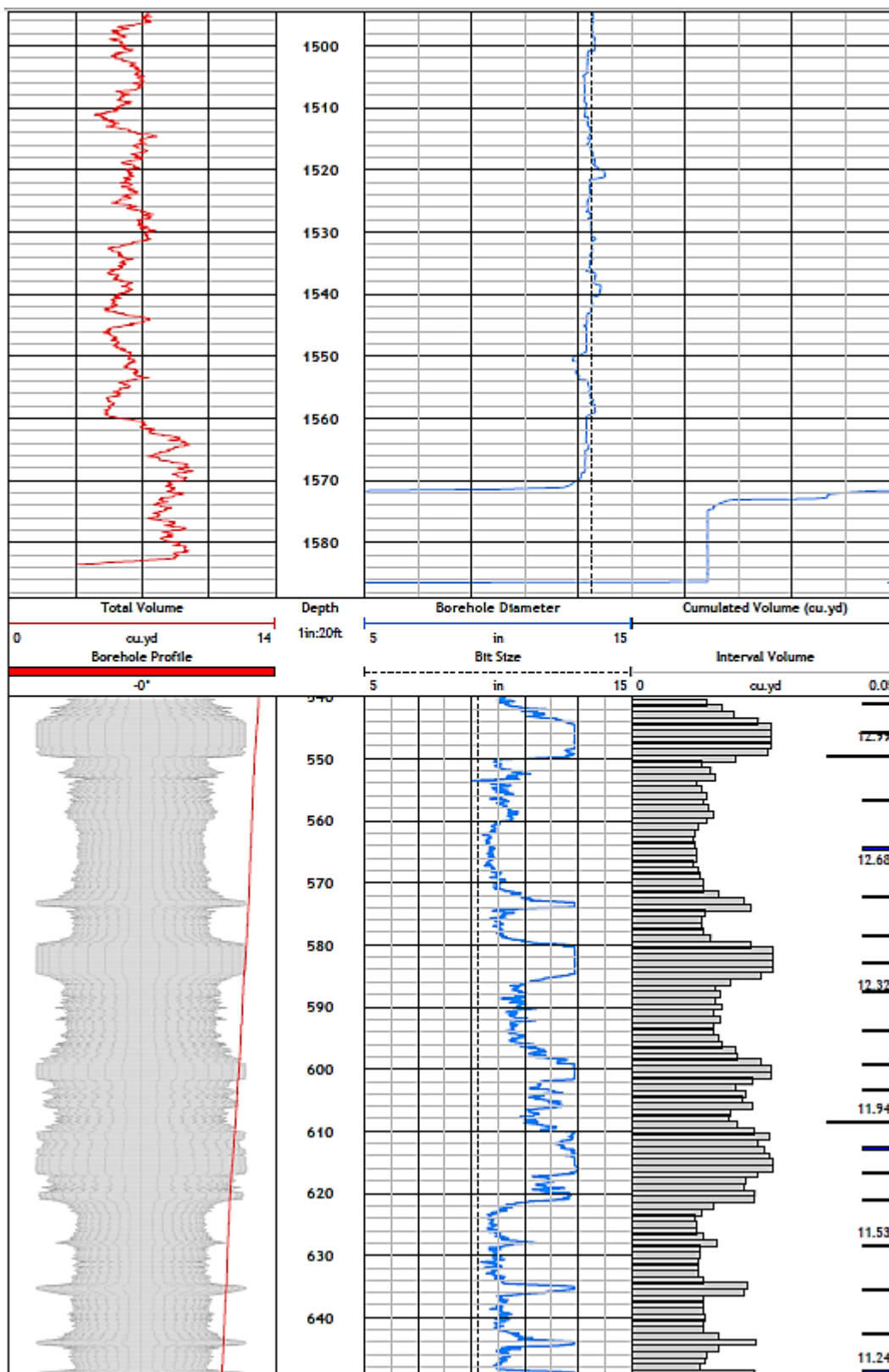


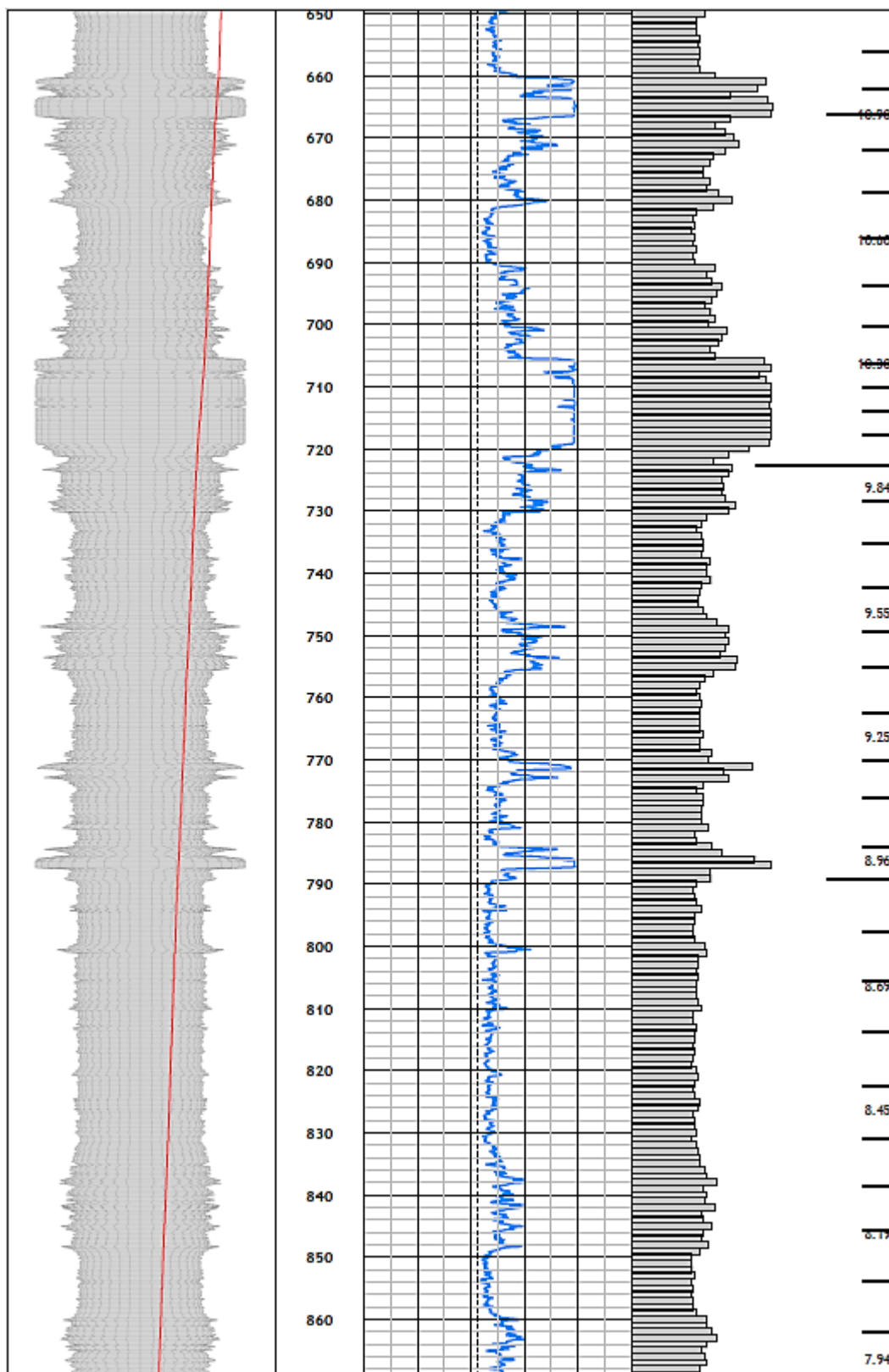


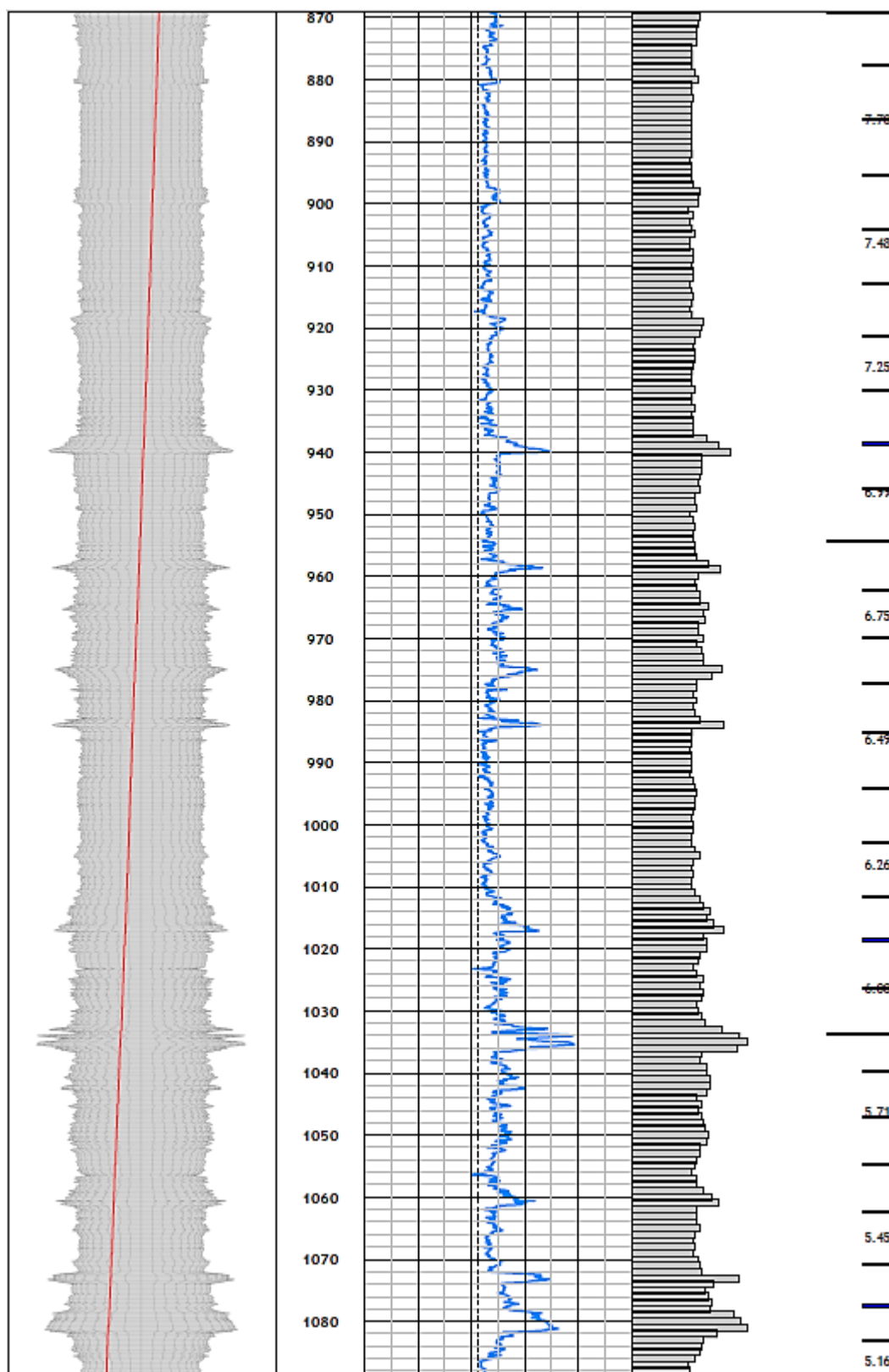


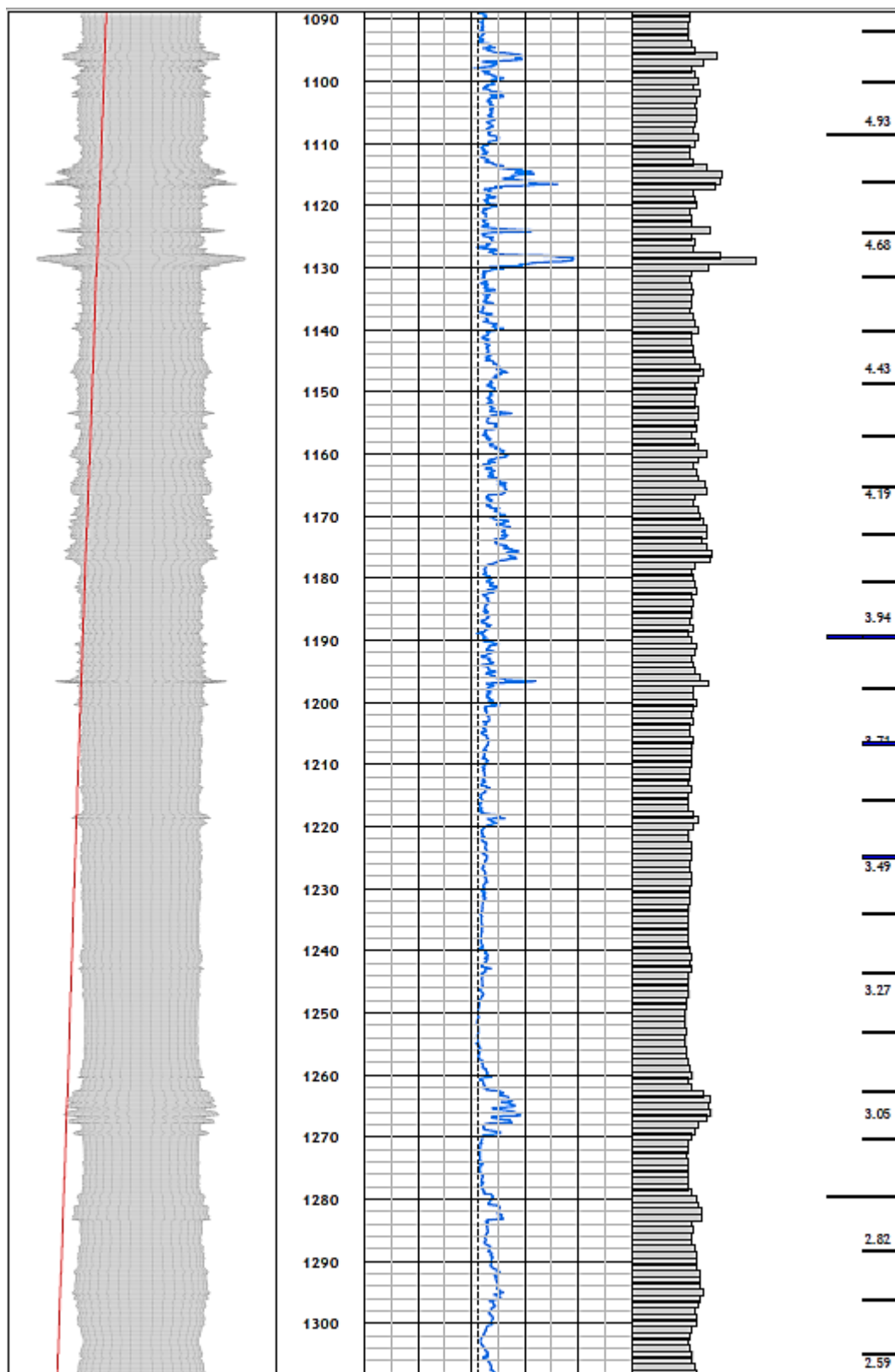


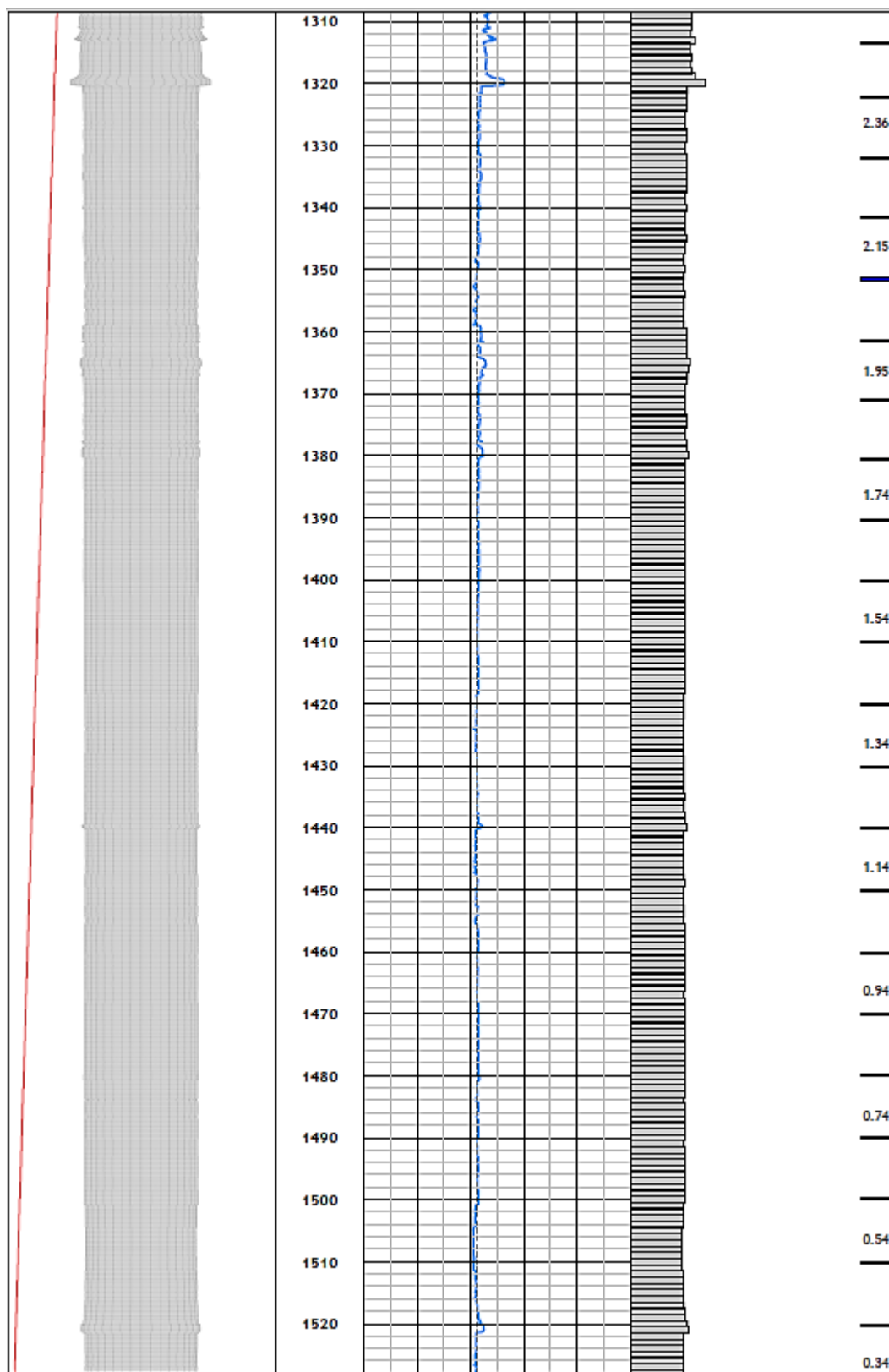


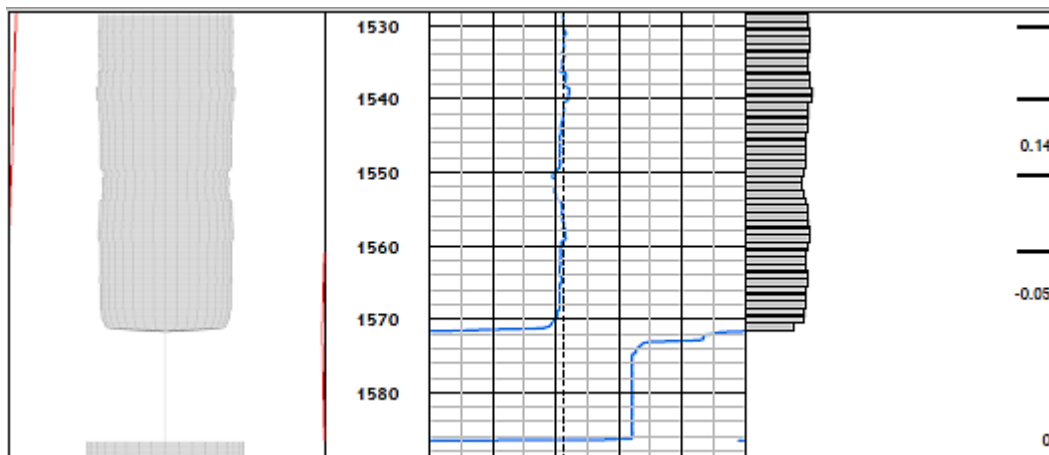












Appendix E: Other Well Reports

Flathead Valley, Montana

TEM and Well Locations

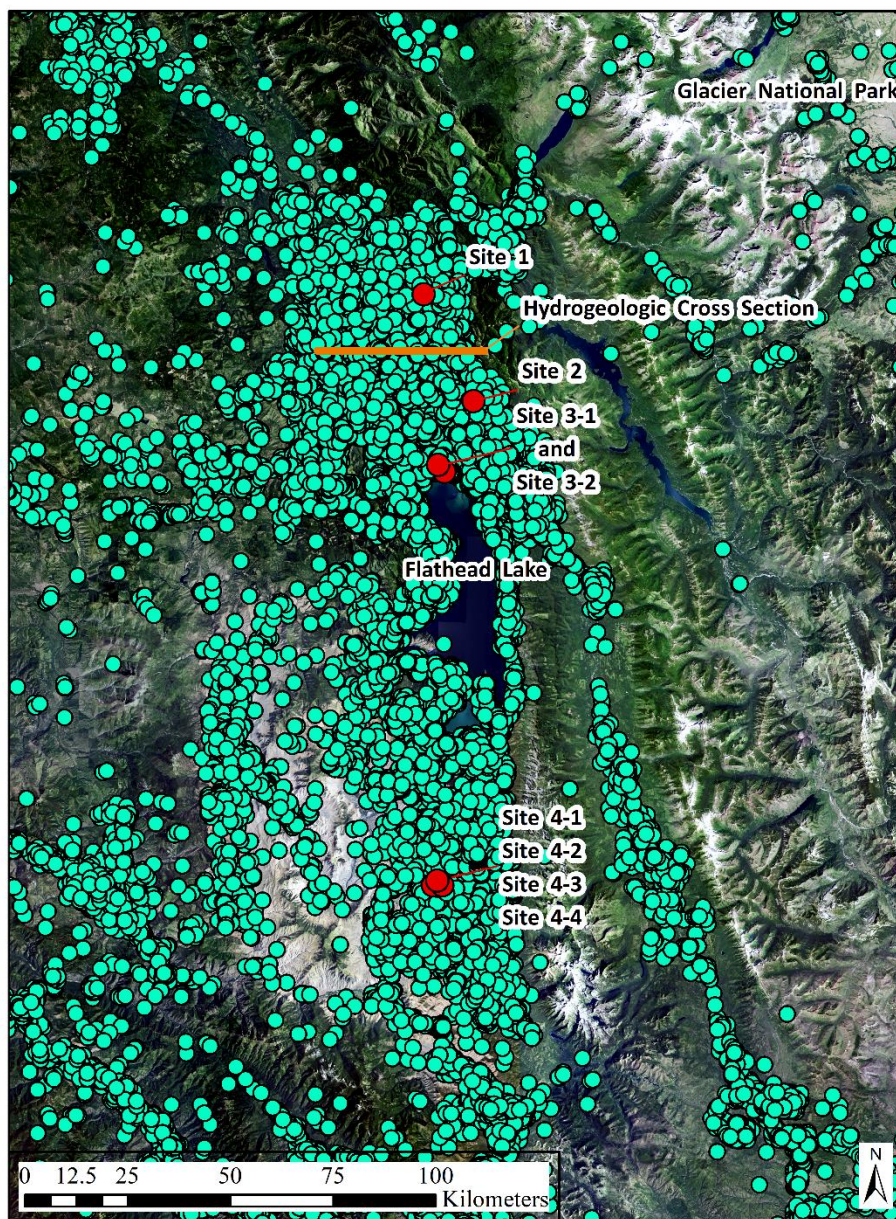


Figure 46. Map of central loop sounding sites and all well locations in the GWIC database for the Flathead Valley, Montana (Montana State Library GIS Services; Ground Water Information Center; Montana Bureau of Mines and Geology; Montana Technological University, 1998-2022) Annotation of TEM sounding sites in red and the hydrogeologic cross section from Figure 4. Only a small percentage of the wells in the GWIC system contain well completion reports with lithology, many are only mapped locations with no additional information available.

Flathead Valley, Montana
Site 1
TEM and Well Completion Report



Figure 47. Site 1 TEM location and locations of all nearby wells in the GWIC database located on or near the Kokanee Bend of the Flathead River (Montana State Library GIS Services). Star indicates well (85605) with a well completion report with lithology (Ground Water Information Center; Montana Bureau of Mines and Geology; Montana Technological University, 1998-2022). All wells within the image were checked for the availability of a well completion report with lithology to use.

Table 9. QWIC ID 85605 well completion report with lithology for comparison with 1D geoelectric resistivity model at Site 1 (Ground Water Information Center; Montana Bureau of Mines and Geology; Montana Technological University, 1998-2022).

Site Name: BOWERMAN BEN * FV-N-13

GWIC Id: 85605

DNRC Water Right: 9985

Section 1: Well Owner(s)

1) BOWERMAN, BEN (WELL)
259 KOKANEE BEND DRIVE
COLUMBIA FALLS MT 59912 [06/27/2019]
2) BOWERMAN, BEN (WELL)
259 KOKANEE DR
COLUMBIA FALLS MT 59912 [07/06/1976]

Section 2: Location

Township	Range	Section	Quarter Sections	
30N	20W	19	NE¼ SW¼ NE¼ SW¼	
County			Geocode	
FLATHEAD				
Latitude	Longitude	Geomethod		Datum
48.3456	-114.207889	MAP		WGS84
Ground Surface Altitude	Ground Surface Method	Datum	Date	
2996	LIDAR	NAVD88	8/12/2015	
Measuring Point Altitude	MP Method	Datum	Date Applies	
2997.75	LIDAR	NAVD88	6/27/2019	
Addition	Block		Lot	

Section 3: Proposed Use of Water

DOMESTIC (1)

IRRIGATION (2)

Section 4: Type of Work

Drilling Method: FORWARD ROTARY

Status: NEW WELL

Section 5: Well Completion Date

Date well completed: Tuesday, July 6, 1976

Section 6: Well Construction Details

There are no borehole dimensions assigned to this well.

Casing

From	To	Diameter	Wall Thickness	Pressure Rating	Joint	Type
0	64	6				STEEL

Completion (Perf/Screen)

From	To	Diameter	# of Openings	Size of Openings	Description
56	61	6		1/4X6	SLOTS

Annular Space (Seal/Grout/Packer)

From	To	Description	Cont. Fed?
0	20	DRILL CUTTINGS	

Section 7: Well Test Data

Total Depth: 64
 Static Water Level: 40
 Water Temperature:

Air Test *

35 gpm with drill stem set at feet for 4 hours.
 Time of recovery hours.
 Recovery water level feet.
 Pumping water level 55 feet.

** During the well test the discharge rate shall be as uniform as possible. This rate may or may not be the sustainable yield of the well. Sustainable yield does not include the reservoir of the well casing.*

Section 8: Remarks

SAMPLING PT -HYDRANT NEXT TO WELL

Section 9: Well Log

Geologic Source

112DRFT - GLACIAL DRIFT

From	To	Description
0	10	TOPSOIL
10	14	BOULDERS IN BROWN CLAY
14	36	SAND
36	56	GRAVEL IN BROWN CLAY
56	61	GRAEL & WATER
61	64	GRAVEL IN BROWN CLAY & WATER

Driller Certification

All work performed and reported in this well log is in compliance with the Montana well construction standards. This report is true to the best of my knowledge.

<p>Name: Company: BILLMAYER DRILLING License No: WWC-5 Date Completed: 7/6/1976</p>

Flathead Valley, Montana
Site 2
TEM and Well Completion Reports

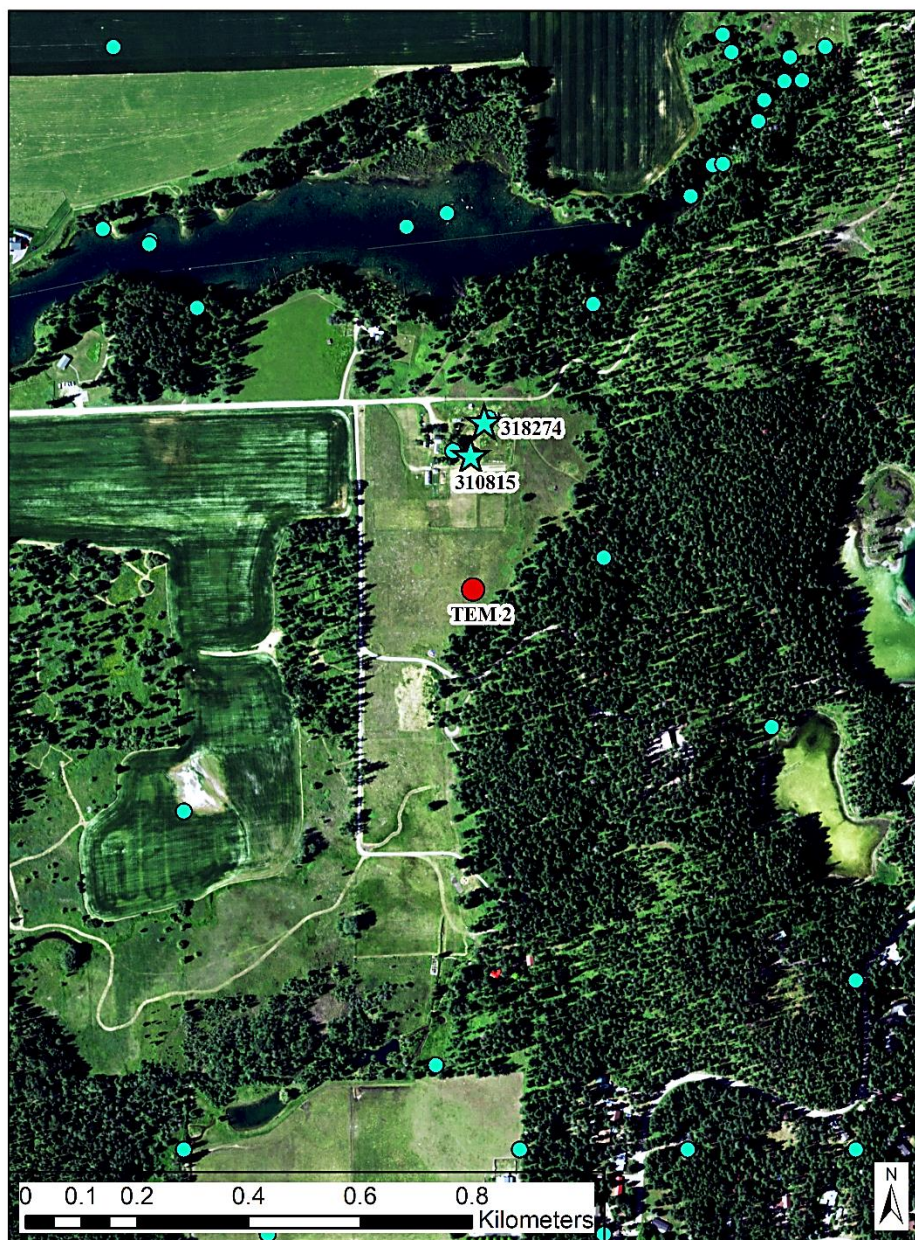


Figure 48. Site 2 TEM and all well locations in the GWIC database located on or near the private property where the soundings were performed (Montana State Library GIS Services). Star indicates GWIP drilled well completion reports with lithology, wells 318274 and 310815 (Ground Water Information Center; Montana Bureau of Mines and Geology; Montana Technological University, 1998-2022).

Table 10. GWIC ID 310815 well completion report with lithology for comparison with 1D geoelectric resistivity model at Site 2 (Ground Water Information Center; Montana Bureau of Mines and Geology; Montana Technological University, 1998-2022).

Site Name: OTTEY , MARK
GWIC Id: 310815

Section 1: Well Owner(s)

1) OTTEY , MARK (MAIL)
270 KAUFFMAN LANE
KALISPELL MT 59901 [10/20/2020]

Section 2: Location

Township	Range	Section	Quarter Sections		
28N	20W	14	NW¼ NW¼ NE¼		
County			Geocode		
FLATHEAD					
Latitude		Longitude		Geomethod	Datum
48.196444486111		-114.105577805556		SUR-GPS	NAD83
Ground Surface Altitude		Ground Surface Method		Datum	Date
2971.28		SUR-GPS		NAVD88	10/19/2021
Measuring Point Altitude		MP Method	Datum	Date Applies	
2973.07		SUR-GPS	NAVD88	12/10/2020	
Addition		Block	Lot		

Section 3: Proposed Use of Water

DOMESTIC (1)

Section 4: Type of Work

Drilling Method: DUAL ROTARY
Status: NEW WELL

Section 5: Well Completion Date

Date well completed: Tuesday, October 20, 2020

Section 6: Well Construction Details

Borehole dimensions

From	To	Diameter
0	280	6

Casing

From	To	Diameter	Wall Thickness	Pressure Rating	Joint	Type
-2	280	6.6	0.25		WELDED	A53B STEEL

Completion (Perf/Screen)

From	To	Diameter	# of Openings	Size of Openings	Description
0	280	6.6			OPEN BOTTOM

Annular Space (Seal/Grout/Packer)

From	To	Description	Cont. Fed?
0	10	CASING SEAL	

Section 7: Well Test Data

Total Depth: 280
 Static Water Level: 18
 Water Temperature:

Air Test *

10 gpm with drill stem set at 260 feet for 1 hours.
 Time of recovery 1 hours.
 Recovery water level 18 feet.
 Pumping water level feet.

** During the well test the discharge rate shall be as uniform as possible. This rate may or may not be the sustainable yield of the well. Sustainable yield does not include the reservoir of the well casing.*

Section 8: Remarks

WELL DRILLED BY PETER CHINIKAYLO AKD

Section 9: Well Log**Geologic Source**

Unassigned

From	To	Description
0	1	BLACK TOPSOIL
1	7	REDDISH BROWN SILTY MEDIUM SAND WITH SOME COBBLES AND GRAVEL
7	17	MULTICOLORED (BELT) COBBLES
17	19	MULTICOLORED (BELT) GRAVEL WITH LITTLE REDDISH BROWN SAND
19	29	REDDISH BROWN SILTY SAND WITH LITTLE FINE GRAVEL
29	34	REDDISH BROWN SILTY SAND AND FINE TO MEDIUM MULTICOLORED (BELT) GRAVEL
34	39	MULTICOLORED (BELT) COBBLES
39	43	MULTICOLORED (BELT) MEDIUM TO COARSE SAND AND FINE TO MEDIUM GRAVEL
43	44	MULTICOLORED (BELT) COBBLES
44	47	MULTICOLORED (BELT) MEDIUM TO COARSE SAND AND FINE TO MEDIUM GRAVEL
47	48	MULTICOLORED (BELT) COBBLES
48	54	MULTICOLORED (BELT) MEDIUM TO COARSE SAND AND FINE TO MEDIUM GRAVEL
54	64	MULTICOLORED (BELT) MEDIUM TO COARSE SAND AND FINE TO MEDIUM GRAVEL WITH LITTLE BLACK SILT
64	69	MULTICOLORED (BELT) MEDIUM TO COARSE SAND AND FINE TO MEDIUM GRAVEL WITH LITTLE BLACK SILT AND SOME COBBLES
69	74	REDDISH BROWN MEDIUM TO COARSE SAND WITH LITTLE FINE MULTICOLORED (BELT) GRAVEL

Driller Certification

All work performed and reported in this well log is in compliance with the Montana well construction standards. This report is true to the best of my knowledge.

Name: MARTIN WILSON
Company: AK DRILLING INC
License No: WWC-624
Date Completed: 10/20/2020

Site Name: OTTEY , MARK		
GWIC Id: 310815		
Additional Lithology Records		
From	To	Description
74	83	MEDIUM TO COARSE SAND WITH SOME FINE MULTICOLORED (BELT) GRAVEL AND FEW COBBLES
83	86	MEDIUM TO COARSE SAND
86	103	FINE TO MEDIUM SAND WITH SOME FINE MULTICOLORED (BELT) GRAVEL AND SOME COARSE SAND
103	116	MULTICOLORED (BELT) FINE TO MEDIUM GRAVEL AND MEDIUM TO COARSE SAND
116	124	MEDIUM TO COARSE SAND WITH SOME FINE MULTICOLORED (BELT) GRAVEL
124	134	MEDIUM TO COARSE SAND WITH LITTLE FINE MULTICOLORED (BELT) GRAVEL
134	176	FINE WELL SORTED SAND
176	183	MEDIUM TO COARSE SAND WITH SOME FINE GRAVEL
183	189	FINE TO MEDIUM SAND
189	208	FINE SAND
208	219	MEDIUM TO COARSE SAND WITH SOME MULTICOLORED (BELT) FINE GRAVEL
219	225	MULTICOLORED (BELT) FINE TO MEDIUM GRAVEL WITH SOME COARSE SAND
225	245	MEDIUM TO COARSE SAND WITH SOME FINE MULTICOLORED (BELT) GRAVEL
245	250	MEDIUM TO COARSE SAND AND FINE TO MEDIUM MULTICOLORED (BELT) GRAVEL
250	270	MEDIUM TO COARSE SAND WITH SOME FINE MULTICOLORED (BELT) GRAVEL
270	280	MEDIUM TO COARSE SAND AND FINE TO MEDIUM MULTICOLORED (BELT) GRAVEL

Table 11. GWIC ID 318274 well completion report with lithology for comparison with 1D geoelectric resistivity model at Site 2 (Ground Water Information Center; Montana Bureau of Mines and Geology; Montana Technological University, 1998-2022).

Site Name: OTTEY, MARK
GWIC Id: 318274

Section 1: Well Owner(s)

1) OTTEY, MARK (MAIL)
270 KAUFFMAN LANE
KALISPELL MT 59901 [10/27/2021]

Section 2: Location

Township	Range	Section	Quarter Sections	
28N	20W	14	NE¼ NW¼	
County			Geocode	
FLATHEAD				
Latitude	Longitude	Geomethod	Datum	
48.196797	-114.105436	SUR-GPS	WGS84	
Ground Surface Altitude	Ground Surface Method	Datum	Date	
2985.49	SURVEY	NAVD88	10/19/2021	
Measuring Point Altitude	MP Method	Datum	Date Applies	
2987.99	SURVEY	NAVD88	10/19/2021	
Addition	Block	Lot		

Section 3: Proposed Use of Water

DOMESTIC (1)

Section 4: Type of Work

Drilling Method: ROTARY DR
Status: NEW WELL

Section 5: Well Completion Date

Date well completed: Wednesday, October 27, 2021

Section 6: Well Construction Details

Borehole dimensions

From	To	Diameter
0	300	6

Casing

From	To	Diameter	Wall Thickness	Pressure Rating	Joint	Type
-2	278	6	0.25		WELDED	A53B STEEL

Completion (Perf/Screen)

From	To	Diameter	# of Openings	Size of Openings	Description
278	298	6		.050	SCREEN-CONTINUOUS-STAINLESS

Annular Space (Seal/Grout/Packer)

From	To	Description	Cont. Fed?
276	276	K-PACKER	

Section 7: Well Test Data

Total Depth: 300
 Static Water Level: 30
 Water Temperature:

Air Test *

35 gpm with drill stem set at 296 feet for 2.5 hours.
 Time of recovery 1 hours.
 Recovery water level 30 feet.
 Pumping water level feet.

** During the well test the discharge rate shall be as uniform as possible. This rate may or may not be the sustainable yield of the well. Sustainable yield does not include the reservoir of the well casing.*

Section 8: Remarks

Section 9: Well Log

Geologic Source
 Unassigned

From	To	Description
0	1	TOP SOIL
1	8	GRAVELS
8	15	SAND, SILT AND CLAY
15	42	GRAVELS
42	85	SILT
85	150	SAND AND GRAVELS
150	300	GRAVEL

Driller Certification

All work performed and reported in this well log is in compliance with the Montana well construction standards. This report is true to the best of my knowledge.

Name: MIKE DOWNEY Company: OKEEFE DRILLING CO License No: WWD-90 Date Completed: 10/27/2021
--

Flathead Valley, Montana
Site 3-2
TEM and Well Completion Report

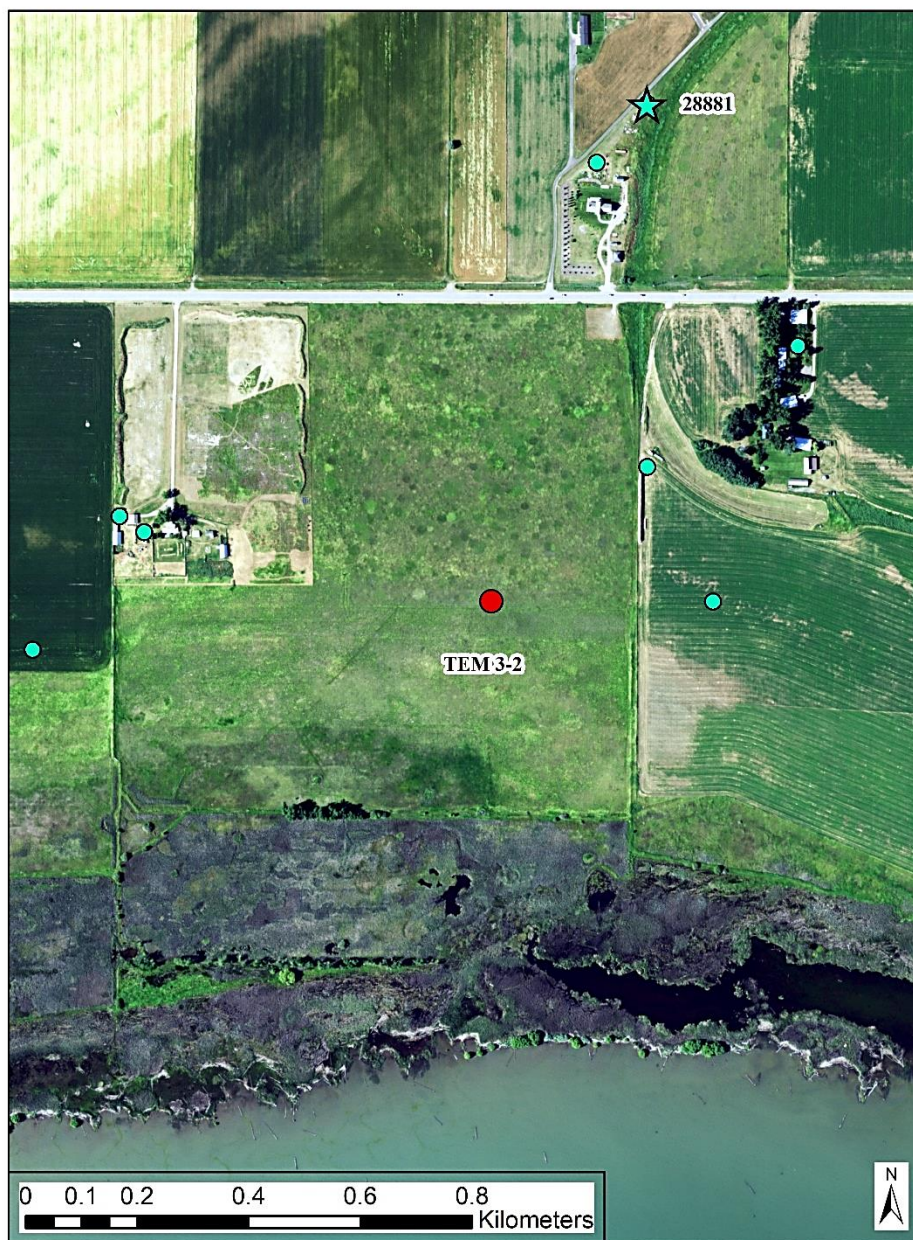


Figure 49. Site 3-2 TEM and all well locations in the GWIC database located on or near the Flathead Waterfowl Production Area under management of U.S. Fish & Wildlife Services (Montana State Library GIS Services). Star indicates well 28881 with well completion report with lithology (Ground Water Information Center; Montana Bureau of Mines and Geology; Montana Technological University, 1998-2022). All wells within the image were checked for the availability of a well completion report with lithology.

Table 12. QWIC ID 28881 well completion report with lithology for comparison with 1D geoelectric resistivity model at Site 3-2 (Ground Water Information Center; Montana Bureau of Mines and Geology;

Site Name: SIR TONY
GWIC Id: 28881

Section 1: Well Owner(s)

1) SIR, TONY (MAIL)
N/A
LINDSAY MT 59339 [10/18/1993]

Section 2: Location

Township	Range	Section	Quarter Sections	
16N	50E	4	SE¼	NE¼ SE¼ SE¼
County			Geocode	
PRAIRIE				
Latitude	Longitude	Geomethod	Datum	
47.1677	-105.3883	MAP	NAD27	
Ground Surface Altitude	Ground Surface Method		Datum	Date
3207				
Measuring Point Altitude	MP Method	Datum	Date Applies	
3207.58			10/18/1993 1:00:00 PM	
Addition	Block		Lot	

Section 3: Proposed Use of Water

STOCKWATER (1)

Section 4: Type of Work

Drilling Method: CABLE TOOLS
Status: NEW WELL

Section 5: Well Completion Date

Date well completed: Thursday, October 5, 1967

Section 6: Well Construction Details

There are no borehole dimensions assigned to this well.

Casing

From	To	Diameter	Wall Thickness	Pressure Rating	Joint	Type
0	29	8				
26	47	6				

Completion (Perf/Screen)

From	To	Diameter	# of Openings	Size of Openings	Description
29	47	6		3/8	DRILLED HOLES

Annular Space (Seal/Grout/Packer)

There are no annular space records assigned to this well.

Montana Technological University, 1998-2022).

Section 7: Well Test Data

Total Depth: 47
 Static Water Level: 8
 Water Temperature:

Pump Test *

Depth pump set for test _ feet.
 4 gpm pump rate with _ feet of drawdown after 24 hours of pumping.
 Time of recovery _ hours.
 Recovery water level _ feet.
 Pumping water level 45 feet.

** During the well test the discharge rate shall be as uniform as possible. This rate may or may not be the sustainable yield of the well. Sustainable yield does not include the reservoir of the well casing.*

Section 8: Remarks

OLD PUMP JACK CONVERTED TO ELECTRICITY.

Section 9: Well Log

Geologic Source

125TGRV - TONGUE RIVER MEMBER (OF FT UNION FM.)

From	To	Description
0	6	GRAVEL
6	20	YELLOW LOAM AND QUICKSAND
20	31	BLUE QUICKSAND
31	47	GRAY SANDSTONE W/WATER

Driller Certification

All work performed and reported in this well log is in compliance with the Montana well construction standards. This report is true to the best of my knowledge.

<p>Name: Company: JOHNSON License No: WWC-22 Date Completed: 10/5/1967</p>
--

Flathead Valley, Montana

Site 4

TEM and Well Completion Reports

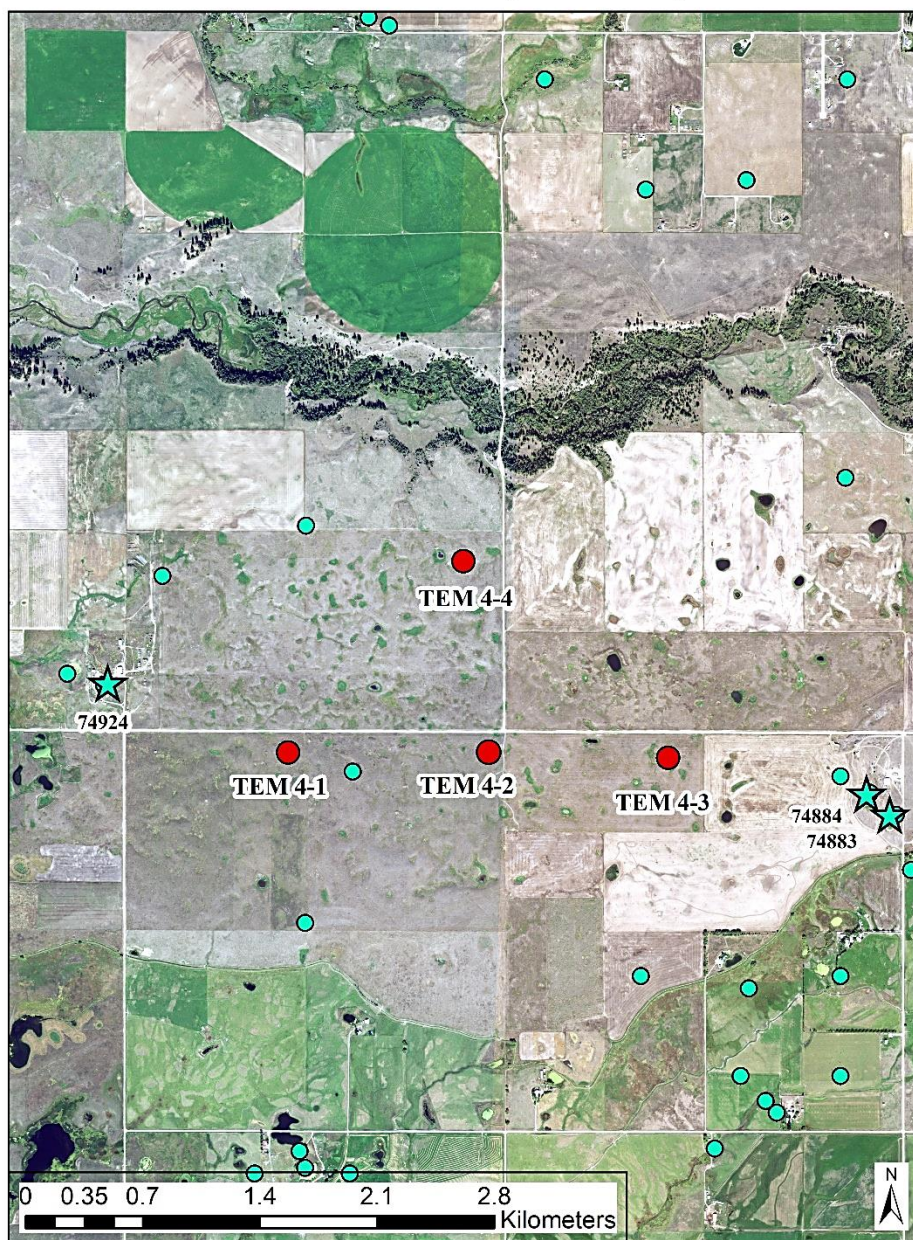


Figure 50. Site 4 TEM and all well locations in the GWIC database located on or near the Crow Waterfowl Production Area under management of U.S. Fish & Wildlife Services (Montana State Library GIS Services). Star indicates wells 74924, 74883 and 74884 with well completion reports with lithology (Ground Water Information Center; Montana Bureau of Mines and Geology; Montana Technological University, 1998-2022). All wells within the image were checked for the availability of a well completion report with lithology to use for correlation with the 1D geoelectric resistivity models.

Table 13. QWIC ID 74883 well completion report with lithology for comparison with 1D geoelectric resistivity model at Site 4 (Ground Water Information Center; Montana Bureau of Mines and Geology;

Site Name: BAUER KIM
GWIC Id: 74883

Section 1: Well Owner(s)

1) BAUER, KIM (MAIL)
 3084 ROCKY BUTTE RD
 RONAN MT 59864 [09/08/1996]
 2) THIEL, BOB (MAIL)
 N/A
 RONAN MT 59864 [10/16/1980]

Section 2: Location

Township	Range	Section	Quarter Sections	
20N	20W	20	SE¼ SE¼ NE¼ NE¼	
County			Geocode	
LAKE				
Latitude	Longitude	Geomethod	Datum	
47.4833	-114.1605	MAP	NAD27	
Ground Surface Altitude		Ground Surface Method	Datum	Date
3065				
Measuring Point Altitude		MP Method	Datum	Date Applies
3066.5				9/8/1996 4:25:00 PM
Addition	Block		Lot	

Section 3: Proposed Use of Water

DOMESTIC (1)
 UNKNOWN (2)

Section 4: Type of Work

Drilling Method: FORWARD ROTARY
 Status: NEW WELL

Section 5: Well Completion Date

Date well completed: Thursday, October 16, 1980

Section 6: Well Construction Details

There are no borehole dimensions assigned to this well.

Casing

From	To	Diameter	Wall Thickness	Pressure Rating	Joint	Type
0	39	6				

There are no completion records assigned to this well.

Annular Space (Seal/Grout/Packer)

From	To	Description	Cont. Fed?
0	15	PUDDLED CLAY	

Montana Technological University, 1998-2022).

Section 7: Well Test Data

Total Depth: 160
Static Water Level: 102
Water Temperature:

Air Test *

11 gpm with drill stem set at feet for 1 hours.
Time of recovery hours.
Recovery water level feet.
Pumping water level 130 feet.

** During the well test the discharge rate shall be as uniform as possible. This rate may or may not be the sustainable yield of the well. Sustainable yield does not include the reservoir of the well casing.*

Section 8: Remarks

E-LINE HANGS UP ON WAY DOWN. BE CAREFUL.

Section 9: Well Log

Geologic Source
400RVLL - RAVALLI GROUP

From	To	Description
0	1	BLK.DIRT
1	87	HARD GRAY ROCK
87	105	MED. HARD BROWN & GRAY ROCK
105	117	HARD GRAY ROCK
117	125	SOFT BROWN ROCK & A LITTLE WATER
125	140	BROKEN BROWN & QUARTZ ROCK WATER
140	150	MED. HARD BROWN ROCK & A LITTLE WATER
150	160	HARD GRAY ROCK

Driller Certification

All work performed and reported in this well log is in compliance with the Montana well construction standards. This report is true to the best of my knowledge.

Name: Company: CASTLIO DRILLING License No: WWC-387 Date Completed: 10/16/1980

Table 14. QWIC ID 74884 well completion report with lithology for comparison with 1D geoelectric resistivity model at Site 4 (Ground Water Information Center; Montana Bureau of Mines and Geology;

Site Name: BAUER DON
GWIC Id: 74884
DNRC Water Right: 54345

Section 1: Well Owner(s)

1) BAUER, DON (MAIL)
 ROCKY BUTTE RD
 RONAN MT 59864 [11/18/1983]

Section 2: Location

Township	Range	Section	Quarter Sections		
20N	20W	20	NW¼ SE¼ NE¼ NE¼		
County			Geocode		
LAKE					
Latitude	Longitude	Geomethod		Datum	
47.4841	-114.1619	MAP		NAD27	
Ground Surface Altitude		Ground Surface Method		Datum	Date
3125					
Measuring Point Altitude		MP Method	Datum	Date Applies	
3125.3				9/8/1996 5:37:00 PM	
Addition		Block	Lot		

Section 3: Proposed Use of Water

DOMESTIC (1)

Section 4: Type of Work

Drilling Method: FORWARD ROTARY
 Status: NEW WELL

Section 5: Well Completion Date

Date well completed: Friday, November 18, 1983

Section 6: Well Construction Details

There are no borehole dimensions assigned to this well.

Casing

From	To	Diameter	Wall Thickness	Pressure Rating	Joint	Type
0	40	6				

There are no completion records assigned to this well.

Annular Space (Seal/Grout/Packer)

From	To	Description	Cont. Fed?
0	20	PUDDLED CLAY	

Montana Technological University, 1998-2022).

Section 7: Well Test Data

Total Depth: 303
 Static Water Level: 165
 Water Temperature:

Air Test *

10 gpm with drill stem set at feet for 1.5 hours.
 Time of recovery hours.
 Recovery water level feet.
 Pumping water level 250 feet.

** During the well test the discharge rate shall be as uniform as possible. This rate may or may not be the sustainable yield of the well. Sustainable yield does not include the reservoir of the well casing.*

Section 8: Remarks

NEW CAP.

Section 9: Well Log**Geologic Source**

400RVLL - RAVALLI GROUP

From	To	Description
0	1	BLACK DIRT
1	15	BROKEN GRAY ROCK
15	140	MED HARD GRAY ROCK
140	145	SOFT BROWN ROCK
145	163	MED HARD GRAY ROCK
163	180	SOFT GREEN & BROWN ROCK & A LITTLE WATER(2-3 GPM)
180	223	MED HARD GRAY ROCK
223	260	MED HARD GRAY ROCK
260	295	HARD GRAY ROCK
295	297	SOFT BROWN ROCK & WATER
297	303	HARD GRAY ROCK

Driller Certification

All work performed and reported in this well log is in compliance with the Montana well construction standards. This report is true to the best of my knowledge.

Name: Company: CASTLIO DRILLING License No: WWC-387 Date Completed: 11/18/1983

Table 15. QWIC ID 74924 well completion report with lithology for comparison with 1D geoelectric resistivity model at Site 4 (Ground Water Information Center; Montana Bureau of Mines and Geology;

Site Name: JOHNSON ALICE
GWIC Id: 74924

Section 1: Well Owner(s)

1) JOHNSON, ALICE (MAIL)
 5052 JOHNSON RD
 RONAN MT 59864 [10/18/1996]
 2) JOHNSON, WAYLAND (MAIL)
 RTE. 2
 RONAN MT 59864 [11/01/1972]

Section 2: Location

Township	Range	Section	Quarter Sections	
20N	21W	13	NW¼ SE¼ SE¼ SE¼	
County			Geocode	
LAKE				
Latitude	Longitude	Geomethod	Datum	
47.488	-114.203	MAP	NAD27	
Ground Surface Altitude	Ground Surface Method	Datum	Date	
3000				
Measuring Point Altitude	MP Method	Datum	Date Applies	
3001.5			10/18/1996 12:42:00 PM	
Addition	Block	Lot		

Section 3: Proposed Use of Water

DOMESTIC (1)
 STOCKWATER (2)

Section 4: Type of Work

Drilling Method: CABLE
 Status: NEW WELL

Section 5: Well Completion Date

Date well completed: Wednesday, November 1, 1972

Section 6: Well Construction Details

Borehole dimensions

From	To	Diameter
0	389	6

Casing

From	To	Diameter	Wall Thickness	Pressure Rating	Joint	Type
-1.5	380	6				STEEL

Completion (Perf/Screen)

From	To	Diameter	# of Openings	Size of Openings	Description
380	389	6			OPEN HOLE

Annular Space (Seal/Grout/Packer)

There are no annular space records assigned to this well.
 Montana Technological University, 1998-2022).

Section 7: Well Test Data

Total Depth: 380
 Static Water Level: 100
 Water Temperature:

Bailer Test *

22 gpm with feet of drawdown after 3 hours.
 Time of recovery hours.
 Recovery water level feet.
 Pumping water level 270 feet.

** During the well test the discharge rate shall be as uniform as possible. This rate may or may not be the sustainable yield of the well. Sustainable yield does not include the reservoir of the well casing.*

Section 8: Remarks

E LINE NEARLY GOT STUCK. FRIENDLY OWNER SAMPLING PT -HYDRANT SW OF WELL.

Section 9: Well Log**Geologic Source**

400RVLL - RAVALLI GROUP

From	To	Description
0	115	TAN CLAY W/GRAVEL
115	125	WET CLAY
125	145	QUICK SAND
145	155	CLAY W/SAND
155	180	LIGHT BLUE CLAY W/SAND
180	265	CLAY & GRAVEL
265	273	GRAVEL & CLAY
273	335	TAN CLAY W/GRAVEL
335	345	WET STICKEY CLAY
345	376	CLAY & GRAVEL
376	379	GRAVEL & CLAY
379	389	ROCK;LIGHT GREY FRACTURE WWATER

Driller Certification

All work performed and reported in this well log is in compliance with the Montana well construction standards. This report is true to the best of my knowledge.

Name: HENRY I. JOHNSON
 Company: JOHNSON WATER WELL SERVICE
 License No: WWC-22
 Date Completed: 11/1/1972

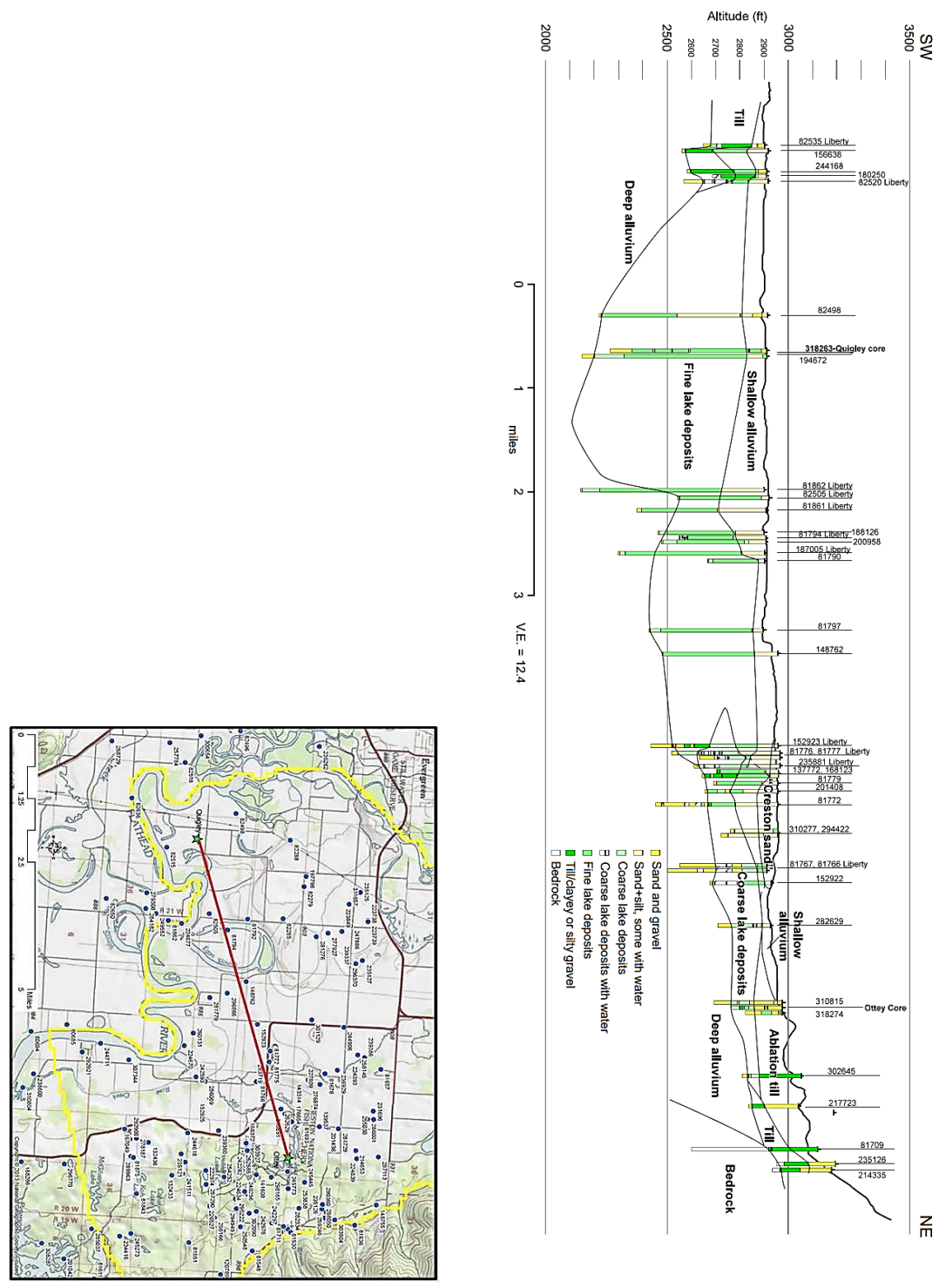


Figure 51. Southwest to northeast cross section of lithology defining the near subsurface between Quigley on the north bank of the Flathead River near Kalispell, Montana and Ottey at Site 2 near the Creston Fish Hatchery (Smith, Flathead SW-NE Cross Section of Deep Aquifer Drilling Report, report in preparation 2022).